



University
of Glasgow

Murray, Lynn (2010) *The role of E-cadherin in colon cancer drug resistance*. PhD thesis.

<http://theses.gla.ac.uk/1943/>

Copyright and moral rights for this thesis are retained by the Author

A copy can be downloaded for personal non-commercial research or study, without prior permission or charge

This thesis cannot be reproduced or quoted extensively from without first obtaining permission in writing from the Author

The content must not be changed in any way or sold commercially in any format or medium without the formal permission of the Author

When referring to this work, full bibliographic details including the author, title, awarding institution and date of the thesis must be given

The Role of E-cadherin in Colon Cancer Drug Resistance

by

Lynn Murray

This thesis is submitted to the University of Glasgow as part fulfilment of the requirements for the degree of Doctor of Philosophy.

The Faculty of Medicine
University of Glasgow
Glasgow

The Beatson Institute for
Cancer Research
Cancer Research U.K.
Laboratories
Bearsden
Glasgow

Edinburgh Cancer Research
Centre
University of Edinburgh
Western General Hospital
Edinburgh

Abstract

As resistance to current therapies remains one of the major hurdles to the successful treatment of advanced colorectal cancer, we need to understand the mechanisms by which cancer cells evade therapy-induced cell death. I have investigated whether there is a link between epithelial cell adhesions, and acquired resistance to 5-fluorouracil (5-FU). I compared three pairs of human colorectal 5-FU-sensitive and -resistant cell lines, and investigated whether there was a direct role for E-cadherin and/or the Src family kinase, c-Yes (which is co-amplified with thymidylate synthase) in promoting resistance to 5-FU. I found that while knockdown of c-Yes expression had no effect, disruption of E-cadherin using a blocking antibody caused a reduction in colon cancer cell proliferation and some re-sensitisation to 5-FU. The resistant cells displayed intrinsically higher activities of putative survival pathways, namely the PI3-kinase/Akt and the MEK/MAP kinase pathways, and these were suppressed when E-cadherin function was blocked. Furthermore, the resistant cells displayed a greater dependence on signalling via the PI3-kinase/Akt pathway for their survival. Finally, preliminary experiments established a possible link between the integrity of E-cadherin-mediated cell-cell junctions, signalling through the PI3-kinase/Akt pathway and nuclear localisation of the apoptotic regulatory tumour suppressor protein p53 in modulation of 5-FU-resistance.

Acknowledgements

First and foremost, I would like to thank my supervisors, Margaret Frame and Valerie Brunton for their continuous help and support during my PhD and without whom this thesis would not have been completed. Also, I would like to thank the Frame and Brunton laboratory members past and present, again without which my project would have been that little bit more difficult. In addition, thank you to Central Services for ensuring the continual smooth running of the laboratory throughout.

A big thank you to my fiancé, best friend and soulmate, Steve, whose love kept me going and to whom I can now finally marry. Thank you to my parents, Robbie and Carol Murray and brother, Ross, who have always supported me and are always there when I need them. Further, thank you to all my close friends who stood by me during the stressful times as well as the good ones.

Finally, I also wish to thank the Beatson Institute for Cancer Research, Edinburgh Cancer Research Centre and Cancer Research U.K. for funding this thesis.

Table of Contents

Abstract	i
Acknowledgements	ii
Table of Contents	iii
List of Figures	vi
Abbreviations	ix
Declaration	xiii
1. Introduction	1
1.1. Colorectal Cancer Incidence.....	1
1.2. Treatment of Colorectal Cancer	2
1.2.1. <i>Mechanism of Action of 5-FU</i>	4
1.3. Resistance in the Clinic	10
1.3.1. <i>Inherent Resistance</i>	10
1.3.2. <i>Acquired Resistance</i>	12
1.4. Resistance in the Laboratory	14
1.5. Protein Tyrosine Kinases (PTKs).....	14
1.6. Src Family Kinases (SFKs)	15
1.6.1. <i>Structure of SFKs</i>	17
1.6.2. <i>Control of SFKs Activation</i>	20
1.6.3. <i>SFKs in Cancer</i>	21
1.6.4. <i>Roles of SFKs</i>	23
1.6.4.1. <i>SFKs at Focal Adhesions</i>	23
1.6.4.2. <i>SFKs at Adherens (Cell-Cell) Junctions</i>	26
1.6.4.3. <i>Differing Roles of Src and Yes</i>	27
1.7. Cadherin Family Proteins	31
1.7.1. <i>Role of E-cadherin at Adherens Junctions</i>	32
1.7.2. <i>Regulation of Adherens Junctions: a Role for GTPases and p120-catenin</i> .33	
1.7.3. <i>Cross-Talk Between Adherens Junctions and Focal Adhesions</i>	34
1.7.4. <i>Signalling Downstream of Adherens Junctions</i>	35
1.8. Epithelial-to-Mesenchymal Transition (EMT).....	42
1.8.1. <i>Key Alterations and Factors That Govern EMT</i>	43
1.8.2. <i>EMT / MET and Drug Resistance</i>	49
1.9. Thesis Aims	51

2. Materials and Methods	52
2.1. Materials	52
2.1.1. <i>Cell Culture Reagents</i>	52
2.1.2. <i>Cell Culture Plasticware and Supplies</i>	53
2.1.3. <i>Cell Culture Drugs</i>	53
2.1.4. <i>Immunocytochemistry</i>	53
2.1.5. <i>Co-Immunoprecipitation</i>	54
2.1.6. <i>Immunoblot Analysis</i>	54
2.1.7. <i>SRB Cell Proliferation Assay</i>	57
2.1.8. <i>Reverse Transcription (RT)-PCR</i>	57
2.1.9. <i>Stock Solutions and Buffers</i>	57
2.2. Methods	62
2.2.1. <i>Routine Cell Culture</i>	62
2.2.2. <i>Generation of Cell Lines</i>	62
2.2.3. <i>Decma Treatment</i>	63
2.2.4. <i>Immunoblotting and Immunoprecipitation</i>	63
2.2.5. <i>Phase Contrast and EmGFP Images</i>	64
2.2.6. <i>Immunocytochemistry</i>	65
2.2.7. <i>Fluorescence Recovery After Photobleaching (FRAP)</i>	66
2.2.8. <i>SRB Cell Proliferation Assay</i>	66
2.2.9. <i>Aggregation Assay</i>	67
2.2.10. <i>Clonogenic Assay</i>	68
2.2.11. <i>3-Dimensional Analysis of HCT-116 and HCT-116-FR cells</i>	68
2.2.12. <i>Tunel Staining of HCT-116 and HCT-116-FR Cells</i>	69
2.2.13. <i>RT-PCR for Thymidylate Synthase</i>	69
3. Characterisation of Three Pairs of 5-FU Sensitive and Resistant Colon Cancer Cell Lines	72
3.1. Morphology	73
3.2. Gene Up-regulation and Resistance to 5-FU.....	77
3.3. Characterisation of Adhesion Protein Expression.....	82
3.4. Adhesion Protein Localisation.....	87
3.5. Monitoring E-cadherin Dynamics in HCT-116 and HCT-116-FR Cells	95
3.6. Assessment of Cell-Cell Junctions by Aggregation Assay	96
3.7. Summary.....	107
4. Assessing the Role of SFK Yes in Resistance to 5-FU	108
4.1. Co-localisation of Yes and E-cadherin.....	108
4.2. Vector Based RNAi System	109

4.3.	Morphology of Single Cell Clones	117
4.4.	Resistance to 5-FU.....	121
4.5.	Characterisation of Adhesion Protein Expression in RNAi Clones	123
4.6.	Adhesion Protein Localisation in RNAi Clones.....	125
4.7.	Assessment of Cell-Cell Junctions of RNAi Clones by Aggregation Assay	126
4.8.	Summary.....	133
5.	Modulation of Adherens Junctions and 5-FU Resistance	134
5.1.	Co-immunoprecipitation of E-cadherin and β -catenin	134
5.2.	Disruption of Adherens Junctions using <i>Decma</i>	136
5.3.	Adhesion Protein Localisation in <i>Decma</i> -treated Cells.....	141
5.4.	The Effect of <i>Decma</i> Treatment on Proliferation.....	145
5.5.	The Effect of <i>Decma</i> Washout on Adherens Junctions and Proliferation.....	145
5.6.	Cell Survival after <i>Decma</i> Treatment.....	150
5.7.	Signalling Effects of <i>Decma</i> Treatment	155
5.7.1.	<i>Signalling Effect via the PI3-kinase/Akt and MAP Kinase Pathways.....</i>	<i>159</i>
5.8.	Clonogenic Assays	165
5.9.	Use of siRNA as Another Approach	172
5.10.	Summary.....	180
6.	Discussion.....	182
6.1.	Models of 5-FU Resistance	182
6.2.	5-FU Resistance and E-cadherin	183
6.3.	Role of Yes in 5-FU Resistance	186
6.4.	Effects of Yes Knock-down on E-cadherin Junctions.....	187
6.5.	Modulation of E-cadherin and EMT as Strategies to Overcome Drug Resistance	188
6.6.	Signalling From Adherens Junctions.....	193
7.	Future Work.....	203
8.	References	205

List of Figures

Figure 1 – Thymidylate Production	6
Figure 2 – Structures of DNA Nucleotides and 5-Fluorouracil Metabolism	8
Figure 3 – Inhibition of Thymidylate Synthase (TS) by 5-Fluorouracil (5-FU).....	9
Figure 4 – The Structure and Conformation of Src Family Kinases.....	19
Figure 5 – SFKs at Focal Adhesions.....	29
Figure 6 – SFKs at Adherens (Cell-Cell) Junctions.....	30
Figure 7 – The PI3-Kinase Pathway	40
Figure 8 – The MAP Kinase Pathway.....	41
Figure 9 – Epithelial to Mesenchymal Transition.....	44
Figure 10 – Development of Cancer Metastasis	45
Figure 11 - Phase Contrast Images of H630 and H630-FR Cells	74
Figure 12 - Phase Contrast Images of HT29 and HT29-FR Cells	75
Figure 13 - Phase Contrast Images of HCT-116 and HCT-116-FR Cells	76
Figure 14 - Properties of H630 and H630-FR Cells	79
Figure 15 - Properties of HT29 and HT29-FR Cells	80
Figure 16 - Properties of HCT-116 and HCT-116-FR Cells	81
Figure 17 – Immunoblotting: Adhesion Proteins in H630 and H630-FR Cells.....	83
Figure 18 – Immunoblotting: Adhesion Proteins in HT29 and HT29-FR Cells.....	84
Figure 19 – Immunoblotting: Adhesion Proteins in HCT-116 and HCT-116-FR Cells.....	85
Figure 20 - Localisation of Src Family Kinase Proteins in H630 and H630-FR Cells.....	89
Figure 21 - Localisation of Src Family Kinase Proteins in HT29 and HT29-FR Cells.....	90
Figure 22 - Localisation of Src Family Kinase Proteins in HCT-116 and HCT-116-FR Cells.....	91
Figure 23 - Localisation of Adherens Junction Proteins in H630 and H630-FR Cells.....	92
Figure 24 – Localisation of Adherens Junction Proteins in HT29 and HT29-FR Cells	93
Figure 25 - Localisation of Adherens Junction Proteins in HCT-116 and HCT-116-FR Cells.....	94
Figure 26 - Fluorescence Recovery After Photobleaching (FRAP).....	98
Figure 27 - eGFP-E-cadherin in HCT-116 and HCT-116-FR Cells	99
Figure 28 - FRAP in HCT-116 and HCT-116-FR Cells	100
Figure 29 - Aggregation Assay with H630 and H630-FR Cells	101
Figure 30 – Aggregation Assay with HT29 and HT29-FR Cells	103
Figure 31 - Aggregation Assay with HCT-116 and HCT-116-FR Cells	105
Figure 32 - Localisation of Yes and E-cadherin in HCT-116 and HCT-116-FR Cells	111
Figure 33 - pcDNA™ 6.2-EmGFP-miR Vector used for Yes RNAi Expression.....	112

Figure 34 – Schematic Diagram Depicting the Strategy for Generation of Yes RNAi Expressing Cell Clones	113
Figure 35 - Mixed Population of Transfected Cells after Blasticidin Selection	114
Figure 36 - Immunoblot Analysis of RNAi Expressing Single Cell Clones.....	115
Figure 37 - Densitometry of Single Cell Clones Chosen for Further Characterisation	116
Figure 38 - Phase Contrast and EmGFP Images of HCT-116-FR Control (HFRC) RNAi Clones.....	118
Figure 39 - Phase Contrast and EmGFP Images of HCT-116-FR Yes 2 (HFRY2) RNAi Clones.....	119
Figure 40 - EmGFP Analysis of HFRC RNAi Clones and HFRY2 RNAi Clones	120
Figure 41 - Resistance to 5-FU in HFRC RNAi Clones and HFRY2 RNAi Clones.....	122
Figure 42 - Immunoblotting of HFRC RNAi Clones and HFRY2 RNAi Clones	124
Figure 43 - Localisation of Yes and Phospho-Src/Yes/Fyn in HFRC RNAi Clones	128
Figure 44 - Localisation of Yes and Phospho-Src/Yes/Fyn in HFRY2 RNAi Clones	129
Figure 45 - Localisation of Adherens Junction Proteins in HFRC RNAi Clones.....	130
Figure 46 - Localisation of Adherens Junction Proteins in HFRY2 RNAi Clones	131
Figure 47 - Average Area of Aggregates Formed.....	132
Figure 48 - Immunoprecipitation of E-cadherin and β -catenin in HCT-116-FR Cells.....	135
Figure 49 - <i>Decma</i> Antibody Treatment of HCT-116 and HCT-116-FR Cells.....	138
Figure 50 - Immunofluorescence of HCT-116 and HCT-116-FR Cells Treated with <i>Decma</i>	139
Figure 51 - Immunofluorescence of HCT-116 and HCT-116-FR Cells Treated With <i>Decma</i>	142
Figure 52 - Immunofluorescence of HCT-116 and HCT-116-FR Cells after <i>Decma</i> Treatment	143
Figure 53 - <i>Decma</i> Treatment in the Pairs of Sensitive and Resistant Cell lines.....	147
Figure 54 - Immunofluorescence of HCT-116 and HCT-116-FR Cells Treated with <i>Decma</i> before Removal for 7 days	148
Figure 55 - Proliferation in HCT-116 and HCT-116-FR Cells after Removal of <i>Decma</i> .	149
Figure 56 - Tunel Staining of HCT-116 Cells Treated with <i>Decma</i>	152
Figure 57 - Tunel Staining of HCT-116-FR Cells Treated with <i>Decma</i>	153
Figure 58 - p53 Localisation in HCT-116 and HCT-116-FR Cells	154
Figure 59 - Immunoblotting Signalling Effects in HCT-116 and HCT-116-FR Cells	158
Figure 60 - Proliferation of HCT-116 and HCT-116-FR Cells Treated with GDC-0941 .	161
Figure 61 - Signalling in HCT-116 and HCT-116-FR Cells Treated with GDC-0941	162
Figure 62 - Proliferation of HCT-116 and HCT-116-FR Cells Treated with U0126	163
Figure 63 - Signalling in HCT-116 and HCT-116-FR Cells Treated with U0126	164
Figure 64 - Clonogenic Assay of the HCT-116 and HCT-116-FR Cells.....	168
Figure 65 - Average Area of Colonies in HCT-116 and HCT-116-FR Cells	169

Figure 66 - Clonogenic Assays of HCT-116 and HCT-116-FR Cells.....	170
Figure 67 - 3-Dimensional (3-D) Analysis of HCT-116 and HCT-116-FR Cell Colonies	171
Figure 68 - Immunofluorescence of HCT-116 and HCT-116-FR Cells after siRNA.....	175
Figure 69 - Immunofluorescence of HCT-116 and HCT-116-FR Cells after siRNA.....	176
Figure 70 - Effects of siRNA Treatment on Proliferation of HCT-116 and HCT-116-FR Cells.....	177
Figure 71 – Immunoblotting of siRNA Treated HCT-116 and HCT-116-FR Cells.....	178
Figure 72 – Immunoblotting of siRNA Treated HCT-116 and HCT-116-FR Cells.....	179
Figure 73 – Theory Regarding Cell Death in HCT-116-FR Cells upon Junction Loss.....	199

Abbreviations

%	Percent
5-FU	5-fluorouracil
21G	21 gauge
-/-	Null
α	Alpha
Ab	Polyclonal antibody Keratinocyte basal medium
AJs	Adherins junctions
APC	Adenomatous Polyposis Coli
APS	Ammonium persulphate
ARP	Actin related protein
ATCC	American Type Culture Collection
β	Beta
BCA	Bicinchoninic acid assay
bp	Base pair
BSA	Bovine serum albumin
CDB	Cell dissociation buffer
CH ₂ H ₄ folate or CH ₂ THF	N ₅ -N ₁₀ -methylene tetrahydrofolate
CHK	CSK-homologous kinase
CSK	c-terminal Src kinase
DHF (or H ₂ folate)	Dihydrofolate
DMEM	Dulbecco's modified eagle's medium
DMSO	Dimethyl sulfoxide
DNA	Deoxyribonucleic acid
dTMP	Thymidine monophosphate or thymidylate thymidine triphosphate
dTTP	Thymidine triphosphate
DTT	Dithiothreitol
dUMP	Deoxyuridine monophosphate
E-cadherin	Epithelial-cadherin
ECL	Enhanced chemiluminescence
ECM	Extracellular matrix
EDTA	Ethylene diamine tetra-acetic acid
EGFR	Epidermal growth factor receptor

eGFP	Enhanced green fluorescent protein
EGTA	Ethylene glycol tetra-acetic acid
EmGFP	Emerald green fluorescent protein
EMT	Epithelial-to-Mesenchymal Transition
ERK	Extracellular regulated kinase
FA	Focal Adhesion
FACS	Fluorescence-activated cell sorting
FAK	Focal adhesion kinase
FBS	Foetal bovine serum 5-fluorodeoxyuridine monophosphate
FdUMP	5-fluorodeoxyuridine monophosphate
FdUTP	5-fluorodeoxyuridine triphosphate
FGFR	Fibroblast growth factor receptor
FITC	Fluorescein isothiocyanate
FRAP	Fluorescence recovery after photo bleaching
FUTP	5-fluorouridine triphosphate
H ₂ O	Water (Dihydrogen monoxide)
HCl	Hydrogen chloride
HER2	Human Epidermal growth factor Receptor 2
HGF	Hepatocyte growth factor human epidermal growth factor receptor 2
HIF	Hypoxia-Inducible Factor
HSP	Heat Shock Protein
IgG	Immunoglobulin G
KBM	Keratinocyte basal medium
LEF-1	Lymphoid Enhancer Factor-1
mAb	Monoclonal antibody
MAPK	Mitogen-activated protein kinase
MET	Mesenchymal-to-Epithelial Transition
MgCl ₂	Magnesium chloride
ml	Millilitres
mm	Millimetre
mTOR	Mammalian Target Of Rapamycin
Na ₃ VO ₄	Sodium orthovanadate
Na ₄ P ₂ O ₇	Sodium pyrophosphate
NaCl	Sodium chloride CH ₂ H ₄ folate or CH ₂ THF
NaOH	Sodium hydroxide
NCAM	Neuronal Cell Adhesion Molecule

N-cadherin	Neural-cadherin
NF	Sodium fluoride
NRTK	Non-receptor tyrosine kinase
OPRT	Orotate phosphoribosyltransferase
PBS	Phosphate buffered saline
P-cadherin	Placental-cadherin
PDGFR	Platelet-Derived Growth Factor Receptor
PH	Pleckstrin homology
pH	The Potential of Hydrogen
PI3-kinase	Phosphatidylinositol-3-kinase
PMSF	Phenylmethylsulphonyl fluoride
PRK-2	Protein kinase C-related kinase-2
PRPP	Phosphoribosyl pyrophosphate protein kinase C-related kinase-2
PtdIns	Phosphatidylinositol
PTEN	Phosphatase and Tensin homologue
PTK	Protein tyrosine kinase
PTP	Protein tyrosine phosphatase
Raptor	Regulatory Associated Protein of TOR
RNAi	RNA interference Regulatory Associated Protein of TOR
RPMI	Roswell Park Memorial Institute
RSV	Rous sarcoma virus
RT	Reverse transcription
RT-PCR	Reverse transcription polymerase chain reaction
S	Serine
SCC	Squamous cell carcinoma
SDS	Sodium dodecyl sulphate
SDS-PAGE	Sodium dodecyl sulphate-polyacrylamide gel electrophoresis
SFK	Src family kinase
SH	Src Homology
SRB	Sulforhodamine B
T	Thymidine
T	Tyrosine
TCA	Trichloroacetic acid
TEMED	Tetramethylethylenediamine
TGF- β	Transforming growth factor- β thymidine monophosphate kinase
TMPK	Thymidine monophosphate kinase

TP	Thymidine phosphorylase
TRITC	Tetramethyl rhodamine isocyanate
TS	Thymidylate synthase
Tunel	Terminal deoxynucleotidyl transferase mediated dUTP nick end labelling
U0126	U0126 monoethanolate uridine kinase
U.K.	United Kingdom
UK	Uridine kinase
wt	wild type
Y	Tyrosine
ZO	Zona occludens

Declaration

I declare that all the work in this thesis was performed personally unless stated otherwise.

No part of this work has been submitted for consideration as part of any other degree or award.

1. Introduction

1.1. Colorectal Cancer Incidence

In the United Kingdom, colorectal cancer accounts for 13% of all diagnosed cancers per year (37,514 people diagnosed/year (2006)). It is the second most common cancer affecting women (after breast cancer) and the third most common cancer found in men (after prostate and lung cancer). In 2007, colorectal cancer claimed the lives of 16,007 people (CRUK, 2009; Office-for-National-Statistics, 2008). This incidence is strongly related to age, with nearly 85% of all cases arising in people aged 60 years or over. Colorectal cancer can be classified by a system called Dukes' staging ranging from stage A to stage D. The Dukes' stage describes the extent of invasion or spread of a tumour and correlates with overall survival, i.e. patients have an 83% survival chance with a Dukes' stage A tumour versus 3% chance of survival if diagnosed with Dukes' stage D, both over five years (Campbell et al., 2001; CRUK, 2009). However, response rates to 5-FU have been shown to be greater in later stages of carcinoma when compared to cancers displaying an earlier staging (Adlard et al., 2002).

There are a number of genetic abnormalities that result in colorectal cancer formation. In approximately 90% of all colorectal cancers, there are mutations in proteins involved in the Wnt signalling pathway (Walther et al., 2009). A key regulator of the Wnt pathway is a tumour-suppressor protein called Adenomatous Polyposis Coli (APC) which is known to be mutated in over half of colorectal cancers (Thorstensen et al., 2005; Waldner and Neurath, 2010). APC is responsible for the degradation and nuclear export of β -catenin which, upon activation of the Wnt pathway, regulates genes involved in control of the cell cycle. Mutations in the tumour-suppressor, Phosphatase and Tensin homologue (PTEN), also contribute to colon carcinogenesis. PTEN not only negatively regulates the pro-survival Phosphatidylinositol-3-kinase (PI3-kinase) pathway, but it also plays an additional

role in the degradation of β -catenin, thus inhibiting the Wnt signalling pathway (Hill and Wu, 2009; Thorstensen et al., 2005). Accumulation of β -catenin in the cytoplasm results in stabilisation of the p53 tumour-suppressor protein (Thorstensen et al., 2005).

In normal cells, p53 acts as the 'guardian of the genome' by halting the cell cycle prior to DNA replication or division if any impairment is present, so allowing time for repair of any DNA damage that is detected before entry into the next stage of the cell cycle (Lane, 1992). To overcome the stalling of cell cycle progression imposed by p53, approximately 60% of colon cancer cells harbour mutant p53 rather than their normal 'wild type' (wt) form (Soussi, 2000). This enables cancer cells to continue to divide even in the presence of DNA abnormalities, for example, increases or decreases in gene expression which confer resistance.

Another early event found in approximately 30% of colorectal cancers are mutations resulting in constitutive activation of the Ras GTPase superfamily, which normally play a role in driving cell proliferation, apoptosis and differentiation by transducing signals from cellular receptors to signalling cascades within the cell (Waldner and Neurath, 2010).

Thus, there are a great number of cellular events that contribute to the development of colorectal cancer, some of which are mentioned above. Next I will describe the current chemotherapy that is the predominant method of treatment in the clinic.

1.2. Treatment of Colorectal Cancer

First line treatment for colorectal cancer is surgery followed by chemotherapy to try to kill any residual disease (Rosen et al., 2000). Surgery is curative in 60% of patients, but many patients present with metastatic lesions, and the spread to distant sites means that further chemotherapy is required. Traditionally, the most common chemotherapeutic treatment for advanced colorectal cancer has been 5-fluorouracil (5-FU) since its development in 1957

by Heidelberger (Curreri et al., 1958). 5-FU is a molecule that is converted to an active metabolite and inhibits DNA synthesis and repair by forming a stable ternary complex with thymidylate synthase (TS) (de Gramont et al., 1997). However, response rates after 5-FU treatment are disappointing, only 12% (Peters and van Groeningen, 1991). More recently, combination regimes have been used with some greater success, but generally these all are still based on 5-FU as the core drug (Goldberg and Gill, 2004).

An orally active fluoropyrimidine pro-drug, namely capecitabine, has changed the way 5-FU is administered. Capecitabine is converted to 5-FU by two enzymes, namely thymidine phosphorylase (TP) and/or uridine phosphorylase (UP) which are thought to be more active in tumour cells (Longley et al., 2003), hence potentially increasing the therapeutic window. 5-FU (or capecitabine) is most commonly used in combination with leucovorin (folinic acid), which can often be combined with irinotecan (also known as CPT-11, a topoisomerase I inhibitor) often termed FOLFIRI [FOL from folinic acid, F from 5-FU and IRI from irinotecan] or combined with oxaliplatin (a platinum-based compound that forms DNA adducts) often termed FOLFOX [OX from oxaliplatin] when used in combination (Goldberg and Gill, 2004).

Toxicity to FOLFIRI and FOLFOX combinations are manageable, but both treatments can result in toxicities including diarrhoea, nausea and neurotoxicity (Falcone et al., 2007; Ramanathan et al., 2003). In addition, some patients can experience pulmonary toxicity culminating in FOLFOX-induced interstitial pneumonia from the combination of oxaliplatin with 5-FU / leucovorin. This can be reversed by removing the oxaliplatin from the combination, and treating with only 5-FU and leucovorin (Muneoka et al., 2009). By treating patients with a FOLFOXIRI combination, improved response rates have been achieved although this is at the expense of increased, but generally manageable, toxicities when compared to FOLFIRI treatment (Falcone et al., 2007; Montagnani et al., 2010).

Side effects frequently limit patient treatment and there are a number of new drugs that aim to improve efficacy of treatment while reducing side effects, or to supplement a regime in an attempt to improve survival. Some examples are S-1, bevacizumab (Avastin), cetuximab (Erbix), panitumumab, adriamycin (doxorubicin hydrochloride), mitomycin, 5'-deoxy-5-fluorouridine (5'-DFUR) and uracil-tegafur (UFT).

Although initial response rates are now higher due to combination therapy, subsequent re-treatment is usually unsuccessful due to the development of resistance (Peters and van Groeningen, 1991). Indeed, resistance to chemotherapeutic agents remains one of the major reasons for death of colon cancer patients after surgery. Thus, new strategies for the effective treatment of colon cancer are urgently required, and this would include re-sensitisation of tumours to 5-FU-based therapies. The latter requires that we better understand the determinants of 5-FU resistance in colon cancer cells.

1.2.1. Mechanism of Action of 5-FU

I am going to describe what is currently known about the mechanism of action of 5-FU. I will first describe how the highly conserved enzyme thymidylate synthase (TS) operates. This will also be relevant later when considering changes in colon cancer cells that have acquired resistance to 5-FU.

DNA replication and repair requires the production of the deoxyribonucleic acid (DNA) pyrimidine base, thymine (T). This is catalysed by TS (composed of two identical dimers of 30-35kDa each), which serves to create the only *de novo* source of thymidine monophosphate (dTMP) and dihydrofolate (H₂folate or DHF) in cells. TS is able to generate these products from the reduction of deoxyuridine monophosphate (dUMP) by the co-factor N₅-N₁₀-methylene tetrahydrofolate (CH₂H₄folate or CH₂THF) (**Figure 1a**) (Carreras and Santi, 1995; Longley et al., 2003; Takeishi et al., 1985). A ternary complex is formed between two molecules of dUMP and two molecules of CH₂THF, one molecule

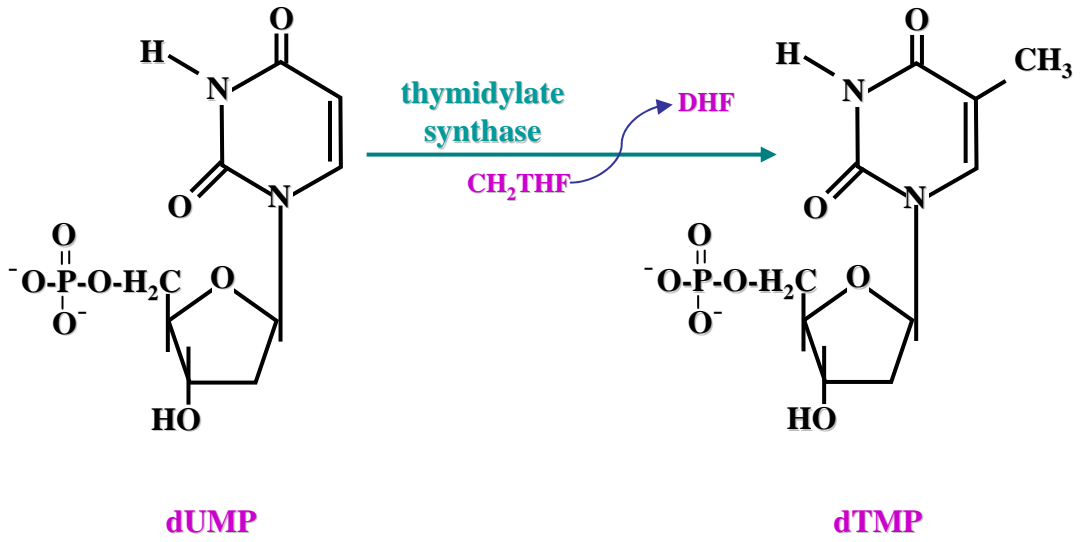
per TS dimer. The CH₂THF donates its methyl group, as well as two hydrogen atoms, in order to create the nucleotide dTMP and the bi-product is DHF (**Figure 1b**) (Kanaan et al., 2007). The nucleotide dTMP, also known as thymidylate, undergoes the addition of two further phosphate groups, and this is catalysed by the enzyme thymidine monophosphate kinase (TMPK) to create dTTP (thymidine triphosphate) (Carnrot et al., 2008). The dTTP nucleotide is composed of a thymine base, attached to a pentose sugar (deoxyribose) and three phosphate groups, which can react with the hydroxyl group of the neighbouring nucleotide, ultimately producing new DNA strands or to aid in the repair of damaged or mis-matched DNA (Smellie, 1965).

Figure 1 – Thymidylate Production

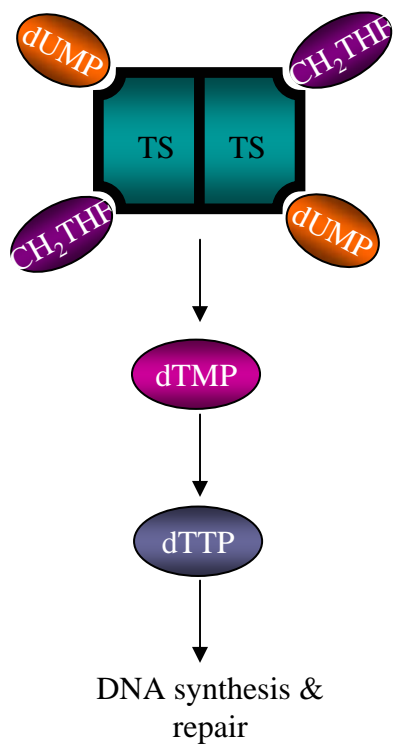
a) Production of thymidine monophosphate (dTMP) from deoxyuridine monophosphate (dUMP) is performed by thymidylate synthase (TS) using the co-factor CH_2THF . dihydrofolate (DHF) is released. **b)** dTMP is produced from the ternary complex of TS with dUMP and CH_2THF . The addition of two phosphate moieties to dTMP creates thymidine triphosphate (dTTP) which is used in the process of DNA synthesis and repair.

Figure 1

a



b



The pyrimidine, uracil, is an un-methylated form of the pyrimidine, thymine and it was noticed in the 1950s that cancers could use uracil in the DNA nucleotide, dTTP, rather than the normal thymine. This resulted in the creation of a fluorinated form of uracil which was used to exploit this occurrence, called 5-FU (**Figure 2a**) (Liu, 2009).

5-FU enters cells in the same manner as uracil by either non-facilitated diffusion or via the adenine-nucleotide carrier (Domin et al., 1993). It is metabolised by multiple mechanisms to form three active metabolites, namely, an analog of dUMP called 5-fluorodeoxyuridine monophosphate (FdUMP), 5-fluorodeoxyuridine triphosphate (FdUTP) and 5-fluorouridine triphosphate (FUTP) (**Figure 2b**). The primary 5-FU activation route is by orotate phosphoribosyltransferase (OPRT) which converts 5-FU to FUTP using the co-factor phosphoribosyl pyrophosphate (PRPP). Indirectly, FUTP can be made by conversion to fluorouridine (FUR) by UP and uridine kinase (UK) sequentially, leading into the FUTP pathway.

5-FU metabolism occurs in two stages. Firstly, 5-FU can be metabolised by TP to generate fluorodeoxyuridine (FdUDR) in a reversible reaction, and then it is converted to FdUMP by thymidine kinase (TK). There is an indirect mechanism of FdUMP production from the FUTP pathway, where fluorouridine biphosphate (FUDP) is converted to 5-fluorodeoxyuridine monophosphate (FdUMP) through de-phosphorylation of FdUDP by ribonucleotide reductase (RNR) (Longley et al., 2003). Phosphorylation of FdUDP produces FdUTP, and both this and FUTP can become incorporated into DNA and RNA respectively, resulting in lesions in DNA (for example, breaks in the DNA) that can trigger cell death via a p53 dependant mechanism (Li et al., 2009), as well as aberrant expression, processing and function of RNA (**Figure 2b**) (Longley et al., 2003).

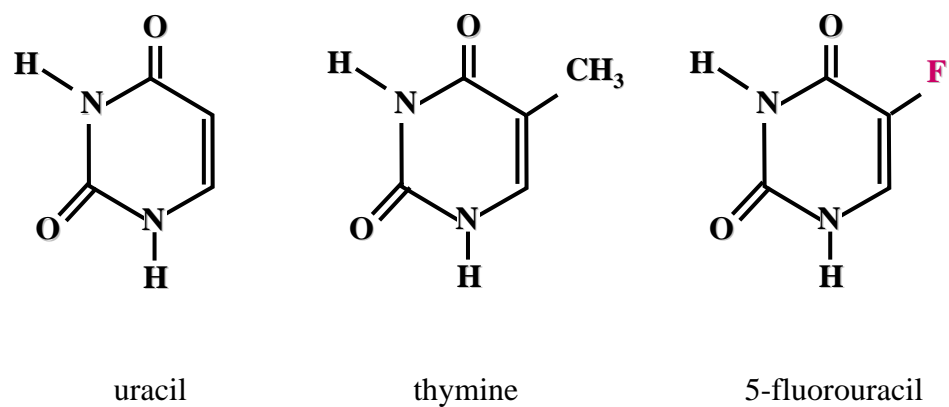
The other metabolite of 5-FU, FdUMP, competitively binds covalently to the active site of TS resulting in the formation of a catalytically inactive ternary complex (**Figure 3**).

Figure 2 – Structures of DNA Nucleotides and 5-Fluorouracil Metabolism

a) Uracil is an un-methylated form of the pyrimidine, thymine. 5-FU has been modelled on uracil and thymine by replacing the hydrogen/methyl group with a fluorine atom at position 5. **b)** 5-FU is catabolised by dihydropyrimidine dehydrogenase (DPD) in the liver or the cell to create 5-fluoro-5,6-dihydrouracil (5-FDHU). Metabolism of 5-FU by thymidine phosphorylase (TP) in a reversible reaction generates fluorodeoxyuridine (FUDR) which produces FdUMP after treatment with thymidine kinase (TK). FdUMP is able to directly inhibit thymidylate synthase (TS). FUMP is created by sequential action of uridine phosphorylase (UP) and uridine kinase (UK) with fluorouridine (FUR) as the intermediate or primarily by orotate phosphoribosyltransferase (OPRT) using phosphoribosyl pyrophosphate (PRPP) as a cofactor. FUMP conversion to FUTP can then be incorporated directly into RNA culminating in aberrant expression, processing and function of RNA. Fluorouridine biphosphate (FUDP) can be converted to 5-fluorodeoxyuridine diphosphate (FdUDP) by ribonucleotide reductase (RNR) which can also be created from FdUMP. FdUTP can be directly incorporated into DNA resulting in breaks occurring.

Figure 2

a



b

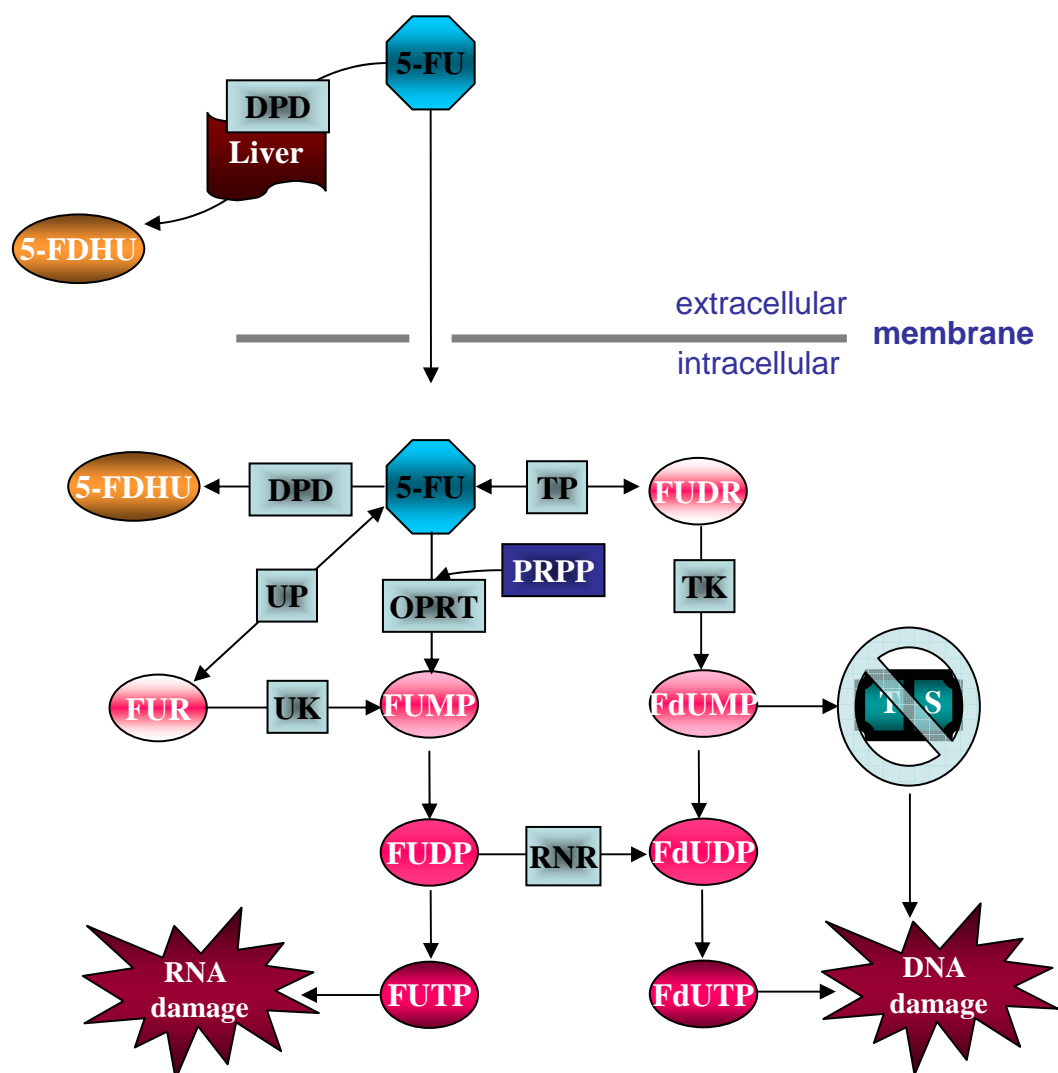
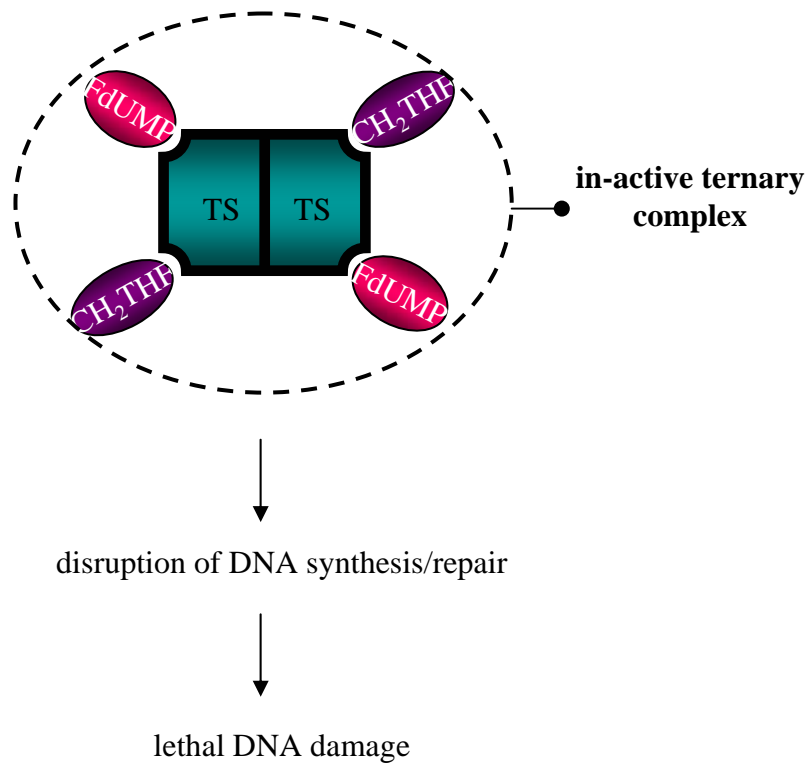


Figure 3**Inhibition of Thymidylate Synthase (TS) by 5-Fluorouracil (5-FU)**

The 5-FU metabolite, FdUMP competitively binds covalently to TS resulting in the formation of a catalytically inactive ternary complex with the co-factor CH₂THF. This leads to disruption of DNA synthesis and repair leading to lethal DNA damage.

The competitive, covalent, binding of FdUMP to TS results in the reduction of catalytically active ternary complexes between dUMP, CH₂THF and TS. As a consequence, the amount of thymidylate being produced is reduced, culminating in increased DNA damage from inhibited DNA repair (Hughey et al., 1993).

As mentioned previously, the mechanisms of action of 5-FU, and hence drug efficacy, are often poorly effective, as a result of drug resistance. The net effect is to allow cancer cells to overcome the damaging effects of 5-FU, so enabling them to evade cell death.

1.3. Resistance in the Clinic

Treatment with chemotherapy is sometimes unsuccessful with poor response rates in the clinic as a result of acquisition of chemo-resistance. Resistance is believed to be the main cause of failed treatment in around 90% of patients with metastatic disease (Longley and Johnston, 2005). This can be attributed to two different types of resistance that can arise; inherent (*de novo*) or acquired resistance. Even in targeted therapies, for example the monoclonal antibody treatment erlotinib, which is used in the treatment of breast cancer, resistance occurs as a result of both intrinsic and acquired forms (Kruser and Wheeler, 2010). In regard to colorectal cancer, the two types of resistance are described below.

1.3.1. Inherent Resistance

Inherent resistance, also known as *de novo* or intrinsic resistance occurs in cancer cells that have a particular characteristic(s) that render them resistant to certain chemotherapeutics prior to exposure. There are a number of inherent resistant mechanisms that cells utilise to reduce the effectiveness of drugs like 5-FU.

Generic mechanisms involved in resistance include the employment of multi-drug resistance (MDR) transporters which can be present on the cell membrane and enable the cell to excrete a variety of different drugs from their cytoplasm. This results in reduced

drug concentration inside the cell (Hooijberg et al., 2006). Some cancers have an innate resistance due to the presence of one or more of such transporters on their surface conferring the ability of cells to pump out agents like 5-FU (Liu, 2009).

Specifically concerning 5-FU, the main mode of *de novo* resistance is due to inherently high levels of TS expressed in cancer cells that have had no previous exposure to 5-FU (Ooyama et al., 2007). The higher number of TS molecules *per se*, or alternatively cells possessing a high proportion of the normal TS substrate dUMP, can have a degree of resistance because of increased competition with the active metabolite, FdUMP, for TS (Spears et al., 1988). Inherent resistance also arises because of the low rate of conversion of the inactive 5-FU to the active metabolite FdUMP. Inherent resistance mechanisms involving 5-FU metabolism pathways occur where cells express low levels of RNR (resulting in reduced FdUMP production) or low levels of TP (resulting in reduced conversion of 5-FU to FUDP) (Metzger et al., 1998; Ooyama et al., 2007).

Low treatment success rates have been linked to the rapid turnover of 5-FU in colorectal tumours with an 'intrinsic' high level of dihydropyrimidine dehydrogenase (DPD). This is the enzyme responsible for the catabolism of 5-FU in the liver and is associated with chemo-resistance. This enzyme converts 80% of administered 5-FU to its first inactive catabolite, 5-fluoro-5,6-dihydrouracil (5-FDHU) (Di Paolo et al., 2002). Patients with low levels of TS, TP, and DPD (prior to any 5-FU treatment) show a greater survival response than patients with higher expression of one or more of these proteins (Johnston et al., 1994; Johnston et al., 1995; Leichman et al., 1997; Salonga et al., 2000). However, there are also reports of the opposite, where patients presenting with cancers displaying high TS levels apparently respond better than those with low expression (Edler et al., 2002; Kornmann et al., 2003). These patients also displayed low DPD, the enzyme that catabolises 5-FU, which has been shown previously to be linked with higher response rates. However, levels of other proteins known to be involved in resistance to 5-FU were not assessed in this

study, suggesting that high TS and low DPD may not be the only factors that determine drug response, and hence survival (Kornmann et al., 2003). These apparently contradictory reports on survival responses emphasise the potential importance of determining levels of key proteins involved with resistance to 5-FU at disease diagnosis, and evaluating properly a signature for 'likelihood of response'. This may allow the identification of patients who will respond to 5-FU-based therapies or drug combinations, such that patients who are likely to benefit can be treated with 5-FU, while those that are not can be spared this form of unnecessary chemotherapy and avoid the unpleasant side effects linked with the treatment (Ooyama et al., 2007; Shimizu et al., 2005).

1.3.2. Acquired Resistance

Acquired resistance occurs subsequent to treatment with a chemotherapeutic agent and may arise as a result of multiple mechanisms. Such mechanisms can either be specific to the drug itself, or be more generic and utilised by many cancers and different drugs.

As mentioned above, one generic mode of acquired resistance has already been described in the context of inherent resistance, namely via the activity of the MDR transporters on the cell surface which promote drug efflux. Although MDR transporters on a cancer cell prior to treatment can confer innate resistance, this can also be acquired by up-regulation of the MDR channels after treatment with chemotherapeutic agents (Calcagno and Ambudkar, 2010). In colon cancer, increased expression of MDR channels has been shown to cause reduced 5-FU accumulation in cancer cells, hence lowering response to the drug (Hooijberg et al., 2006).

The innate resistance mechanisms can also be exploited by cancer cells to acquire resistance following 5-FU treatment. For example, low formation of FdUDP which occurs as a consequence of 5-FU treatment, results in decreased RNR enzyme levels (Fukushima et al., 2001). Treatment with 5-FU can also induce expression of DPD in patients who

initially responded, but who experienced toxic side effects from having low levels of DPD. Catabolism of 5-FU by DPD is not the only rate limiting step however. When there is a reduction in the available uninhibited TS as a consequence of treatment with 5-FU, cells are potentially able to overcome the lack of newly produced thymidylate by exploiting the thymidine salvage pathway (Grem and Fischer, 1989). This pathway allows thymidylate to be salvaged from the degradation of DNA (Kinsella et al., 1997). However, although this method may be used by cells to overcome the molecular consequences of 5-FU treatment, inhibition of this pathway does not reverse resistance to 5-FU in terms of rescuing biological response. This implies that it is unlikely to be one of the major contributory mechanisms underlying acquired resistance (Pickard and Kinsella, 1996).

The likely, most important gene and protein up-regulation associated with 5-FU resistance is the increase in the TS gene (Copur et al., 1995). The main target of 5-FU, TS, binds to dUMP and CH_2TF to form an active complex, leading to the subsequent formation of dTMP. Cancer cells compensate for the inhibition of TS by 5-FU with enhanced expression of the TS gene after 5-FU treatment (Johnston et al., 1995). This increased expression is often associated with TS gene amplification, enabling cancer cells to counteract the amount of inactive ternary complexes formed between the active metabolite of 5-FU, FdUMP, the cofactor CH_2TF , and TS (**Figure 3**) (Copur et al., 1995; Kanaan et al., 2007).

1.4. Resistance in the Laboratory

In the laboratory, the development of colon cancer cell lines resistant to 5-FU allow the study of modes and molecular determinants of chemotherapeutic resistance, and enable attempts to be made to define appropriate intervention strategies that will re-induce drug sensitivity.

In this thesis, I investigated three pairs of 5-FU sensitive and resistant colorectal cancer cell lines, which will be described later. The increase in TS protein which occurs with acquired resistance to 5-FU is examined in these cell lines, and linked to other changes I observed, specifically those involving cell morphology and adhesion proteins. In this regard, it is noteworthy that the TS gene is located on chromosome 18, specifically mapping to position 18p11.32 (Hori et al., 1990). Interestingly, the gene encoding the Src family kinase (SFK) member, c-Yes (Yes), is located on the same amplicon, less than 50kb away from the gene encoding TS. As a direct consequence of the close proximity of these two genes in the amplicon, the up-regulation of Yes protein is coincident with TS over-expression in 5-FU resistant cells (Silverman et al., 1993), raising the possibility that Yes may play a role in colorectal cancer cells that have acquired resistance to 5-FU.

1.5. Protein Tyrosine Kinases (PTKs)

There are two different classes of Protein Tyrosine Kinases (PTK). There are membrane spanning Receptor Tyrosine Kinases (RTKs) and Non-Receptor Tyrosine Kinases (NRTKs), which are usually cytoplasmic and often attached to cellular membranes. RTKs can dimerise and autophosphorylate upon activation as a result of binding extracellular ligands, such as growth factors. This typically promotes downstream activation of intracellular signalling pathways in the cell, by triggering specific tyrosine phosphorylation and recruitment events. RTKs are essential for normal cellular functions, but they have

also been implicated in the development and progression of human cancers. For example, the Epidermal Growth Factor Receptor (EGFR), which is a member of the Human Epidermal Growth Factor Receptor (HER) family of RTKs, is responsible for aberrant signalling in a number of epithelial cancers including breast, colorectal, and lung (Wheeler et al., 2008; Zwick et al., 2001). SFKs are members of the NRTKs which associate with, but do not cross the cell membrane and these can activate target proteins by tyrosine phosphorylation. NRTKs are themselves activated by tyrosine phosphorylation, often autophosphorylation, after activation of RTKs and other cell surface receptors, such as G protein-coupled receptors. SFKs play an essential role in many signal transduction pathways and regulate many biological processes during development and cancer (Frame, 2004). Many NRTKs are implicated in various aspects of cancer and have been shown to be encoded by proto-oncogenes, and oncogenes in the case of their viral counterparts (Hubbard and Till, 2000). One such oncoprotein which, as previously mentioned, is co-elevated with TS in resistance to 5-FU is Yes. Hence, I will discuss Yes, along with the prototypic member of the SFKs (Src), in the next section.

1.6. Src Family Kinases (SFKs)

When I started my PhD, the Frame and Brunton group was focused on Src and its role in adhesion regulation and cancer. They had generated a 5-FU resistant colon cancer cell line and this led me to consider differences between 5-FU-sensitive and -resistant cells with respect to morphology, cellular adhesions and SFKs. Amongst early observations, which will be discussed later in the Results section, was the predicted co-increase in Yes expression in 5-FU resistant cells, concomitant with up-regulation of TS. I discuss below the origin and functions of SFKs, in particular, Yes and Src.

Yes is one of nine SFKs that include c-Src (Src; the prototypical family member) and Fyn, which along with Yes, are ubiquitously expressed in most tissues. Others like Blk, Yrk, c-

Fgr, Hck, Lck and Lyn have a more limited tissue distribution (Frame, 2002), and are not generally present in colon cancer cells.

The gene encoding Src was the first proto-oncogene to be discovered, stemming from studies made decades earlier of a viral homologue, v-Src, which caused malignant sarcomas in chickens. This was first investigated in 1909 by Peyton Rous when he hypothesised, with great scepticism from his peers, that an infectious agent, now known as Rous sarcoma virus (RSV), was causing the formation of tumours in donor chickens upon injection of cell-free filtrate from affected chickens (Rous, 1983). It was later discovered that a single gene, identified as the first oncogene, v-Src, was responsible for tumour induction (Martin, 2004; Wang et al., 1976). The discovery of the first oncogene elucidated further investigations into other viruses that caused cancer. Two viruses called Yamaguchi 73 and Esh sarcoma viruses were discovered and these attracted a lot of interest because they encoded a protein that had strong homology (82%) to v-Src, and was called v-Yes (Ghysdael et al., 1981; Sukegawa et al., 1987; Summy et al., 2003b). It took many years before the complete identification of the cellular counterparts of these viral genes, known as cellular-Src (c-Src; Src) and cellular-Yes (c-Yes; Yes), both of which are implicated in the development of a number of human malignancies (Frame, 2002; Martin, 2003). To summarise what we now know, Src and Yes are NRTKs involved in complex cell signalling networks, regulating a number of cellular processes such as adhesion, cell migration, survival and promotion through the cell cycle. Importantly, during cellular transformation active Src, or Yes, can directly influence tumour cell behaviour (Frame, 2002; Summy et al., 2003a).

1.6.1. *Structure of SFKs*

SFKs are composed of four highly conserved Src homology (SH) domains, a carboxy-terminal tail and an amino-terminus with amino acid sequences that are distinct between family members (**Figure 4a**). Membrane attachment of SFKs is mediated by amino-terminal acylation moieties, which target SFKs to the plasma membrane where they function to trigger downstream signalling (Kaplan et al., 1990).

The SH domains have differing functions. Initially NRTKs were believed to only possess the ability to phosphorylate target proteins via their kinase (SH1) domain. However, as the modular domains of proteins and the appreciation of protein-protein interaction domains became evident, it was clear that the SH2 and SH3 domains acted as scaffolding domains by binding partner proteins (Martin, 2001). Both SH2 and SH3 domains have now been identified in a large number of proteins involved in signalling pathways, including those that control transcription, ubiquitination and cytoskeleton rearrangement (Pawson and Gish, 1992; Pawson et al., 2001). Typically, the SH2 domain interacts in a sequence specific manner with phospho-tyrosine-containing sequences in other proteins, while the SH3 domain interacts with proline-rich regions in target proteins (Li, 2005; Pawson et al., 2001).

In the inactive state SFKs adopt a 'closed' conformation and this is 'opened' upon auto-phosphorylation at tyrosine residue 419 (Y419 in humans, or Y416 in chickens) and the de-phosphorylation of the regulatory inhibitory tyrosine residue at position 530 (Y530 in humans, Y527 in chickens). This results in the loss of binding of the SH2 domain with the carboxy-terminal tail, culminating in an 'open' conformation (as depicted in **Figure 4b**). Alternatively, it is believed that stronger binding of SH2 and/or SH3 domain partners are able to displace the intermolecular interactions, and hence 'open' the catalytic site and enable substrate binding (Bjorge et al., 2000). As an example, the progesterone receptor

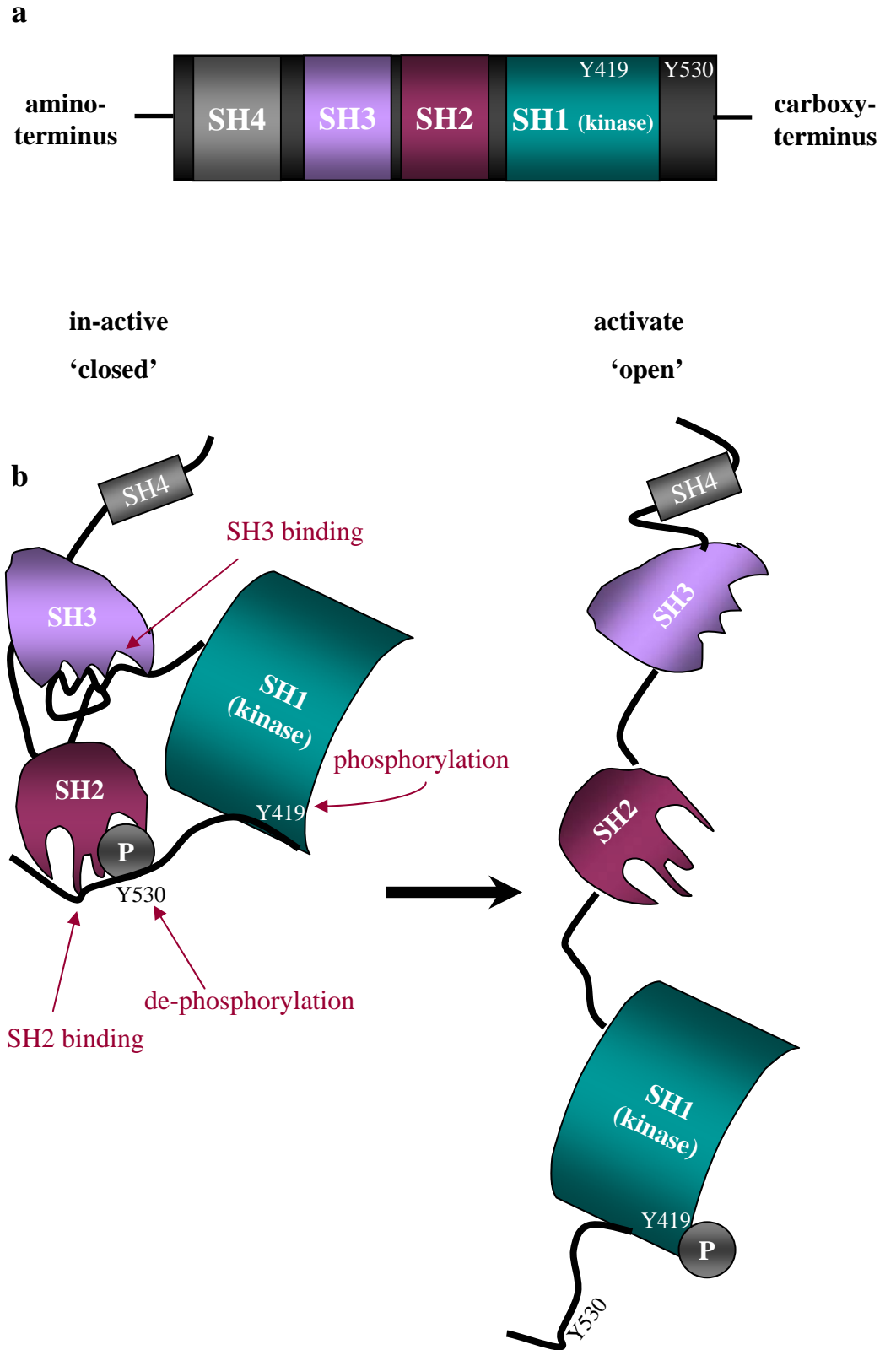
has been shown to have a high affinity for the SH3 domain of Src and can displace its auto-inhibitory intra-molecular binding, leading to catalytic activation (Boonyaratanakornkit et al., 2001). In my experimental work, I made use of an antibody to detect Src/Fyn/Yes auto-phosphorylation of Y419 that is commonly used as a surrogate readout for catalytic activation of these SFKs.

Protein interactions via the SH2 and SH3 domains ultimately result in the downstream activation of many signalling pathways as a result of tyrosine phosphorylation by the kinase (SH1) domain (Frame, 2002; Kaplan et al., 1994; Yeatman, 2004). Substrates may be recruited via the protein interaction SH domains. Binding of the substrate to the SH2 domain can also enable Src to hold target proteins at their required localisation in the cell (Pawson, 1995; Thomas and Brugge, 1997). Below I describe the ways in which SFKs can be activated.

Figure 4 – The Structure and Conformation of Src Family Kinases

a) Molecular structure of SFKs with Src Homology (SH) 1 (kinase) domain (which contains the auto-phosphorylation site Y419), SH2 and SH3 protein binding domains and SH4 unique domain. The carboxy-terminus contains the inhibitory Y530 and the amino-terminus mediates interaction with cell membranes. **b)** Inactive SFKs adopt a ‘closed’ conformation in which Y527 interacts with the SH2 domain, and the SH3 domain interacts with the linker between the catalytic domain and the SH2 domain. During activation Y527 is de-phosphorylated and the Y419 is auto-phosphorylated, relieving the intra-molecular constraints.

Figure 4



1.6.2. Control of SFKs Activation

The activation of SFKs is tightly controlled by the phosphorylation/de-phosphorylation status of Y530. This is in stark contrast to v-Src which lacks the negative auto-regulatory region at its carboxy-terminus and therefore adopts a constitutively active conformation, leading to unregulated and promiscuous phosphorylation of substrates and transformation (Martin, 2001).

The control of SFKs inactivation is attributed to the actions of carboxy-terminal Src kinase (CSK) (structurally related to Src but lacks the regulatory region (Ogawa et al., 2002)) and its homologue CSK-homologous kinase (CHK) (Bjorge et al., 2000). Once the adaptor protein CSK Binding Protein (CBP) is bound to the SFK, it recruits CSK or CHK, which in turn causes inactivation by phosphorylating Y530 (Avraham et al., 1995; Ingley et al., 2006; Nada et al., 1991).

Activation of SFKs occurs by phosphatase-mediated de-phosphorylation of Y530. Candidate phosphatases are protein tyrosine phosphatase- α (PTP- α), protein tyrosine phosphatase-1 (PTP1), SH2-containing phosphatase-1 (SHP-1) and SH2-containing phosphatase-2 (SHP-2) (Frame, 2002; Somani et al., 1997). These phosphatases may activate SFKs by de-phosphorylating the inhibitory tyrosine at Y530 after auto-phosphorylation of Y419 (Yeatman, 2004). However, PTP- α is also able to activate SFKs via a phospho-tyrosine displacement mechanism. This involves displacement of the negative regulatory inter-molecular binding interaction between the SH2 domain and the carboxy-terminal Y530 (Zheng et al., 2000). This mode of activation has been proposed for other SFKs, for example Hck, where displacement of the SH3 domain occurs upon binding of a stronger affinity ligand, namely the Nef protein from the human immunodeficiency virus (HIV-1) (Moarefi et al., 1997). As mentioned above, aberrant activation of SFKs has been linked to a variety of cancers.

1.6.3. SFKs in Cancer

Src is involved in many cell signalling networks and is known to regulate a number of cellular processes such as adhesion, invasion and motility which can directly influence tumour cell behaviour (Summy et al., 2003a). For this reason, much interest in Src as a target for drug therapy has emerged and a number of Src kinase inhibitors are currently in early or late Phase III trials in Europe and the USA for solid tumours (Brunton and Frame, 2008). Increased expression of the Src protein and its aberrant activation has been linked to colon, breast, pancreatic and brain tumours, but the methods by which irregular Src activation occurs are not completely understood (Frame, 2002). Elevated Src expression and activity may contribute to the ability of colon cancer cells to proliferate and/or progress to invasive and metastatic disease. Src levels correlate with malignant potential, as displayed in pre-malignant lesions and adenomas, with the highest levels of Src expression being observed in polyps with malignant potential (Cartwright et al., 1989; Cartwright et al., 1990). Further increases in Src protein are also seen in metastatic lesions, suggesting an additional role for Src in late stage progression of colon tumours (Aligayer et al., 2002). More recently, increased Src kinase activity in colon tumours was identified as an independent indicator of poor prognosis in all stages of human colon cancer (Aligayer et al., 2002).

Specifically in colon cancer, the increased activity of SFKs is not only due to increased protein expression (Bolen et al., 1987). A decrease in the expression level of the SFK negative regulator CHK has been linked with increased Src activation in colon cancer, in which levels of CSK remain unaltered (Zhu et al., 2008). A reduction of CSK expression in colon cancer cells has also been proposed to elevate Src activity and in studies using CSK over-expression, there was reduced metastasis *in vivo*. The tumourigenicity of cells was not altered in that study, thus suggesting that CSK is a metastasis suppressor (Nakagawa et al., 2000). Conversely, over-expression of PTP- α or SHP-1 *in vitro* induced

activation of Src by causing the de-phosphorylation of the inhibitory Y530, suggesting that these PTPs may cause increased Src activity (Khanna et al., 2007; Zheng et al., 1992).

Alteration of the ubiquitin ligase pathways can also contribute to increased steady state levels of Src in cancer cells. For example, a protein called Suppressor Of Cytokine Signalling 1 (SOCS1) actively promotes ubiquitination of Src in normal cells and this process is synergistic with the actions of c-Cbl (Kim et al., 2004; Yokouchi et al., 2001). c-Cbl acts as a Src scaffolding protein, but can also operate as a ubiquitin ligase to target SFKs for degradation (Kim et al., 2004; Yokouchi et al., 2001). The SH3 domain of Src binds the proline rich region of c-Cbl causing phosphorylation by active Src, resulting in increased degradation of c-Cbl, and the bound Src. In a number of malignancies where SFKs are up-regulated, increased phosphorylation of c-Cbl has been shown, suggesting that there is increased ubiquitination and degradation of c-Cbl in cancer cells which would permit maintenance of steady levels of Src (Kamei et al., 2000).

A number of mutations in Src sequence have been identified allowing its aberrant activation. In late stage colon cancer, mutations in the gene encoding Src were reported and proposed to lead to the production of a truncated, constitutively active Src protein (Irby et al., 1999); however, no further studies detected such mutations, and so it is unclear how generally important such reported gene mutations are (Daigo et al., 1999; Nilbert and Fernebro, 2000; Wang et al., 2000).

Although a lot of the emphasis has been on mis-regulation of Src in cancer, there have been suggestions that Yes protein levels and activity are elevated in colon carcinomas and in adenomas (particularly in benign tumours that maybe at risk of progressing to carcinomas) (Cartwright et al., 1994; Irby and Yeatman, 2000; Pena et al., 1995). In the colon carcinomas studied, the increase in Yes activity was paralleled by an increase in

protein level, and so, probably not a result of specific catalytic activation by altered phosphorylation of its inhibitory Y530 residue (Park et al., 1993).

RTKs are often over-expressed in many tumours that also display elevated Src expression, thus implying that RTKs and SFKs work together to promote tumourigenesis via cooperative or synergistic functional interactions that require the increased activities of Src or Yes and their downstream effectors (Zwick et al., 2001).

1.6.4. Roles of SFKs

SFKs are upstream of key signalling pathways that control cell proliferation and survival, amongst their biological functions (Frame, 2002; Summy et al., 2003a). Here, I examined Src and Yes in 5-FU-sensitive and -resistant colon cancer cell pairs, and considered whether Yes in particular, played a role in 5-FU resistance. The particular reason for focussing on Yes was its co-amplification with the gene encoding TS during acquisition of 5-FU resistance. SFKs operate predominantly at two distinct sites of cell adhesion, namely, integrin-linked focal adhesions and cadherin-mediated cell-cell junctions.

1.6.4.1. SFKs at Focal Adhesions

The attachment of cells to the extracellular matrix (ECM) is primarily mediated by integrin-dependent dynamic structures termed focal adhesions or focal contacts (depicted in **Figure 5**). These consist of complexes of proteins which serve to link integrins to the actin cytoskeleton, and are dynamically regulated sites of bi-directional signalling which control the actin cytoskeleton. Src and a key Src binding partner and substrate, Focal Adhesion Kinase (FAK), are key components of these complexes and govern processes including focal adhesion turnover, cell migration and survival (Fincham and Frame, 1998; Klinghoffer et al., 1999). Src may also affect invasion of cancer cells by activating FAK,

which controls up-regulated expression of matrix metalloproteinases (MMPs) that facilitate the degradation of the basement membrane (Mitra et al., 2005; Schlaepfer et al., 2004).

The ECM is composed of a number of different types of constituent proteins, for example fibronectin, laminins and collagens (Hynes, 2009). Binding to the ECM is mediated by trans-membrane integrin receptors which consist of alpha (α) and beta (β) subunits, each containing multiple different members. With 18 α subunits and 8 β subunits, there are 24 distinct integrin hetero-dimer combinations, giving rise to many possible $\alpha\beta$ integrin hetero-dimers that can bind to specific ECM ligands. For example, $\alpha_5\beta_1$ binds specifically to the ECM protein fibronectin by recognising a tripeptide sequence in the protein, namely RGD (Arginine – Glycine – Aspartic acid) (Jin and Varner, 2004).

Integrins are clustered and activated by ECM binding and clustered activated integrins recruit focal adhesion proteins such as paxillin and talin, which in turn recruit FAK and vinculin to sites of integrin clustering (Schlaepfer et al., 2004). Talin has a particularly important role in integrin activation and in permitting full signalling responses after ECM ligand binding (Calderwood, 2004). The binding of paxillin and talin to the carboxy-terminal of FAK allows the auto-phosphorylation of FAK-Y397 (Schlaepfer and Mitra, 2004). FAK-Y397 phosphorylation (monitored by a phospho-specific antibody), will be used as a surrogate readout for FAK activation in the latter Results chapters. However, activation of FAK occurs, as with Src, with the relief of inhibitory interactions within the domain structure of the FAK protein before phosphorylation of Y397 can occur to allow full activation of FAK (Dunty et al., 2004; Schlaepfer and Hunter, 1996). Integrin-induced auto-phosphorylation at this site recruits SFKs via binding SH2 binding domains (Mitra et al., 2005). FAK's binding to active Src permits Src-mediated trans-phosphorylation of multiple tyrosine residues in both the kinase domain and carboxy-terminal regions of FAK. The two tyrosine phosphorylation sites in the carboxy-terminal domain of FAK are at

Y861 and Y925 and their phosphorylation can be monitored by phospho-specific antibodies to measure Src-mediated FAK phosphorylation (Mitra et al., 2005). A complex of Src and FAK allows the phosphorylation of paxillin, which provides SH2 binding sites for Crk and the adaptor protein p130^{Cas}, which is thought to stabilise actin filaments and control focal adhesion dynamics (Chodniewicz and Klemke, 2004; Turner, 2000). Src phosphorylation of p130^{Cas} allows activation of the Rho-family GTPase, Rac1 which directs the formation of actin filaments in lamellipodia (Hanks et al., 2003). Phosphorylation of paxillin by Src may recruit CSK to binding sites on paxillin at focal adhesions (Sabe et al., 1994). CSK may then phosphorylate Src Y530 and suppress signalling downstream of Src, for example, to block further phosphorylation of p130^{Cas} (Sabe et al., 1994; Turner, 2000), thus acting as a negative regulatory switch. Linkage of integrins through focal adhesion protein complexes to the actin cytoskeleton allows tensile strength from the ECM to cellular sub-structures; Src and FAK promote the dynamic regulation of integrin-linked adhesions and the associated filamentous actin network, so controlling cell motility and invasion. Phosphorylation of α -actinin by Src-activated FAK and phosphorylation of vinculin by Src, reduces binding of each protein to the cytoskeleton, providing dynamic regulation of focal contacts (Izaguirre et al., 2001).

In addition to the role of Src in regulating attachment and dynamic regulation of integrin complexes to the actin cytoskeleton, the phosphorylation of FAK at Y925 by Src provides a docking site for the GRB2 adaptor protein, which signals through Ras to the pro-survival ERK/mitogen-activated protein (MAP) kinase pathway (Schlaepfer et al., 1994). The auto-phosphorylation of FAK on Y397 enables connection to another important cellular pro-survival signalling pathway, namely the PI3-kinase pathway. Through direct binding of FAK to the p85 regulatory subunit of PI3-kinase, the PI3-kinase pathway can be engaged (Guinebault et al., 1995) (PI3-kinase subunits are described later in **section 1.7.4**).

Thus, SFK regulation of focal adhesions by phosphorylation of key components, such as FAK, promotes dynamic regulation of these adhesions and links integrin complexes to the actin cytoskeleton. In addition, Src and FAK promote downstream signalling pathways involved in cell survival. SFKs also have a role in the other adhesion complex, adherens junctions, and SFKs' role in the regulation of these will be discussed below.

1.6.4.2. SFKs at Adherens (Cell-Cell) Junctions

Adherens (cell-cell) junctions are found in epithelial tissues where they enable interaction and secure barrier formation by tight interaction with neighbouring cells, as well as allowing signals initiated at such cell to cell contacts to be transduced to the cell interior. Adherens junctions are mediated by the stable formation of E-cadherin dimers between adjacent cells (described in more detail in **section 1.7**). This is a calcium-dependent process and requires E-cadherin to bind β -catenin, α -catenin and p120-catenin (**Figure 6**) (Yagi and Takeichi, 2000). This complex regulates a variety of fundamental biological processes, including proliferation, differentiation and cellular invasion (Gumbiner, 2005).

There are multiple ways of regulating adherens junctions. SFKs can promote the disassembly of cadherin-mediated cell-cell adhesions, potentially increasing invasion and motility in cancer cells where Src is induced or activated (Owens et al., 2000). Src is recruited by the E-cadherin binding protein p120-catenin upon homeotypic dimerisation of E-cadherin molecules in adjacent cells (Gumbiner, 2005). Activation of SFKs directly mediates the tyrosine phosphorylation of β -catenin, reducing its binding to E-cadherin (Roura et al., 1999). It has been reported that SFK-mediated phosphorylation of E-cadherin causes displacement of p120-catenin allowing the association of the E3 ligase Hakai with E-cadherin. Hakai, together with another E3 ligase, the proto-oncogene c-Cbl, and E1 and E2 ubiquitination enzymes, targets β -catenin and E-cadherin for degradation by the proteasome as a result of ubiquitination of both Src-phosphorylated proteins (Frame,

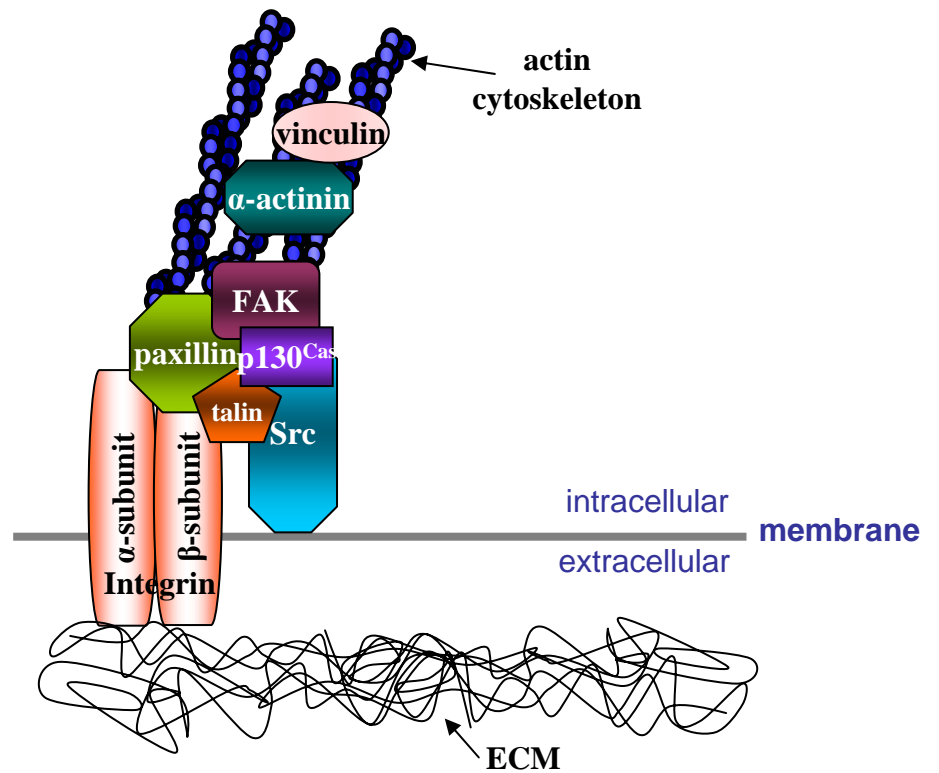
2002; Fujita et al., 2002). SFKs can also phosphorylate p120-catenin resulting in a stronger affinity of p120-catenin for E-cadherin binding (Roura et al., 1999).

1.6.4.3. Differing Roles of Src and Yes

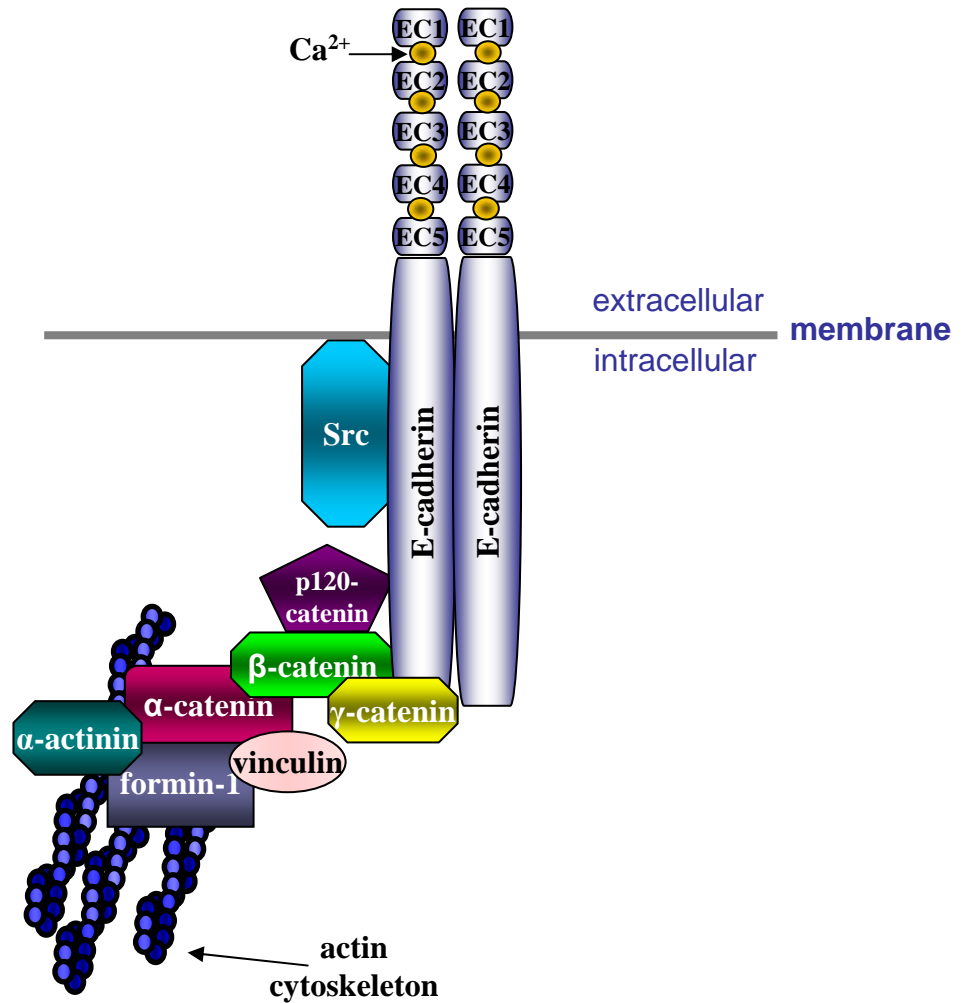
There are studies that have examined the similarities/differences between Src and Yes signalling and functions. Despite being the most homologous proteins amongst the Src family, Src and Yes have been reported to perform distinct functions, as well as overlapping functions (Summy et al., 2003b). In addition to Src, the other two ubiquitously expressed SFKs, Yes and Fyn, localise at adherens junctions, but there have been no reports that suggest differing functions at adherens junctions (Owens et al., 2000; Tsukita et al., 1991). However, another type of cell-cell contact, called tight junctions (also known as zonula occludin (ZO) junctions) may be regulated differently by Yes and Src. Yes, but not Src, has been shown to co-localise and co-immunoprecipitate with occludin, the main component of ZO junctions, and inhibition of SFKs activity results in disruption of ZO junctions in canine kidney epithelial cells because of the dissociation of occludin/Yes binding (Chen and Lu, 2003; Chen et al., 2002; Nusrat et al., 2000). It was predicted however, that Src may aid the dissociation of ZO junctions because Src binds to Raf-1 via its SH3 domain, a function which could not be substituted by the Yes SH3 domain, and Raf-1 is responsible for the down-regulation of occludin (Summy et al., 2003b). These studies concluded that the Raf-1 interaction with Src, but not Yes, may result in the disruption of tight junctions (Summy et al., 2003a; Summy et al., 2003b). Distinct functions of Src and Yes were confirmed when chimeras of the Src/Yes proteins demonstrated that Yes could not compensate functionally for Src when the non-catalytic domains of a constitutively active Src^{527F} mutant were replaced by those of Yes (Summy et al., 2003a). Despite the implied differences in ZO junctions, the 80% homology of Src and Yes (outwith their unique domains) implies there are overlapping functions; which is supported by the *in vivo* observations that neither Src nor Yes deficiency causes embryonic

lethality in mice, but combined deficiency of both does result in embryonic lethality (Roche et al., 1995; Summy et al., 2003a). Mice that were deficient in Src had perturbed osteoclast formation, preventing bone resorption, highlighting a specific role for Src that is not shared by Yes (Soriano et al., 1991). Yes-deficient mice displayed reduced signalling downstream of the polymeric Immunoglobulin A (IgA) receptor implicating Yes as the SFK responsible for specific signalling in cellular defence against pathogens (Luton et al., 1999).

In addition to the above findings on overlapping and unique functions of Src and Yes, it was found that regulation of Src and Yes throughout the cell cycle in colon carcinoma cells appears to differ. Specifically, there was elevated Src activity but decreased Yes activity, and abundance during mitosis, suggesting dissimilar regulation and perhaps functions for Src and Yes at this point in the cell cycle (Park and Cartwright, 1995).

Figure 5**Src at Focal Adhesions**

The $\alpha\beta$ subunits of integrins bind to the extracellular matrix (ECM) resulting in the recruitment of FAK and Src to the site of integrin clustering. A complex of FAK and Src enables the phosphorylation of a number of proteins and provides a docking site for proteins such as the adaptor protein p130^{Cas}, which, along with α -actinin and vinculin, enables dynamic attachment of integrins to the actin cytoskeleton.

Figure 6

Src at Adherens (Cell-Cell) Junctions

Stable formation of E-cadherin dimers in the presence of calcium recruit p120-catenin, β-catenin and γ-catenin to the cell membrane. Binding of β-catenin to α-catenin provides a bridge to the actin cytoskeleton mediated by interaction with α-actinin, formin-1 and vinculin (described in more detail in section 1.7). p120-catenin is able to recruit Src, which disassembles adherens junctions by phosphorylation of E-cadherin and β-catenin.

1.7. Cadherin Family Proteins

Cadherin proteins are a super-family consisting of a number of different subcategories. The cadherin proteins are calcium dependent, homophilic, cell-cell adhesion molecules that are primarily involved in adhesion, but also cell signalling (**section 1.6.4.2**) (Kartenbeck et al., 1991). One subcategory of the cadherin superfamily is the *classical cadherins*, which is further divided into two categories. These are Type I; which contains Epithelial-cadherin (E-cadherin), Neuronal-cadherin (N-cadherin) and Placental-cadherin (P-cadherin), and Type II; which contains vascular endothelial-cadherin (VE-cadherin) and kidney-cadherin (K-cadherin) (Hulpiau and van Roy, 2009). Although these cadherins are named after the tissue in which they were predominantly expressed, it is now known that they are not confined to expression in one tissue type (Rudini and Dejana, 2008). Their roles in adhesion and cell signalling have also linked the cadherin proteins to cancer progression.

In some cancer cells, ‘cadherin switching’ occurs where the expression of particular cadherin types changes; for example, tumour progression is associated with reduced E-cadherin expression and increased N-cadherin expression (described in more detail in **section 1.8**) (Jager et al., 2010). Furthermore, over-expression of P-cadherin in breast cancer correlates with decreased patient survival and it has been shown that up-regulation of P-cadherin *in vitro* induces MMP production - MMPs are responsible for the degradation of the basement membrane, and promote cancer cell invasion (Ribeiro et al., 2009). N-cadherin has also been linked with a more migratory phenotype and hence promotion of invasion and metastasis in cancers that display elevated N-cadherin expression (Blaschuk and Devemy, 2009).

In contrast to the pro-tumour activities associated with N- and P-cadherin mentioned above, the prototypic member of the Type I cadherins, namely E-cadherin, is known to be

a multi-tissue tumour suppressor protein. It is a familial tumour suppressor protein in gastric cancer, with germline transmission of a truncating mutation in the E-cadherin gene promoting tumour progression (Guilford et al., 1998; Humar and Guilford, 2009). In the work I present here, I observed changes in E-cadherin in 5-FU resistant colorectal cancer cells, and so I focussed on the role of E-cadherin in colon cancer cell survival and 5-FU resistance; hence I mainly discuss the E-cadherin member of the superfamily during the rest of my thesis. N-cadherin was not present in two of the three cell pairs investigated, and while P-cadherin was present, it did not rescue the effects of perturbing E-cadherin in my experiments. Thus, E-cadherin is the cadherin I focus on in the discussion below.

1.7.1. Role of E-cadherin at Adherens Junctions

E-cadherin is a 120kDa transmembrane protein that consists of a cytoplasmic domain, a transmembrane domain and five extracellular domains (linked in a rod-like structure) (depicted in **Figure 6**). The extracellular domains of E-cadherin molecules interact with other E-cadherin molecules on adjacent cells to form adherens junctions in the presence of calcium (described in **section 1.6.4.2**).

The cytoplasmic domain of E-cadherin interacts with three catenin proteins, p120-catenin (membrane proximal region of E-cadherin), β -catenin (membrane distal region of E-cadherin) and γ -catenin (membrane distal region of E-cadherin) (Knudsen and Wheelock, 1992; Liwosz et al., 2006; Ozawa et al., 1989; Reynolds et al., 1994; Thoreson et al., 2000). β -catenin acts as a bridge between E-cadherin and the actin cytoskeleton by binding to α -catenin (Drubin and Nelson, 1996; Gumbiner, 2000) (depicted in **Figure 6**). α -catenin binds to the actin cytoskeleton directly, or through the actin binding proteins, α -actinin, formin-1 and vinculin. Association of the cell membrane with the actin cytoskeleton is essential to maintain epithelial cell shape and to allow cells to polarise and to move, in addition to allowing a cell to sense external cues and forces (Pollard and

Cooper, 2009). Thus, E-cadherin is vital for sensing epithelial cell environments, and for permitting appropriate cellular responses.

There is cross talk between adherens junctions and integrin adhesions that controls and coordinates key aspects of epithelial cell behaviour, signalling, proliferation and survival (Brunton et al., 2004). In terms of proteins in common, α -actinin and vinculin, as well as SFKs, are co-located at both focal adhesions and adherens junctions. At focal adhesions, α -actinin is able to bind to the β_1 -integrin subunit directly, providing a linkage to the actin cytoskeleton (Otey et al., 1990). It is thought that α -actinin can move between focal adhesions and adherens junctions and that upon α -actinin binding to the actin cytoskeleton at adherens junctions, it cross-links adjacent actin filaments promoting their stabilisation. This drives the actin filaments to the sites of focal adhesions at the base of the cell, with the help of vinculin and talin (Jamora and Fuchs, 2002; Otey and Carpen, 2004; Ziegler et al., 2008).

1.7.2. Regulation of Adherens Junctions: a Role for GTPases and p120-catenin

The tethering of adherens junctions to the actin cytoskeleton is not required to enable extracellular binding of E-cadherin, but it almost certainly aids the strengthening of the junctions once formed (Braga et al., 1997). The association of adherens junctions to the actin cytoskeleton may be due in part to the activities of the small GTPases of the Rho family, Rac1, RhoA and cdc42. Activation of all three GTPases occurs upon binding of the extracellular domains of adjacent E-cadherin molecules and their activities are required to stabilise E-cadherin-mediated adherens junctions (Braga, 2002). It is interesting to note that activation of Rac1 enables its association with p120-catenin at sites of cell-cell contact, and this promotes actin polymerisation via the Arp2/3 protein complex (Braga and Yap, 2005; Wildenberg et al., 2006).

Thus, the catenin proteins and intracellular signalling proteins, including SFKs, regulate the stabilisation and breakdown of adherens junctions, controlling their dynamics and enabling cellular responses that require dynamic adhesion changes, such as motility. In this regard, p120-catenin is known to control E-cadherin stabilisation and internalisation at the plasma membrane (Reynolds and Roczniak-Ferguson, 2004). p120-catenin acts by protecting (covering) a dileucine motif on E-cadherin, which prevents binding to adaptor proteins involved in clathrin dependent internalisation of membrane proteins (Miyashita and Ozawa, 2007). Knock-down of p120-catenin protein by RNAi, or inhibition of p120-catenin binding to E-cadherin results in an increased rate of endocytosis of E-cadherin and E-cadherin degradation (Miyashita and Ozawa, 2007).

1.7.3. Cross-Talk Between Adherens Junctions and Focal Adhesions

There is considerable evidence of cross-talk between cell-cell and cell-matrix adhesions. For example, the ability of Src to dynamically regulate adherens junctions is not unrelated to Src-dependent events at focal adhesions and there is clear cross talk between these two important adhesion types, which may be subverted in cancer (Avizienyte et al., 2002). Specifically in colon cancer cells, integrin- and Src-dependent phosphorylation of FAK on Y861 and Y925 is required for efficient de-regulation of E-cadherin-mediated adherens junctions by Src (Avizienyte et al., 2002). Another recently identified protein involved in crosstalk between the actin cytoskeleton and adherens junctions is called 4.1R (Yang et al., 2009). 4.1R is a member of the 4.1 protein family originally discovered in the blood and new work has found that it may associate with β -catenin. Loss of 4.1R results in weaker formation of E-cadherin with the actin cytoskeleton (Yang et al., 2009), although whether it plays a role in integrin-cadherin crosstalk or not, remains to be established.

Thus, the regulation and functions of E-cadherin-dependent adherens junctions and integrin-mediated focal adhesions are linked by common protein components and

signalling pathway outputs. The actin cytoskeleton is regulated by both and there is significant crosstalk that remains to be fully elucidated, although current knowledge implies the Src/FAK pathway and the activities of small GTPases lies at the heart of such crosstalk. Importantly, the predominance of these adhesion types and signals originating there determines the epithelial to mesenchymal balance of individual cells of epithelial origin and can drive them to becoming more mesenchymal in morphology. In the cancer context, cells often undergo an epithelial to mesenchymal transition (EMT) that is thought to promote cancer invasion and metastasis, and epithelial plasticity may be a key determinant of clinical outcome. In my work I wished to investigate whether there was a link between the epithelial/mesenchymal balance, and the relevant adhesion proteins, in acquired resistance to 5-FU (discussed in **section 1.8**).

1.7.4. Signalling Downstream of Adherens Junctions

In addition to sites of cell to cell contact and adhesion, adherens junctions are sites of origin of a number of signalling pathways, including those that promote cell survival (Yap et al., 1997). As my work evolved, I became interested in the activation of pathways involved in cell proliferation and survival, originating at adherens junctions which seemed to have a role in resistance to 5-FU. Hence, I will discuss survival signalling originating at adherens junctions.

It has been shown that the formation of AJs can initiate binding to, and the activation of, the PI3-kinase pathway, which is important in transducing survival signals (**Figure 7**) (Laprise et al., 2002; Pece et al., 1999; Rivard, 2009). PI3-kinases can also be activated by RTKs or activated by integrins at the cell membrane (Datta et al., 1999; Vivanco and Sawyers, 2002). The PI3-kinases are composed of three classes, namely I, II and III, and they have in common their ability to catalyse the phosphorylation of the 3' position of phosphatidylinositols (PtdIns), inositol-containing lipids. Class I PI3-kinases convert

PtdIns(4,5)P₂ (PIP₂) to PtdIns(3,4,5)P₃ (PIP₃) and are involved in downstream signalling pathways that promote survival and proliferation, for example by the downstream activation of the mammalian Target Of Rapamycin (also known as FRAP1 or mTOR) protein by Akt (Hawkins et al., 2006). Class II PI3-kinases are involved in clathrin-dependent vesicle formation and are associated with the Golgi sorting apparatus (Gaidarov et al., 2001). Class III PI3-kinases are involved in autophagy and vesicle formation, and they have also been implicated in control of mTOR, a role primarily undertaken by Class I proteins, suggesting they may play a part in cell growth, however currently not much is known about the role of Class III enzymes in this pathway (Engelman et al., 2006). Class I PI3-kinases are further subdivided into IA and IB. I will only discuss Class IA PI3-kinases (which will be referred to as PI3-kinase from here on) because of its specific role in mediating proliferative and survival effects. PI3-kinase consists of a regulatory subunit, p85, which binds to the catalytic domain, p110, both of which are encoded by three genes, α , β and δ (Otsu et al., 1991; Vivanco and Sawyers, 2002). I will later use an inhibitor, GDC-0941, that selectively inhibits the catalytic function of the p110 α subunit of PI3-kinase (Folkes et al., 2008; Kong and Yamori, 2009).

RTKs or integrins activated from ECM stimuli are able to recruit PI3-kinase by a binding domain present on the regulatory p85 subunit. This binding results in activation of the catalytic subunit after a conformational change (Vivanco and Sawyers, 2002). As mentioned, activation of PI3-kinase can also occur during adherens junction formation where AJs are able to recruit PI3-kinase which can bind to either β -catenin and/or γ -catenin at the formed junctions (Laprise et al., 2002; Pece et al., 1999; Rivard, 2009). Recruitment by both RTKs/integrins or by adherens junctions result in the PI3-kinase being in close proximity to PIP₂ which is bound to the peripheral cell membrane, where the active PI3-kinase is able to convert PIP₂ to PIP₃ using ATP as a co-factor (Datta et al., 1999). This process can be reversed by the phosphatase PTEN, which de-phosphorylates the PIP₃

product (Maehama and Dixon, 1998). As previously mentioned, PTEN is often aberrant in cancers, including colon cancers, enabling cells to experience net high activity of the PI3-kinase survival pathway (Hill and Wu, 2009).

Production of PIP₃ enables translocation of Akt isoforms (also known as Protein Kinase B) from the cytoplasm to the membrane upon binding of PIP₃ to the Akt Pleckstrin Homology (PH) domain resulting in a conformational change (Liu et al., 2009). This binding to the PH domain alone can activate Akt by the phosphorylation of threonine 308 (T308) and serine 473 (S473). In future experiments, I will use the phosphorylation of Akt at S473 (by use of a phospho-specific antibody) as a surrogate readout for PI3-kinase activation (Franke et al., 1997; Klippel et al., 1996). However, phosphorylation of T308 has also been shown to be catalysed by the 3-phosphoinositide-dependent protein kinase (PDK1) which is activated upon PI3-kinase stimulation; nevertheless, this still requires the conformational change induced by the PH domain binding to PIP₃ (Alessi et al., 1997; Cohen et al., 1997; Datta et al., 1999). A complex of PDK1 and another kinase, protein kinase C-related kinase-2 (PRK-2), is able to phosphorylate both T308 and S473 of Akt upon Akt PH domain binding to PIP₃ (Balendran et al., 1999a). However, the phosphorylation of Akt S473 is a valid readout of pathway activation.

Upon Akt activation, signalling is mediated by downstream effectors that are involved in cell proliferation, growth and survival, (Hawkins et al., 2006). Amongst the effector pathways are the mTOR / p70 S6 kinase and the Mdm2 / p53 pathways, which I will now describe (Vivanco and Sawyers, 2002). Activated Akt is able to bind and activate mTOR, which can function as a sensing molecule for available nutrients. It activates the downstream protein, p70 S6 kinase and phosphorylates and inactivates the 4E-binding protein 1 (4-EBP1). This pathway regulates genes involved in cell growth and proliferation (Kroczyńska et al., 2009). mTOR is able to phosphorylate its substrate proteins with the help of an adaptor protein called Raptor (Regulatory Associated Protein

of TOR) which, upon binding to mTOR, can recruit 4-EBP1 and p70 S6 kinase (Hara et al., 2002; Hay and Sonenberg, 2004). I will later use phosphorylation of p70 S6 kinase at T389 (monitored by use of a phospho-specific antibody) as a read-out for signalling via this pathway, although phosphorylation of p70 S6 kinase at T229 is also important for its activation (Balendran et al., 1999b). Activated p70 S6 kinase phosphorylates the ribosomal protein S6, as well as regulating the translation elongation factor eEF2, and inactivation of 4-EBP1 which allows the process of mRNA translation to occur; these events are linked to cell survival (Nave et al., 1999).

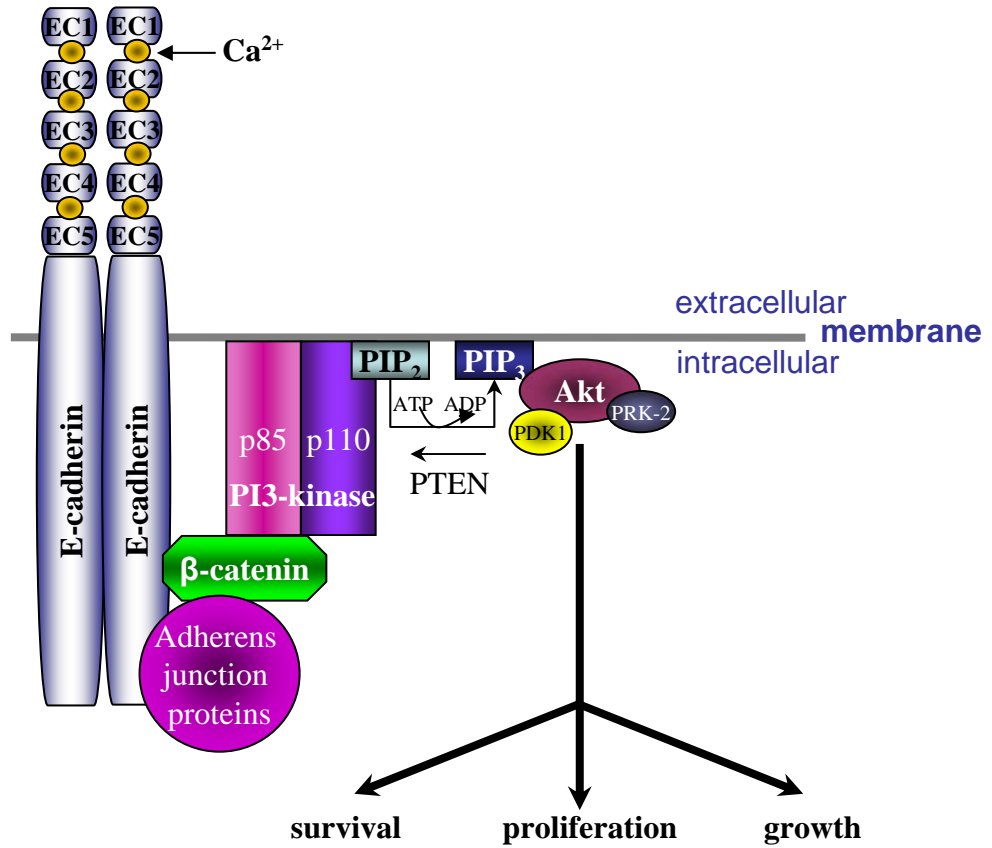
PI3-kinase activation of Akt enables the phosphorylation of the pro-apoptotic Bcl-2 family member BAD. Upon phosphorylation of the BAD protein, which is a BH3 domain-containing protein, it is unable to induce apoptosis through activation of downstream target genes, resulting in increased cell survival (Datta et al., 1997).

Activated Akt can also inhibit Mdm2, the negative regulator of p53. Activation of the Mdm2 protein causes a negative feedback loop resulting in ubiquitination and degradation of p53, which plays a crucial role in cell-cycle arrest or apoptosis in times of DNA damage or other stress (Datta et al., 1999; Vousden and Lane, 2007).

Activation of the PI3-kinase pathway also occurs when the p110 catalytic subunit binds to the MAP kinase upstream regulator Ras, either directly or via Raf1, at the plasma membrane (Kodaki et al., 1994) in the vicinity of its substrate PIP₂ (Kodaki et al., 1994; Rodriguez-Viciano et al., 1996). MAP kinase signalling is another of the cells' major signal transduction pathways and is an important survival pathway that is activated upon adherens junctions formation (**Figure 8**) (Pece and Gutkind, 2000). Adherens junctions formation is also able to activate the MAP kinase pathway indirectly, by ligand independent activation of the EGFR (Pece and Gutkind, 2000). Upon growth factor receptor activation or stimulation of adherens junctions assembly, activation of Ras occurs

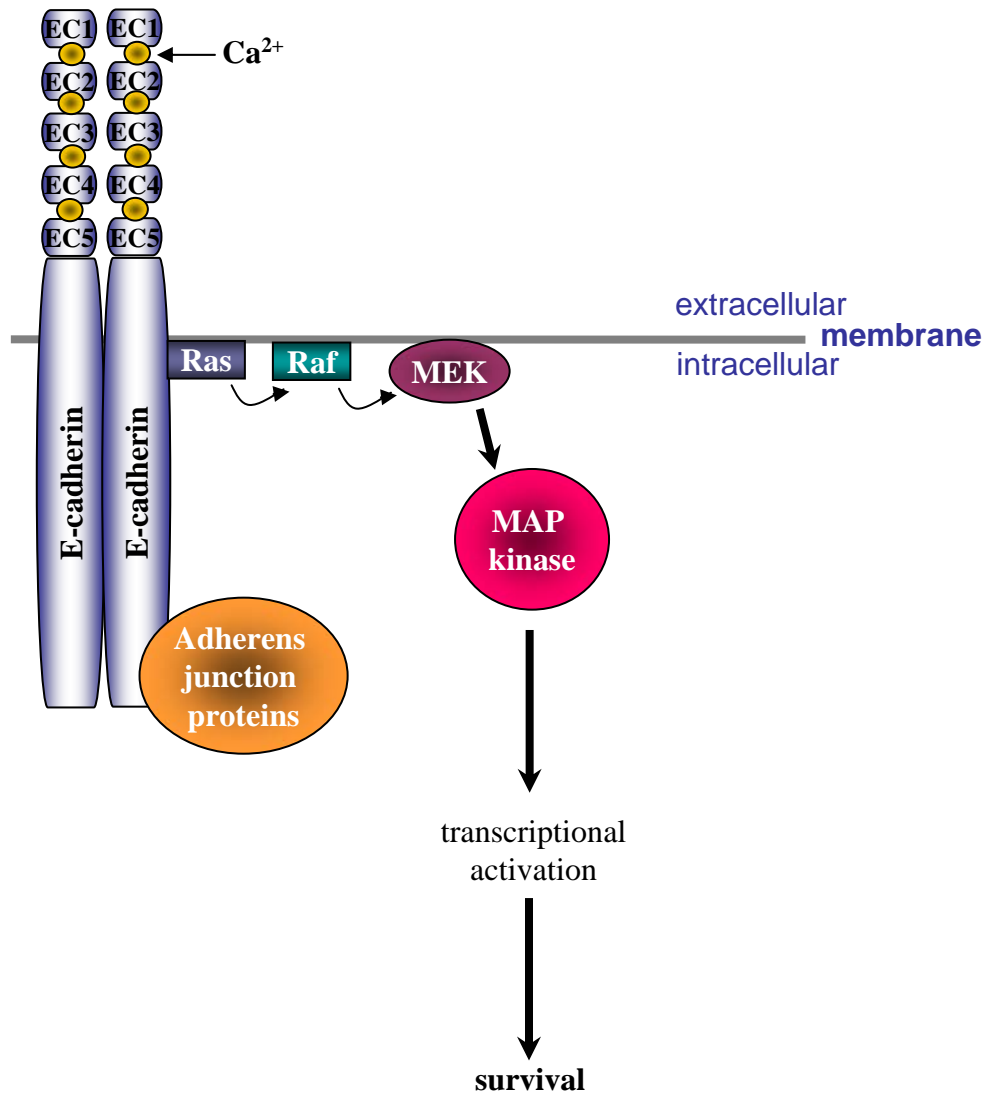
which, in turn, recruits and activates Raf kinases at the cell membrane (Orton et al., 2005). Raf kinases are then able to recruit MEK to the plasma membrane and it becomes activated by phosphorylation of two serine residues present in the MEK activation loop (Kolch, 2000). This constitutes the MAP kinase signal transduction cascade, leading to phosphorylation and activation of MAP kinase (p44/42; also known as ERK-1 and ERK-2) on a Threonine-Glutamine-Tyrosine (TEY) motif in the MAP kinase activation loop (Kolch, 2000). Active MAP kinase has a vast number of downstream targets, some of which control the activities of transcription of genes whose products can promote cell survival (Bonni et al., 1999). Additionally, MAP kinase activation has also been shown to provide cell survival by the phosphorylation, and hence inhibition, of the pro-apoptotic protein BAD (Bonni et al., 1999).

The survival signals that may originate at adherens junctions could be amongst those that provide cancer cells with mechanisms to evade cell death under stress conditions, such as those provided by treatment with chemotherapeutic agents. During cancer progression, the reliance on normal pro-survival signals can be subverted, perhaps allowing the generation of survival in the absence of normal adhesion-dependent signalling.

Figure 7

PI3-Kinase Pathway Activation by Adherens Junctions

Adherens junction formation recruits PI3-kinase to bind to β-catenin (or γ-catenin; not shown) resulting in its close proximity to the PI3-kinase substrate, phosphatidylinositols(4,5)P₂ (PIP₂) allowing conversion to phosphatidylinositols(3,4,5)P₃ using ATP as a co-factor, a process that can be reversed by the phosphatase PTEN. Translocation of Akt, PDK1 and PRK-2 to the membrane enables activation of downstream pathways by Akt providing cell survival, cell proliferation and cell growth.

Figure 8

MAP Kinase Pathway Activation by Adherens Junctions

Adherens junction formation recruits Ras and activates it at the cell membrane. This, in turn recruits Raf resulting in downstream activation of MEK and then MAP kinase. Active MAP kinase has a vast number of downstream targets which can activate transcription and allow cell survival.

1.8. Epithelial-to-Mesenchymal Transition (EMT)

Adherens junctions between adjacent cells provide survival signals via a number of signalling pathways (**section 1.7.4**). Cancer metastasis, in addition to the development of resistance, provides a major problem in the clinic. In order for a cancer cell to invade and metastasise, it often de-regulates both cell-cell and cell-matrix adhesions, becoming more migratory in nature and acquiring the ability to survive and proliferate in the absence of signals generated from these adhesions.

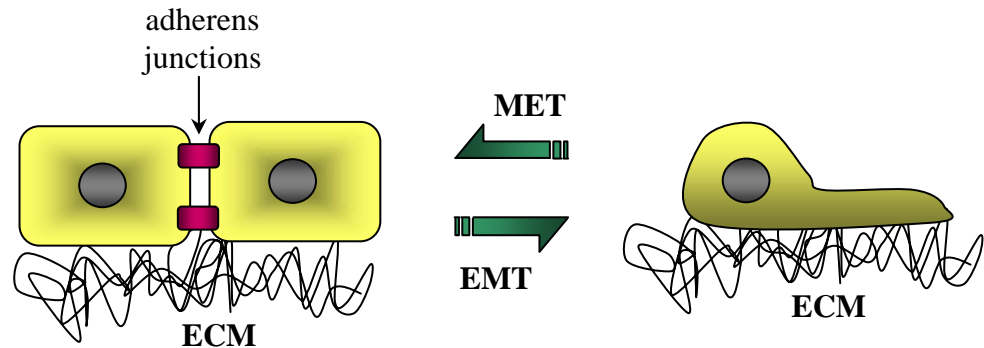
A process termed Epithelial-to-Mesenchymal Transition (EMT) is one of the hallmarks of human cancer, where cells lose their apical-basal polarity and epithelial architecture and adopt a more mesenchymal phenotype which displays a front-rear polarity (**Figure 9**) (Christiansen and Rajasekaran, 2006; Voulgari and Pintzas, 2009). This promotes the dissemination of cells from the primary tumour, entry into the vascular or lymphatic system through pre-existing or newly formed blood or lymph vessels, and travel to a distal site where they may create one or more metastatic lesions. On arrival at the ectopic secondary site, often the mesenchymal cells revert to a more epithelial morphology in a reverse process appropriately named Mesenchymal-to-Epithelial transition (MET) (**Figure 10**) (Geiger and Peeper, 2009; Thiery, 2002). However, the process of EMT may not be a complete ‘all or nothing’ conversion between an epithelial and mesenchymal phenotype and there are several reports that suggest a full EMT, or even a partial one, may not be necessary for the metastatic phenotype as some cells can probably remain epithelial and still be invasive (Christiansen and Rajasekaran, 2006).

The processes of EMT and MET do occur in normal tissues, for example during embryonic development, organ creation and tissue repair (Kalluri, 2009). The process of EMT in tissue repair can become aberrant, resulting in the formation of fibrosis in many organs, including the liver and kidney (Rastaldi et al., 2002; Zeisberg et al., 2007). This is due to

the persistence of cytokines that stimulate EMT after organ damage repair has ceased, resulting in the overproduction of mesenchymal (fibroblast) cells which form excessive extracellular matrix (ECM). This process can destroy organ structure and may eventually inhibit organ function (Zeisberg et al., 2007). Another example of EMT is provided by the inflammatory disorder, Crohn's disease, which is an autoimmune disease that affects the gastrointestinal tract. This is associated with increased production of mesenchymal cells implying that EMT may play a role in this disease (Bataille et al., 2008).

1.8.1. Key Alterations and Factors That Govern EMT

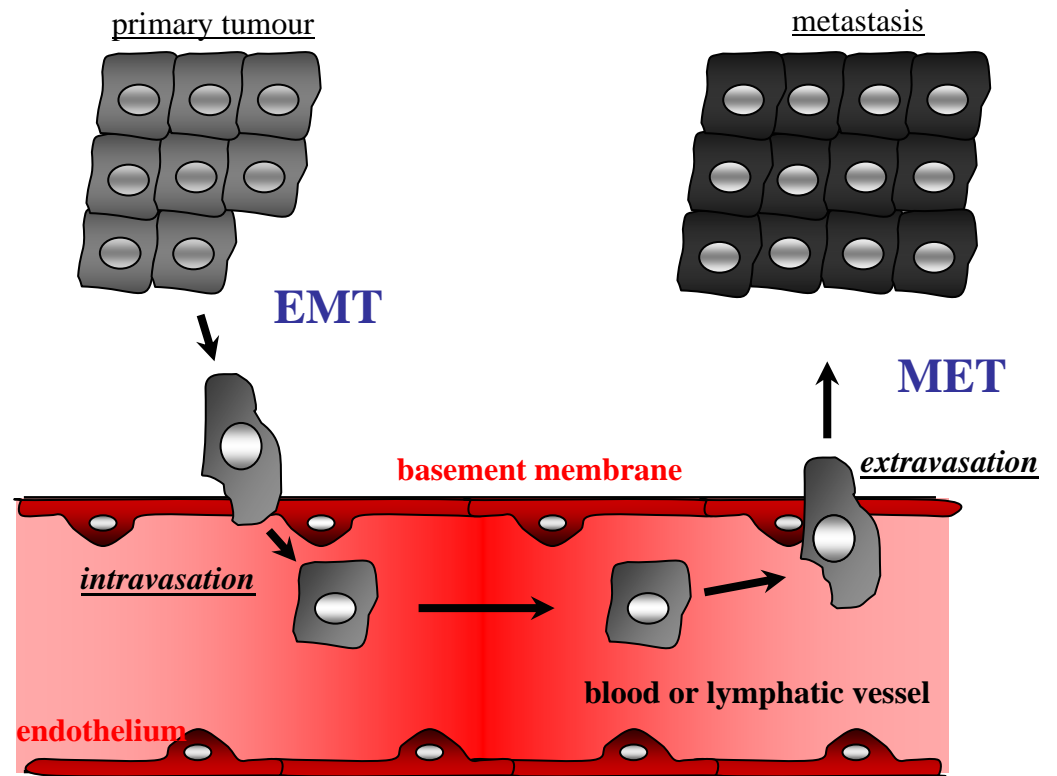
A number of key alterations occur, and several markers have been identified, that distinguish between epithelial and mesenchymal cells (**Figure 9**). Initially the perturbation of cellular junctions is required. This not only requires the loss of adherens junctions, but also the loss of tight junctions, gap junctions and desmosomes. Loss of E-cadherin is a commonly associated marker of EMT (Voulgari and Pintzas, 2009). A 'cadherin switch' where epithelial cells down regulate E-cadherin and up-regulate N-cadherin is often associated with EMT. This results in the breakdown, or loosening, of cell-cell contacts and the cells adopt a more migratory phenotype due to the pro-migratory role of N-cadherin (Maeda et al., 2005). Another key marker of EMT is the gain of expression of vimentin, an intermediate filament family member which is commonly used as a marker of mesenchymal cells, but other mesenchymal markers include, Zeb-1, Zeb-2, Snail, Slug and MMPs. The up-regulation of MMPs, specifically MMP2 and MMP9 in mesenchymal cells can be associated with EMT. For example, MMP activities enable the degradation of the basement membrane and ECM to allow the more motile and invasive N-cadherin-expressing mesenchymal-like colon cancer cells to infiltrate into the surrounding tissues and body circulatory systems (Curran and Murray, 1999).

Figure 9

	Epithelial	Mesenchymal
Morphology	Apical/basolateral polarity	Leading/trailing edge
Physical characteristics	Cell adhesion and contact inhibition	Cell migration and invasion
Intercellular junctions	Adherens, tight, gap and desmosomes	Focal adhesions and transient gap junctions
Molecular markers	E-cadherin, cytokeratins	N-cadherin, vimentin, MMPs and fibronectin

Epithelial to Mesenchymal Transition (EMT)

Epithelial cells are well differentiated, highly polarised and form strong intercellular junctions. Upon transition to a mesenchymal morphology the cells become de-differentiated, lose E-cadherin and associated junctions and acquire a highly motile invasive phenotype. The Table represents some of the key physical and molecular changes that take place during EMT.

Figure 10

Development of Cancer Metastasis

Cells from the primary tumour, break away and invade through the basement membrane and intravasate into the blood or lymphatic vessels. At a distant site the cells attach to the endothelium and extravasate back through the basement membrane forming and then grow and colonise at distant sites to form metastatic lesions.

EMT can be induced by a variety of different stimuli (growth factors / cytokines) including Hepatocyte Growth Factor (HGF), Transforming Growth Factor (TGF)- β , Platelet-Derived Growth Factor Receptor (PDGFR), Wnt and Hedgehog (Christiansen and Rajasekaran, 2006; Kalluri, 2009; Moustakas and Heldin, 2007). TGF- β is a major inducer of EMT, resulting in suppressed expression of various epithelial proteins such as E-cadherin and enhanced mesenchymal proteins such as fibronectin and vimentin. TGF- β operates as both a tumour suppressor and promoter by acting via Smad (e.g. Smad 2 and 4) or non-Smad (e.g. c-Myc, PI3-kinase and MAPK) pathways (Massague, 1998). Key targets of TGF- β signalling are the transcriptional repressors of E-cadherin: Snail, Slug and Twist, Zeb-1 and Zeb-2. Members of the miR200 family of micro-RNAs also play a role in mediating the effects of TGF- β . miR200 binds to the mRNA encoding Zeb-1 and Zeb-2 preventing translation of these E-cadherin repressors (Gregory et al., 2008; Korpala et al., 2008; Park et al., 2008). TGF- β down-regulates miR200 which results in expression of Zeb-1 and Zeb-2 and down regulation of E-cadherin. Zeb-1 and Zeb-2 proteins themselves, are able to abolish the functions of the miR-200 family suggesting the presence of a feedback mechanism at the levels of mRNA (McConkey et al., 2009).

Wnt signalling is also a key regulator of EMT during cancer progression. The canonical β -catenin-dependent Wnt signalling pathway results in the nuclear accumulation of β -catenin. This causes transcriptional activation of target genes, involved in EMT, through the lymphoid enhancer factor 1 (LEF-1)/TCF transcription factors (Nawshad et al., 2007). These include vimentin and fibronectin, which are both markers of a mesenchymal morphology (Nawshad et al., 2007). Wnt signalling and TGF- β can also co-operate to regulate EMT. For example, LEF-1 is activated by TGF- β -induced Smad2-Smad4, culminating in LEF-1 binding to the promoter of E-cadherin directly and suppressing its transcription (Nawshad et al., 2007). In addition, down regulation of E-cadherin following

TGF- β activation (or via other EMT regulators) disrupts the association of E-cadherin and β -catenin at the cell membrane and leads to accumulation of β -catenin within the nucleus (Xu et al., 2009). The non-Smad dependent targets of TGF- β include the cancer oncoprotein c-Myc, which is mutated in a number of colon and breast cancers and can activate EMT by binding to Max and functioning as a transcription factor for genes involved in cell cycle, proliferation, adhesion and apoptosis (Cho et al., 2010). c-Myc is also a key downstream target of the Wnt / β -catenin signalling pathway in colon cancer (Sansom et al., 2007), where EMT may play an important role at the invasive front of tumours.

The Hedgehog pathway has also been implicated in EMT. Studies in prostate cancer cells have shown that Hedgehog signalling leads to induction of Snail and loss of E-cadherin, which correlates with a more metastatic phenotype (Karhadkar et al., 2004). Hedgehog can also co-operate with TGF- β to regulate EMT by inducing TGF- β secretion, and also by the Wnt signalling pathway, via the E-cadherin transcriptional repressors (Katoh and Katoh, 2008).

The down-regulation of adherens junctions and induction of EMT can also be initiated by signalling from the PDGFR, which activates Src-dependent phosphorylation of β -catenin which, in turn, disrupts the binding of E-cadherin / β -catenin to α -catenin, ultimately dissociating adherens junctions from the actin cytoskeleton (Thiery and Sleeman, 2006). Furthermore activation of Src downstream of the c-Met receptor can also induce EMT by disrupting the adherens junctions (Kypta et al., 1990; Thiery, 2002; Vogelmann et al., 2005). Activation of Src not only directly disrupts the adherens junctions by direct phosphorylation of β -catenin, but it initiates signalling through STAT3 which controls nuclear localisation of the negative E-cadherin repressor, Snail, by activation of LIV-1,

which allows Snail to reduce E-cadherin transcription by directly binding to the E-cadherin promoter (Huber et al., 2005).

TGF- β -induced EMT also requires PDGFR signalling in hepatocellular carcinomas. This involves a pathway in which PDGF regulates β -catenin translocation to the nucleus and its association with the transcription factor LEF-1, in a Wnt-independent manner (Fischer et al., 2007). TGF- β activation of Fibroblast Growth Factor Receptor (FGFR) can also induce expression of Snail, in addition to another two E-cadherin negative transcriptional factors, Twist and Slug, thus promoting induction of EMT as a consequence of lowered E-cadherin protein (Moustakas and Heldin, 2007; Thuault et al., 2006).

There is evidence of cross-talk between adherens junctions and integrin mediated focal adhesions (**section 1.7.3**). Src-mediated phosphorylation of FAK, which is a key downstream effector of integrins, promotes the disassembly of E-cadherin junctions and induction of EMT (Avizienyte et al., 2002). In another study, a reduction in E-cadherin protein occurred with up-regulation of the Neuronal Cell Adhesion Molecule (NCAM), which promotes the turnover of focal adhesions and a more migratory phenotype in a pathway involving activation of Fyn and phosphorylation of FAK. NCAM may therefore play a pivotal role in co-ordinating signals from adherens junctions to integrin adhesions that regulates the EMT phenotype (Lehembre et al., 2008).

The tumour microenvironment plays an important role in the induction of EMT. For example, reduced oxygen and activation of Hypoxia-Inducible Factor (HIF)- α results in the downstream activation of latent TGF- β , which triggers signalling for survival (Copple et al., 2009; Webb et al., 2009; Xu et al., 2009).

1.8.2. EMT / MET and Drug Resistance

Alterations in both cell-cell and cell-matrix contacts have been linked to resistance in the clinic in a number of different types of malignancies (Acloque et al., 2009; Voulgari and Pintzas, 2009). Resistance is usually linked with an EMT resulting from the loss of E-cadherin. For example, in colorectal cancer a Snail-induced loss of E-cadherin is associated with increased resistance to 5-FU (Hoshino et al., 2009). In pancreatic cancer, an inverse relationship between E-cadherin loss and gain of Zeb-1 correlates with resistance to a number of cytotoxic agents that can be reversed by silencing Zeb-1 by siRNA (Arumugam et al., 2009). EMT is also associated with resistance to some targeted therapies. For example, lung cancer cells that are resistant to the EGFR inhibitor erlotinib have also been shown to display EMT characteristics (Yauch et al., 2005). In bladder cancer, sensitivity to EGFR inhibition is also associated with an epithelial phenotype that can apparently be reversed by miRNA-mediated loss of E-cadherin (McConkey et al., 2009).

Treatment with a number of anti-cancer drugs has also been shown to induce EMT in different tumour types. Oxaliplatin treatment of colorectal cancer cells induces EMT via increased expression of Snail and down-regulation of E-cadherin (Yang et al., 2006), while in breast cancer cells adriamycin-induced EMT can be reversed by reducing the expression of Twist1 which also partially restores sensitivity to adriamycin (Li et al., 2009). In addition, breast cancer cells that are resistant to tamoxifen also display a phenotype consistent with that of cells having undergone EMT (Hiscox et al., 2006). This phenotype is accompanied by an increase in the metastatic potential of the tamoxifen resistant cells and enhanced basal motility (Hiscox et al., 2004).

Obviously, EMT is not the only cellular determinant of chemo-resistance. The converse, MET, or indeed the gain of adherens junctions by the up-regulation of E-cadherin, can

increase sensitivity to a number of cytotoxics in some situations, for example, colon cancer cells (Green et al., 2004). Another example of MET playing a role in resistance is shown by the increased differentiation in the crypt-villi of the intestine, which correlates with increased adherens junction protein expression and formation of cell to cell adhesion. Upon increased cell-cell adhesion, there is increased resistance to genotoxin-induced cell death, which occurs by an adherens junction-induced activation of the PI3-kinase / Akt pathway resulting in increased cell survival (Chae et al., 2009). In addition, disruption of cell-cell adhesion in mammary tumour cells by hyaluronidase also results in re-sensitisation to the alkylating agent, cyclophosphamide (Croix et al., 1996). The use of hyaluronidase in the treatment of breast cancer models both *in vitro* and *in vivo* increases the efficacy of adriamycin (Beckenlehner et al., 1992). A similar increase in chemosensitivity has also shown in glioblastoma cells, where inhibiting cell-cell adhesions in the absence of cell-matrix contacts sensitises cells to apoptosis during irradiation and anti-cancer drugs (Westhoff et al., 2008). Studies in mice have further confirmed a role for cell-cell adhesion in the survival of epithelial cells where a skin-specific reduction in E-cadherin, and also P-cadherin, results in a loss of cell-cell adhesion that is accompanied by an increase in apoptosis (Tinkle et al., 2008). Recently, induction of EMT in mammary epithelial cells was associated with stem cell properties such as self-renewal and the ability to generate new tumours which are more resistant to chemotherapy treatment (Mani et al., 2008).

Hence, there are a number of different lines of evidence that imply a role for epithelial to mesenchymal balance (i.e. EMT or MET transitions) in sensitivity and resistance to anti-cancer drugs. Even with targeted therapies - for example, the EGFR inhibitor erlotinib, which is used in the treatment of breast, lung and pancreas cancer - resistance occurs due to both intrinsic and acquired mechanisms (Kruser and Wheeler, 2010), which is associated with the mesenchymal phenotype (Yauch et al., 2005). Drug resistance remains a problem

with new molecularly targeted signal transduction inhibitors. The specific roles of the epithelial to mesenchymal balance, and the associated cell adhesion proteins and their downstream effectors, deserves further attention for both conventional and novel forms of therapeutic agents.

Therefore, I decided to look at morphology, adhesion proteins and drug resistance to 5-FU in colon cancer cells.

1.9. Thesis Aims

For the reasons discussed in this Introduction Chapter 1, I set out to:

- characterise three pairs of 5-FU-sensitive and -resistant colon cell lines with respect to thymidylate synthase, Src family kinases, and adhesions (and related proteins) associated with the epithelial/mesenchymal balance
- determine whether the Src family kinase, Yes, which is co-amplified with thymidylate synthase, plays a role in acquisition of resistance
- address whether the epithelial-mesenchymal status of cells correlates with sensitivity and resistance to 5-FU
- modulate E-cadherin function, and signalling downstream, to begin to determine whether, and if so how, E-cadherin-mediated adhesions contribute to drug resistance

2. Materials and Methods

2.1. Materials

2.1.1. Cell Culture Reagents

Supplier: Invitrogen Life Sciences Ltd, Paisley, U.K.

RPMI 1640
 DMEM
 McCoy's 5A
 Foetal bovine serum (FBS), dialysed
 200mM L-glutamine
 2.5% trypsin solution
 Penicillin (10,000units/ml)
 Streptomycin (10mg/ml)
 Calcium Chloride solution (0.2M)
 Cell dissociation buffer
 Blasticidin (10mg/ml stock)
 Block-iT™ Yes 1 RNAi
 Block-iT™ Yes 2 RNAi
 Block-iT™ Control RNAi
 Lipofectamine™ 2000
 Cell Dissociation Buffer (CDB)

Supplier: Lonza, Slough, U.K.

Keratinocyte basal medium (KBM)
 Keratinocyte growth medium singlequots

Supplier: Qiagen, Crawley, U.K.

RNeasy Mini Kit
 SuperScript® First-Strand Synthesis System for RT-PCR
 E-cadherin siRNA
 p120-catenin siRNA
 Control siRNA

Supplier: Roche Products Limited, Hertfordshire, U.K.

In Situ Cell Death Detection Kit, Fluorescein (Tunel kit)

Supplier: Sigma Chemical Co, Poole, U.K.

Monoclonal Anti-Uvomorulin/E-cadherin *decma-1* (4mg/ml IgG concentration)
 Dimethyl sulfoxide (DMSO)
 IgG from rat serum (4mg/ml IgG concentration)

Supplier: Kind gift from Jennifer Stow

pcDNA 3.1-eGFP-E-cadherin (eGFP-E-cadherin)

2.1.2. Cell Culture Plasticware and Supplies

Supplier: BD Biosciences, Oxford, U.K.

21 gauge (21G) needles
5ml sterile syringes
15ml falcon tubes

Supplier: Sigma Chemical Co, Poole, U.K.

Scienceware® cloning discs

Supplier: TCS biologicals, Botolph Claydon, U.K.

Nunc tissue culture flasks
Nunc cryotubes

Supplier: Techno Plastic Products (TPP), Trasadingen, Switzerland

Tissue culture dishes (60mm, 90mm and 150mm)
Tissue culture plates (6 well, 12 well, 24 well and 96 well)

Supplier: Iwaki Cell Biology, Sterilin Ltd., United Kingdom

Glass-bottomed 30mm tissue culture dishes

2.1.3. Cell Culture Drugs

Supplier: Chemietek, Indianapolis, U.S.A.

GDC-0941 – a specific inhibitor of PI3-kinase p110- α subunit

Supplier: Sigma Chemical Co, Poole, U.K.

5-fluorouracil (5-FU) – inhibits thymidylate synthase
U0126 monoethanolate (U0126) - MAP kinase kinase (MEK) inhibitor

2.1.4. Immunocytochemistry

Supplier: Fisher, Loughborough, U.K.

19mm glass coverslips
Microscope slides

Supplier: Invitrogen, Paisley, U.K.

Alexa Fluor® 488 goat anti-mouse IgG
Alexa Fluor® 488 goat anti-rabbit IgG
Alexa Fluor® 594 goat anti-rabbit IgG
Phospho-Y397-FAK Ab
Calcein, AM

Supplier: Merck Biosciences, Sussex, U.K.

p53 (Ab-1) mAb

Supplier: New England Biolabs, Hertfordshire, U.K.

Src (36D10) Ab
Phospho-Src/Yes/Fyn Ab
E-cadherin Ab
P-cadherin Ab

Supplier: Sigma Chemical Co, Poole, U.K.

Formaldehyde
Paraformaldehyde
Sodium hydroxide (NaOH)
Pipes
Magnesium chloride (MgCl₂)
EGTA
Triton X-100
Bovine serum albumin (BSA)
TRITC-phalloidin

Supplier: Transduction Laboratories, BD Biosciences, Oxford, U.K.

p120-catenin mAb
β-catenin mAb
P-cadherin Ab
E-cadherin mAb
N-cadherin mAb
Yes mAb

2.1.5. Co-Immunoprecipitation

Supplier: Sigma Chemical Co, Poole, U.K.

Mouse IgG (whole molecule)-Agarose
Anti-mouse IgG-Agarose
Lithium Chloride

Supplier: Transduction Laboratories, BD Biosciences, Oxford, U.K.

β-catenin mAb
E-cadherin mAb

2.1.6. Immunoblot Analysis

Supplier: Abcam plc, Cambridge, U.K.

Phospho-T389-S6 kinase Ab

Supplier: The Beatson Institute for Cancer Research Antibody Development

Src mAb

Supplier: Chemicon International, Harrow, U.K.

Re-blot kit, strong

Supplier: GE Healthcare, Little Chalfont, U.K.

ECL reagent

High molecular weight rainbow markers

Supplier: Genetic Research Instrumentation, Dunmow, U.K.

Atto protein electrophoresis apparatus

Supplier: Invitrogen, Paisley, U.K.

Phospho-Y397-FAK Ab

Phospho-Y861-FAK Ab

Phospho-Y925-FAK Ab

Supplier: Jencons, Leighton Buzzard, U.K.

Immunoblotting apparatus

Supplier: Merck Biosciences, Sussex, U.K.

p53 (Ab-1) mAb

Supplier: New England Biolabs, Hertfordshire, U.K.

Phospho-Src/Yes/Fyn Ab (recognises phospho-tyrosine at position 416)

FAK Ab

Phospho-S473-Akt mAb

Akt Ab

Phospho-Thr202/Tyr204-MAP kinase (p44/42) Ab

MAP kinase mAb

Anti-mouse/horseradish peroxidase conjugate

Anti-rabbit/horseradish peroxidase conjugate

Supplier: PERBIO, Glasgow, U.K.

Micro BCA protein assay kit

Supplier: Schleicher and Schuell, London, U.K.

Nitrocellulose membrane

Supplier: Severn Biotech Ltd, Kidderminster, U.K.

Design-a-gel 30% acrylamide

Supplier: Sigma Chemical Co, Poole, U.K.

Ammonium persulphate (APS)
Actin mAb
0.1% (v/v) aprotinin
Bovine serum albumin (BSA)
2mM phenylmethylsulphonyl fluoride (PMSF)
TEMED
Sodium fluoride (NF)
Sodium orthovanadate (Na_3VO_4)
Sodium chloride (NaCl)
Sodium pyrophosphate ($\text{Na}_4\text{P}_2\text{O}_7$)
Sodium dodecyl sulphate (SDS)
Tris base
Tris/HCl
Magnesium chloride (MgCl_2)
EGTA
Sodium deoxycholate
Triton X-100
NP40
Leupeptin
Benzamidine
DTT
2-mercaptoethanol
Glycerol
Bromophenol blue
Glycine
Methanol
Tween 20

Supplier: Transduction Laboratories, BD Biosciences, Oxford, U.K.

p120-catenin mAb
 β -catenin mAb
 α -catenin mAb
P-cadherin Ab
E-cadherin mAb
N-cadherin mAb
Yes mAb

Supplier: Vector Laboratories Ltd, Peterborough, U.K.

Vectashield mounting medium with DAPI

Supplier: Whatman, Maidstone, U.K.

3MM filter paper

2.1.7. SRB Cell Proliferation Assay

Supplier: Sigma Chemical Co, Poole, U.K.

Trichloroacetic acid (TCA)
Tris base
Sulforhodamine B
Glacial acetic acid

2.1.8. Reverse Transcription (RT)-PCR

Supplier: Invitrogen Life Sciences Ltd, Paisley, U.K.

SuperScript® First-Strand Synthesis System for RT-PCR

Supplier: Qiagen, Crawley, U.K.

RNeasy Mini Kit
PCR master mix

Supplier: Sigma Chemical Co, Poole, U.K.

Ethidium bromide

2.1.9. Stock Solutions and Buffers

Cell Culture Solutions

Cell culture medium – complete medium – H630 cells

1x RPMI 1640 supplemented with
10% dialysed FBS
2mM L-glutamine
50 units/ml penicillin
10µg/ml streptomycin

Cell culture medium – complete medium – HT29 cells

1x DMEM supplemented with
10% dialysed FBS
2mM L-glutamine
50 units/ml penicillin
10µg/ml streptomycin

Cell culture medium – complete medium – HCT-116 cells

1x McCoy's 5A supplemented with
10% dialysed FBS
50 units/ml penicillin
10µg/ml streptomycin

Cell culture medium – serum free medium – HCT-116 cells

1x McCoy's 5A supplemented with
 50 units/ml penicillin
 10µg/ml streptomycin

Aggregation assay low calcium medium – all cell types

Keratinocyte basal medium (KBM)
 Keratinocyte growth medium single quotes
 0.03mM CaCl₂

Aggregation assay high calcium medium – all cell types

Keratinocyte basal medium (KBM)
 Keratinocyte growth medium singlequotes
 1.5mM CaCl₂

Trypsin

0.25% trypsin in sterile PBS/1mM EDTA

FACS solution

PBS containing 2% dialysed FBS

Immunocytochemistry*Formaldehyde Method**Fix and permeabilisation buffer*

1ml formaldehyde
 1ml 100mM EGTA
 4ml 250mM Pipes
 10µl 1M MgCl₂
 20µl Triton X-100
 3.7ml H₂O

Wash buffer

100ml PBS
 100µl Triton X-100

Block buffer

100ml PBS
 100µl Triton X-100
 2g BSA

Paraformaldehyde Method

Fix buffer

100ml PBS
3g paraformaldehyde
Heat on hot stirrer and pH to 7.4 / 7.6 with NaOH

Permeabilisation buffer

10ml PBS
50µl Triton X-100
0.1g BSA

Wash buffer

10ml PBS
2.5µl Tween 80

Block buffer

9ml PBS
1ml FBS

GFP fix Method/3-D Cell Analysis Fix

Fix buffer

9ml PBS
1ml formaldehyde

Protein Extraction and Elution

RIPA buffer

50mM Tris/HCl, pH 7.4
150mM NaCl
1% Triton X-100
1% Sodium deoxycholate
1% NP40
0.1% SDS
5mM EGTA
100µM Na₃VO₄
10mM Na₄P₂O₇
1mM PMSF
10µg/ml aprotinin
100mM NaF
10µg/ml leupeptin
10µg/ml benzamidine

Co-Immunoprecipitation buffer

50mM Tris/HCl, pH 7.6
200mM NaCl
5mM MgCl₂
0.1% NP40
1mM DTT
25mM NF
1mM PMSF
10µg/ml aprotinin
100µM Na₃VO₄

Immunoblotting*Acrylamide gel – 10%*

13.3ml 30% acrylamide
15ml Tris base pH 8.8
11.7ml H₂O
400µl 10% SDS
375µl 10% APS
20µl TEMED

Stacker gel

3.2ml 30% acrylamide
2.5ml Tris base pH 6.8
14ml H₂O
200µl 10% SDS
200µl 10% APS
20µl TEMED

SDS Sample buffer – 2x

800µl 2-mercaptoethanol
1.3ml Tris base pH 6.8
2ml glycerol
5ml 10% SDS
1.3ml H₂O
Bromophenol blue to colour

Tank buffer – 10x

0.05M Tris base
0.05M glycine
0.1% SDS

Transfer buffer

50mM Tris base
40mM glycine
0.04% SDS

20% methanol

Wash buffer

0.2% Tween 20 in Tris Base Solution

Block buffer

0.2% Tween 20 in Tris Base Solution
5% BSA

SRB Cell Proliferation Assay

Fix solution

25% trichloroacetic acid (TCA) solution in distilled water.

Wash solution

1% glacial acetic acid in distilled water.

Staining solution

0.4% Sulforhodamine B (SRB) solution in 1% acetic acid.

SRB solubilising solution

10mM Tris base pH 10.5 in distilled water with pH adjusted using 1M sodium Hydroxide.

2.2. Methods

2.2.1. Routine Cell Culture

H630 and H630-FR cells (a kind gift from Weiguang Wang, Department of Medical Oncology, University of Glasgow) were cultured at 37°C in RPMI 1640 supplemented with 10% dialysed FBS and 2mM L-glutamine. HT29 cells were cultured at 37°C in DMEM supplemented with 10% dialysed FBS and 2mM L-glutamine. HCT-116 and HCT-116-FR cells (a kind gift from Patrick Johnston, Queen's University, Belfast) were cultured at 37°C in McCoy's 5A medium supplemented with 10% dialysed FBS.

Sub-culturing of adherent cells was achieved by aspirating the media, washing with PBS and then treatment with 0.25% trypsin in sterile PBS/1mM EDTA. Cells were re-suspended in appropriate media, counted and then transferred into tissue culture flasks or plates. All cells were maintained at 37°C with 5% CO₂ in a humid incubator.

2.2.2. Generation of Cell Lines

5-FU resistant cell lines were generated by treating parental cells with increasing concentrations of 5-FU over a period of 10 months which eventually rendered them less sensitive to the drug. I was not involved in the development of any of the 5-FU resistant cell lines.

To make stable cell lines expressing RNAi for Yes, cells were either transfected with pcDNATM 6.2-EmGFP-miR (which contains two separate RNAi sequences against Yes; Yes 1 RNAi and Yes 2 RNAi), or with a scrambled control. Transfections were carried out using LipofectamineTM 2000 as per manufacturers' instructions and cells were selected in 10µg/ml blasticidin for 21 days. Cells were then FACS sorted using a Becton Dickinson

FACS Aria II cell sorter and single cell clones generated; HFRY2 RNAi clones 1 and 12 and HFRC RNAi clones 3 and 24 were chosen to undergo further investigation.

2.2.3. *Decma Treatment*

HCT-116 and HCT-116-FR cells were counted and single cells generated using a 21G needle and syringe. Cells were plated on dishes or glass coverslips in complete McCoy's 5A medium containing *decma* or rat IgG at 1:100 (40µg/ml final concentration). Cells were grown for 7 days and then harvested for immunoblotting, fixed and stained for immunofluorescence or fixed for SRB assays. Other concentrations of *decma* used were; 1:75 (53µg/ml final concentration), 1:300 (13µg/ml final concentration), 1:1000 (4µg/ml final concentration) and 1:3000 (1.3µg/ml final concentration).

2.2.4. *Immunoblotting and Immunoprecipitation*

Cells were plated at a density of 1×10^6 cells on 60mm dishes and incubated for 2 days. Dishes were transferred directly from the incubator onto ice. Cells were then washed twice with PBS and then lysed in ice-cold RIPA buffer for 15 minutes. Cells were scraped off the tissue culture plastic using a disposable cell scraper and the lysate transferred to a microcentrifuge tube. The lysate was then clarified by centrifugation at 14,000g for 15 minutes at 4°C. Protein concentration was determined using the Micro BCA™ Protein Assay Kit and light absorbance then measured with a DU® 650 spectrophotometer (Beckman) at a wavelength of 562nm.

Cell lysates (20µg as measured by Micro BCA™ Protein Assay Kit; Pierce Ltd.) were supplemented with 2x SDS sample buffer and incubated at 99°C for 10 minutes. Proteins were separated by SDS-PAGE (10% acrylamide gel and stacker gel in tank buffer; 180V, 200mA for 1 hour) and transferred to a nitrocellulose membrane (buffered by 3MM paper in transfer solution; 100V, 400mA for 1 hour). Membrane was then incubated in block

buffer for one hour before being immunoblotted with the following antibodies; p120-catenin, β -catenin, α -catenin, P-cadherin, E-cadherin, N-cadherin, Src, Yes, phospho-Src/Yes/Fyn, p53 (Ab-1), FAK, phospho-Y397-FAK, phospho-Y861-FAK, phospho-Y925-FAK, Akt, phospho-S473-Akt, phospho-Thr202/Tyr204-MAP kinase (p44/42), MAP kinase, phospho-T389-S6 kinase and actin at a 1 in 1000 dilution overnight at 4°C. The blots were then washed three times in wash buffer (15 minutes each) and incubated with horseradish peroxidase conjugated secondary antibodies at 1 in 5000 for 45 minutes. The blots were again washed three times in wash buffer (15 minutes each) and ECL reagent added for 1 minute. The proteins were then visualized using a film processor. When necessary, blots were stripped using the Re-Blot Plus Strong Antibody Stripping Solution according to manufacturer's instruction. Densitometry was carried out using Image J software and is shown throughout as a fold change relative to the appropriate control.

For immunoprecipitation experiments, 1mg of cell lysate was incubated with 2 μ g of β -catenin or E-cadherin antibody overnight at 4°C. Immune complexes were collected using anti-mouse IgG (whole molecule)-agarose beads for 1 hour at 4°C. Beads were washed three times with ice-cold RIPA buffer and once with ice-cold 0.6M lithium chloride before 2x SDS sample buffer was added and Western blotting carried out.

2.2.5. Phase Contrast and EmGFP Images

Phase contrast images of cells were taken using a Leica microscope with Qimaging Retiga EXi Fast 1394 camera at 10x and 20x magnification. In conjunction with phase contrast images, EmGFP images were taken with an exposure time of 4 seconds at 10x magnification and 2 seconds at 20x magnification for each image to allow direct comparisons between cell lines. For aggregation assay, images were taken at 4x magnification.

2.2.6. Immunocytochemistry

For immunocytochemistry using the 'formaldehyde method', 0.5×10^5 cells were grown on 19mm glass coverslips, rinsed twice in ice-cold PBS and treated with fix and permeabilisation buffer for 10 minutes. Cells were then washed in wash buffer and blocked in block buffer for a minimum of 1 hour followed by incubation with the primary antibody overnight (4°C, in the dark; primary antibodies at 1:100 dilution). Antibodies used were p120-catenin, β -catenin, P-cadherin, E-cadherin, N-cadherin, Src (36D10), Yes, phospho-Src/Yes/Fyn, p53 (Ab-1), FAK, phospho-Y397-FAK, E-cadherin and TRITC-phalloidin. Coverslips were then washed three times with wash buffer before incubation for 45 minutes with secondary antibodies; Alexa Fluor® 488 goat anti-mouse IgG, Alexa Fluor® 488 goat anti-rabbit IgG or Alexa Fluor® 594 goat anti-rabbit IgG (room temperature, in the dark; 1:200 dilution). Coverslips were mounted using Vectashield mounting medium with DAPI to visualise the nuclei.

For E-cadherin immunocytochemistry cells were treated using the 'paraformaldehyde method' where the cells were fixed for 10 minutes with fix buffer before being treated with permeabilisation buffer for 15 minutes and blocked for a minimum of 30 minutes. Antibodies were added as above and slides mounted using Vectashield mounting medium with DAPI.

Cells were visualised by confocal microscopy using the Olympus FV1000 confocal microscope. These experiments were repeated a minimum of three times and the images shown are representative of the localisation observed in the majority of cells. A cell count of positively stained p53 nuclei in HCT-116 and HCT-116-FR cells was presented as a percentage calculated from total nuclei in 15 images (greater than 250 cells) analysed.

2.2.7. Fluorescence Recovery After Photobleaching (FRAP)

HCT-116 and HCT-116-FR cells were transiently transfected with pcDNA 3.1-eGFP-E-cadherin (eGFP-E-cadherin) using Lipofectamine™ 2000. After 24 hours, cells were trypsinised and 1×10^6 cells were plated onto glass-bottomed 30mm tissue culture dishes for 2 days. Culture media was replaced prior to imaging and FRAP was performed using an Olympus FV1000 confocal microscope with SIM scanner. Cells were maintained at 37°C in a temperature controlled chamber and imaging performed using the following settings: pixel dwell time 4µs/pixel, pixel resolution 512 x 512, 5% 488nm laser power.

Effective photobleaching was achieved using: 50% 405nm laser power, 20µs/pixel dwell time, 1 frame bleach time. Images were captured every 5 seconds for 120 frames and up to 15 cells were imaged for each cell line.

Fluorescence intensity measurements, derived from the region of interest used to bleach, were averaged and used to plot recovery curves. Average measurements for each time point were exported into Sigma Plot (Systat Inc.) for exponential curve fitting. The data was fit using the following exponential function: $y = y_0 + a \cdot (1 - e^{-bt})$. The half-time of recovery ($t_{1/2}$) was calculated using the formula: $\ln 2 / b$, where b was obtained from the exponential curve fit. The immobile fraction was calculated as follows using values derived from the curve fit: photo-bleaching : immobile fraction = $100 \cdot (1 - a / (1 - y_0))$, where y_0 is the pre-bleach intensity. Standard error values for y_0 , a , and b were given by Sigma Plot and propagated through the equations for half-time of recovery and immobile fraction listed above.

2.2.8. SRB Cell Proliferation Assay

Cells were trypsinised and single cells generated using a 21G needle and syringe before being counted and plated at 1×10^3 cells/well in a 96 well dish (surface area equals

320mm²/well). Cells were allowed to attach and grow for 48 hours prior to media change at which time drugs were added in 200µl media per well as indicated; 5-FU (0.5µM, 1µM, 2.5µM, 5µM, 10µM, 50µM, 100µM and 200µM), GDC-0941 (0.01µM, 0.03µM, 0.1µM, 0.3µM, 1µM, 3µM, 10µM and 30µM) and U0126 (0.1µM, 0.3µM, 1µM, 3µM, 5µM, 10µM, 20µM and 30µM). Cell plates were routinely fixed at three time points; before drug addition, 2 days and 5 days post addition. Briefly, 50µl fix solution was added to cell media and plates were incubated for 1 hour at 4°C. Plates were washed ten times with water and air dried. Cells were stained using 50µl staining solution for 30 minutes at room temperature before four washes using wash solution. 150µl SRB solubilising solution was added and gentle agitation was employed for 1 hour to solubilise the SRB before reading the absorbance at 540nm with Biohit BP 800 reader.

Dose response curves and IC₅₀ values were generated using Prism GraphPad software (using non-linear regression with sigmoidal curve fit parameters).

2.2.9. Aggregation Assay

Cells were dissociated using Cell Dissociation Buffer (CDB) which chelates calcium ions resulting in a loss of calcium dependent cadherin junctions. Single cells were then generated and 1×10^6 cells collected by high speed centrifugation (16,000g for 1 minute). Cells were re-suspended in Keratinocyte Basal Medium (KBM) supplemented with singlequots with either low calcium (0.03mM) or high calcium (1.5mM) and incubated for 1 hour with constant agitation. Cells were collected by high speed centrifugation (16,000g for 1 minute), re-suspended in PBS and the number of single cells and aggregates formed were counted. Aggregates were classed as a colony of ≥ 10 cells and area was measured using ImageJ software.

2.2.10. Clonogenic Assay

HCT-116 and HCT-116-FR cells were trypsinised and passed three times through a 21G needle to obtain single cells prior to plating 1000 cells per well of a 6 well dish. After 24 hours, media was replaced with or without the IC₅₀ dose of 5-FU (HCT-116 at 2µM 5-FU and HCT-116-FR at 10µM 5-FU). After 12 days cells were fixed by addition of 25% TCA (as in the SRB assay) for 1 hour at 4°C. After ten washes with water, plates were air dried. Cells were stained using SRB staining solution for 30 minutes at room temperature before four washes using SRB wash solution.

Stained colonies were photographed and colony size was determined using ImageJ software.

Further measurement of drug effects was obtained by solubilising the SRB with the addition of 10mM Tris pH 10.5 and gently agitating plates for 1 hour prior to reading the OD with Biohit BP 800 Reader at 540nm. Three replicate plates per treatment were assayed and absorbance values were normalised to those of the DMSO treated control plates.

2.2.11. 3-Dimensional Analysis of HCT-116 and HCT-116-FR cells

HCT-116 and HCT-116-FR cells were trypsinised and single cells generated before 1×10^5 cells were plated on glass-bottomed 30mm tissue culture dishes for 4 days. HCT-116 and HCT-116-FR cells were incubated with calcein, AM, for 1 hour at 37°C and fixed with 3-D cell analysis fix for 15 minutes before being washed twice with PBS. DAPI was added to cells (500nM) for 20 minutes before being washed twice with PBS. Images were taken in 0.5µM sections throughout cell colonies using an Olympus FV1000 confocal microscope. These sections were then compiled to render a 3-dimensional image. The

height of the colony of cells was established using Imaris software (Bitplane Scientific Software, Switzerland).

2.2.12. TUNEL Staining of HCT-116 and HCT-116-FR Cells

HCT-116 and HCT-116-FR cells were counted and single cells generated using a 21G needle and syringe. 9×10^3 cells were plated onto glass coverslips in the presence of *decma* at 1:100 (40 μ g/ml final concentration) or rat IgG at 1:100 (40 μ g/ml final concentration). Cells were grown for 7 days before being washed twice with ice-cold PBS, fixed and permeabilised using the 'formaldehyde method'. TUNEL staining was performed as per manufacturer's instructions and DAPI Vectashield was used to visualise nuclei. DNase (treatment for 5 minutes) was used as a positive control and a sample lacking TUNEL treatment was used as a negative control. Staining was visualised using an Olympus FV1000 confocal microscope.

2.2.13. RT-PCR for Thymidylate Synthase

Cells were trypsinised, counted and 5×10^6 cells were collected by high speed centrifugation (16,000g for 5 minutes). Cells were washed twice in PBS before total RNA extraction was performed using RNeasy Mini Kit (Qiagen, Crawley, UK) as per manufacturer instructions. RNA concentration was determined using UV absorbance from an Eppendorf Biophotometer at a wavelength of 260nm. cDNA was generated from 1 μ g RNA using SuperScript® First-Strand Synthesis System for RT-PCR as per manufacturer instructions. Sense and anti-sense primers of the gene of interest (0.625 μ M final concentration) were added to 2 μ l of cDNA as well as primers for GAPDH (0.625 μ M final concentration), which was selected as a control for normalisation. PCR master mix (which included TAQ DNA polymerase) was then added to the reaction and after 10 minutes at 94°C, 28 PCR cycles (detailed in **Table 1**) were carried out. A final incubation step of 72°C for 7 minutes was included before PCR products were resolved on a 1.5% agarose

gel containing ethidium bromide. Products were visualised under a UV light source and the image was captured by a Syngenes gel documentation system. Experiments were repeated three times and representative images are shown.

Table 1**Primer Sequences and PCR Cycle Conditions for Genes of Interest:**

Gene	Sense Primer Sequence (5' - 3')	Anti-sense Primer Sequence (5' - 3')	Cycle Conditions	Fragment Size (bp)
TS	TCAGGAAGGA- CGACCGCACG	CTCAGATTTG- AGGGAATAGC	94°C 45 seconds 54°C 45 seconds 72°C 2 minutes <i>28 cycles</i>	1560
GAPDH	GTGGATATTGTG- CCCAATGACATC	GGACTCCACGACGT- ACTCAGCGCCAGCA	94°C 45 seconds 54°C 45 seconds 72°C 2 minutes <i>28 cycles</i>	214

Primer sequences were obtained using Primer3 (Primer3) (<http://frodo.wi.mit.edu/primer3/>). RepeatMasker was used to exclude repeat elements prior to designing the primers (A.F.A. Smit) (RepeatMasker at <http://repeatmasker.org>). All primers are checked for specificity by doing pairwise blast searches with the sensitivity adjusted for short sequences (NCBI).

3. Characterisation of Three Pairs of 5-FU Sensitive and Resistant Colon Cancer Cell Lines

Cell lines obtained from a primary tumour or from metastases that evade chemotherapy treatment are an important tool for the study of colon cancer *in vitro* to increase our understanding of the mechanisms by which they become resistant to 5-FU treatment.

Three cell lines routinely used in the laboratory for the investigation of colorectal cancer are H630, HT29 and HCT-116 colon carcinoma cell lines.

H630 cells (a kind gift from Weiguang Wang, University of Glasgow) were derived from a liver metastasis of a rectal carcinoma of a 60 year old Caucasian male. Prior to resection of the metastatic tumour, the patient received treatment with FAM (5-FU in combination with adriamycin and mitomycin) and radiotherapy. The metastasised cells were moderately differentiated as per their growth characteristics (Copur et al., 1995; Park et al., 1987; Wang et al., 1999).

HT29 cells (obtained from the American Type Culture Collection (ATCC)) were derived from a moderately well-differentiated adenocarcinoma from a 44 year old Caucasian female who had received no prior treatment to resection (Chen et al., 1987).

HCT-116 cells (a kind gift from Paddy Johnston (Queen's University, Belfast)) are a colon carcinoma cell line derived from a primary tumour (Boyer et al., 2004; Traverso et al., 2003).

Creation of 5-FU resistant cell lines with corresponding parental, more sensitive, cell lines enables investigation into acquired resistance and the mechanisms altered to allow survival.

The 5-FU resistant cell lines H630-FR, HT29-FR and HCT-116-FR cells were generated *in vitro* by exposure of the cells to increasing concentrations of 5-FU. Over time, continuous

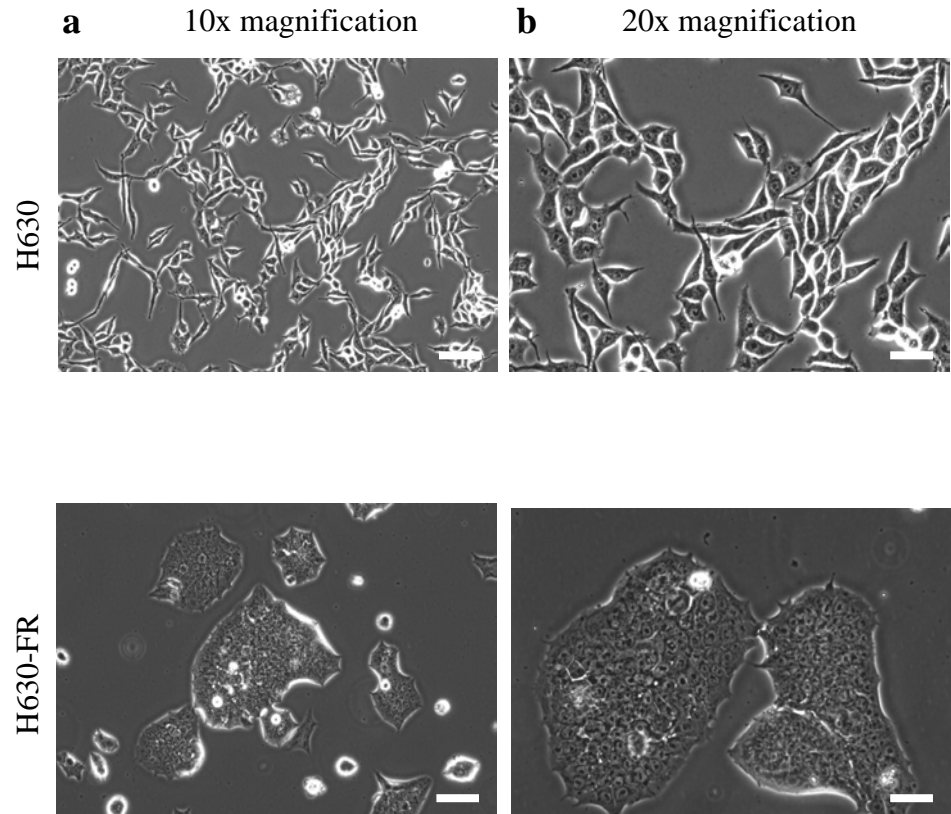
exposure of the 5-FU sensitive cells to 5-FU caused the cells to become resilient to this treatment.

3.1. Morphology

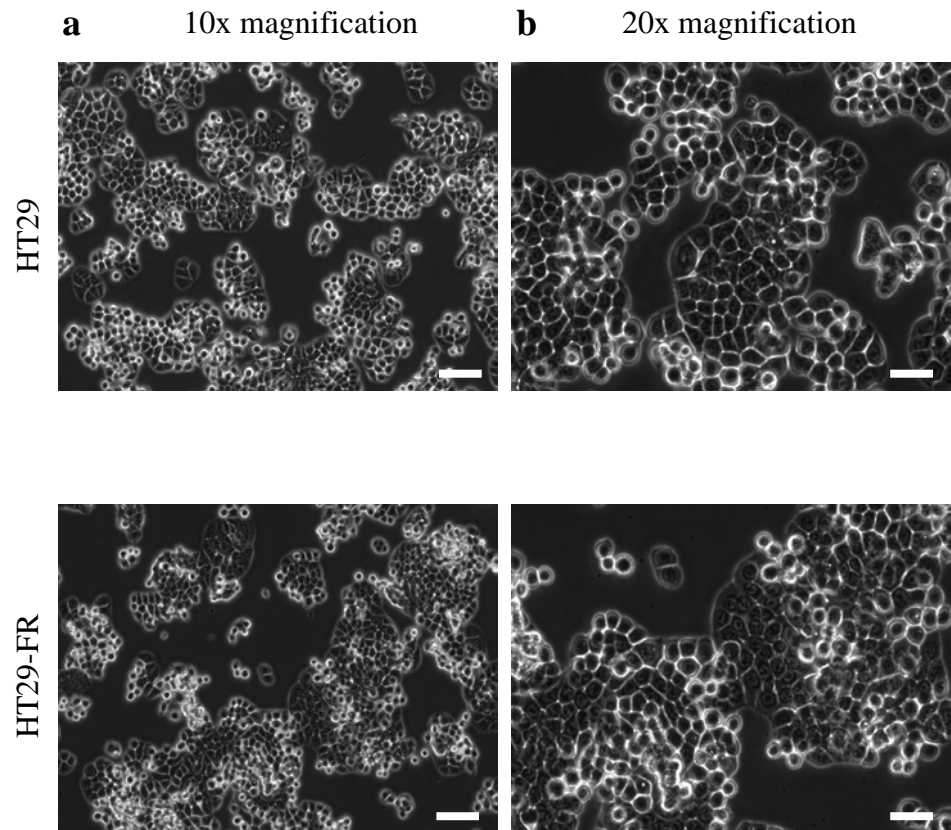
Phase contrast images were used for initial examination of H630 and H630-FR cells. Cells were plated on 60mm dishes for 2 days and images taken at 10x magnification and 20x magnification (**Figure 11a** and **b**, respectively). This analysis was also completed with the HT29 and HT29-FR cells (**Figure 12**) and the HCT-116 and HCT-116-FR cells (**Figure 13**).

Images of all cell line pairs suggested a change in morphology occurred during acquisition of resistance consistent with increased cell-cell association. This was most obvious in the H630-FR cells which appeared to have undergone an MET during acquisition of resistance. Despite the fact that HCT-116 cells are epithelial in origin, their resistant counterparts HCT-116-FR appeared to have additional cells growing above the monolayer, suggesting increased cell-cell adhesion with resistance. This phenotype, although they have some altered morphology, was less obvious in the HT29-FR cells.

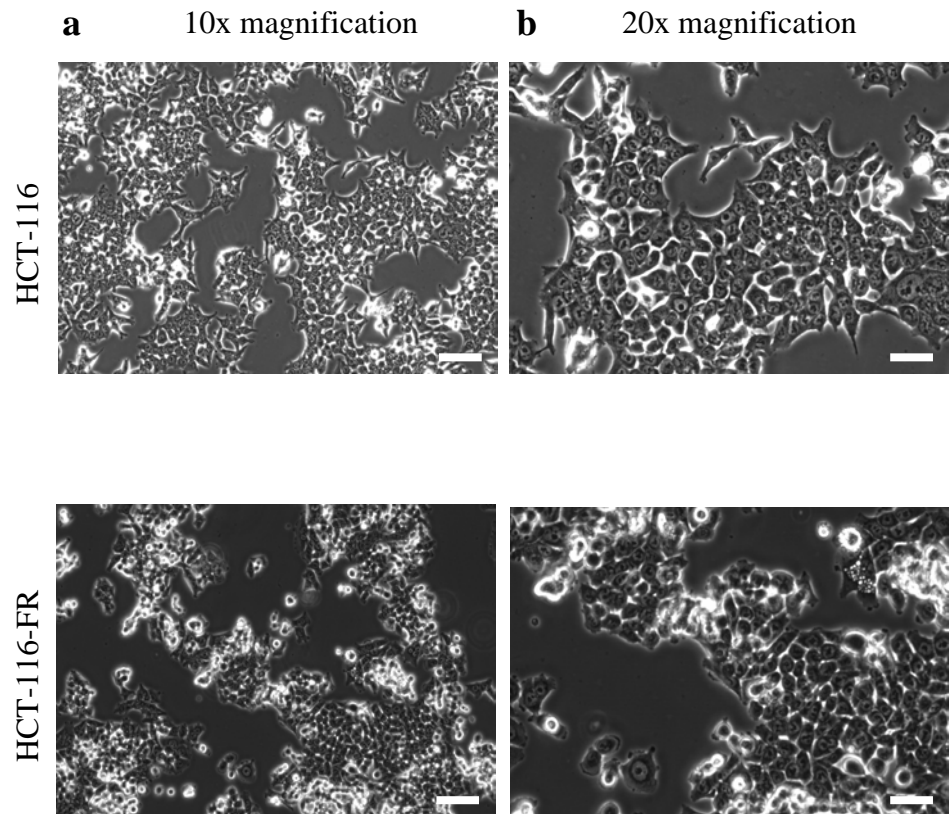
From visualising the cells' appearance, I concluded that there may be a link between increased cell-cell association and resistance to 5-FU. This was addressed in future experiments.

Figure 11**Phase Contrast Images of H630 and H630-FR Cells**

H630 and H630-FR cells were plated at 2×10^6 cells on 60mm dishes for 2 days and photographed at **a)** 10x magnification or **b)** 20x magnification. Scale bars 100 μ m.

Figure 12**Phase Contrast Images of HT29 and HT29-FR Cells**

HT29 and HT29-FR cells were plated at 2×10^6 cells on 60mm dishes for 2 days and photographed at **a)** 10x magnification or **b)** 20x magnification. Scale bars 100 μm .

Figure 13**Phase Contrast Images of HCT-116 and HCT-116-FR Cells**

HCT-116 and HCT-116-FR cells were plated at 2×10^6 cells on 60mm dishes for 2 days and photographed at **a)** 10x magnification or **b)** 20x magnification. Scale bars 100 μ m.

3.2. Gene Up-regulation and Resistance to 5-FU

Further characterisation of the cell line pairs was initiated by performing RT-PCR and immunoblotting to measure the levels of thymidylate synthase (TS) - a protein known to be up-regulated upon acquisition of 5-FU resistance (Johnston et al., 1992). The reason for this is explained as follows: TS binds dUMP and CH₂TF to form an active complex for the subsequent formation of dTMP – a key molecule involved in DNA synthesis and repair. 5-FU treatment results in the formation of an inactive ternary complex between the active metabolite of 5-FU, FdUMP, the cofactor CH₂TF, and TS. Due to the direct inhibition of TS, cancer cells attempt to overcome 5-FU treatment by up-regulating the TS gene in order to lower the proportion of inactive complexes (**Figure 2**) (Kanaan et al., 2007) (Copur et al., 1995).

Levels of TS were investigated for all three cell pairs, namely H630 and H630-FR cells (**Figure 14a** and **b**), HT29 and HT29-FR cells (**Figure 15a** and **b**) and HCT-116 and HCT-116-FR cells (**Figure 16a** and **b**). GAPDH mRNA was used as a control for the RT-PCR and actin was used as a protein loading control for immunoblotting. There was an increase in TS at both the mRNA level and the protein level for all three cell pairs as they acquired 5-FU resistance. This increase was similar in the HT29-FR and HCT-116-FR cell pairs, but was greatest in the H630-FR cells. The level of TS mRNA was reflected in the level of TS protein by immunoblot analysis for the HT29 and the HCT-116 cell pairs (**Figure 15**, compare **a** to **b** and **Figure 16**, compare **a** to **b**, respectively). I consistently found that the H630 cells displayed very low levels of TS mRNA and protein although some expression was still evident (**Figure 14a** and **b**, respectively).

I next tested how cell proliferation was altered upon increasing concentrations of 5-FU exposure in the cell pairs (**Figure 14c**, **Figure 15c** and **Figure 16c**). After 7 days of 5-FU treatment, all cell lines produced sigmoidal dose response curves that experienced a shift to

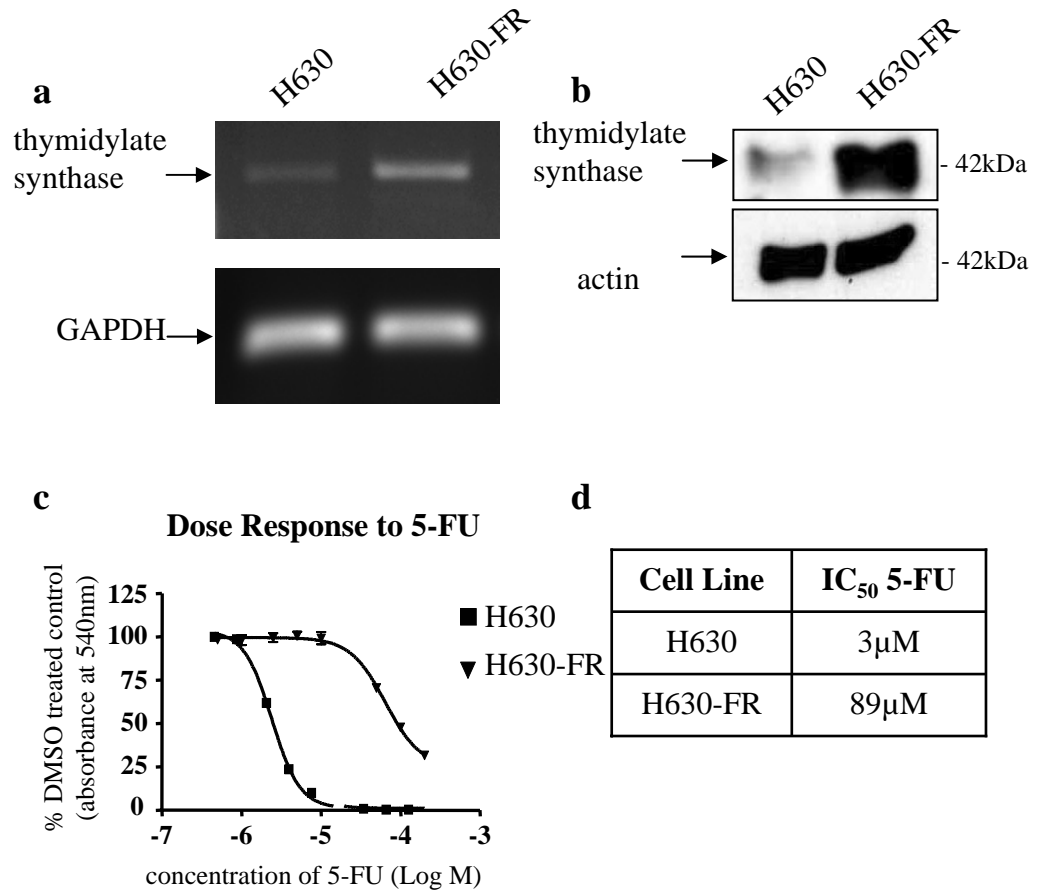
the right in the more resistant cell lines (H630-FR, HT29-FR and HCT-116-FR cells) when compared to their parental, more sensitive, counterparts. This indicated an increase in the IC₅₀ concentration of 5-FU in these cells. The largest increase in IC₅₀ displayed in the three pairs of cell lines was in the H630 and H630-FR, which increased from 3μM to 89μM (**Figure 14d** and **Table 2**). This was consistent with this cell pair having the greatest up-regulation of TS displayed at mRNA and protein levels (**Figure 14a** and **b**). The HCT-116-FR cells displayed a 5-fold increase in resistance to 5-FU, resulting in an IC₅₀ of 10μM (increased from the parental IC₅₀ of 2μM; **Figure 16d** and **Table 1**), and the HT29-FR cells had an IC₅₀ of 3μM (increased from 1μM in the HT29 cells; **Figure 15d** and **Table 2**). Thus, the three cell pairs display acquired resistance to 5-FU, with the degree of resistance being as follows: H630>HCT-116>HT29 (**Table 2**). As discussed at the beginning of this chapter, this resistance was acquired by exposure to increasing concentrations of 5-FU.

Table 2

IC₅₀ Concentrations of 5-FU in Three Cell Line Pairs

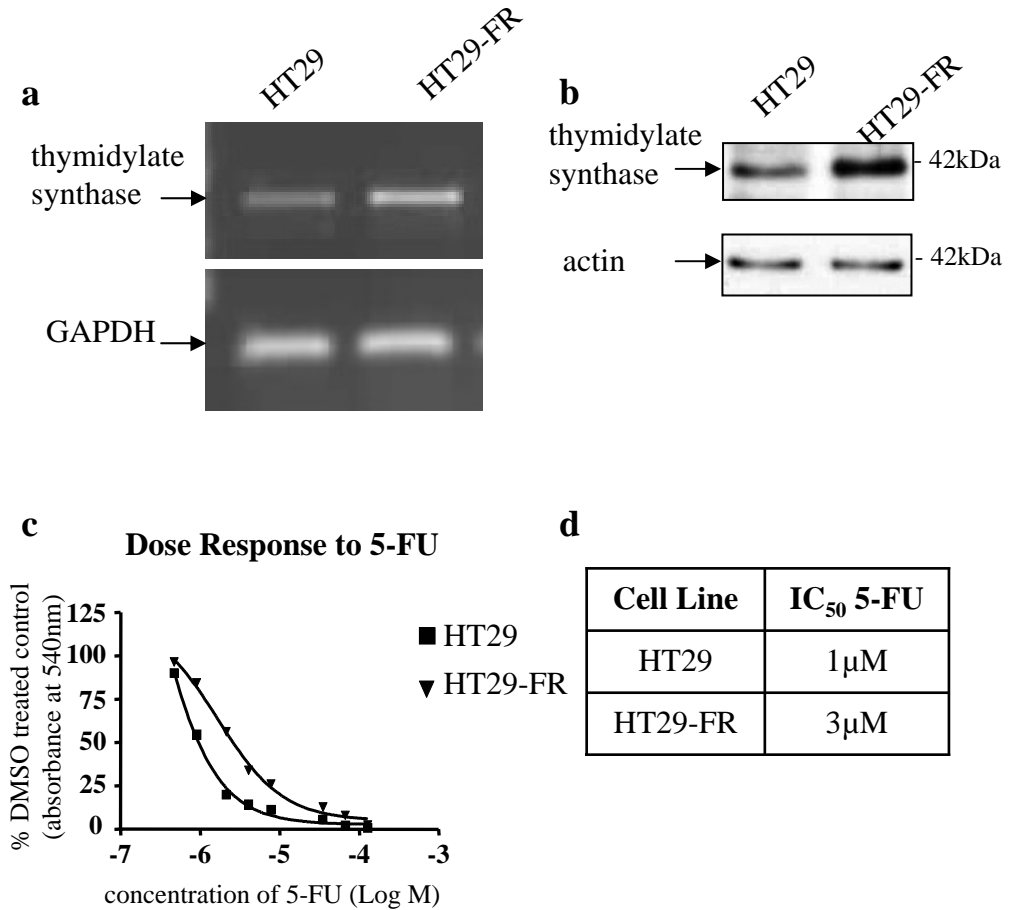
Cell Line	IC ₅₀ 5-FU	Standard Deviation
H630	3μM	0.43 μM
H630-FR	89μM	0.22 μM
HT29	1μM	0.12μM
HT29-FR	3μM	0.08μM
HCT-116	2μM	0.10μM
HCT-116-FR	10μM	0.56μM

I concluded from the results above that all three cell line pairs have; **a**) elevated IC₅₀ values in the resistant counterparts, although to varying degrees, and **b**) gained increased TS expression which correlates with acquisition of 5-FU resistance. However, I noted that the sensitive H630 cells have the same IC₅₀ to 5-FU as the resistant HT29-FR cells. That said, all cell pairs gain a degree of 5-FU resistance upon 5-FU exposure.

Figure 14

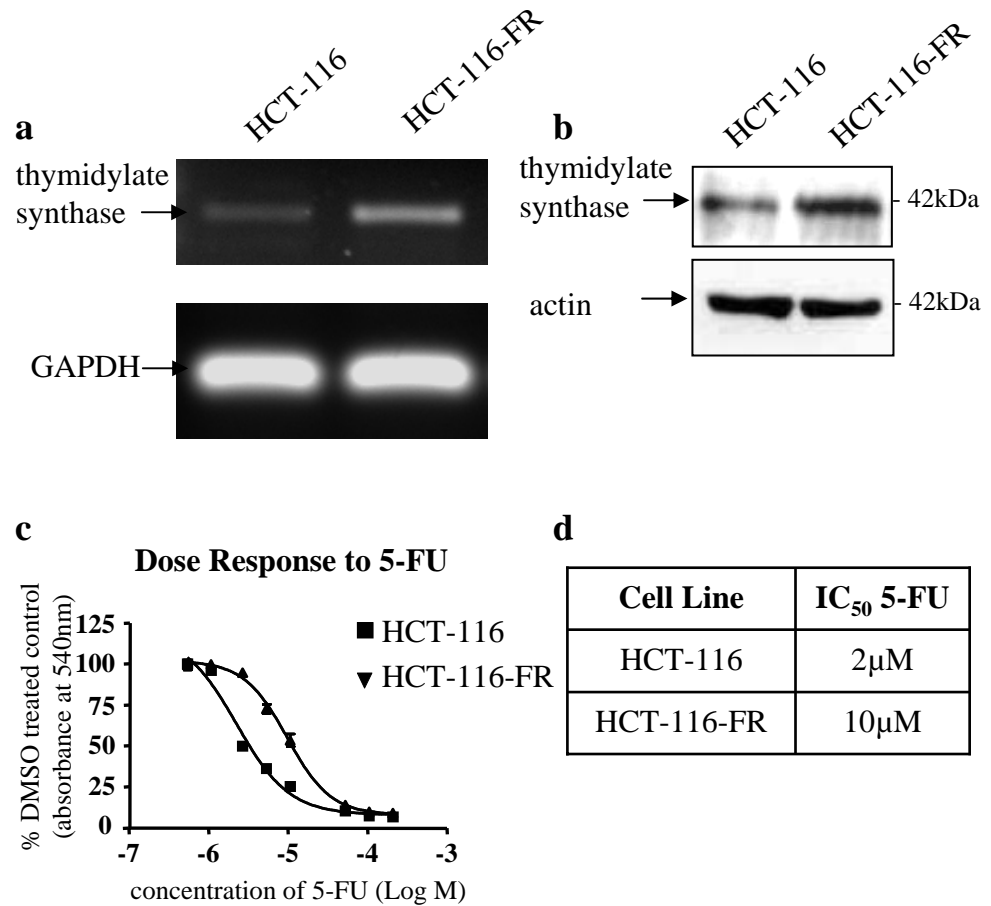
Properties of H630 and H630-FR Cells

Thymidylate synthase in H630 and H630-FR cells was monitored by analysing the following; **a)** mRNA levels via RT-PCR using GAPDH as a loading control, and **b)** protein levels via immunoblotting using actin as a loading control. **c)** Resistance to 5-FU was analysed by performing an SRB cell proliferation assay over 7 days (1×10^3 cells/well 96 well plate ($320\text{mm}^2/\text{well}$)) with a range of 5-FU concentrations (shown on graph as Log Molar concentration). Refer to figure key for cell line coding. Cells that were DMSO treated were used as a control. Absorbance at 540nm of 6 replicates per treatment were averaged and displayed as a percentage of DMSO-treated control. Standard deviation was calculated from the percentage DMSO-treated control values of the 6 replicates. **d)** Graph Pad Prism software was used to calculate IC₅₀ values for 5-FU in H630 and H630-FR cells (described in materials and methods section). A representative experiment is shown.

Figure 15

Properties of HT29 and HT29-FR Cells

Thymidylate synthase in HT29 and HT29-FR cells was monitored by analysing the following; **a**) mRNA levels via RT-PCR using GAPDH as a loading control, and **b**) protein levels via immunoblotting using actin as a loading control. **c**) Resistance to 5-FU was analysed by performing an SRB cell proliferation assay over 7 days (1×10^3 cells/well 96 well plate ($320\text{mm}^2/\text{well}$)) with a range of 5-FU concentrations (shown on graph as Log Molar concentration). Refer to figure key for cell line coding. Cells that were DMSO treated were used as a control. Absorbance at 540nm of 6 replicates per treatment were averaged and displayed as a percentage of DMSO-treated control. Standard deviation was calculated from the percentage DMSO-treated control values of the 6 replicates. **d**) Graph Pad Prism software was used to calculate IC₅₀ values for 5-FU in HT29 and HT29-FR cells (described in material and methods section). A representative experiment is shown.

Figure 16

Properties of HCT-116 and HCT-116-FR Cells

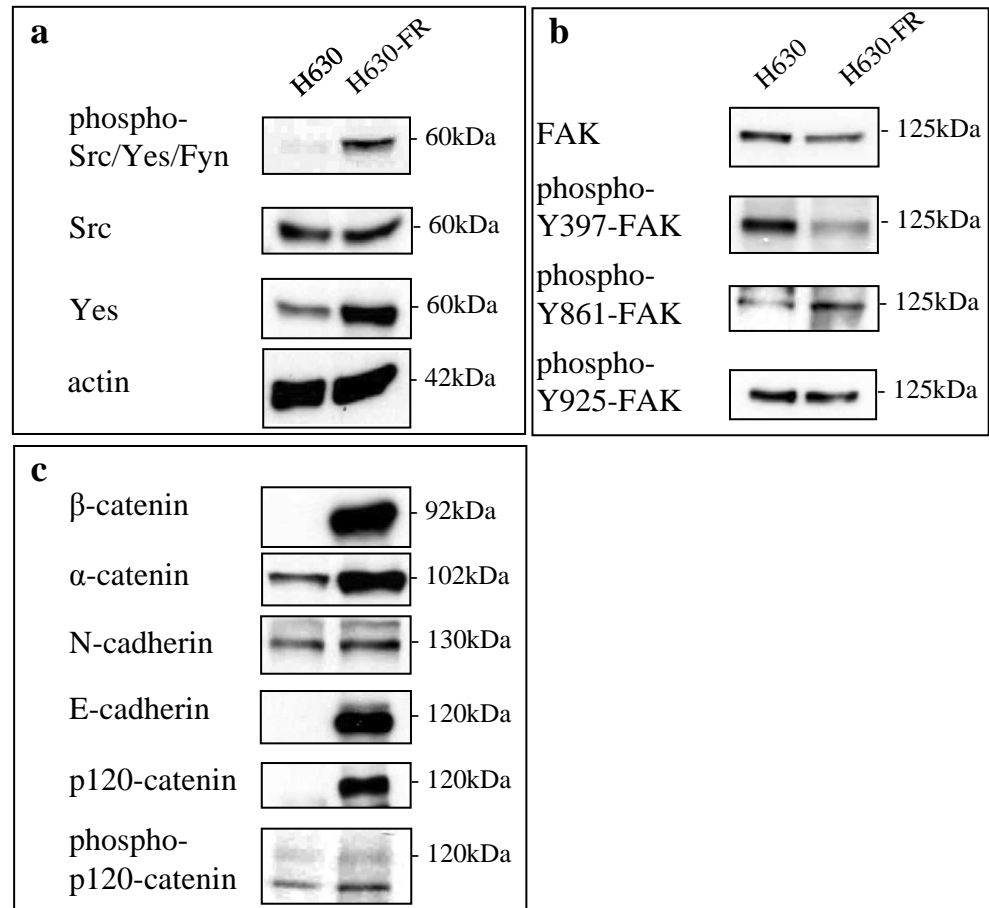
Thymidylate synthase in HCT-116 and HCT-116-FR cells was monitored by analysing the following; **a**) mRNA levels via RT-PCR using GAPDH as a loading control, and **b**) protein levels via immunoblotting using actin as a loading control. **c**) Resistance to 5-FU was analysed by performing an SRB cell proliferation assay over 7 days (1×10^3 cells/well 96 well plate ($320\text{mm}^2/\text{well}$)) with a range of 5-FU concentrations (shown on graph as Log Molar concentration). Refer to figure key for cell line coding. Cells that were DMSO treated were used as a control. Absorbance at 540nm of 6 replicates per treatment were averaged and displayed as a percentage of DMSO-treated control. Standard deviation was calculated from the percentage DMSO-treated control values of the 6 replicates. **d**) Graph Pad Prism software was used to calculate IC₅₀ values for 5-FU in HCT-116 and HCT-116-FR cells (described in material and methods section). A representative experiment is shown.

3.3. Characterisation of Adhesion Protein Expression

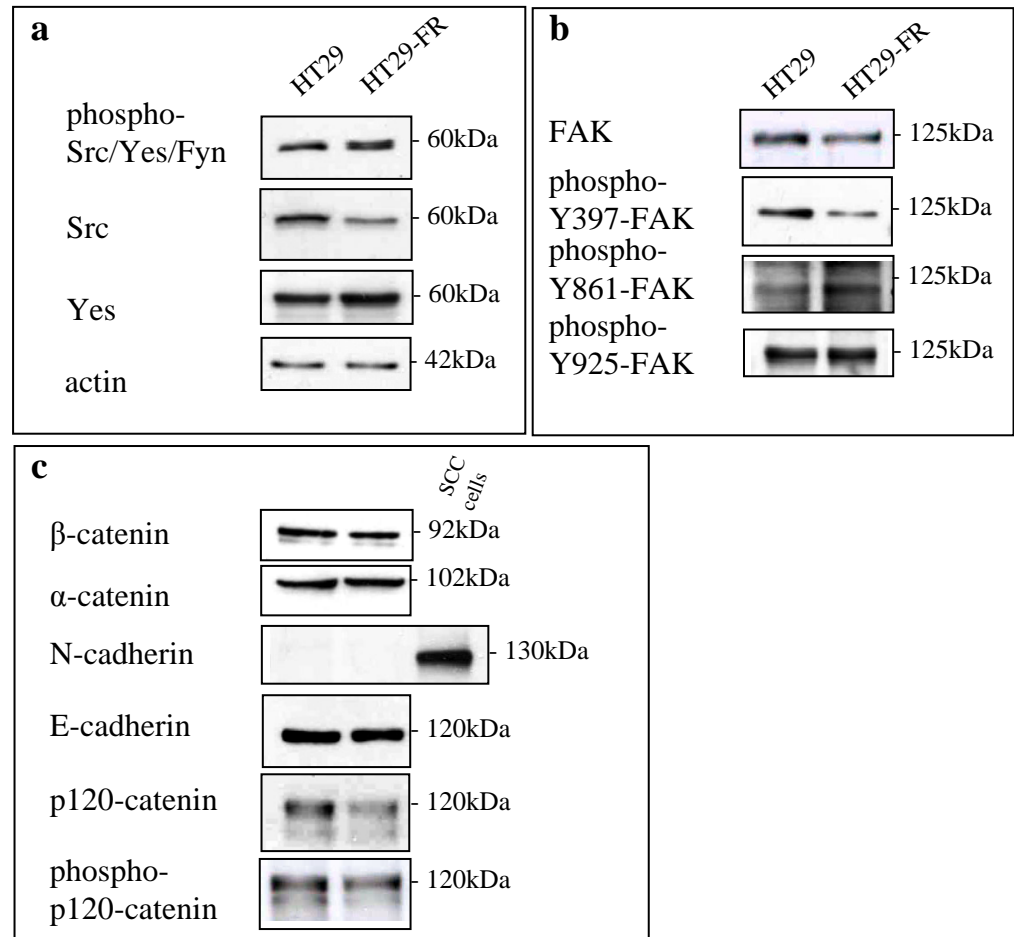
Immunoblotting was performed to investigate protein levels of SFKs and other proteins involved in cell adhesion (**Figures 17-19**) as there were differences in the morphology in all three cell pairs that may be explained by altered adhesions.

The H630 and H630-FR cells displayed similar levels of total Src protein, yet Src family kinase (SFK) phosphorylation (shown by using a phospho-Src/Yes/Fyn antibody) was increased in the H630-FR cells. I therefore examined expression of the other SFKs (**Figure 17a**). I found that the total protein level of Yes was increased in the H630-FR cells when compared to the H630 cells, and this may contribute to the apparent increase in phospho-Src/Yes/Fyn (**Figure 17a**). The SFK member Fyn was not investigated further as suitable high quality specific antibodies were not available.

In both the HT29 and HCT-116 cell pairs, a small, but consistent reduction of Src protein was seen in the resistant cells when compared to their more sensitive counterparts (**Figures 18a and 19a**, respectively). Like the H630-FR cells, both cell pairs displayed an increase in Yes protein level and phospho-Src/Yes/Fyn in the resistant cells, although to a lesser extent than in the H630-FR cells. In addition, I found a small decrease in expression of the cell-matrix attachment protein FAK in the resistant cells from all three cell pairs, and this was mirrored by a decrease in phosphorylation of the integrin-induced auto-phosphorylation site of FAK at tyrosine 397 (**Figures 17b, 18b and 19b**). There was an increase in phosphorylation of FAK-Y861, a Src-dependent phosphorylation site, in the H630-FR and HT29-FR cells, whereas the HCT-116-FR cells showed a decrease in phosphorylation of FAK at this site. Also, no consistent difference was found in the phosphorylation of FAK-Y925 between sensitive and resistant cells in all three pairs.

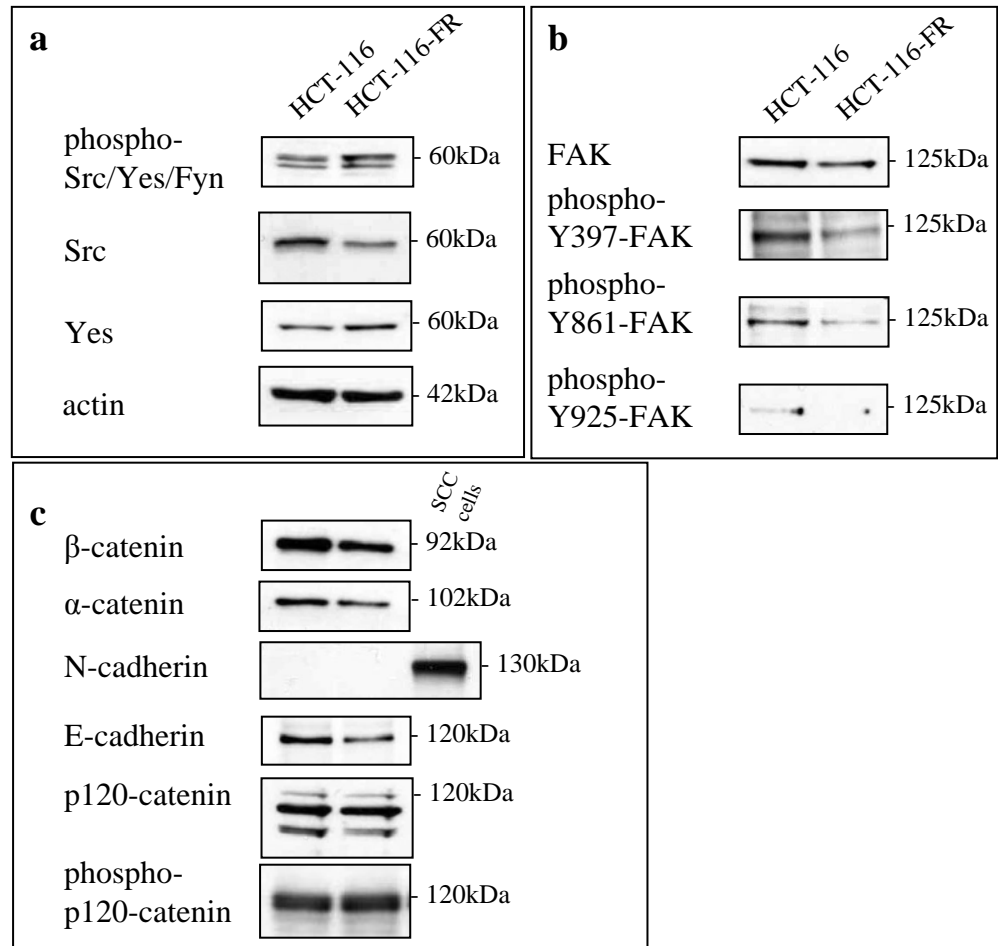
Figure 17**Immunoblotting: Adhesion Proteins in H630 and H630-FR Cells**

Immunoblotting was carried out 2 days after plating 1×10^6 untreated H630 and H630-FR cells on 60mm dishes. Lysates were probed with antibodies against; **a**) Src family kinase proteins (Src, Yes and phospho-Src/Yes/Fyn), **b**) cell-matrix adhesion protein FAK and its phosphorylated versions (phospho-Y397-FAK, phospho-Y861-FAK and phospho-Y925-FAK) and **c**) proteins involved in cell-cell adhesion (β -catenin, α -catenin, N-cadherin, E-cadherin, p120-catenin and phospho-p120-catenin). Actin was used as a loading control in (a). Molecular weight markers are shown.

Figure 18

Immunoblotting: Adhesion Proteins in HT29 and HT29-FR Cells

Immunoblotting was carried out 2 days after plating 1×10^6 untreated HT29 and HT29-FR cells on 60mm dishes. Lysates were probed with antibodies against; **a**) Src family kinase proteins (Src, Yes and phospho-Src/Yes/Fyn), **b**) cell-matrix adhesion protein FAK and its phosphorylated versions (phospho-Y397-FAK, phospho-Y861-FAK and phospho-Y925-FAK) and **c**) proteins involved in cell-cell adhesion (β -catenin, α -catenin, N-cadherin, E-cadherin, p120-catenin and phospho-p120-catenin). Actin was used as a loading control in (a). Squamous cell carcinoma cells were used as a positive control for N-cadherin. Molecular weight markers are shown.

Figure 19**Immunoblotting: Adhesion Proteins in HCT-116 and HCT-116-FR Cells**

Immunoblotting was carried out 2 days after plating 1×10^6 untreated HCT-116 and HCT-116-FR cells on 60mm dishes. Lysates were probed with antibodies against; **a**) Src family kinase proteins (Src, Yes and phospho-Src/Yes/Fyn), **b**) cell-matrix adhesion protein FAK and its phosphorylated versions (phospho-Y397-FAK, phospho-Y861-FAK and phospho-Y925-FAK) and **c**) proteins involved in cell-cell adhesion (β -catenin, α -catenin, N-cadherin, E-cadherin, p120-catenin and phospho-p120-catenin). Actin was used as a loading control in **(a)**. Squamous cell carcinoma cells were used as a positive control for N-cadherin. Molecular weight markers are shown.

Thus, from examining the Src/FAK pathway that operates downstream of integrins, I concluded that all three sensitive cell lines experience a degree of down-regulation of FAK (and resultant decrease of phosphorylated FAK-Y397) upon acquisition of 5-FU resistance. This may be due to decreased cell-matrix adhesion which correlates with increased cell-cell adhesion.

In the H630-FR cells, there was a dramatic increase in all cadherin junction proteins. The largest up-regulation was seen in the levels of β -catenin, E-cadherin and p120-catenin (**Figure 17c**) where no protein was visible in the parental H630 cells by immunoblotting. Although increases were also found in α -catenin, N-cadherin, and phospho-p120-catenin in the H630-FR cells, there was already a basal level of these in the 5-FU-sensitive H630 cells. Such dramatically elevated levels of cell-cell junction proteins were not found for HT29-FR and HCT-116-FR cells, with no increase in expression levels of p120-catenin or phospho-p120-catenin when compared to the more sensitive HT29 or HCT-116 cells (**Figures 18c** and **19c**, respectively). The HT29-FR cells did not display an increase in β -catenin, α -catenin and E-cadherin when compared to the HT29 cells (**Figure 18c**) however, a moderate decrease in these proteins was detected in the HCT-116-FR cells when compared to the HCT-116 parental cells (**Figure 19c**). Neither HT29 nor HCT-116 cell pairs contain N-cadherin; as a positive control here we used squamous cell carcinoma (SCC) cells as these expressed N-cadherin (**Figures 18c** and **19c**, respectively). The actin level in the cells was used as loading controls for the proteins studied (**Figures 17a**, **18a** and **19a**). Thus, in the cell pair that gained the largest resistance acquisition to 5-FU, the H630 cell pair, a mesenchymal to epithelial (MET) transition correlated with 5-FU resistance. The other two cell pairs studied already displayed an epithelial morphology, and hence more sophisticated tests were required to determine if their epithelial adhesions were altered. However, the combined changes in morphology and protein expressions we

observed raised the question of whether the mesenchymal/epithelial balance was involved in acquisition of resistance to 5-FU. Addressing this formed a major component of the experimental work in my thesis.

Therefore, I concluded that there are differences in the expression levels of proteins involved in cell-cell adhesion and in levels/activities of SFKs between the sensitive and resistant cell lines, although the extent of these differences varied between the three cell pairs.

3.4. Adhesion Protein Localisation

As there were differences in the immunoblots (**Figures 14-16**) I next assessed the localisation of these proteins by immunofluorescence. H630 and H630-FR cells, HT29 and HT29-FR cells and HCT-116 and HCT-116-FR cells were grown for 2 days and fixed using the formaldehyde method (as described in the material and methods section; **Figures 20-22**, respectively). Localisation of Src at the sites of cell-cell contacts was evident in both the H630 and H630-FR cells (**Figure 20a**). The H630-FR cells also displayed some diffuse cytoplasmic staining of Src. Immunofluorescence detection of Yes in the H630 and H630-FR cells showed localisation at cell-cell contacts. The increase in Yes was not so obvious by IF, which is not a quantitative technique. Localisation of phospho-Src/Yes/Fyn was seen at the sites of focal adhesions in H630 cells and cell-cell contacts in the resistant H630-FR cells (**Figure 20c**).

In the case of the HT29 and HT29-FR cells, Src and Yes were located at the sites of cell-cell contacts and the increase in Yes protein in the HT29-FR cells, as shown by immunoblotting, was again not obvious by immunofluorescence (**Figure 21a and b**, respectively). Phospho-Src/Yes/Fyn was localised at the sites of focal adhesions in the HT29 and HT29-FR cells with a small proportion locating at cell-cell junctions in the HT29-FR cells only (**Figure 21c and i**).

In the case of HCT-116 and HCT-116-FR cells, Src and Yes both localised at cell-cell adhesions (**Figure 22a** and **b**, respectively). Phospho-Src/Yes/Fyn in the HCT-116 and HCT-116-FR cells localised primarily at the sites of focal adhesions (**Figure 22c**), but some localisation was apparent at cell-cell contacts in both (**Figure 22c, i** and **ii**).

Next I examined the localisation of the cadherin junction proteins namely, E-cadherin, β -catenin and p120-catenin. Immunoblotting showed that H630 cells had no detectable E-cadherin, β -catenin or p120-catenin proteins and there was a substantial increase in all three proteins in the resistant H630-FR cells (**Figure 17c**). However, upon immunofluorescence analysis of H630 cells, some E-cadherin and β -catenin proteins were visible at cell-cell contacts in addition to cytoplasmic staining of E-cadherin (**Figure 23a** and **b**, respectively). Although cytoplasmic staining of p120-catenin was present, it did not appear to be localised to the cell membrane (**Figure 23c**). The H630-FR cells displayed strong cell-cell membrane staining of all three cadherin proteins, although there was also some cytoplasmic staining of β -catenin (**Figure 23**).

In the case of both HT29 and HT29-FR cells, localisation of E-cadherin, β -catenin and p120-catenin proteins was at the site of cell-cell contacts (**Figure 24**). Similarly, in the HCT-116 and HCT-116-FR cells, localisation of E-cadherin, β -catenin and p120-catenin was at the cell membrane in both (**Figure 25**).

I concluded from these experiments that, when present, the adherens junction proteins E-cadherin, β -catenin and p120-catenin localised to sites of cell-cell junctions at the cell membrane. H630 cells have very weak staining of all three cadherin proteins consistent with their mesenchymal morphology and immunoblotting results.

Figure 20 - Localisation of Src Family Kinase Proteins in H630 and H630-FR Cells

H630 and H630-FR cells (5×10^4 cells/19mm glass coverslip) were plated, grown for 2 days and fixed using the formaldehyde method (described in Materials and Methods section), before being probed with antibodies against the SFK proteins; **a)** Src, **b)** Yes, or **c)** phospho-Src/Yes/Fyn (shown in green; Alexa Fluor 488). Vectashield containing DAPI was used to visualise the nuclei (blue) and images were obtained using an Olympus FV1000 confocal microscope with a 60x objective. Scale bars 20 μ m.

Figure 20

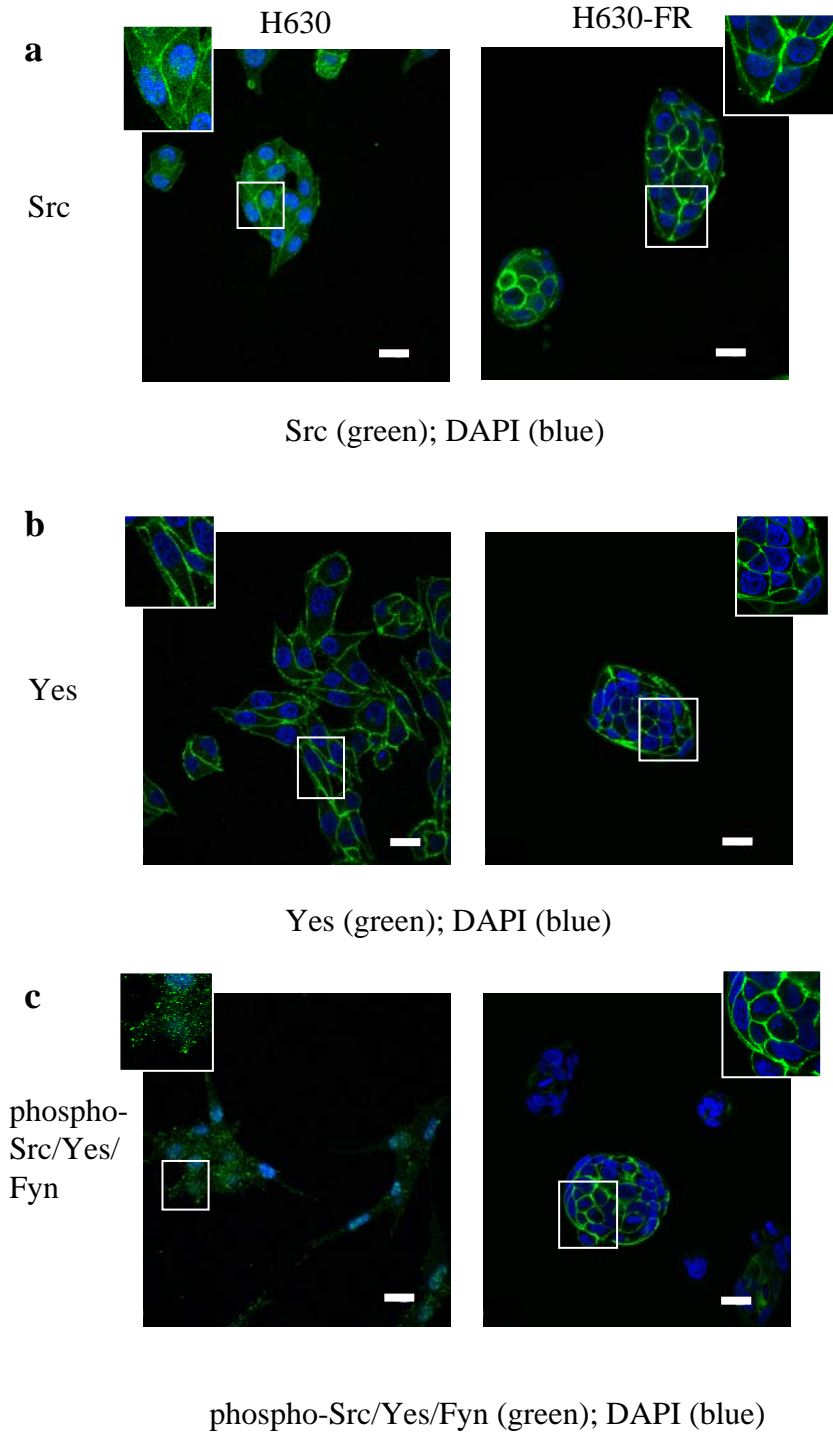


Figure 21 - Localisation of Src Family Kinase Proteins in HT29 and HT29-FR Cells

HT29 and HT29-FR cells (5×10^4 cells/19mm glass coverslip) were plated, grown for 2 days and fixed using the formaldehyde method (described in Materials and Methods section), before being probed with antibodies against the SFK proteins; **a)** Src, **b)** Yes, or **c)** phospho-Src/Yes/Fyn (shown in green; Alexa Fluor 488). **i)** phospho-Src/Yes/Fyn at cell-cell junctions in HT29-FR cells. Vectashield containing DAPI was used to visualise the nuclei (blue). Scale bars 20 μ m.

Figure 21

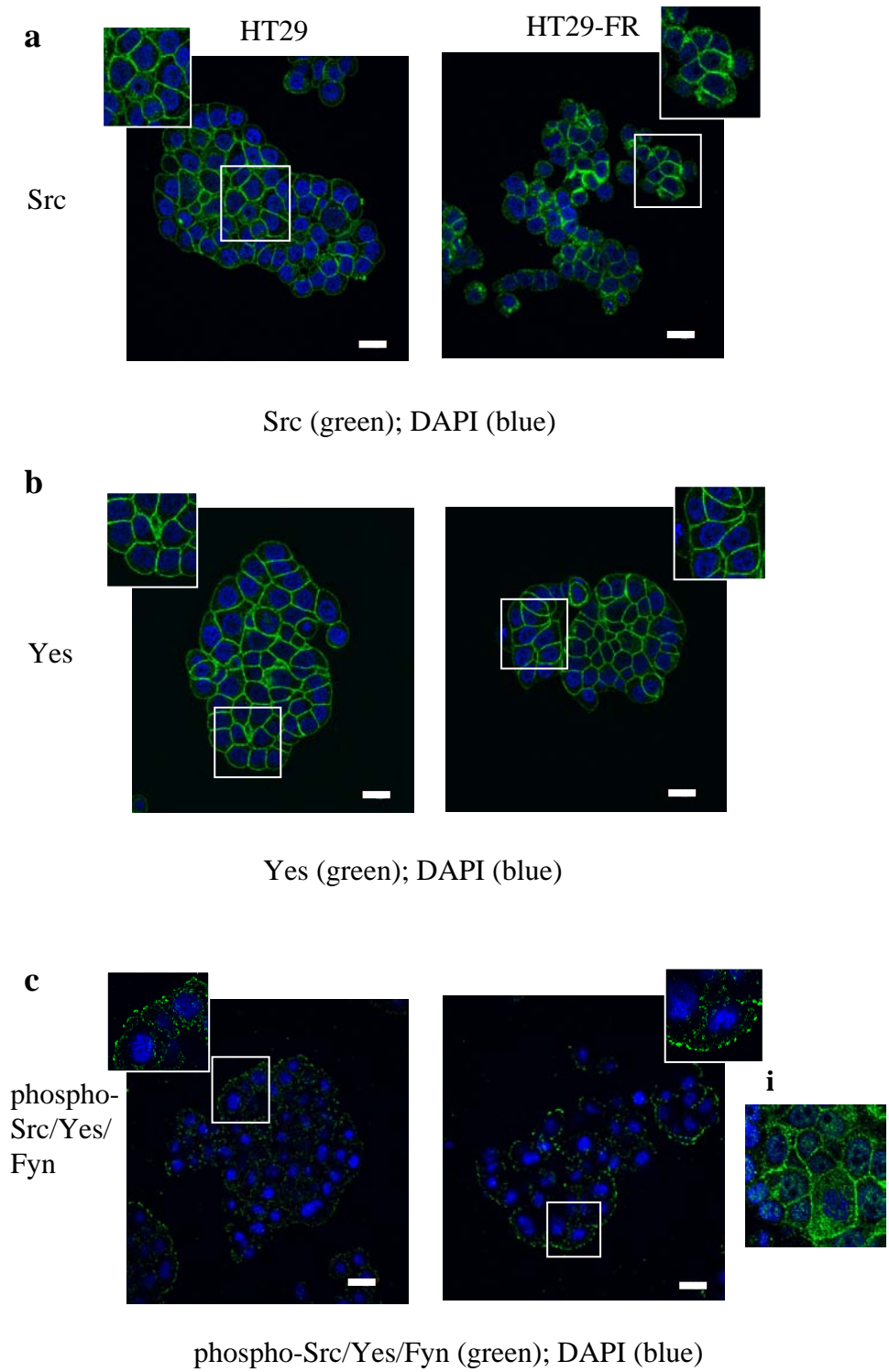


Figure 22 - Localisation of Src Family Kinase Proteins in HCT-116 and HCT-116-

FR Cells

HCT-116 and HCT-116-FR cells (5×10^4 cells/19mm glass coverslip) were plated, grown for 2 days and fixed using the formaldehyde method (described in Materials and Methods section), before being probed with antibodies against the SFK proteins; **a)** Src, **b)** Yes, or **c)** phospho-Src/Yes/Fyn (shown in green; Alexa Fluor 488). **i)** phospho-Src/Yes/Fyn at cell-cell junctions in HCT-116 cells. **ii)** phospho-Src/Yes/Fyn at cell-cell junctions in HCT-116-FR cells. Vectashield containing DAPI was used to visualise the nuclei (blue). Scale bars 20 μ m.

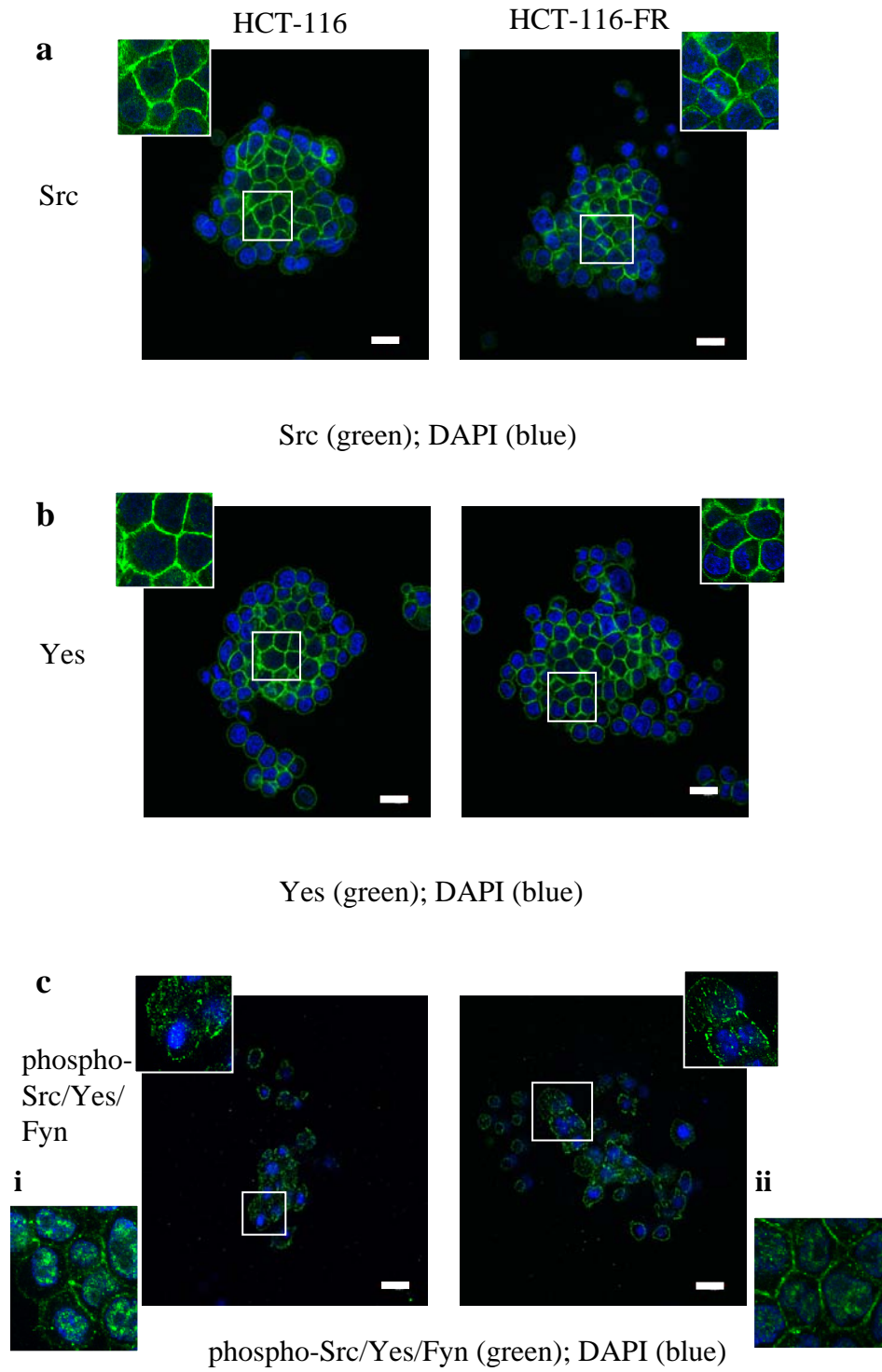
Figure 22

Figure 23 - Localisation of Adherens Junction Proteins in H630 and H630-FR Cells

H630 and H630-FR cells (5×10^4 cells/19mm glass coverslip) were plated, grown for 2 days and fixed using the formaldehyde method (with the exception of E-cadherin which was fixed using the paraformaldehyde method; described in Materials and Methods section), before being probed with antibodies against adherens junction proteins; **a)** E-cadherin, **b)** β -catenin, and **c)** p120-catenin (shown in green; Alexa Fluor 488). Vectashield containing DAPI was used to visualise the nuclei (blue). Faint E-cadherin and β -catenin staining in the H630 cells at cell-cell contacts is indicated by white arrows. Scale bars 20 μ m.

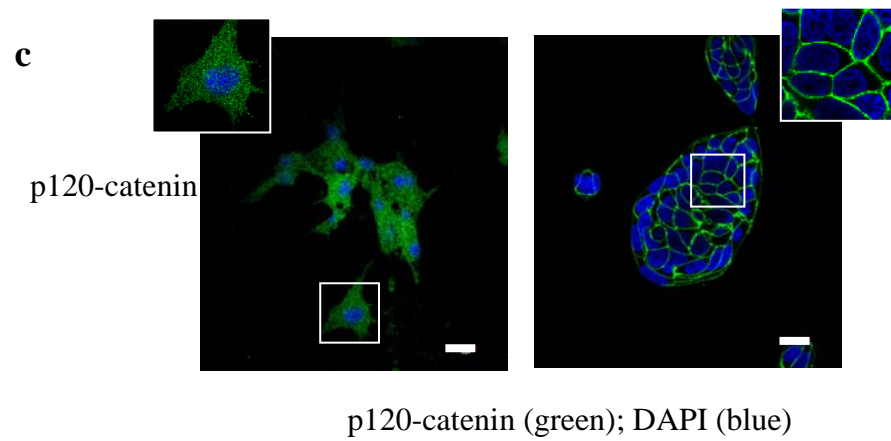
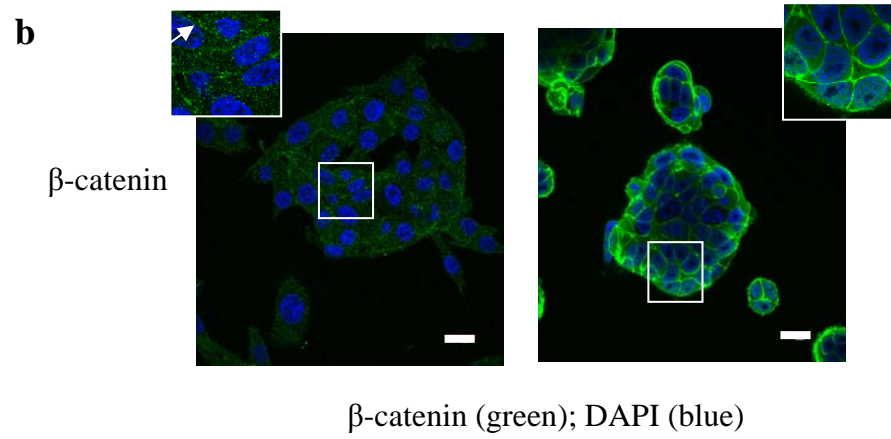
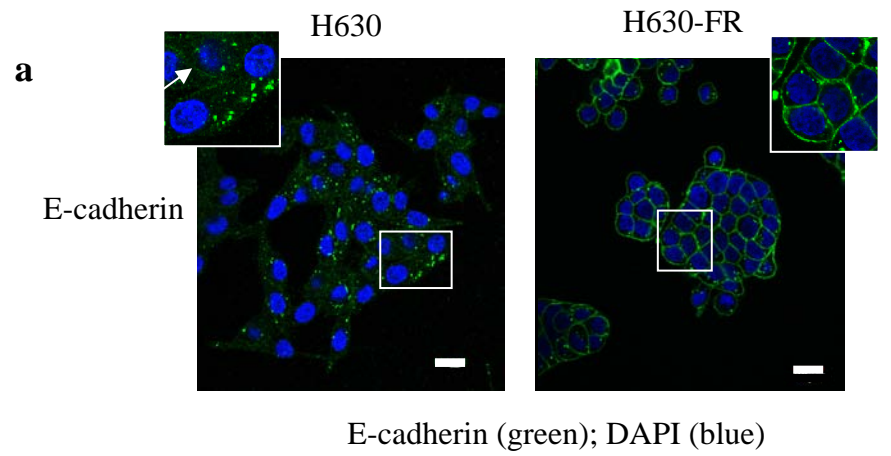
Figure 23

Figure 24 – Localisation of Adherens Junction Proteins in HT29 and HT29-FR Cells

HT29 and HT29-FR cells (5×10^4 cells/19mm glass coverslip) were plated, grown for 2 days and fixed using the formaldehyde method (with the exception of E-cadherin which was fixed using the paraformaldehyde method; described in materials and methods section), before being probed with antibodies against adherens junction proteins; **a)** E-cadherin, **b)** β -catenin, and **c)** p120-catenin (shown in green; Alexa Fluor 488). Vectashield containing DAPI was used to visualise the nuclei (blue). Faint E-cadherin and β -catenin staining in the H630 cells at cell-cell contacts is indicated by white arrows. Scale bars 20 μ m.

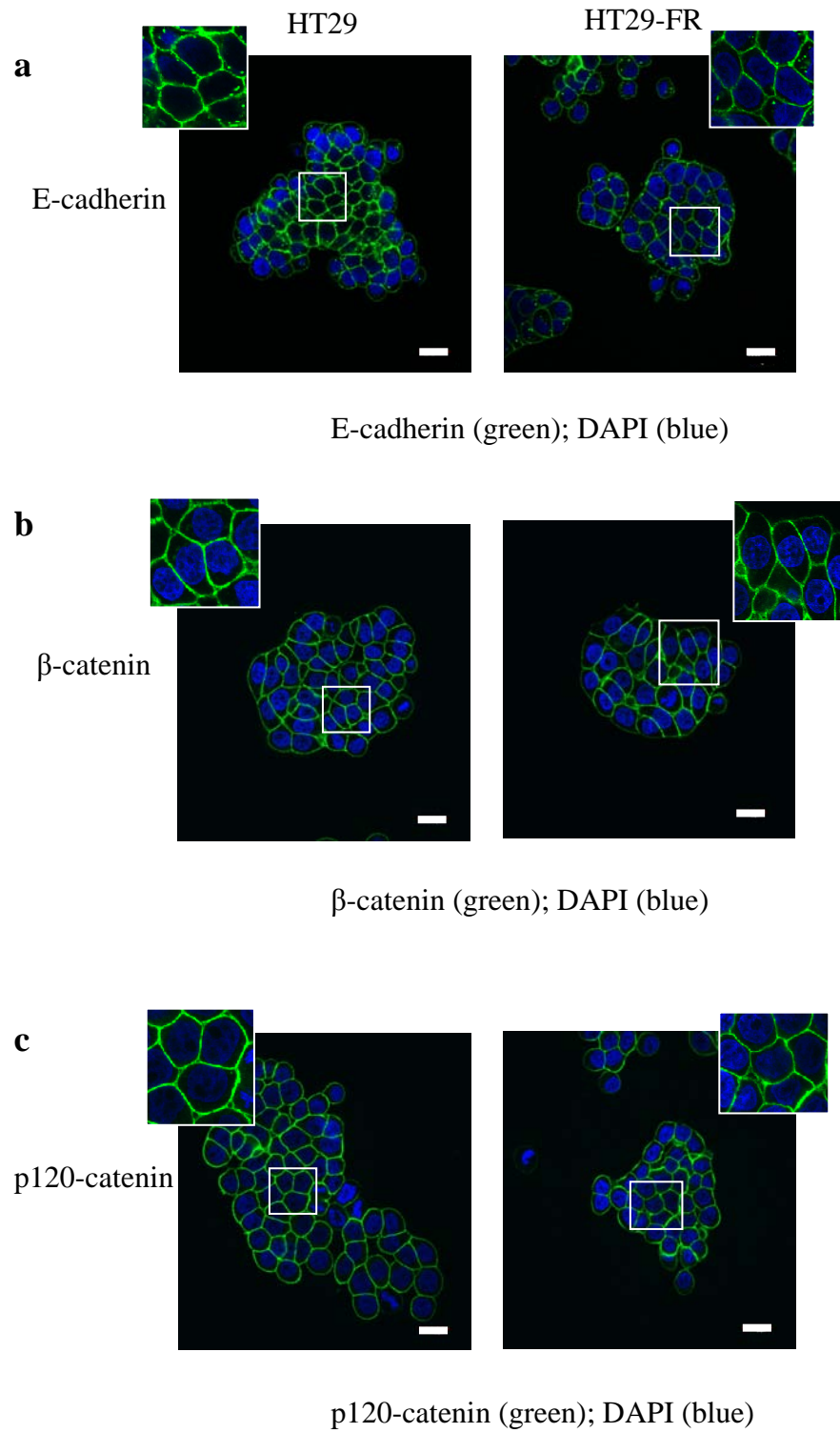
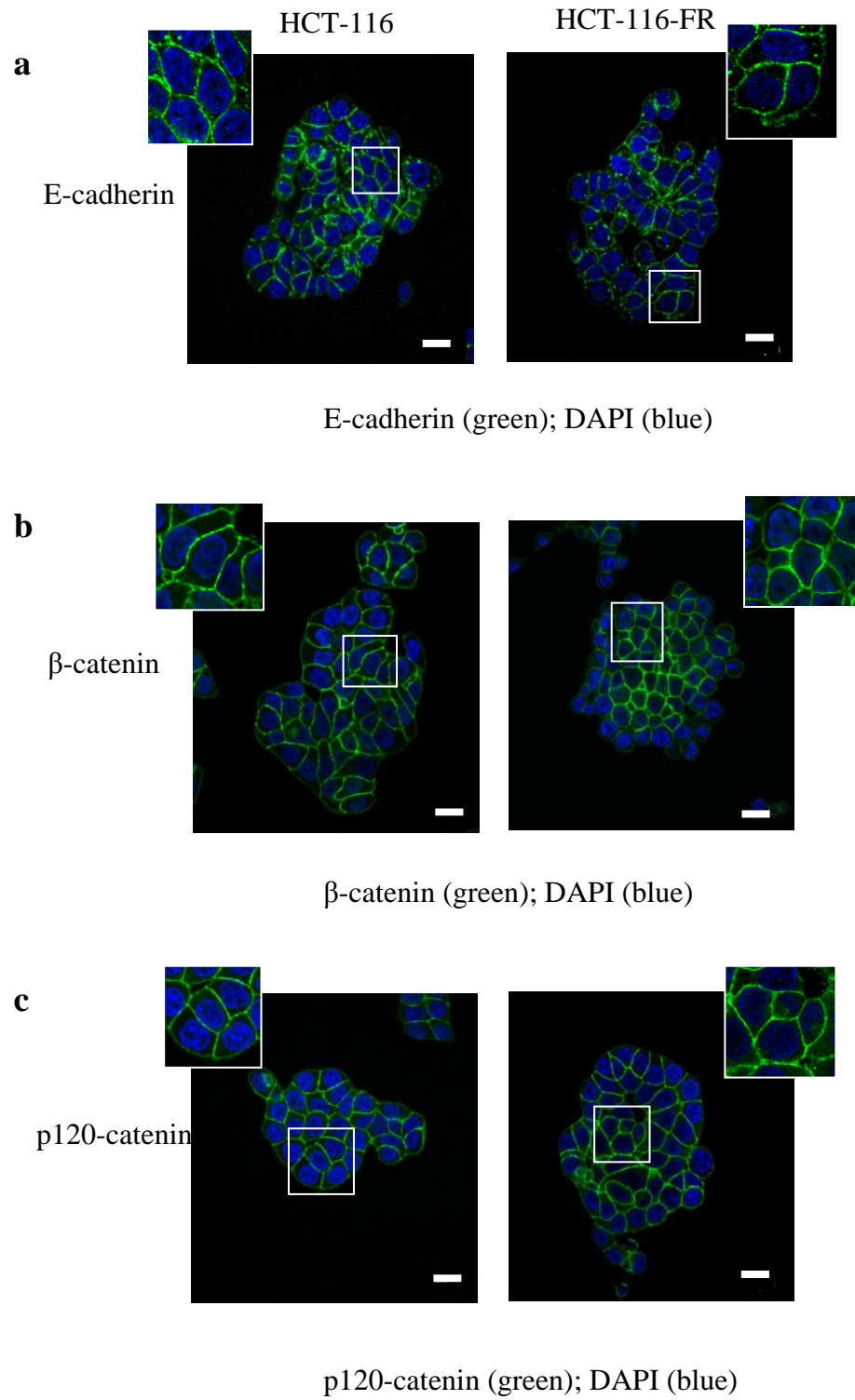
Figure 24

Figure 25 - Localisation of Adherens Junction Proteins in HCT-116 and HCT-116-FR Cells

HCT-116 and HCT-116-FR cells (5×10^4 cells/19mm glass coverslip) were grown for 2 days and fixed using the formaldehyde method (with the exception of E-cadherin which was fixed using the paraformaldehyde method; described in materials and methods section) before being stained with antibodies against cadherin junction proteins; **a)** E-cadherin, **b)** β -catenin, and **c)** p120-catenin (shown in green; Alexa Fluor 488). Vectashield containing DAPI was used to visualise the nuclei (blue). Faint E-cadherin and β -catenin staining in the H630 cells at cell-cell contacts is indicated by white arrows. Scale bars 20 μ m.

Figure 25

3.5. Monitoring E-cadherin Dynamics in HCT-116 and HCT-116-FR Cells

No difference was observed in static images of cell-cell junction proteins between the HCT-116 and HCT-116-FR cells. Therefore, Fluorescence Recovery After Photobleaching (FRAP) was employed as a means of perhaps detecting more subtle differences between dynamic movement of proteins in adherens junctions (Reits and Neefjes, 2001). Enhanced Green Fluorescent Protein-E-cadherin (eGFP-E-cadherin) molecules in a cell membrane are bleached by light emitted at 405nm, resulting in the irreversible removal of the eGFP fluorescence in the bleached region. The recovery of eGFP fluorescence by other molecules of eGFP-E-cadherin in the cells moving into the bleached region, for example, from the plasma membrane or the internal pool of eGFP-E-cadherin, quantified as a value representing the time it takes for 50% of the initial eGFP signal to return ($t_{1/2}$). After the eGFP signal plateaus, the proportion of bleached eGFP-E-cadherin molecules that are unable to move away from the bleached region (immobile fraction) and the proportion of molecules that are able to move (mobile fraction) can be deduced from a graph of fluorescence intensity changes over time (**Figure 26**).

FRAP was carried out using HCT-116 and HCT-116-FR cells because both cell lines displayed epithelial morphology and they showed substantial gain of resistance to 5-FU. E-cadherin with a carboxy-terminal eGFP tag pcDNA 3.1 vector (eGFP-E-cadherin; **Figure 27a**) was transiently transfected into HCT-116 and HCT-116-FR cells using Lipofectamine™ 2000 (**Figure 27b**). The transfection efficiency of eGFP-E-cadherin in these cells was around 20-40% and was sufficient to perform FRAP on an eGFP-E-cadherin expressing colony (**Figure 27b**; described in Materials and Methods section). Prior to bleaching, the eGFP-E-cadherin in both the HCT-116 and resistant HCT-116-FR cells was uniformly localised at the cell membrane and eGFP signal was lost upon bleaching with the laser (**Figure 28a**).

From the fluorescence recovery data collected, the $t_{1/2}$ for the HCT-116 cells was calculated to be around twice as fast, as that obtained for the HCT-116-FR cells (**Figure 28b**). In HCT-116 cells, $t_{1/2}$ was around 26 seconds whereas in the HCT-116-FR cells $t_{1/2}$ was around 54 seconds. The immobile fractions were not substantially different between the cell lines.

This demonstrated that even although we could not visualise differences in E-cadherin localisation by static imaging, there were altered adhesion dynamics resulting in a difference in the rate of recovery of E-cadherin molecules from the plasma membrane between sensitive and resistant cells.

Therefore, I concluded, that a decreased rate of recovery of E-cadherin was evident in the HCT-116-FR cells when compared to the HCT-116 cells, implying that the adhesion dynamics in the resistant cells were altered upon acquisition of 5-FU resistance.

3.6. Assessment of Cell-Cell Junctions by Aggregation Assay

Results from previous figures suggested that there may be differences in the cell-cell contacts between 5-FU-sensitive and -resistant cells. In order to investigate this, aggregation assays were used to measure the ability of single cells to adhere to each other and form aggregates in the presence of low or high calcium. The cell pairs, namely H630 and H630-FR cells, HT29 and HT29-FR cells and HCT-116 and HCT-116-FR cells were dissociated using Cell Dissociation Buffer (CDB) (described in Materials and Methods) and single cells generated using a 21G needle and syringe. 1×10^6 cells were incubated for 1 hour with constant agitation in Keratinocyte Basal Medium (KBM) (described in Materials and Methods) containing either low calcium (0.03mM) or high calcium (1.5mM) before being resuspended in 50 μ l PBS and analysed using a haemocytometer. Differences in single cells, number of aggregates and aggregate areas were monitored. Aggregates were classed as a colony of greater than or equal to 10 cells.

In low calcium medium, no aggregates were formed for any cell lines and the majority of cells remained as single cells (**Figures 29a, 30a and 31a**). In high calcium, the H630 cells remained largely as single cells whereas the H630-FR cells formed an average of 45 aggregates (with an average area of $1012\mu\text{m}^2$) with only 15 single cells remaining (**Figure 29**).

In high calcium, the HT29 and HT29-FR cells displayed a similar number of aggregates, but these differed in size – monitored by the area of the haemocytometer covered, with the aggregates formed by the HT29-FR cells being larger ($2127.98\mu\text{m}^2$ in HT29-FR cells when compared to $943\mu\text{m}^2$ in the HT29 cells). The remaining single cells in the HT29 and HT29-FR cells were similar in number (**Figure 30**).

In high calcium, the HCT-116 and HCT-116-FR cells displayed a similar number of aggregates formed. The average size of aggregates formed was larger in the HCT-116-FR cells ($5417\mu\text{m}^2$ in HCT-116-FR cells when compared to $2662\mu\text{m}^2$ in the HCT-116 cells). A comparable number of single cells remained in the HCT-116 and HCT-116-FR cells (**Figure 31**).

In each resistant cell line a large colony has been highlighted to illustrate how colony size was measured. However, this was for demonstration purposes only and every colony ≥ 10 cells was counted (**Figures 29c, 30c and 31c**).

From these aggregation assays, I concluded that in all three of the 5-FU resistant cell pairs assayed, an increased ability to form aggregates was displayed, each generating aggregates of a greater size than their corresponding sensitive counterparts. This result was consistent with enhanced cell-cell adhesions observed in the resistant cell lines suggesting that adhesion dynamics are altered upon acquisition of 5-FU resistance.

Figure 26 - Fluorescence Recovery After Photobleaching (FRAP)

The basic principle of FRAP is depicted by illustrating eGFP-E-cadherin molecules in a cell membrane being bleached by light emitted at 405nm (at $t_B=t_0$), resulting in the irreversible removal of the eGFP-labelled E-cadherin signal ($I_B=I_0$). The recovery of eGFP fluorescence by other molecules of eGFP-E-cadherin moving into the bleached region is monitored over time – for example the time taken for 50% of the initial eGFP signal ($I_{1/2}$) to return ($t_{1/2}$) to a plateau (I_p). The proportion of bleached eGFP-E-cadherin molecules that are unable to move from the target region (immobile fraction) and the proportion of molecules that are able to move (mobile fraction) were depicted from a graph of fluorescence intensity over time. Initial intensity (I_i)

Figure 26

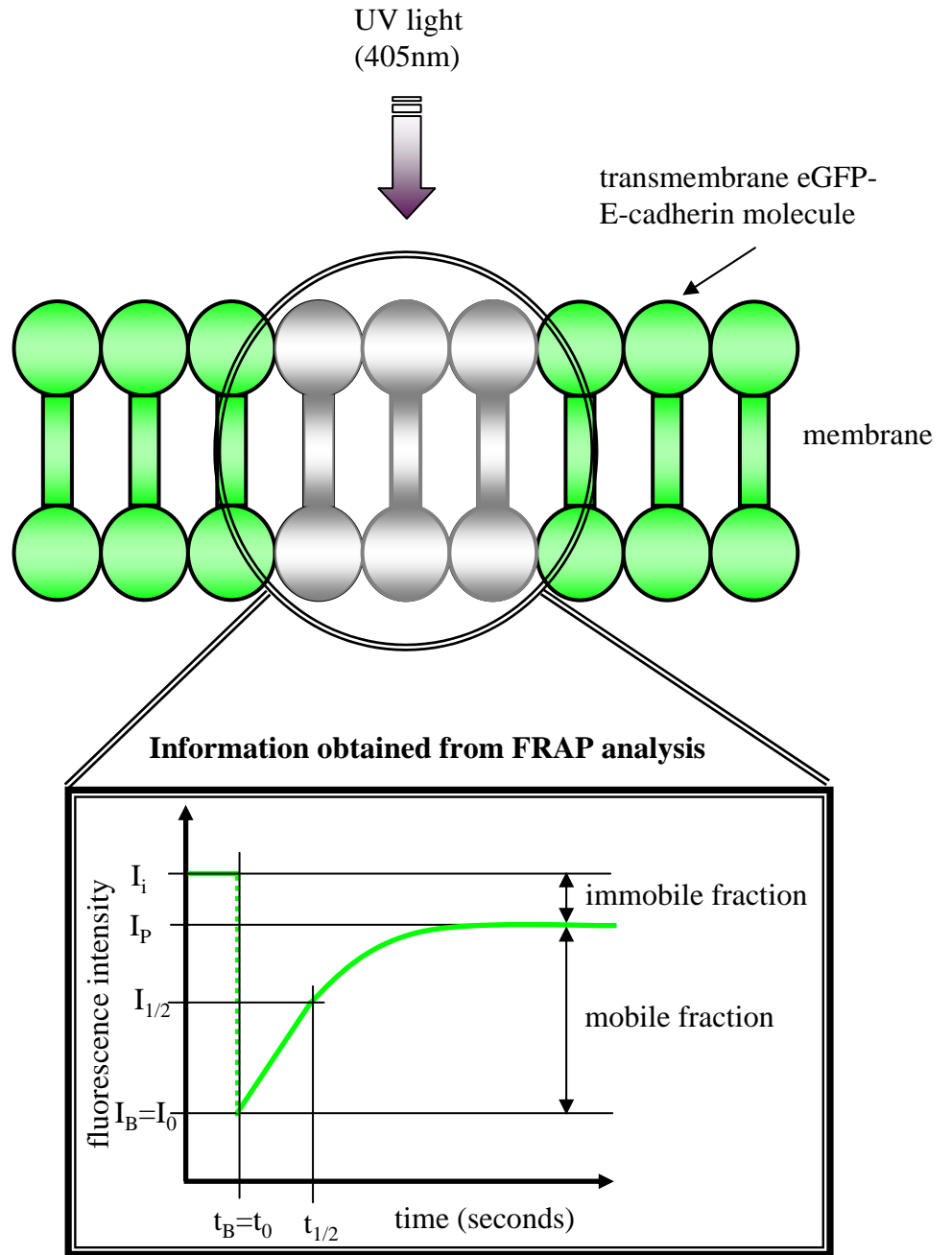
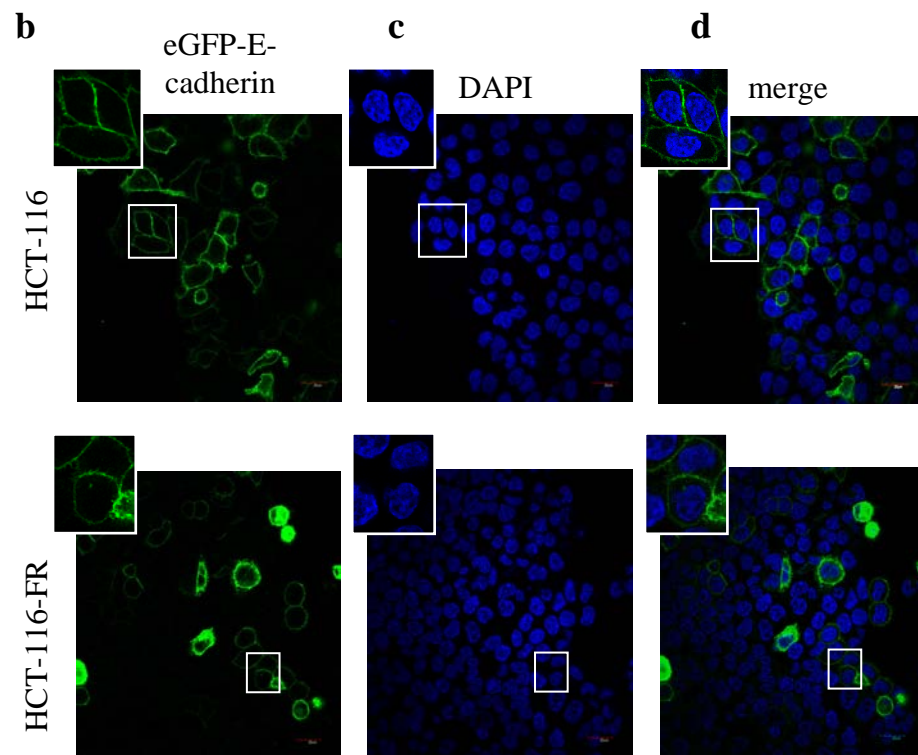
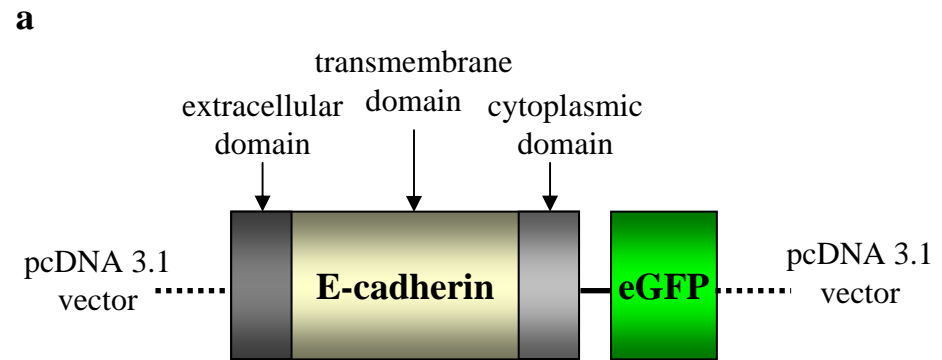
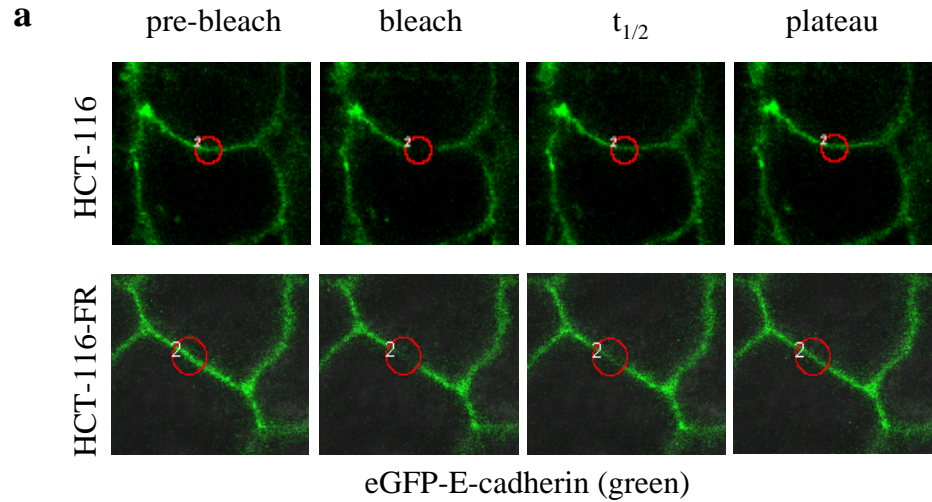


Figure 27 - eGFP-E-cadherin in HCT-116 and HCT-116-FR Cells

a) An illustrative diagram of E-cadherin with carboxy-terminal eGFP tag in the pcDNA 3.1 vector (eGFP-E-cadherin). **b)** 1×10^5 HCT-116 and HCT-116-FR cells were plated onto 19mm coverslips and transiently transfected with eGFP-E-cadherin using Lipofectamine™ 2000. Cells were grown for 2 days before being fixed using the GFP fix method (described in Materials and Methods section). **c)** Vectashield containing DAPI was used to visualise the nuclei. **d)** An overlaid image with both the eGFP-E-cadherin and DAPI staining is also shown.

Figure 27

eGFP-E-cadherin (green); DAPI (blue)

Figure 28**b**

Cell Line	$t_{1/2}$	Immobile Fraction	$t_{1/2}$ Normalised to HCT-116 cells
HCT-116	25.854 sec	11.22%	1
HCT-116-FR	54.321 sec	13.89%	2.1

FRAP in HCT-116 and HCT-116-FR Cells

a) HCT-116 and HCT-116-FR cells were transiently transfected with eGFP-E-cadherin using Lipofectamine™ 2000 and 1×10^6 cells were plated onto to glass-bottomed 30mm tissue culture dish for 2 days (described in Materials and Methods section). FRAP was performed and images were taken at pre-bleach, point of bleach occurring, time of 50% recovery of initial fluorescence ($t_{1/2}$) and point of plateau of fluorescence.

b) From FRAP data collected, a $t_{1/2}$ and immobile fraction were calculated for HCT-116 and HCT-116-FR cells.

Figure 29 - Aggregation Assay with H630 and H630-FR Cells

H630 and H630-FR cells were dissociated by chelating calcium ions using Cell Dissociation Buffer (CDB) and single cells were generated using a 21G needle and syringe, before being incubated in Keratinocyte Basal Medium (KBM) containing either; **a)** low calcium (0.03mM) or **b)** high calcium (1.5mM) for 1 hour at room temperature with constant agitation. After this time I quantified; **d)** single cells remaining, **e)** the number of aggregates formed and **f)** their colony area. Illustration for the measuring of aggregate area using ImageJ software is shown (**c)**). Aggregates were classed as a colony of ≥ 10 cells. Average values were obtained over three experiments and standard deviations were calculated. Average areas of colonies were calculated for a representative experiment and standard deviations were calculated using the colony areas obtained in that experiment.

Figure 29

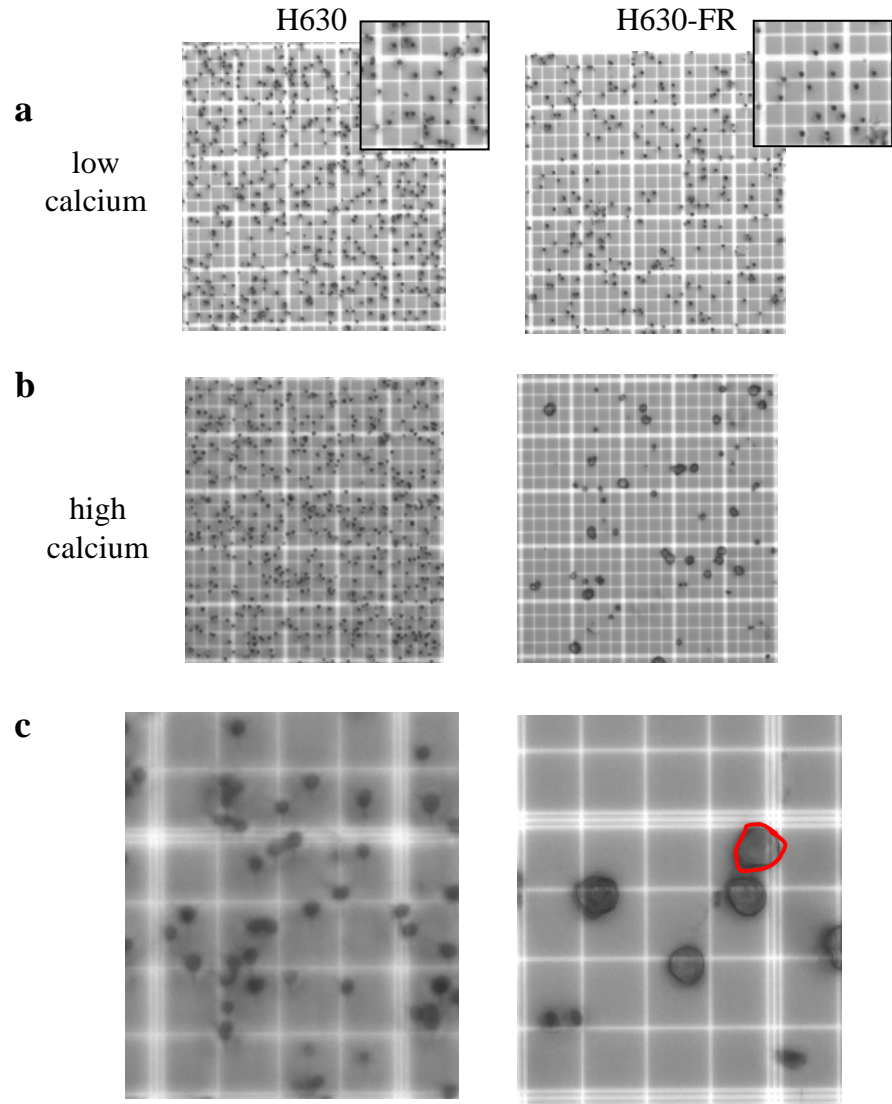
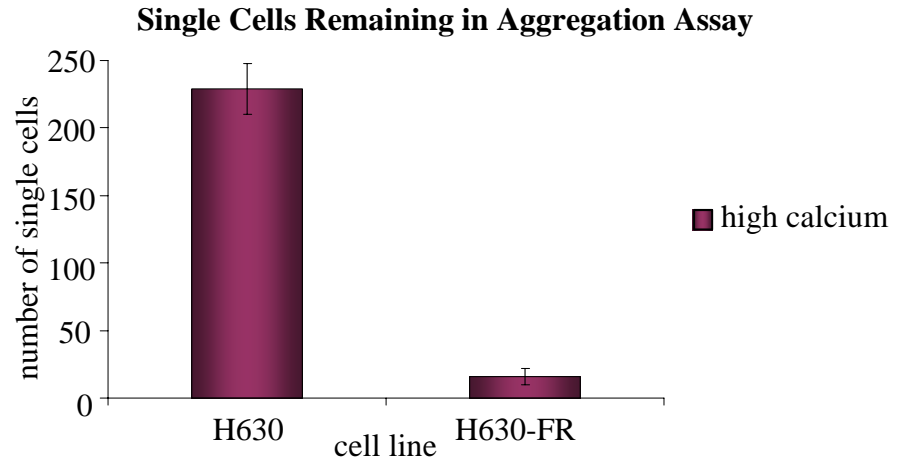
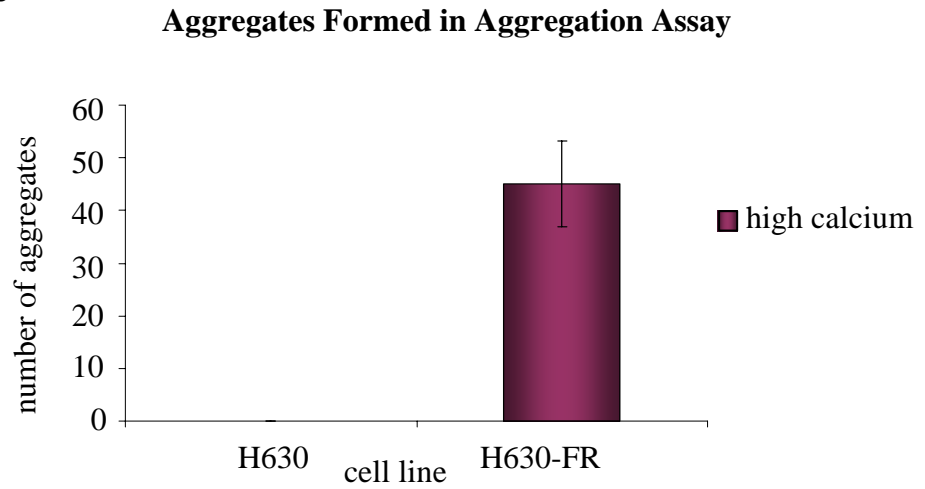


Figure 29 - continued

d



e



f

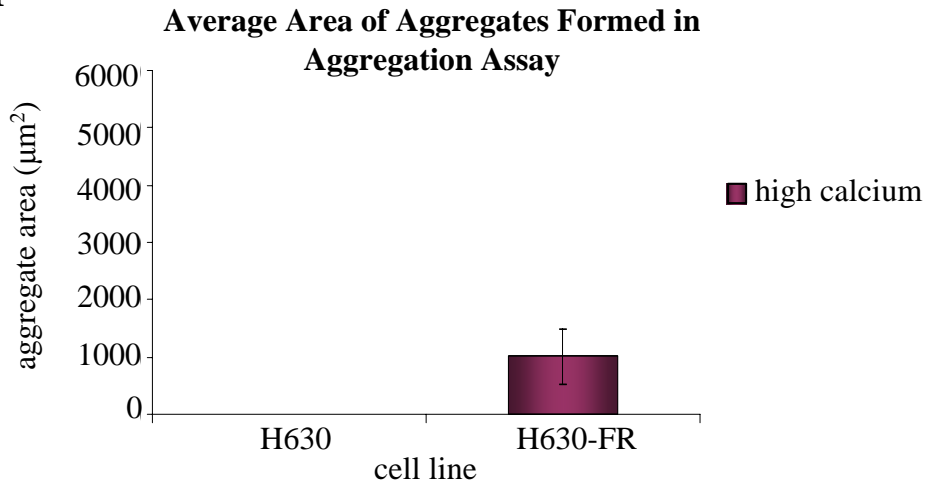
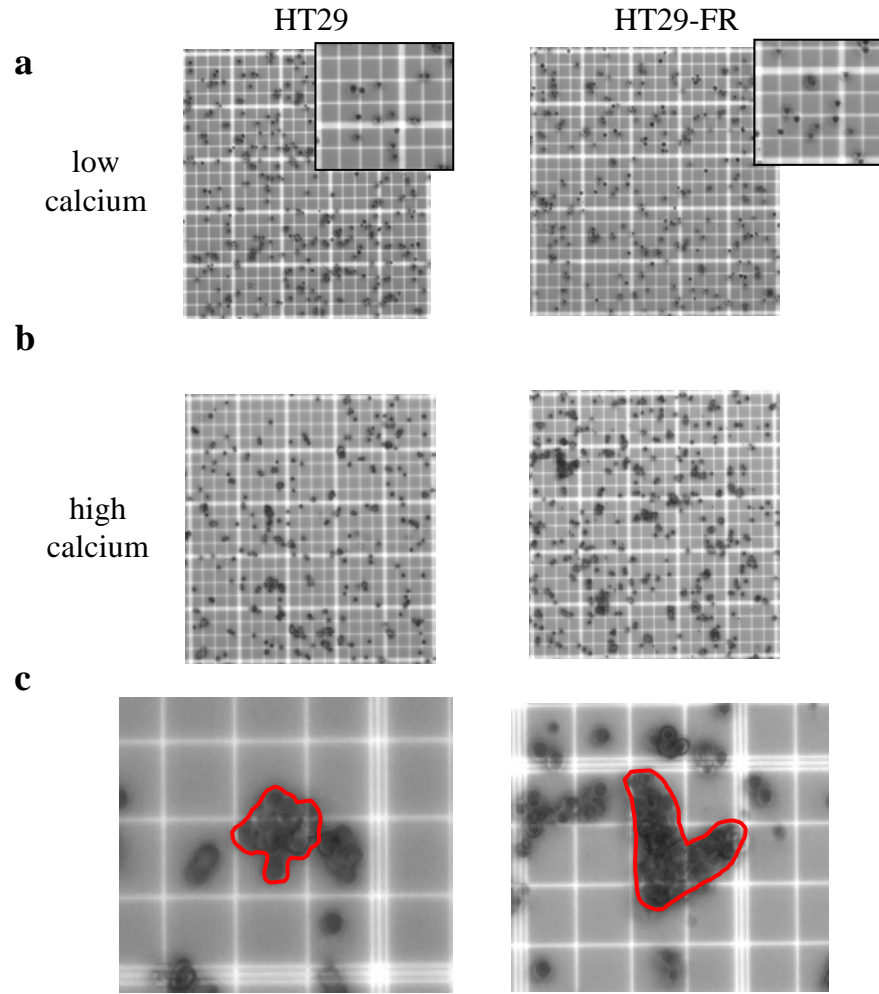


Figure 30 – Aggregation Assay with HT29 and HT29-FR Cells

HT29 and HT29-FR cells were dissociated by chelating calcium ions using CDB and single cells were generated using a 21G needle and syringe, before being incubated in KBM containing either; **a)** low calcium (0.03mM) or **b)** high calcium (1.5mM) for 1 hour at room temperature with constant agitation. After this time I quantified; **d)** single cells remaining, **e)** the number of aggregates formed and **f)** their colony area. Illustration for the measuring of aggregate area using ImageJ software is shown **(c)**. Aggregates were classed as a colony of ≥ 10 cells. Average values were obtained over three experiments and standard deviations were calculated. Average areas of colonies were calculated for a representative experiment and standard deviations were calculated using the colony areas obtained in that experiment.

Figure 30



c

Figure 30 - continued

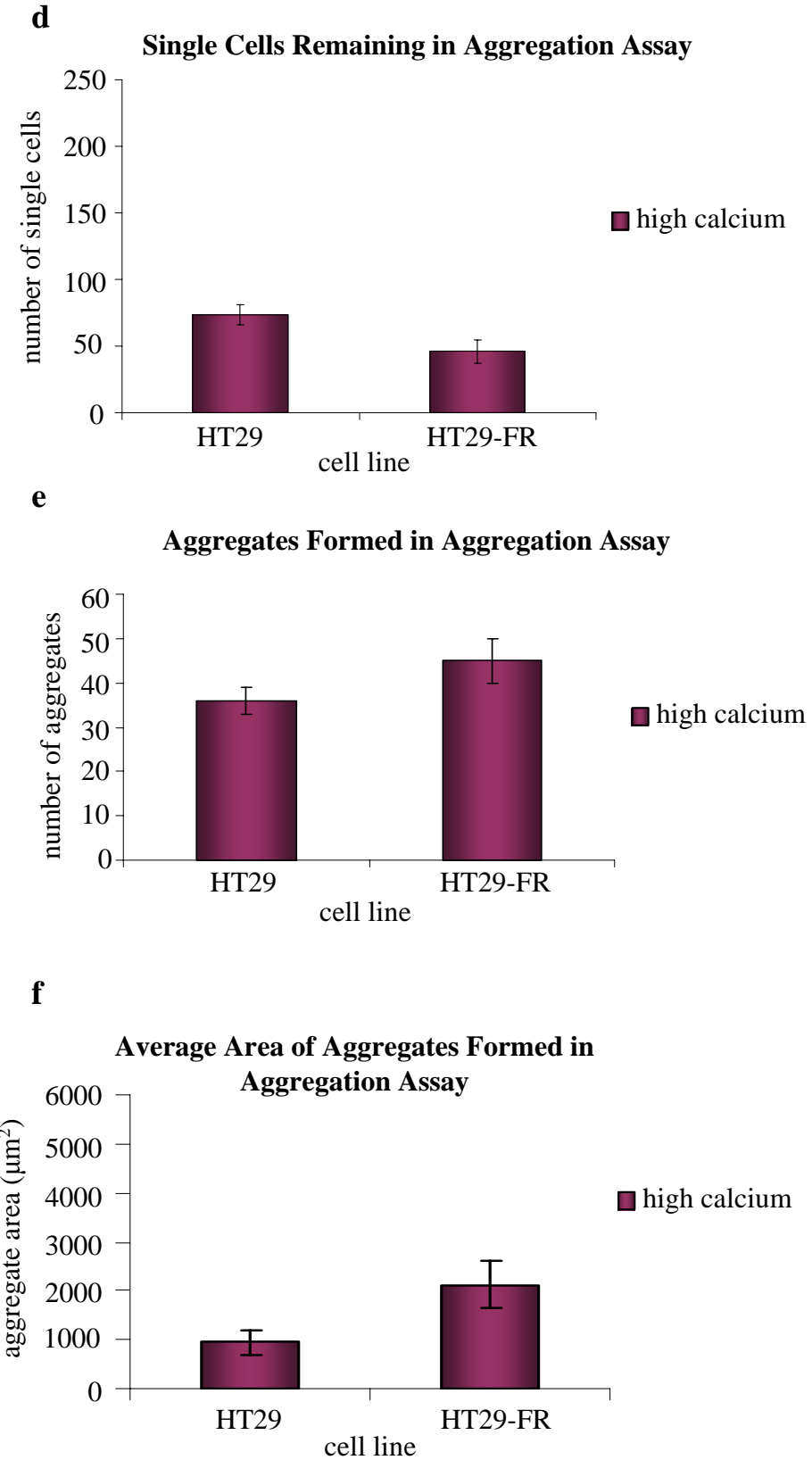


Figure 31 - Aggregation Assay with HCT-116 and HCT-116-FR Cells

HCT-116 and HCT-116-FR cells were dissociated by chelating calcium ions using Cell Dissociation Buffer (CDB) (refer to Materials and Methods section) and single cells were generated using a 21G needle and syringe, before being incubated in Keratinocyte Basal Medium (KBM) containing either; **a**) low calcium (0.03mM) or **b**) high calcium (1.5mM) for 1 hour at room temperature with constant agitation. After this time I quantified; **d**) single cells remaining, **e**) the number of aggregates formed and **f**) their colony area. Illustration for the measuring of aggregate area using ImageJ software is shown (**c**). Aggregates were classed as a colony of ≥ 10 cells. Average values were obtained over three experiments and standard deviations were calculated. Average areas of colonies were calculated for a representative experiment and standard deviations were calculated using the colony areas obtained in that experiment.

Figure 31

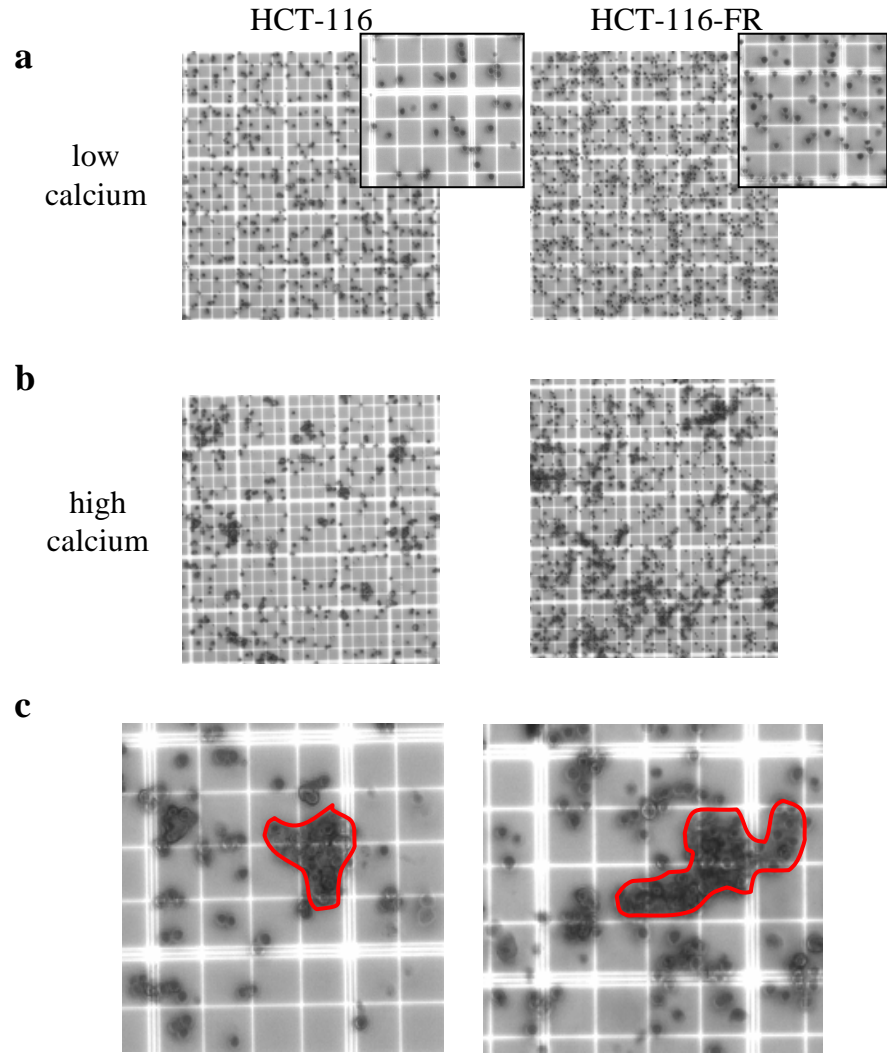
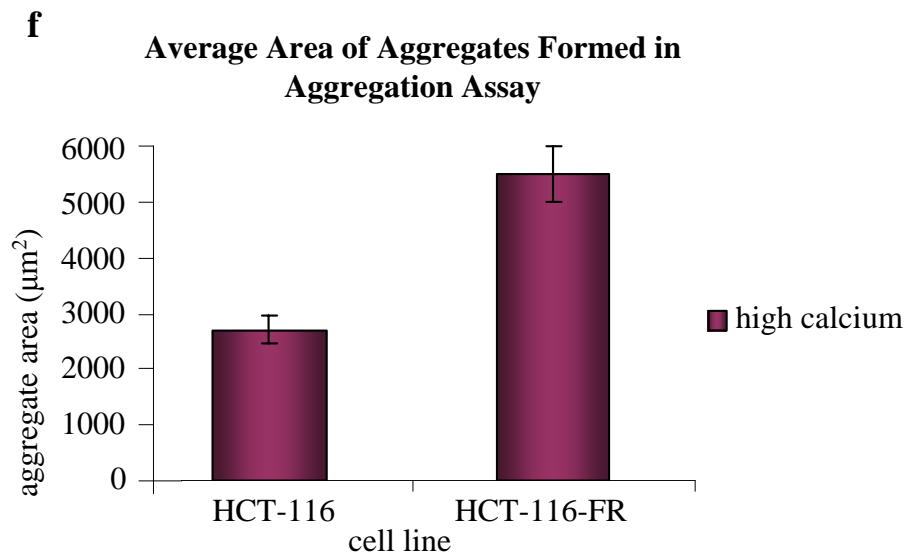
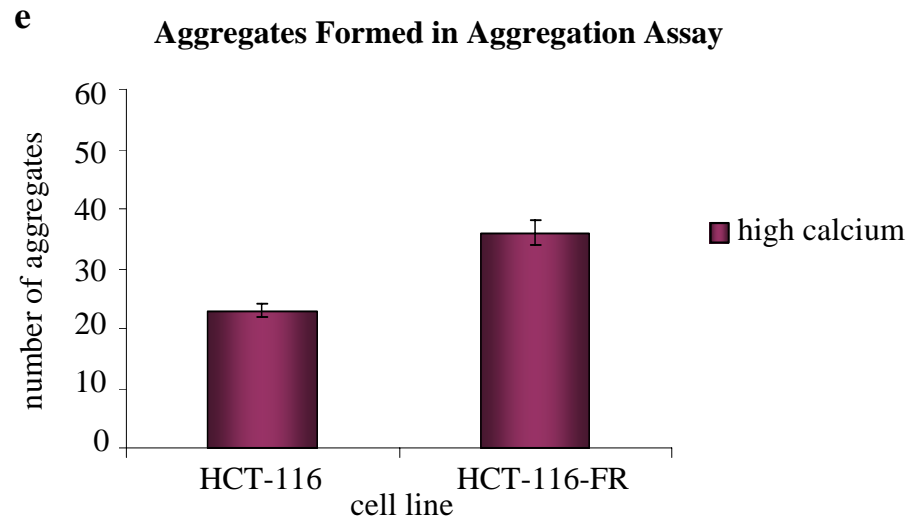
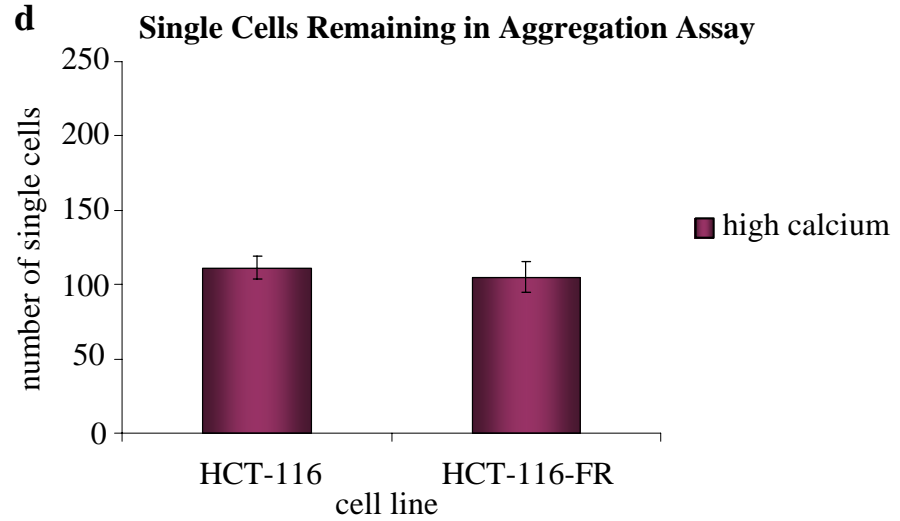


Figure 31 - continued



3.7. Summary

From the data generated during the characterisation of 3 pairs of 5-FU-sensitive and -resistant cell pairs, I concluded that there were morphological changes associated with acquisition of drug resistance, as well as the expected increase in expression of TS. Specifically, there was enhanced cell to cell association, which was evident to varying degrees in the different cell pairs, and this could be linked to alterations in expression and/or activities of adhesion proteins. In one cell pair, acquisition of resistance was associated with a visible mesenchymal to epithelial transition; in the other two cell pairs, the cells were already epithelial in morphology, with E-cadherin present at the cell-cell junctions as judged by static images. However, in one of these, I was able to demonstrate altered E-cadherin dynamics. Finally, the Src family kinases are implicated in control of cell-cell association, and I observed that Yes expression was increased in 5-FU-resistant cells. This was almost certainly a result of coincidental co-amplification of the gene encoding Yes with the gene encoding TS (these are very closely located on chromosome 18). This led to increased activity of Src/Yes/Fyn in the 5-FU-resistant cells.

As a result of these observations, I next investigated whether Yes played a role in the acquisition of 5-FU-resistance using the HCT116 cell pair as a model, and went on to determine whether there was a direct role for the adherens junction protein E-cadherin, and if so, to try to establish the molecular mechanism.

4. Assessing the Role of SFK Yes in Resistance to 5-FU

Cancer cells overcome direct inhibition of TS by 5-FU metabolites by up-regulating the TS gene after 5-FU treatment in order to counteract the amount of inactive ternary complexes formed between the active metabolite of 5-FU, FdUMP, the cofactor CH₂TF, and TS (**Figure 2**) (Copur et al., 1995; Kanaan et al., 2007). The gene encoding a SFK, c-Yes1 tyrosine kinase (Yes) is located on the same amplicon, less than 50kb away from TS (Silverman et al., 1993). The close proximity of these two genes means that Yes expression is increased concurrently with TS over-expression in 5-FU resistant cells, as I showed in all three resistant cell lines (**Figures 17-19**). Therefore, as SFKs regulate adherens junctions, which I also found altered, I next addressed the role, if any, played by the increased Yes protein displayed in the resistant cell line HCT-116-FR, with the aim of possibly linking an increase in Yes protein in 5-FU resistant cells with survival signals generated from E-cadherin. This cell pair was chosen because they displayed epithelial morphology which enables adherens junctions in the HCT-116-FR Yes RNAi cells to be directly compared to adherens junctions in the parental cells, HCT-116 cells. In addition, they also showed an increase in Yes protein with substantial gain of resistance to 5-FU. By knocking down Yes in these cells, could resistance to 5-FU be reversed and hence sensitivity to this chemotherapeutic be restored?

4.1. Co-localisation of Yes and E-cadherin

Firstly, immunofluorescence was performed to assess co-localisation of Yes and E-cadherin proteins in HCT-116 and HCT-116-FR cells to determine if any change in Yes localisation occurred when the protein expression was elevated. Cells were plated and grown for 2 days, fixed and co-stained with antibodies against Yes (**Figure 32a**) and E-cadherin (**Figure 32b**). The merged images demonstrated that Yes and E-cadherin co-localise in both HCT-116 and HCT-116-FR cells (**Figure 32c**; co-localisation shown by

white arrows). Thus, I concluded that the increase in Yes shown in the HCT-116-FR cells concurrent with acquisition of 5-FU resistance does not aberrantly affect the co-localisation of Yes with E-cadherin.

4.2. Vector Based RNAi System

To suppress expression of Yes, I used the two commercially available Yes RNAi's (Yes 1 RNAi and Yes 2 RNAi directed against two differing sections of the Yes protein) available from Invitrogen BlockiT™. The two different Yes RNAi vectors directed against two differing sections of the Yes protein. These were inserted into the pcDNA™ 6.2-EmGFP-miR validated vector. This vector has the advantage of having a pol II promoter allowing co-cistronic expression of Emerald Green Fluorescent Protein (EmGFP) and the Yes RNAi which provided identification of cells successfully transfected with the vector (**Figure 33**). Control RNAi containing a scrambled sequence, which is not directed to any human gene, was used as a control to monitor non-specific effects of the RNAi vector and the selection of RNAi expressing cells (**Figure 35a**). A blasticidin gene marker allows for selection of the vector in transfected cells.

HCT-116-FR Yes 1 (HFRY1) RNAi cells, HCT-116-FR Yes 2 (HFRY2) RNAi cells and HCT-116-FR control (HFRC) RNAi cells were generated by transfection of the respective vectors using Lipofectamine™ 2000 into HCT-116-FR cells (**Figure 34**). Transfected cells were maintained in medium containing 10µg/ml blasticidin for 21 days to select cells expressing the RNAi vector, after which time they were plated onto coverslips and the knockdown of Yes protein analysed by immunofluorescence (**Figure 35b** and **c**). In the control HFRC RNAi cells, no decrease in Yes staining was found in EmGFP positive cells (**Figure 35a**). However, in the case of HFRY1 RNAi and the HFRY2 RNAi cells which expressed EmGFP, there was a visible reduction in Yes protein at cell-cell junctions (**Figure 35b** and **c**; broken white arrows). In HFRY1 RNAi and HFRY2 RNAi cells that

lack EmGFP expression, Yes protein staining was not suppressed (**Figure 35b** and **c**; solid white arrows). Blasticidin was removed for 7 days prior to Fluorescence-Activated Cell Sorting (FACS) using the expressed EmGFP. From this EmGFP-enriched population of cells, single cell clones were generated and immunoblotting was performed to determine Yes protein levels (**Figure 36**). Actin loading was used as a control and uneven loading was normalised to actin using densitometry (only certain clones shown; **Figure 37**). In a number of HFRC RNAi, HFRY1 RNAi and HFRY2 RNAi clones, a faster migrating species (of lower molecular weight than Yes) was present, although its identity or its significance at this time remains unclear.

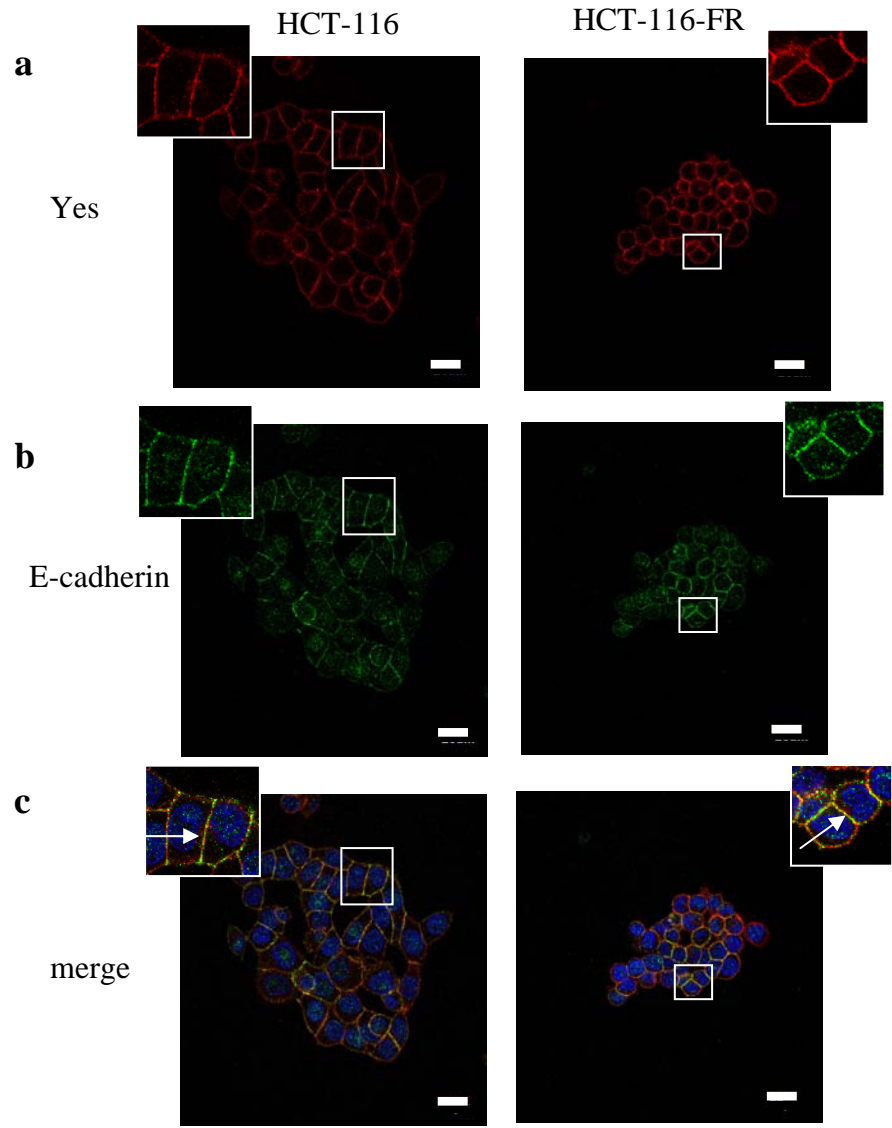
In the 7 HFRC RNAi clones generated, there was no down-regulation of Yes when compared to HCT-116-FR cells (**Figure 36a**). In the HFRY1 RNAi clones, all 7 displayed equal Yes protein expression when compared to the HCT-116-FR cells, showing that Yes protein was not suppressed (**Figure 36b**). However, in the HFRY2 RNAi clones, 2/11 single cell clones displayed a reduction in the total Yes protein (**Figure 36c**). A reduction in Yes protein was not shown in all clones analysed which may have been caused by a number of internal mechanisms. These were not investigated further.

HFRY2 RNAi-clone1 cells displayed a level similar to that of the total Yes protein in the HCT-116 cells, while HFRY2 RNAi-clone 12 cells had an almost complete knockdown of Yes protein (**Figure 36c**). HFRC RNAi clones 3 and 24 were chosen because their EmGFP expression was similar to that of the HFRY2 RNAi clones 1 and 12 respectively (**Figure 37**). Thus, I successfully generated stable Yes knockdown cells, with corresponding control cells that would be used to test the role of Yes as a possible determinant of altered morphology, E-cadherin status and drug resistance.

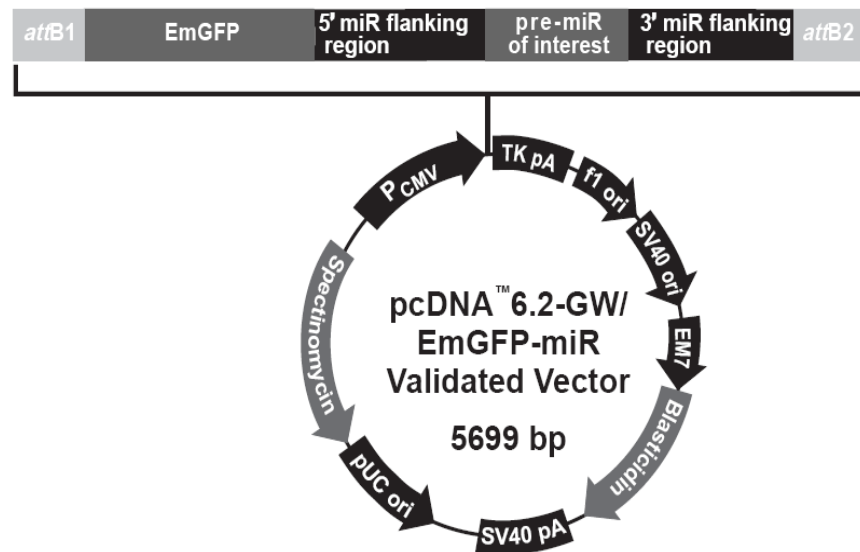
Figure 32 - Localisation of Yes and E-cadherin in HCT-116 and HCT-116-FR Cells

HCT-116 and HCT-116-FR cells (5×10^4 cells/19mm glass coverslip) were plated, grown for 2 days and fixed using the paraformaldehyde method (described in Materials and Methods section) before being probed with antibodies against; **a**) Yes (shown in red; Alexa Fluor 594) and **b**) E-cadherin (shown in green; Alexa Fluor 488). Vectashield containing DAPI was used to visualise the nuclei (blue). **c**) A merged image is also shown. Co-localisation of Yes and E-cadherin is shown (shown in yellow; white arrow). Scale bars 20 μ m.

Figure 32



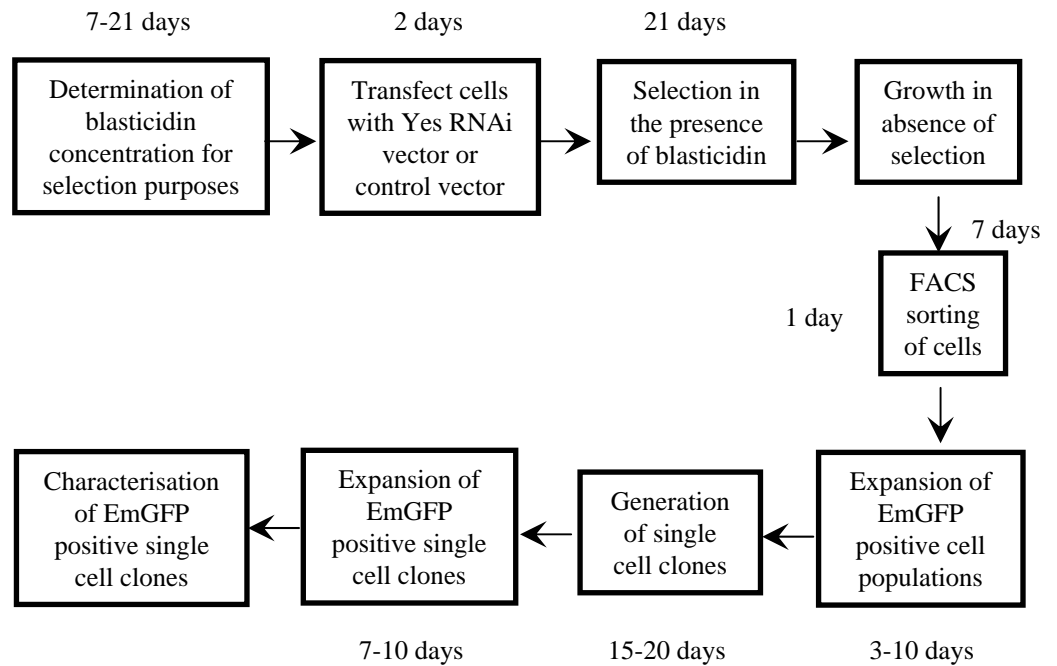
DAPI (blue); Yes (red); E-cadherin (green)

Figure 33

pcDNA™ 6.2-EmGFP-miR Vector Used for Yes RNAi Expression

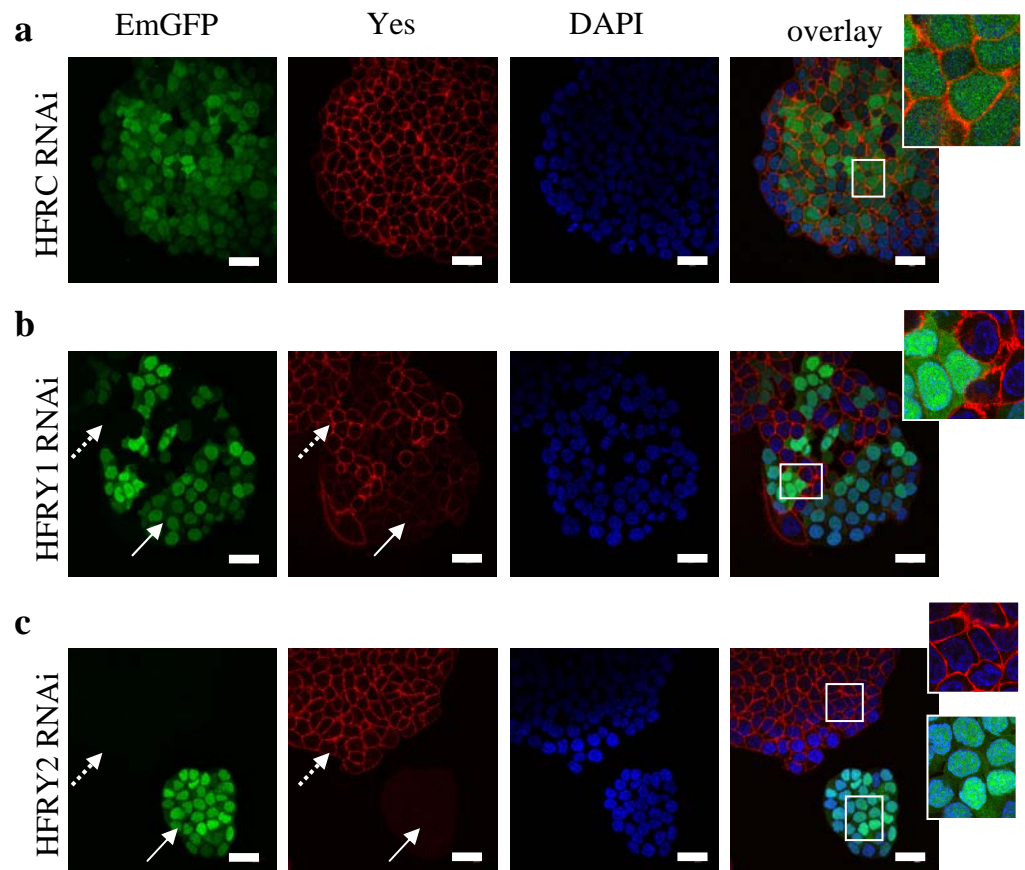
A commercially available pcDNA™ 6.2-EmGFP-miR validated vector containing two separate RNAi sequences against the Src family member, Yes (Yes 1 RNAi and Yes 2 RNAi) or a scrambled sequence (control RNAi) were used. This vector uses a pol II promoter and has co-cistronic expression of EmGFP and the RNAi inserted. A blasticidin gene marker allows for selection of the vector in transfected cells. This figure is taken from Invitrogen documentation.

https://tools.invitrogen.com/content/sfs/vectors/pcdna6_2gwemgfpmir_validated_map.pdf

Figure 34

Schematic Diagram Depicting the Strategy for Generation of Yes RNAi Expressing Cell Clones

HCT-116-FR cells were plated at a density of 1×10^6 cells in a 60mm dish for 24 hours before being transfected with the control RNAi vector, Yes 1 RNAi or Yes 2 RNAi using Lipofectamine™ 2000. The transfected cells were exposed to medium containing 10µg/ml blasticidin for 21 days (a concentration of blasticidin known to kill HCT-116-FR cells which do not express the RNAi vector). Blasticidin was removed for 7 days prior to sorting by FACS using the expressed EmGFP. Single cell clones were generated from the EmGFP enriched population and expanded before characterisation was undertaken.

Figure 35

EmGFP (green); Yes (red); DAPI (blue)

Mixed Population of Transfected Cells after Blasticidin Selection

Immunofluorescence was performed on; **a)** HCT-116-FR control (HFRCA) RNAi cells, **b)** HCT-116-FR Yes 1 (HFRYA1) RNAi, and **c)** HCT-116-FR Yes 2 (HFRYA2) RNAi cells. 5×10^4 cells/19mm glass coverslip were plated, grown for 2 days and fixed using the formaldehyde method before staining with an antibody against Yes (shown in red; Alexa Fluor 594). Vectashield containing DAPI was used to visualise the nuclei (shown in blue) and EmGFP was used to detect the RNAi vector (shown in green). A merged image of Yes, DAPI and EmGFP is also shown. Solid arrows indicate cells expressing Yes RNAi vector and subsequent loss of Yes protein, and broken arrows show cells lacking Yes RNAi expression and containing residual Yes protein. Scale bars 20 μ m.

Figure 36 - Immunoblot Analysis of RNAi Expressing Single Cell Clones

Immunoblotting was carried out on 1×10^6 cells plated on 60mm dishes after 2 days growth from single cell clones generated from; **a)** HCT-116-FR control (HFRC) RNAi cells, **b)** HCT-116-FR Yes 1 (HFRY1) RNAi cells and **c)** HCT-116-FR Yes 2 (HFRY2) RNAi cells. HCT-116 and HCT-116-FR cells were used as controls in all three immunoblots. Lysates were probed with an antibody against the SFK protein, Yes, and actin was used as a loading control. Molecular weight markers are shown.

Figure 36

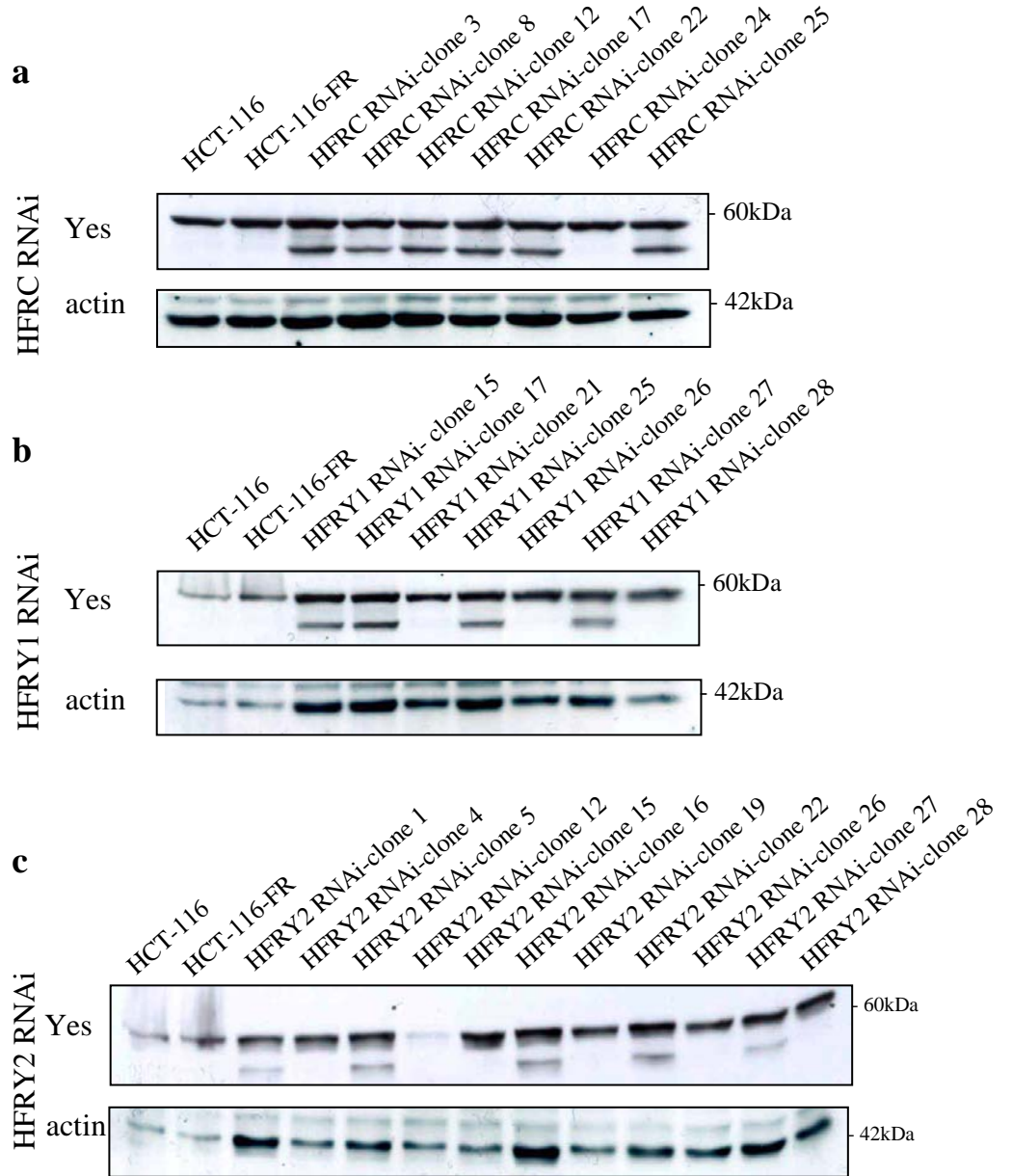
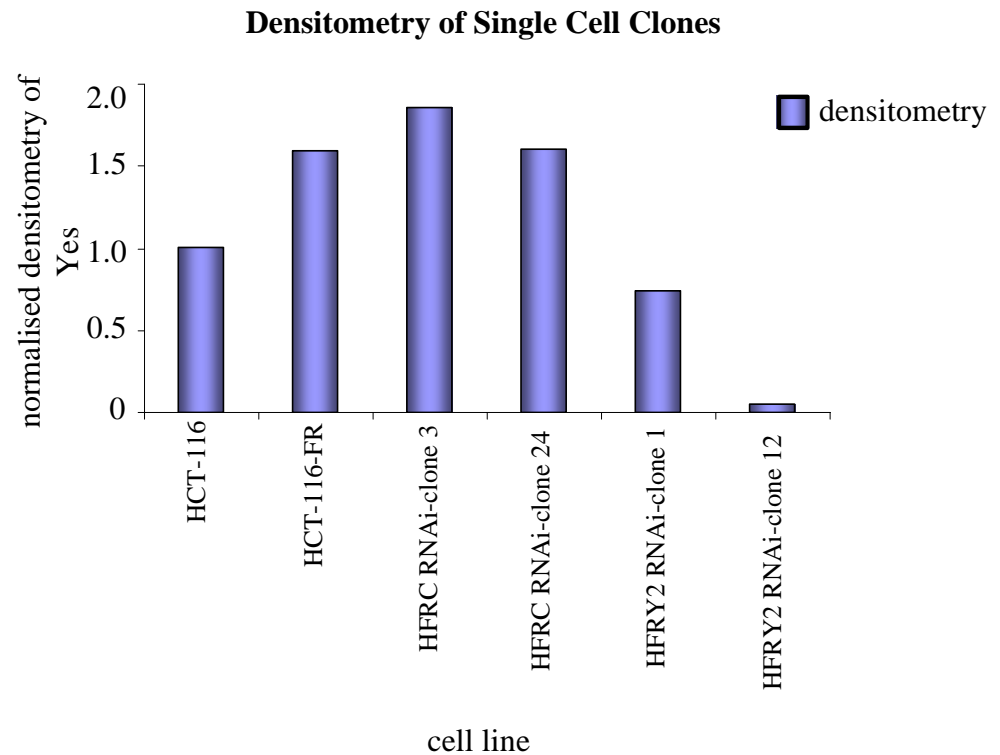


Figure 37

Densitometry of Single Cell Clones Chosen for Further Characterisation

Immunoblotting was carried out after 2 days on single cell clones generated from HFRC RNAi cells, HFRY1 RNAi cells and HFRY2 RNAi cells, to analyse Yes protein levels (**Figure 36**). Actin loading was used as a control and uneven loading was corrected for after densitometry. The densitometry of blotted species from lysates of HFRC RNAi clones 3 and 24 cells and HFRY2 RNAi clones 1 and 12 cells were normalised to HCT-116 and HCT-116-FR cells to allow direct comparison of protein levels. Values were normalised to the Yes level obtained in the HCT-116 cells.

4.3. Morphology of Single Cell Clones

Any changes in morphology between the HCT-116-FR control (HFRC) RNAi clones 3 and 24 (**Figure 38**) and the HCT-116-FR Yes 2 (HFRY2) RNAi clones 1 and 12 was assessed (**Figure 39**). The expression of EmGFP in these cells was used as an expected measure of RNAi expression. I selected HFRC RNAi clones with a similar EmGFP expression to the HFRY2 RNAi clones, allowing valid comparisons. Essentially this controlled for two distinct variables that were non-specific effects caused by either the RNAi vector or the selection process itself. Cells were plated for 2 days and images were taken at 10x and 20x magnification. There were no visible differences in morphology between the HFRC RNAi clones and the HFRY2 RNAi clones (compare **Figure 38** to **Figure 39**) despite the differences in Yes protein expression (**Figure 36**). Thus, knockdown of Yes did not visibly affect morphology.

The EmGFP expression was substantially different between the cell lines. The HFRC RNAi-clone 3 had a comparable low EmGFP expression to that of the HFRY2 RNAi-clone 1 (compare **Figure 38a** to **Figure 39a**) and so were appropriate to compare directly in future experiments. The HFRY2 RNAi-clone 12 had strong EmGFP expression which was most similar to that expressed in the HFRC RNAi-clone 24 (compare **Figure 39b** to **Figure 38b**) so these could also be compared directly.

The EmGFP expression results described above were confirmed by immunofluorescence where cells were plated for 2 days (**Figure 40**). EmGFP expression using fixed cells was clearer, and it confirmed the EmGFP levels described above. Despite being single cell clones, immunofluorescence detection did highlight variations in EmGFP expression within the cell populations of both the HFRC RNAi-clone 3 and the HFRY2 RNAi-clone 2 cells. In contrast, the EmGFP expression of both the HFRC RNAi-clone 24 cells and the HFRY2 RNAi-clone 12 cells was uniform within the same cell population.

Figure 38 - Phase Contrast and EmGFP Images of HCT-116-FR Control (HFRC)

RNAi Clones

HCT-116-FR control RNAi clone 3 (**a**) and clone 24 (**b**) cells were plated at 1×10^6 cells on 60mm dishes for 2 days before phase contrast images and EmGFP images were taken at 10x (scale bars 100 μ m) and 20x magnification (scale bars 50 μ m).

Figure 38

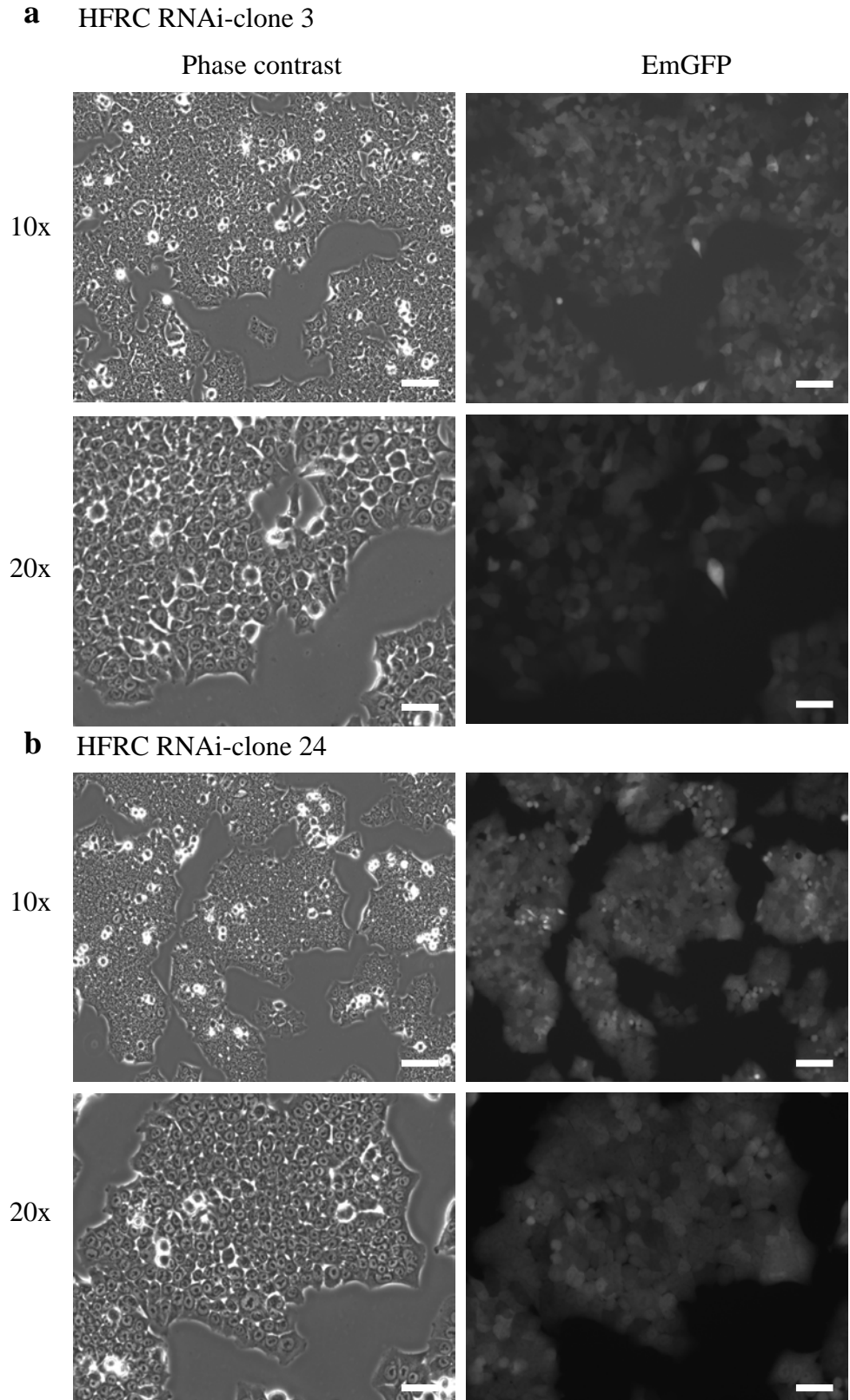


Figure 39 - Phase Contrast and EmGFP Images of HCT-116-FR Yes 2 (HFRY2)

RNAi Clones

HCT-116-FR Yes 2 RNAi clone 1 (**a**) and clone 12 (**b**) cells were plated at 1×10^6 cells on 60mm dishes for 2 days before phase contrast images and EmGFP images were taken at 10x (scale bars 100 μ m) and 20x magnification (scale bars 50 μ m).

Figure 39

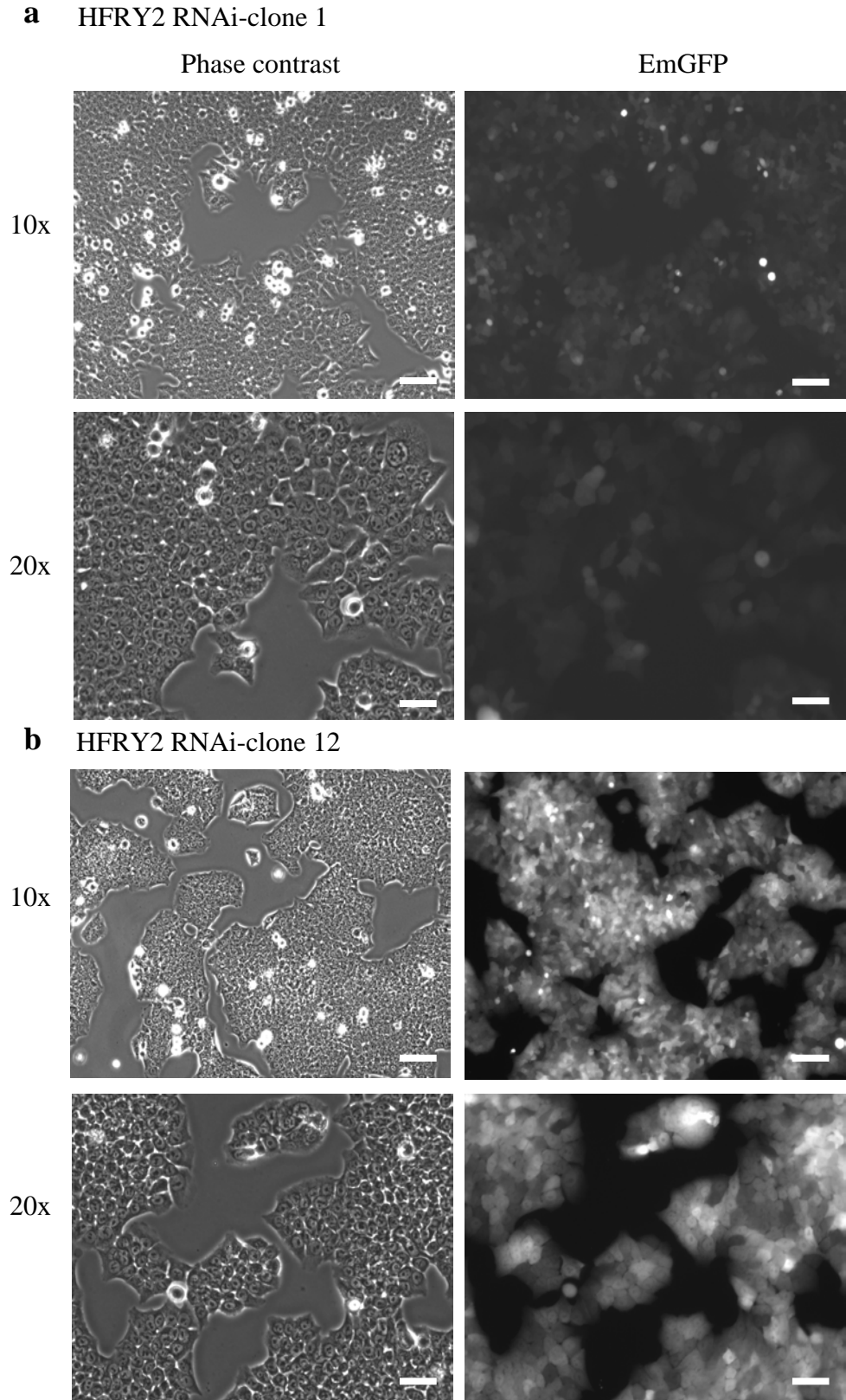
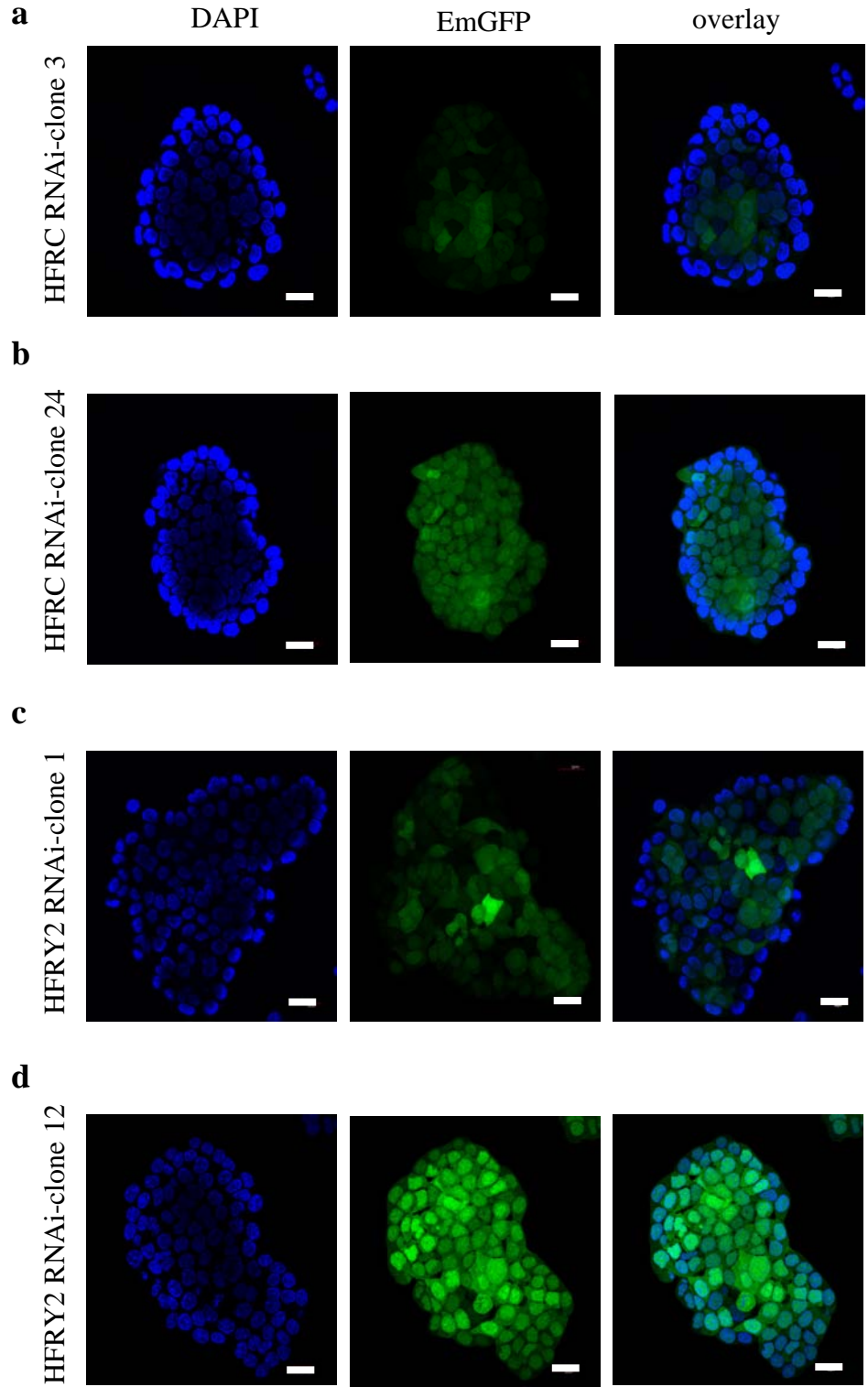


Figure 40 - EmGFP Analysis of HFRC RNAi Clones and HFRY2 RNAi Clones

HCT-116-FR control RNAi clone 3 (**a**) and clone 24 (**b**) cells and HCT-116-FR Yes 2 RNAi clone 1 (**c**) and clone 12 (**d**) cells were grown on coverslips (5×10^4 cells/19mm glass coverslip) for 2 days and then fixed using GFP fix method (described in Materials and Methods section). EmGFP was used to detect expression of the RNAi vector (green) and Vectashield containing DAPI was used to visualise the nuclei (blue). An overlaid image of EmGFP and DAPI is also shown. Scale bars 20 μ m.

Figure 40



DAPI (blue); EmGFP (green)

4.4. Resistance to 5-FU

To determine if resistance to 5-FU was altered by knocking down Yes protein expression, HFRY2 RNAi clones 1 and 12 and most appropriate control clones HFRC RNAi clones 3 and 24, were tested for sensitivity to 5-FU. An SRB cell proliferation assay was performed over 7 days with a range of 5-FU concentrations (**Figure 41**). All cell lines produced sigmoidal dose response curves with varying response to 5-FU (**Figure 41a**).

HFRY2 RNAi-clone 1 cells displayed a similar IC_{50} concentration of 5-FU as their corresponding control, HFRC RNAi-clone 3 (4.5 μ M compared with 3.2 μ M, respectively; **Figure 41b**). HFRY2 RNAi-clone 12 cells, which display a complete knockdown in Yes protein, showed an increased IC_{50} concentration of 5-FU when compared to their corresponding control, HFRC RNAi-clone 24 (11.2 μ M compared with 3.9 μ M, respectively; **Figure 41c**). However, there was no significant difference in IC_{50} concentrations when HFRY2 RNAi-clone 12 cells were compared to the cells from which they originated, HCT-116-FR cells (11.2 μ M compared with 10.1 μ M, respectively; **Figure 41d**).

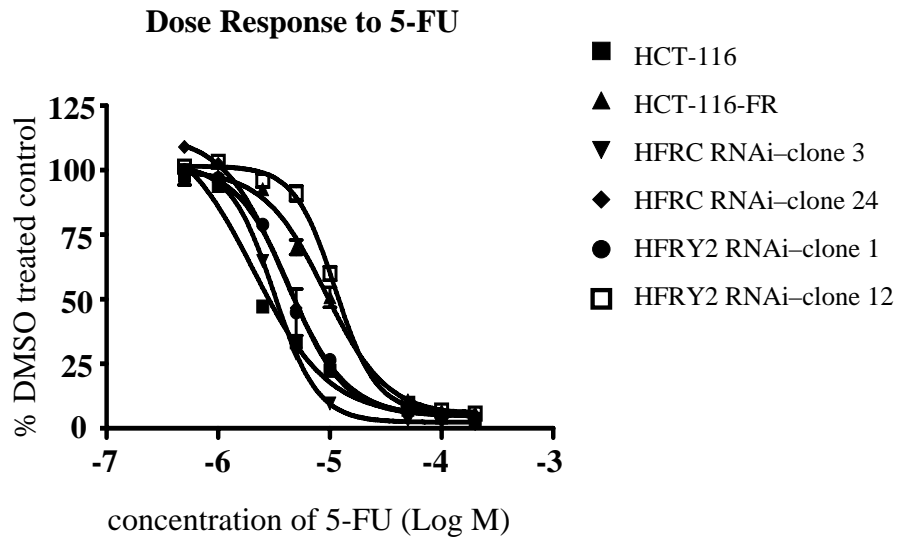
Therefore, I concluded, that Yes protein level did not contribute to 5-FU resistance and any differences observed were from general variation that cannot be attributed to Yes knock-down.

Figure 41 - Resistance to 5-FU in HFRC RNAi Clones and HFRY2 RNAi Clones

a) Resistance to 5-FU was analysed in HCT-116-FR control (HFRC) RNAi clones 3 and 24 and HCT-116-FR Yes 2 (HFRY2) RNAi clones 1 and 12 by performing an SRB cell proliferation assay over 7 days with a range of 5-FU concentrations (shown on graph as Log Molar concentration). Refer to figure key for cell line coding. A representative experiment is shown. HCT-116 and HCT-116-FR cells were used as controls. Cells that were DMSO treated were used as a control to 5-FU treatment. Absorbance at 540nm of 6 replicates per treatment were averaged and percentage values of DMSO treated control were calculated. Standard deviation was calculated from the percentage DMSO treated control values of the 6 replicates. **b)** IC₅₀ values for 5-FU in all cell lines were calculated using Graph Pad Prism software for each cell line (described in Materials and Methods section).

Figure 41

a



b

Cell Line	IC ₅₀ 5-FU
HFRC RNAi-clone 3	3.2µM
HFRY2 RNAi-clone 1	4.5µM

c

Cell Line	IC ₅₀ 5-FU
HFRC RNAi-clone 24	3.9µM
HFRY2 RNAi-clone 12	11.2µM

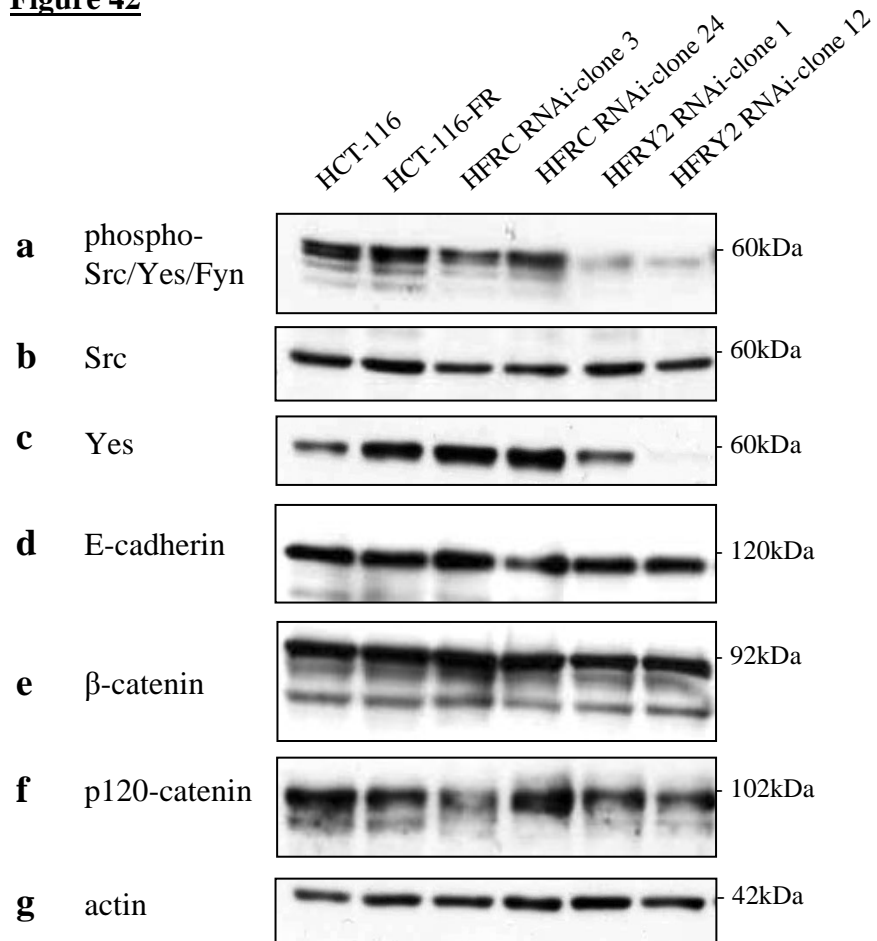
d

Cell Line	IC ₅₀ 5-FU
HCT-116	2µM
HCT-116-FR	10.1µM
HFRY2 RNAi-clone 12	11.2µM

4.5. Characterisation of Adhesion Protein Expression in RNAi Clones

As HCT-116-FR Yes 2 (HFRY2) RNAi clones 1 and 12 displayed a substantial knockdown in Yes protein expression demonstrated by immunoblotting (**Figures 36-37**), I next addressed the effect of this knockdown on phospho-Src/Yes/Fyn, i.e. SFK activities, and levels of expression of adherens junction proteins, E-cadherin, β -catenin and p120-catenin (**Figure 42**). The HFRC RNAi clones 3 and 24, as discussed previously, were used as controls for the Yes RNAi cells. Fyn levels were not analysed as antibodies were uninformative. Hence, lysates of HFRC RNAi clones 3 and 24 and HFRY2 RNAi clones 1 and 12 were probed with antibodies against these proteins. HCT-116 and HCT-116-FR cell lysates were included for comparison. Actin levels were used to control for protein loading (**Figure 42g**).

In the HFRC RNAi clones 3 and 24 cells, there was no reduction in levels of phospho-Src/Yes/Fyn, total Yes or total Src when compared to the HCT-116-FR cells (**Figure 42a, b and c**, respectively). Protein levels of E-cadherin, β -catenin and p120-catenin proteins also remained unchanged (**Figure 42d, e and f**, respectively). In the case of the HFRY2 RNAi clones 1 and 12 cells, a reduction in total Yes protein was evident (**Figure 36c and Figure 42c**). HFRY2 RNAi-clone 1 cells displayed a level similar to that of the total Yes protein found in the HCT-116 cells, while HFRY2 RNAi-clone 12 cells had an almost complete knockdown in total Yes protein (**Figure 36c and Figure 42c**). Thus, these 2 clones allowed me to determine effects of complete knockdown and knockdown of Yes in chemoresistant cells to a similar level to that found in their chemosensitive counterparts. As expected, a reduction in phospho-Src/Yes/Fyn in both HFRY2 RNAi clones 1 and 12 was shown when compared to their respective HFRC RNAi clones 3 and 24 (**Figure 42a**). Levels of Src and the cadherin/catenin proteins, E-cadherin, β -catenin and p120-catenin, remained unchanged (**Figure 42b, d, e and f**, respectively).

Figure 42

Immunoblotting of HFRC RNAi Clones and HFRY2 RNAi Clones

Immunoblotting was carried out on HCT-116-FR control (HFRC) RNAi clones 3 and 24 and HCT-116-FR Yes 2 (HFRY2) RNAi clones 1 and 12 cells. Lysates were probed with antibodies against SFK (phospho-Src/Yes/Fyn (**a**), Src (**b**) and Yes (**c**)) and proteins involved in cell-cell adhesion (E-cadherin (**d**), β -catenin (**e**) and p120-catenin (**f**)). HCT-116 and HCT-116-FR cell lysates were used for comparison. Actin levels were used as a protein loading control (**g**). Molecular weight markers are shown.

4.6. Adhesion Protein Localisation in RNAi Clones

As HCT-116-FR Yes 2 (HFRY2) RNAi clones 1 and 12 displayed a knockdown of Yes protein (**Figure 36-37**), we examined whether reduced expression was evident by immunofluorescence and whether localisation was altered (**Figure 44**). The effect of Yes knockdown in the HFRY2 RNAi clones 1 and 12 on the localisation of phospho-Src/Yes/Fyn and the adherens junction proteins, E-cadherin, anti- β -catenin and anti-p120-catenin, was also investigated (**Figures 44** and **46**, respectively). The HFRC RNAi clones 3 and 24 were used for comparison (**Figures 43** and **45**).

The HFRC RNAi clones 3 and 24 displayed no change in Yes protein staining at sites of cell-cell junctions, when compared to the HCT-116-FR parental cells (compare **Figure 43a** to **Figure 22b**). Localisation of phospho-Src/Yes/Fyn at the sites of focal adhesions and E-cadherin, β -catenin and p120-catenin at the cell membrane also remained unaltered in the HFRC RNAi clones 3 and 24 (compare **Figure 43c** to **Figure 22c** and compare **Figure 45** to **25**).

In the case of the HFRY2 RNAi clones 1 and 12 there was no alteration to the localisation of phospho-Src/Yes/Fyn at sites of focal adhesions at the edge of cells (compare **Figure 44b** to **43b**). However, staining of Yes at cell-cell adhesions was very low in both the HFRY2 RNAi clones 1 and 12, particularly notable in the HFRY2 RNAi-clone 12 cells (**Figure 44a**). Localisation of E-cadherin, β -catenin and p120-catenin at the cell membrane remained unaltered in both the HFRY2 RNAi clones 1 and 12 (**Figure 46**) implying that perturbation of Yes did not influence adherens junctions.

Thus, Yes staining at cell-cell adhesion sites was greatly reduced in the HFRY2 RNAi clones 1 and 12 when compared to the HFRC RNAi clones 3 and 24, respectively. Phospho-Src/Yes/Fyn, E-cadherin, β -catenin and p120-catenin proteins localisation

remained unchanged in all the RNAi clones investigated despite a large reduction in phospho-Src/Yes/Fyn (as shown by immunoblotting). Although E-cadherin expression was similar in all RNAi clones, as observed by judging static images, this does not rule out changes in dynamics. Unfortunately, I was not able to test this without complication, using eGFP-E-cadherin as RNAi transfected cells were already EmGFP positive. I considered using a mCherry-tagged-E-cadherin, but early experiments indicated that the fluorescence was not stable enough to allow FRAP analysis.

4.7. Assessment of Cell-Cell Junctions of RNAi Clones by Aggregation Assay

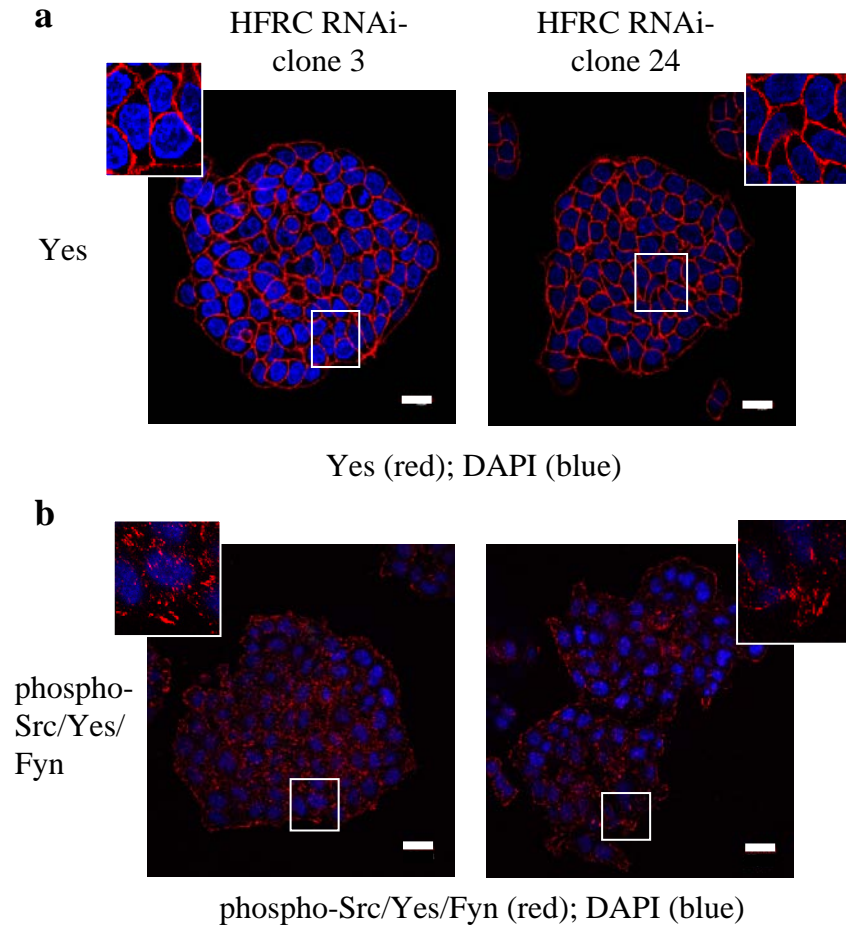
I showed that there was no difference in the level or localisation of the adherens junction proteins, E-cadherin, β -catenin and p120-catenin in HFRY2 RNAi clones 1 and 12. However, there may be differences in the ability for cell-cell contacts to join caused by the knockdown of Yes protein. To investigate this, an aggregation assay was performed to measure the ability of single cells to adhere to each other and form aggregates in the presence of low and high calcium (as was described previously for **Figures 29-31**). This was performed using HFRY2 RNAi clones 1 and 12 with HFRC RNAi clones 3 and 24 used for comparison (**Figure 47**).

No aggregates formed in low calcium and the majority of cells remained as single cells in all cell lines tested (data not shown). In high calcium, similar numbers of cell aggregates were formed in all cell lines (data not shown). However, a difference in aggregate area was apparent between the cell lines. As shown previously (**Figure 31**), the average area of aggregates formed in the HCT-116-FR cells were larger when compared to the HCT-116 cells ($5367\mu\text{m}^2$ in HCT-116-FR cells when compared to $2262\mu\text{m}^2$ in the HCT-116 cells). HFRC RNAi clones 3 and 24 had equivalent aggregate areas to those displayed in the HCT-116-FR cells ($5420\mu\text{m}^2$ in HFRC RNAi-clone 3 cells and $5221\mu\text{m}^2$ in HFRC RNAi-clone 24 cells). However, the aggregate area in both the HFRY2 RNAi clones 1 and 12 were much smaller in comparison to HFRC RNAi clones 3 and 24, respectively. The

HFRY2 RNAi-clone 1, which displayed a level of Yes protein equivalent to the Yes protein level in the HCT-116 cells, displayed a reduced aggregate area of $2804\mu\text{m}^2$ in comparison to HFRC RNAi-clone 3 ($5420\mu\text{m}^2$). However, the HFRY2 RNAi-clone 12, which showed an almost complete knockdown of Yes protein, displayed a reduction in aggregate area to $2587\mu\text{m}^2$ in comparison to HFRC RNAi-clone 24 ($5221\mu\text{m}^2$). The aggregate area shown by HFRY2 RNAi-clone 12 was comparable to that shown in the HCT-116 cells ($2587\mu\text{m}^2$ compared to $2262\mu\text{m}^2$ respectively).

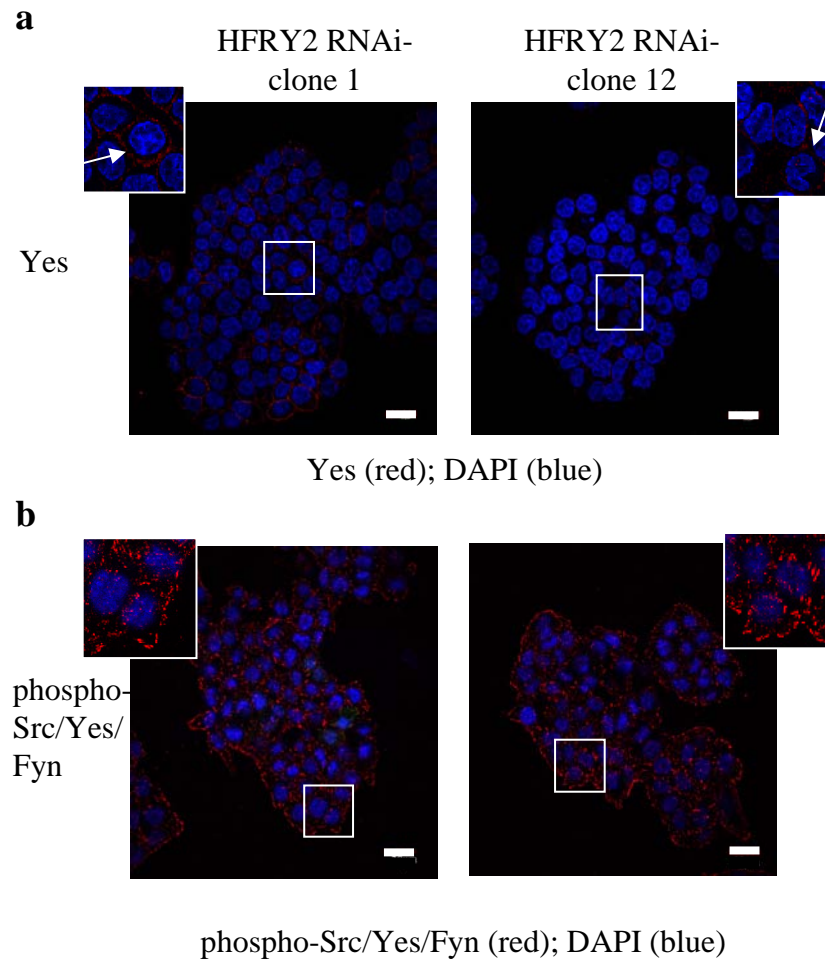
Thus, I demonstrated a robust reduction in area from these aggregation assay results when Yes protein was reduced in HCT-116-FR cells. I concluded that when Yes was reduced, E-cadherin on the cell surface may be more able to 'release' binding to adjacent cells resulting in a smaller area of formed aggregates. For that reason, resistant cells, which display an increase in Yes may then have an increased ability to form aggregates containing a larger cell number, and hence area. If true, this suggested more adhesive properties when Yes was present. Src is known to de-regulate cell-cell contacts mediated by E-cadherin (Avizienyte et al., 2002), however in this assay, increased Yes does not show the same effect, in fact, these results suggest an opposing role at adherens junctions between Src and Yes in these cells. This contradicts previous literature that states that Yes, along with Src, acts to disrupt adherens junctions, a function that is blocked when chemically inhibited (Owens et al., 2000). However, I did not test other functions of Yes in the tumourgenicity of these cells.

Despite the apparent alterations of cell-cell adhesion capacity in the aggregation assay when Yes was knocked-down; these alterations were not accompanied by changes to 5-FU resistance.

Figure 43

Localisation of Yes and Phospho-Src/Yes/Fyn in HFRC RNAi Clones

HCT-116-FR control (HFRC) RNAi clones 3 and 24 cells (5×10^4 cells/19mm glass coverslip) were grown for 2 days after plating and fixed using the formaldehyde method before being probed with antibodies against **a**) Yes or **b**) phospho-Src/Yes/Fyn (shown in red; Alexa Fluor 594). Vectashield containing DAPI was used to visualise the nuclei (blue). Scale bars $20\mu\text{m}$.

Figure 44

Localisation of Yes and Phospho-Src/Yes/Fyn in HFRY2 RNAi Clones

HCT-116-FR Yes 2 (HFRY2) RNAi clones 1 and 12 cells (5×10^4 cells/19mm glass coverslip) were grown for 2 days after plating and fixed using the formaldehyde method before being probed with antibodies against **a**) Yes or **b**) phospho-Src/Yes/Fyn (shown in red; Alexa Fluor 594). Vectashield containing DAPI was used to visualise the nuclei (blue). Faint Yes staining at cell-cell contacts was indicated by white arrows. Scale bars 20 μ m.

Figure 45 - Localisation of Adherens Junction Proteins in HFRC RNAi Clones

HCT-116-FR control (HFRC) RNAi clones 3 and 24 cells (5×10^4 cells/19mm glass coverslip) were grown for 2 days after plating and fixed using the formaldehyde method (with the exception of E-cadherin which was fixed using the paraformaldehyde method) before being probed with antibodies against **a**) E-cadherin, **b**) β -catenin or **c**) anti-p120-catenin (shown in red; Alexa Fluor 594). Vectashield containing DAPI was used to visualise the nuclei (blue). Scale bars 20 μ m.

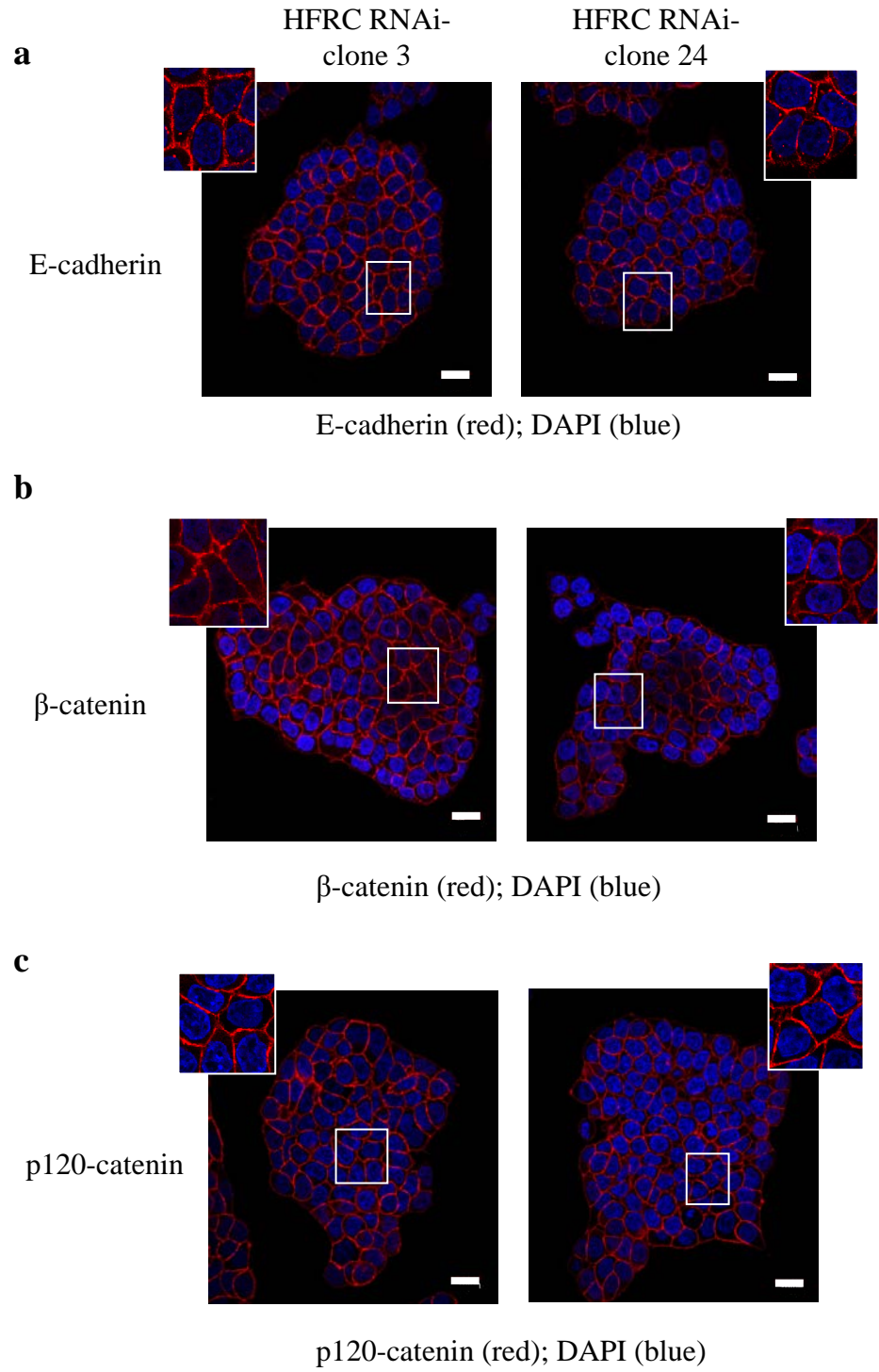
Figure 45

Figure 46 - Localisation of Adherens Junction Proteins in HFRY2 RNAi Clones

HCT-116-FR Yes 2 (HFRY2) RNAi clones 1 and 12 cells (5×10^4 cells/19mm glass coverslip) were grown for 2 days after plating and fixed using the formaldehyde method (with the exception of E-cadherin which was fixed using the paraformaldehyde method) before being probed with antibodies against **a)** E-cadherin, **b)** β -catenin or **c)** p120-catenin (shown in red; Alexa Fluor 594). Vectashield containing DAPI was used to visualise the nuclei (blue). Scale bars 20 μ m.

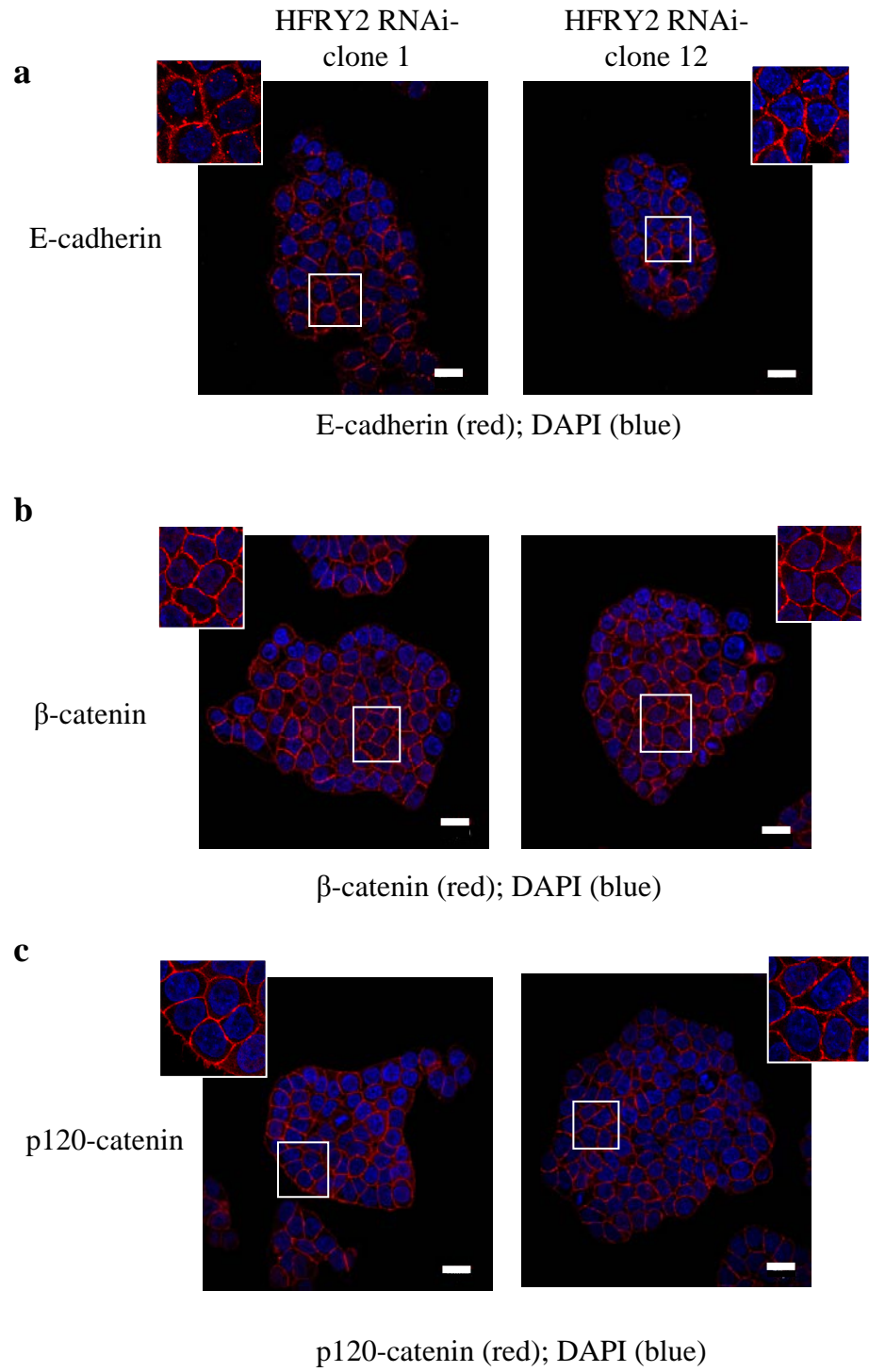
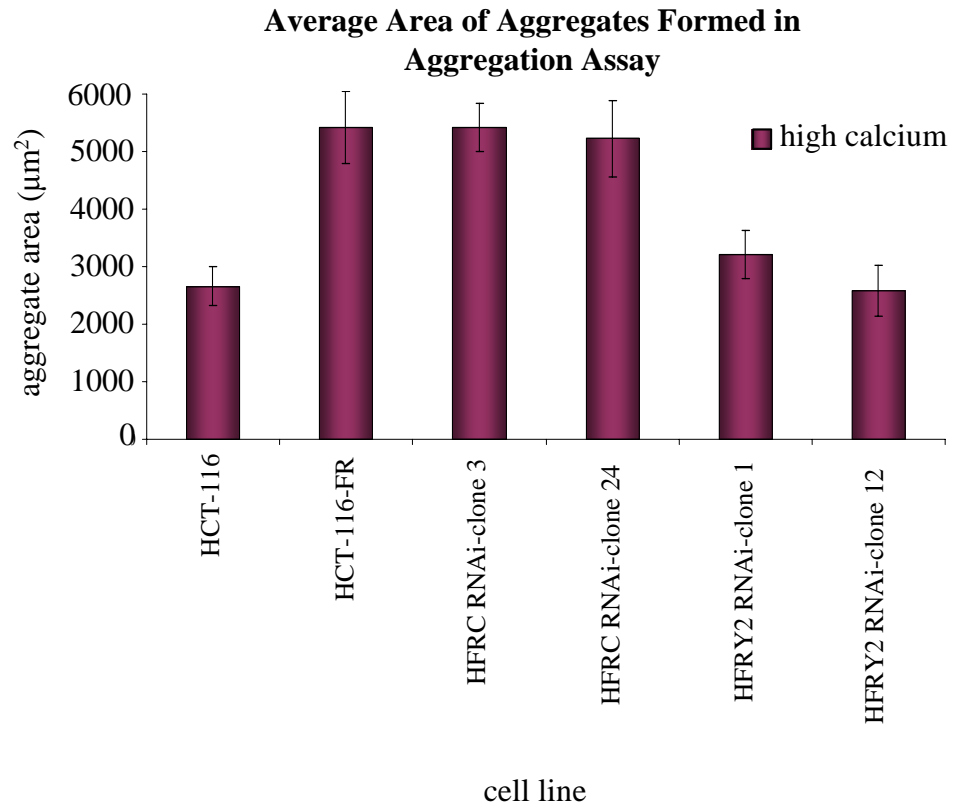
Figure 46

Figure 47

Average Area of Aggregates Formed

HFRC RNAi clones 3 and 24 cells and HFRY2 RNAi clones 1 and 12 cells were dissociated using CDB and single cells were generated using a 21G needle and syringe, before being incubated in KBM containing high calcium (1.5mM) for 1 hour at room temperature with constant agitation. After this time the area of the aggregates formed was measured. HCT-116 and HCT-116-FR cells were used as controls for the HFRC RNAi clones. Aggregates were classed as a colony of ≥ 10 cells. Average areas of colonies were calculated for a representative experiment and standard deviations were calculated using the colony areas obtained in that experiment.

4.8. Summary

By using a vector-based RNAi system, 2 HCT116-FR clones expressing RNAi to induce Yes knockdown were generated. In one of these, Yes protein was suppressed to levels that were similar to those of HCT116 cells and in the other, Yes was almost completely ablated. In neither case was sensitivity to 5-FU restored. RNAi provided a useful interventionist approach, and allowed me to conclude that despite increased Yes protein (as a result of its co-amplification with TS), it did not play a role in acquired resistance to 5-FU. I did find that there was some modulation of cell-cell adhesiveness when Yes was suppressed, suggesting a role for Yes in E-cadherin function in these colon cancer cells. However, as Yes knockdown did not affect drug resistance, the consequences for cell to cell association were not pursued any further.

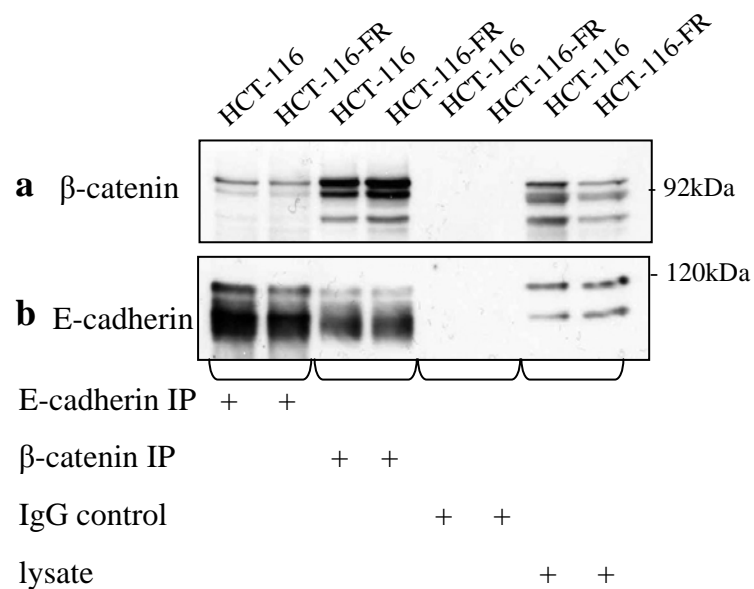
5. Modulation of Adherens Junctions and 5-FU Resistance

5.1. Co-immunoprecipitation of E-cadherin and β -catenin

Next I wished to interfere with E-cadherin function and address its role in drug resistance. Although I had shown that E-cadherin was present at adherens junctions, I also wanted to determine if the complex between E-cadherin and one of the components of the adherens junctions, in this case β -catenin, was intact in the HCT-116-FR cells (**Figure 48**). Co-immunoprecipitation does not provide information that the junctions are functionally intact, but it does show whether these two components of an adherens junction have bound to one another suggesting functional interaction is taking place. Thus, E-cadherin and β -catenin were immunoprecipitated from the lysates of HCT-116 and HCT-116-FR cells before being immunoblotted using antibodies against β -catenin (**Figure 48a**) and E-cadherin (**Figure 48b**).

In HCT-116 and HCT-116-FR cells, both E-cadherin and β -catenin co-immunoprecipitated β -catenin and E-cadherin, implying that in both cell lines, E-cadherin binds to β -catenin. There were a number of additional species present in the immunoblots for both E-cadherin and β -catenin. Interestingly, only two of the three species of β -catenin bound to the E-cadherin immunoprecipitation. I do not know the reason for binding to the highest molecular weight species and it was not clear what the differences were between this and the faster migrating species.

Thus, association of E-cadherin to β -catenin in HCT-116-FR cells was unaltered as HCT-116 cells acquired 5-FU resistance.

Figure 48

Immunoprecipitation of E-cadherin and β -catenin in HCT-116-FR Cells

E-cadherin and β -catenin were immunoprecipitated from lysates of HCT-116 and HCT-116-FR cells that were plated at 1×10^6 cells on 60mm dishes then grown for 2 days. Immunoprecipitates were then immunoblotted using antibodies against **a**) β -catenin and **b**) E-cadherin. HCT-116 and HCT-116-FR lysates were probed to identify the E-cadherin and β -catenin proteins. Mouse IgG was used as an immunoprecipitation control. Molecular weight markers are shown.

5.2. Disruption of Adherens Junctions using *Decma*

Next I examined the effect of disrupting E-cadherin mediated cell-cell junctions by use of an interfering antibody – *decma*. *Decma* works by recognising and binding to the extracellular domain of E-cadherin, preventing binding to E-cadherin presented on an adjacent cell (**Figure 49a**) (Ozawa et al., 1990). Cells left untreated, or treated with rat IgG control, were able to form adherens junctions upon contact and this allowed comparison of the effects on junction formation in cell lines treated with *decma*. Initial examination of the phase contrast images of *decma*-treated cells, suggested that there was a reduction in cell-cell contact. In addition there were fewer cells than in control cultures (**Figure 49b**). This effect was more noticeable in the 5-FU resistant cells when compared to their more sensitive counterparts (**Figure 49b**). HCT-116 and HCT-116-FR cells were then incubated with a range of dilutions of *decma* antibody (4mg/ml IgG stock concentration) to determine the optimal dilution to use for further investigations. HCT-116 and HCT-116-FR cells were incubated on coverslips with *decma* at 1:75 (53µg/ml final concentration of *decma*; **Figure 50a**), 1:100 (40µg/ml final concentration of *decma*; **Figure 50b**) and 1:300 (13µg/ml final concentration of *decma*; **Figure 50c**) dilutions. Incubation with rat IgG at 1:100 dilution (40µg/ml final concentration of IgG) was used as a control sample (**Figure 50d**). Cells were incubated for 7 days before being fixed using the paraformaldehyde method and stained with an E-cadherin antibody. Rat IgG control coverslips for both the HCT-116 and HCT-116-FR cells had grown to near confluence (100%) with E-cadherin junctions remaining intact (**Figure 50d**).

Treatment with *decma* resulted in a concentration dependant reduction in the number of cell-cell junctions, as well as reduced cell number when compared to the corresponding rat IgG control samples (**Figure 50a, b and c** compared to **d**). This visual observation of reduced cell-cell adhesion was quantified and confirmed by counting the number of cells

that contained adherens junctions and presenting that number as a percentage of total cell number (**Figure 50e**). To address why there was reduced cell number upon *decma* treatment, an SRB cell proliferation assay was performed with *decma* at a number of dilutions (**Figure 50f**). After *decma* treatment of HCT-116-FR cells for 7 days, the cells showed reduced proliferation when compared to HCT-116 cells at both 1:100 and 1:300 dilutions. At weaker dilutions (1:1000 and 1:3000), no effect on proliferation was evident in either cell line. As the difference between *decma* at 1:75 and 1:100 dilutions being small, the concentration of *decma* chosen for future experiments was the 1:100 dilution (40µg/ml final concentration of *decma*). In addition, I concluded that HCT-116-FR cells are more reliant on their cell-cell junctions in order to proliferate, than the HCT-116 cells.

Figure 49 - *Decma* Antibody Treatment of HCT-116 and HCT-116-FR Cells

a) This diagram is a representation of the way in which *decma* antibody operates to prevent E-cadherin binding between adjacent cells. Single cells incubated in normal media without *decma* (i.e. rat IgG treated) retain the ability to form cadherin based cell-cell junctions. Addition of *decma* prevents E-cadherin in adjacent cells from binding. Diagram is not to scale. **b)** HCT-116 and HCT-116-FR cells were trypsinised and single cells generated before 1×10^3 cells/well of a 96 well plate ($320\text{mm}^2/\text{well}$) were incubated with rat IgG or *decma* (both at 1:100 dilution; $40\mu\text{g}/\text{ml}$ final IgG concentration). Phase contrast images were taken after 7 days treatment. Scale bars $100\mu\text{m}$.

Figure 49

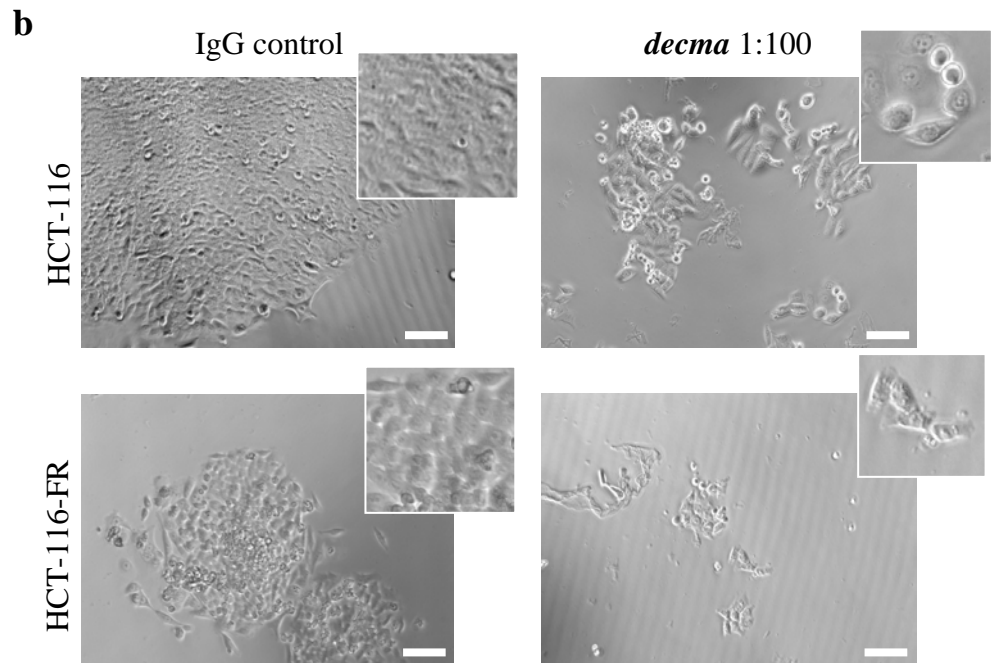
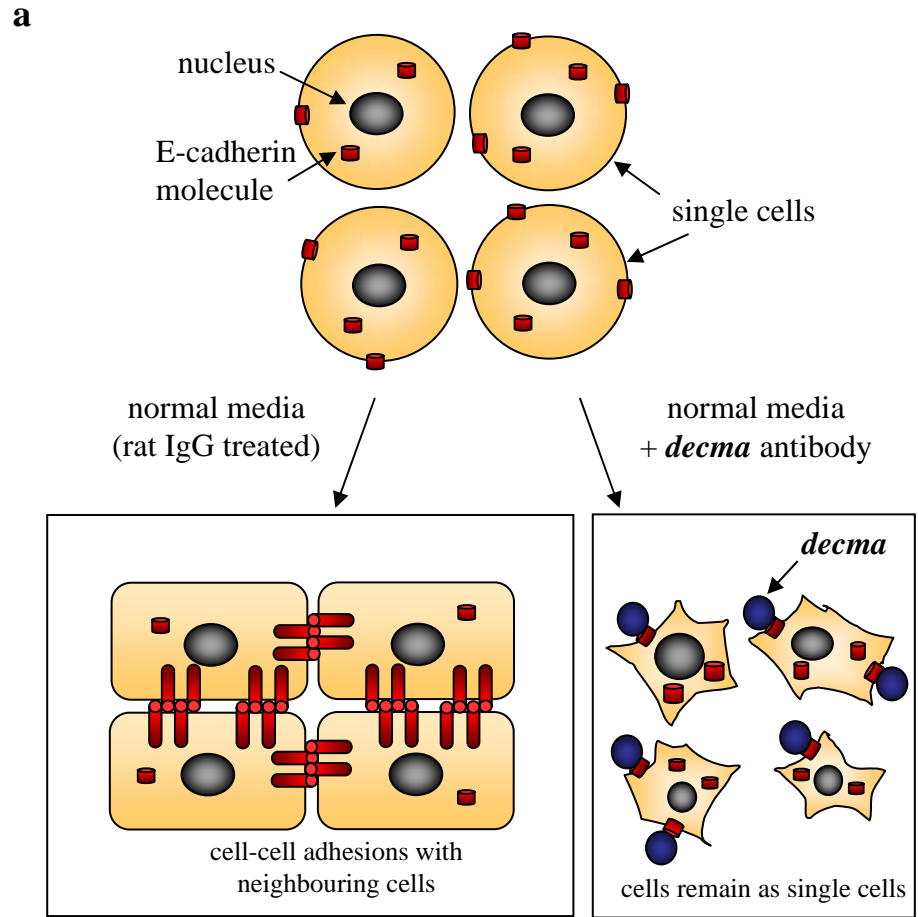


Figure 50 - Immunofluorescence of HCT-116 and HCT-116-FR Cells Treated with *Decma*

HCT-116 and HCT-116-FR cells were trypsinised and single cells generated. 9×10^3 cells were plated on 19mm coverslips and incubated with *decma* antibody at; **a)** 1:75, **b)** 1:100, or **c)** 1:300 dilution (of a 4mg/ml IgG stock concentration) and grown for 7 days. Cells were then fixed using the paraformaldehyde method and stained with an antibody against E-cadherin (shown in green; Alexa Fluor 488). **d)** Incubation with rat IgG was used as a control (refer to **Figure 25** for non-confluent E-cadherin staining). Vectashield containing DAPI was used to visualise the nuclei (blue). Scale bars 20 μ m. **e)** An average number of cells with E-cadherin junctions was determined and displayed as a percentage of total cells. **f)** An SRB proliferation assay was performed over 7 days on HCT-116 and HCT-116-FR cells which were treated with a range of dilutions of *decma* antibody (1:100, 1:300, 1:1000 and 1:3000). Cells that were untreated or treated with rat IgG were used as controls (refer to figure key for cell line colour coding). Absorbance at 540nm of 6 replicates per treatment were averaged and displayed as a percentage of rat IgG-treated control. Standard deviation was calculated from the percentage rat IgG-treated control values of the 6 replicates. A representative experiment is shown.

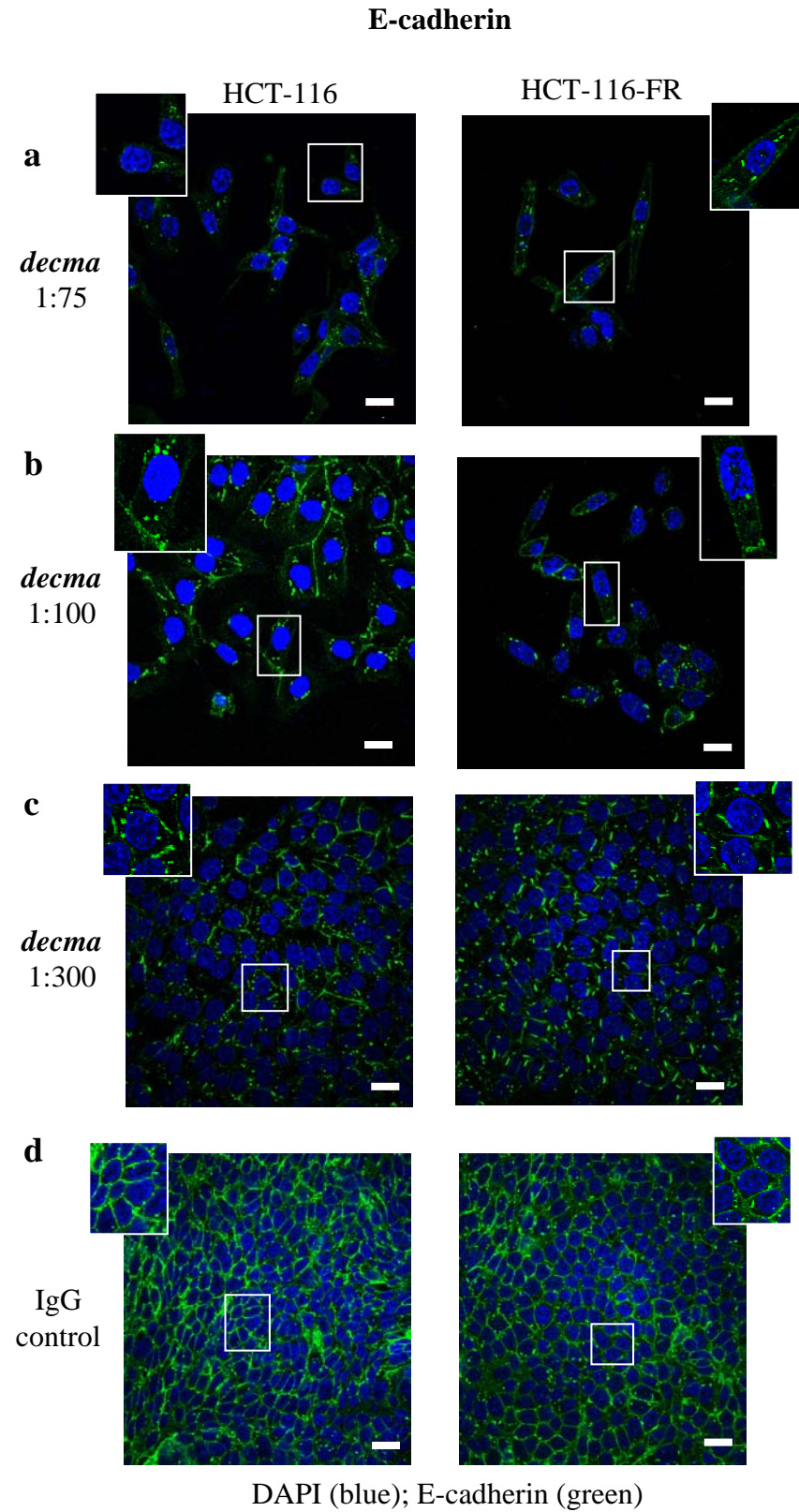
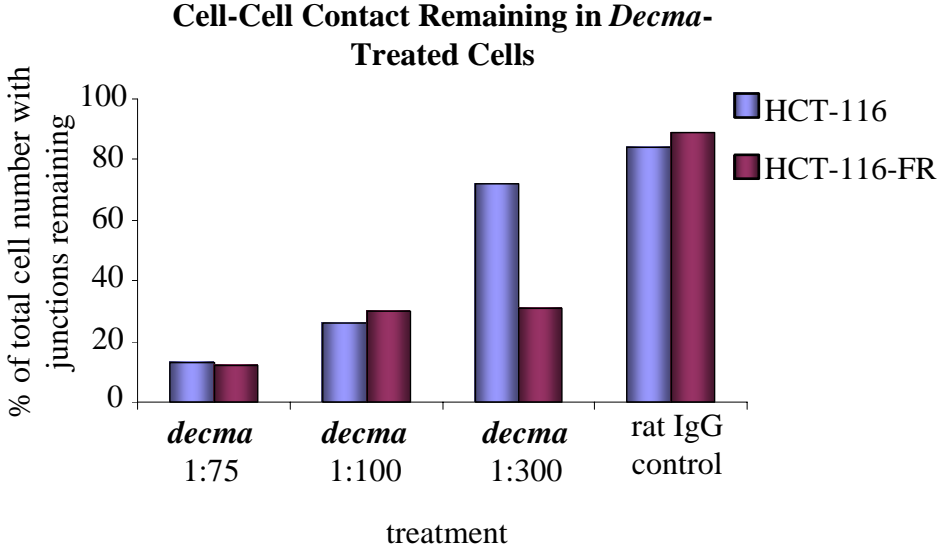
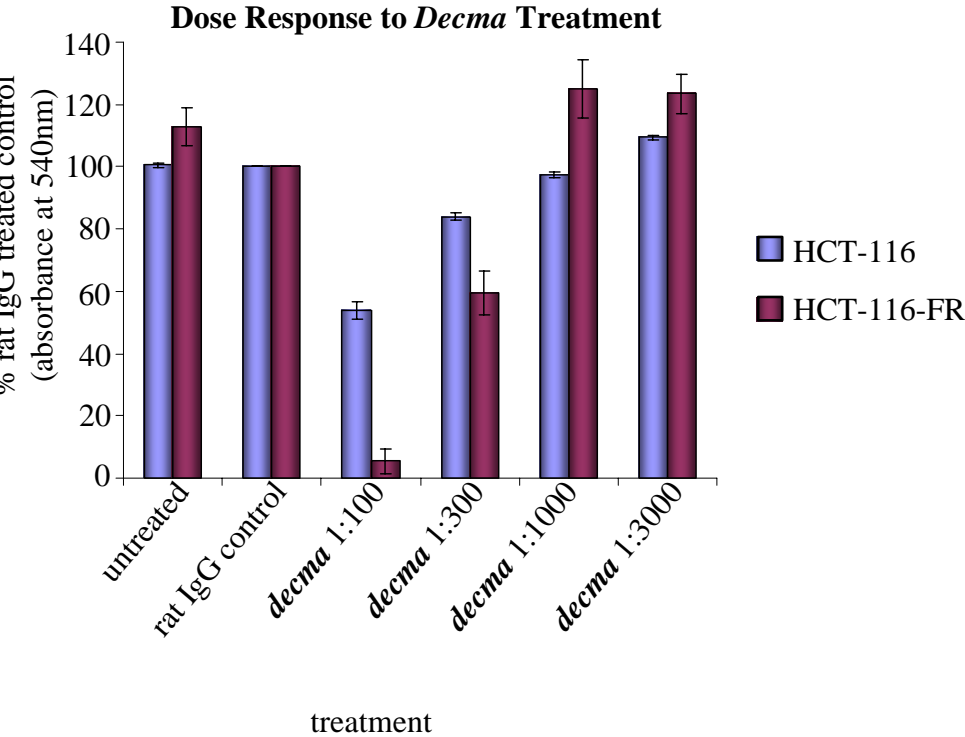
Figure 50

Figure 50 - continued

e



f



5.3. Adhesion Protein Localisation in *Decma*-treated Cells

As the *decma* antibody had the effect of disrupting cell-cell junctions by binding to the extracellular domain of cell surface E-cadherin in both HCT-116 and HCT-116-FR cells, I examined the localisation of other adherens junction proteins to assess the effect of *decma* treatment on those. Cells treated with *decma* at 1:100 dilution for 7 days were fixed and stained with antibodies against p120-catenin (**Figure 51a**) or β -catenin (**Figure 51b**). In both HCT-116 and HCT-116-FR cells treated with rat IgG, p120-catenin and β -catenin proteins localised at the sites of cell-cell junctions at the cell membrane. However, upon *decma* treatment, the p120-catenin and β -catenin protein staining was not as strong and was more diffuse in both the HCT-116 and HCT-116-FR cells when compared to their corresponding rat IgG treated controls, even though the proteins remained at the cell membrane.

Previously I showed immunofluorescence of 7 days *decma*-treated cells. I wanted to confirm that this time frame was optimum for investigating the effects of *decma* by fixing coverslips after 2 days and 4 days treatment, in addition to 7 days (**Figure 52**). Disruption of cell-cell junctions in both HCT-116 (**Figure 52a**) and HCT-116-FR (**Figure 52b**) cells was evident after 2 days and 4 days. However, I concluded that the observation of the effect of *decma* is most apparent after 7 days in both cell lines. Therefore, 7 days *decma* treatment was used in future experiments.

**Figure 51 - Immunofluorescence of HCT-116 and HCT-116-FR Cells Treated With
*Decma***

HCT-116 and HCT-116-FR cells were trypsinised and single cells generated. 9×10^3 cells were plated on 19mm coverslips and incubated with *decma* antibody at 1:100 dilution for 7 days, before being fixed and stained with antibodies against; **a**) p120-catenin and **b**) β -catenin (shown in green; Alexa Fluor 488). Incubation with rat IgG was used as a control. Vectashield containing DAPI was used to visualise the nuclei (blue). Scale bars 20 μ m.

Figure 51

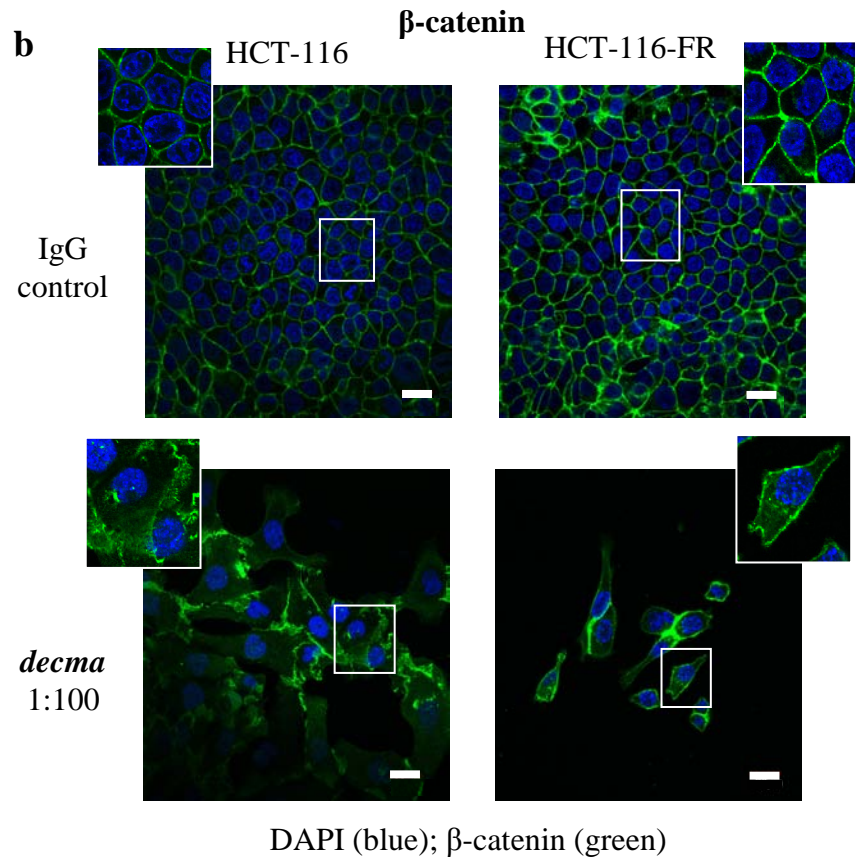
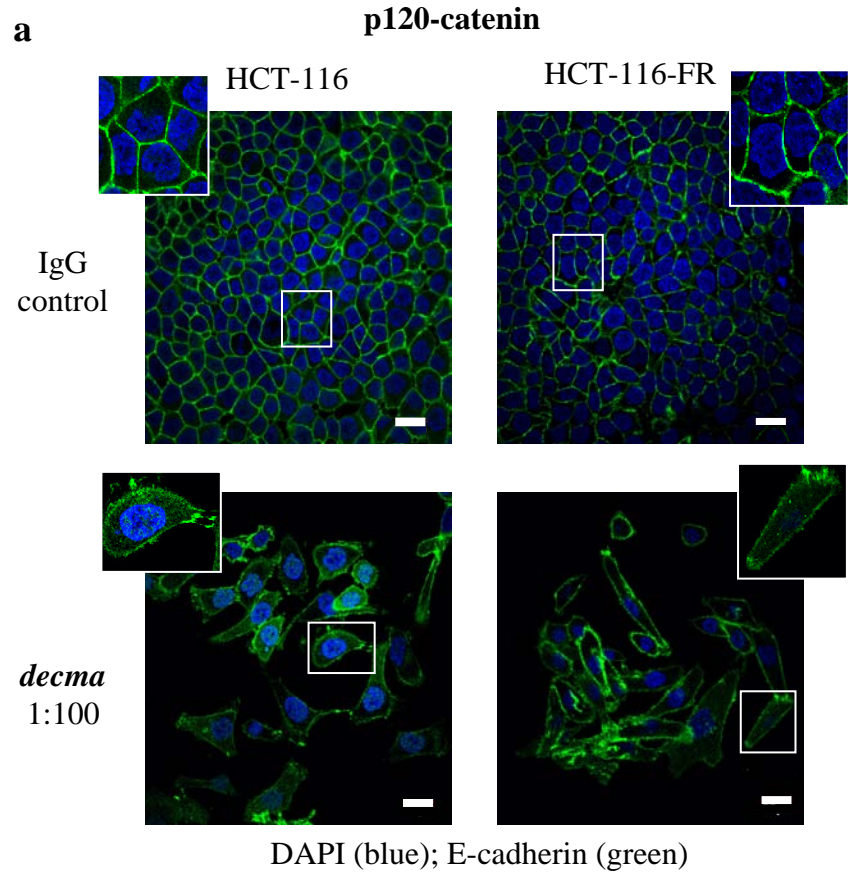


Figure 52 - Immunofluorescence of HCT-116 and HCT-116-FR Cells after *Decma* Treatment

a) HCT-116 and **b)** HCT-116-FR cells were trypsinised and single cells generated. 9×10^3 cells were plated on 19mm coverslips and incubated with *decma* antibody at 1:100 and grown for 2 days, 4 days and 7 days before being fixed and stained with an antibody against E-cadherin (shown in green; Alexa Fluor 488). Incubation with rat IgG was used as a control. Vectashield containing DAPI was used to visualise the nuclei (blue) and TRITC-phalloidin (red) was used to visualise the actin cytoskeleton. Scale bars 20 μ m.

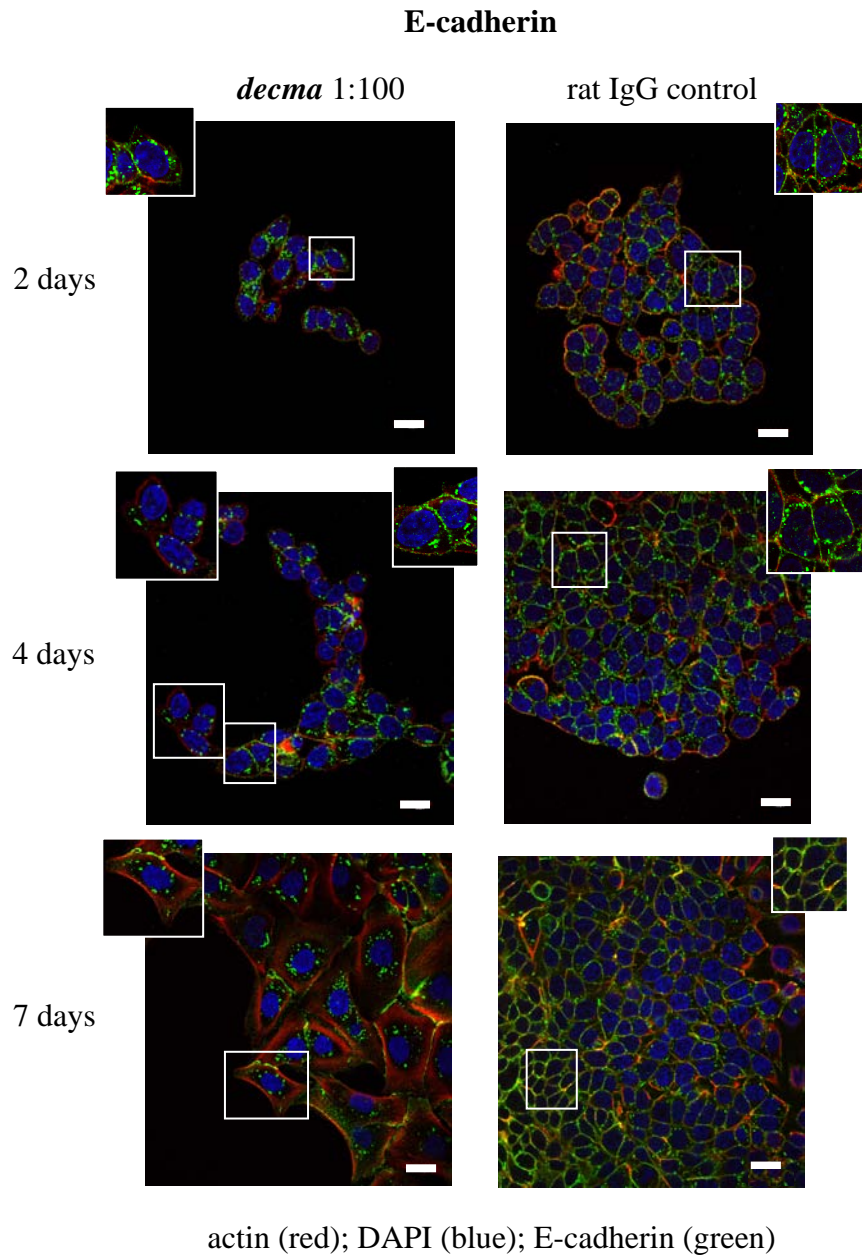
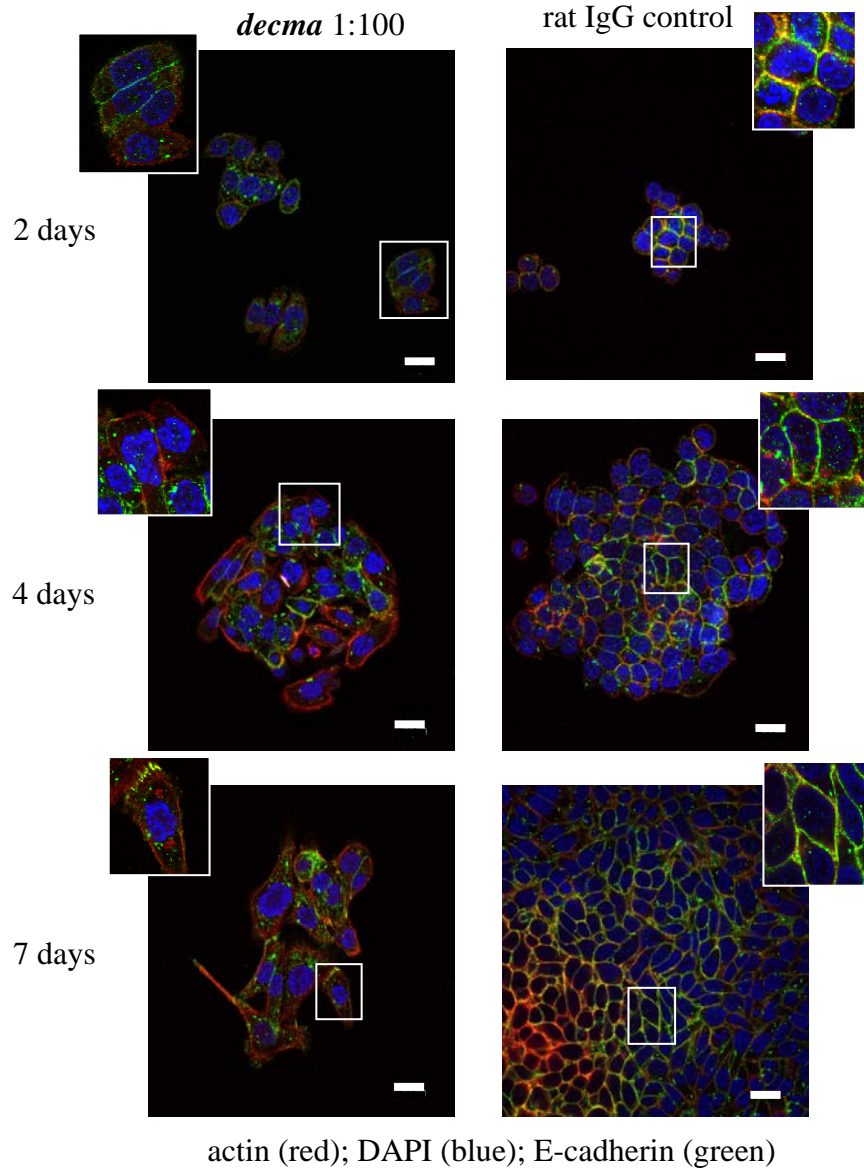
Figure 52**a**

Figure 52 - continued

b

E-cadherin



5.4. The Effect of *Decma* Treatment on Proliferation

Immunofluorescence of *decma*-treated cells over 2, 4 and 7 days further highlighted the decrease in cell number displayed during *decma* treatment in both HCT-116 and HCT-116-FR cells. As the HCT-116-FR cells experienced a more obvious decrease in cell number, the results suggested that sensitivity to 5-FU may also be modulated by disruption of cell-cell contacts. This was tested by treating cells with their respective IC₅₀ concentration of 5-FU in addition to *decma* and measuring proliferation over 7 days (**Figure 53c**). Both cell lines were more sensitive to treatment with 5-FU during *decma* exposure. This was most evident in the HCT-116-FR cells. This same trend was found in the most resistant cell pair, namely H630 and H630-FR cells (**Figure 53a**). However, a similar trend was not observed for the least resistant cell pair, namely HT29 and HT29-FR cells, which both showed reduced proliferation upon *decma* treatment, as well as with IC₅₀ concentration of 5-FU plus *decma*, but there was no substantial difference between resistant and sensitive cells from this pair (**Figure 53b**).

5.5. The Effect of *Decma* Washout on Adherens Junctions and Proliferation

When *decma* was removed from cultures and cells were grown for a further 7 days without *decma* treatment, cell-cell junctions were restored (**Figure 54**). Junction recovery was visualised by localisation of E-cadherin at the sites of cell-cell contact in both the HCT-116 and HCT-116-FR cells, and this was comparable to their IgG control samples (**Figure 54a**). *Decma* removal also resulted in β -catenin staining being much stronger at sites of cell-cell junctions, resembling β -catenin in cells treated with IgG control (**Figure 54b**). As cell number also appeared to be restored after 7 days proliferation without *decma* present, I investigated whether the inhibition of proliferation was reversible. By performing an SRB

cell proliferation it was observed that proliferation resumed, resulting in HCT-116 cells treated with *decma* only (1:100) and *decma* (1:100) plus their IC₅₀ concentration of 5-FU, proliferating to levels similar to untreated cells (**Figure 55**). HCT-116-FR cells treated with *decma* only (1:100) proliferated to levels similar to untreated cells. HCT-116-FR cells treated with *decma* (1:100) plus the IC₅₀ concentration of 5-FU, regained proliferation but did not recover to control levels after 7 days.

Therefore, I concluded that proliferation of both HCT-116 and HCT-116-FR cells resumed upon removal of *decma* treatment for 7 days, but full recovery of HCT-116-FR cells was not achieved when treated with *decma* and their IC₅₀ concentration of 5-FU. This was probably because the 5-FU-resistant HCT-116-FR cells were more sensitive to their IC₅₀ concentration of 5-FU when cell-cell contacts were lost, further implying that resistant HCT-116-FR are more reliant on their cell-cell adhesions for proliferation than their sensitive counterparts.

Figure 53 - *Decma* Treatment in the Pairs of Sensitive and Resistant Cell lines

An SRB proliferation assay was performed over 7 days on the pairs of sensitive and resistant cell lines; **a)** H630 and H630-FR cells, **b)** HT29 and HT29-FR cells, and, **c)** HCT-116 and HCT-116-FR cells, (1×10^3 cells/well 96 well plate ($320\text{mm}^2/\text{well}$)), which were treated with their IC_{50} concentration of 5-FU, *decma* at 1:100 dilution, or *decma* at 1:100 dilution plus the IC_{50} concentration of 5-FU. Cells that were untreated, treated with rat IgG or treated with DMSO vehicle were used as controls (refer to figure key for colour coding). Absorbance at 540nm of 6 replicates per treatment were averaged and displayed as a percentage of DMSO-treated control. Standard deviation was calculated from the percentage DMSO-treated control values of the 6 replicates. A representative experiment is shown.

Figure 53

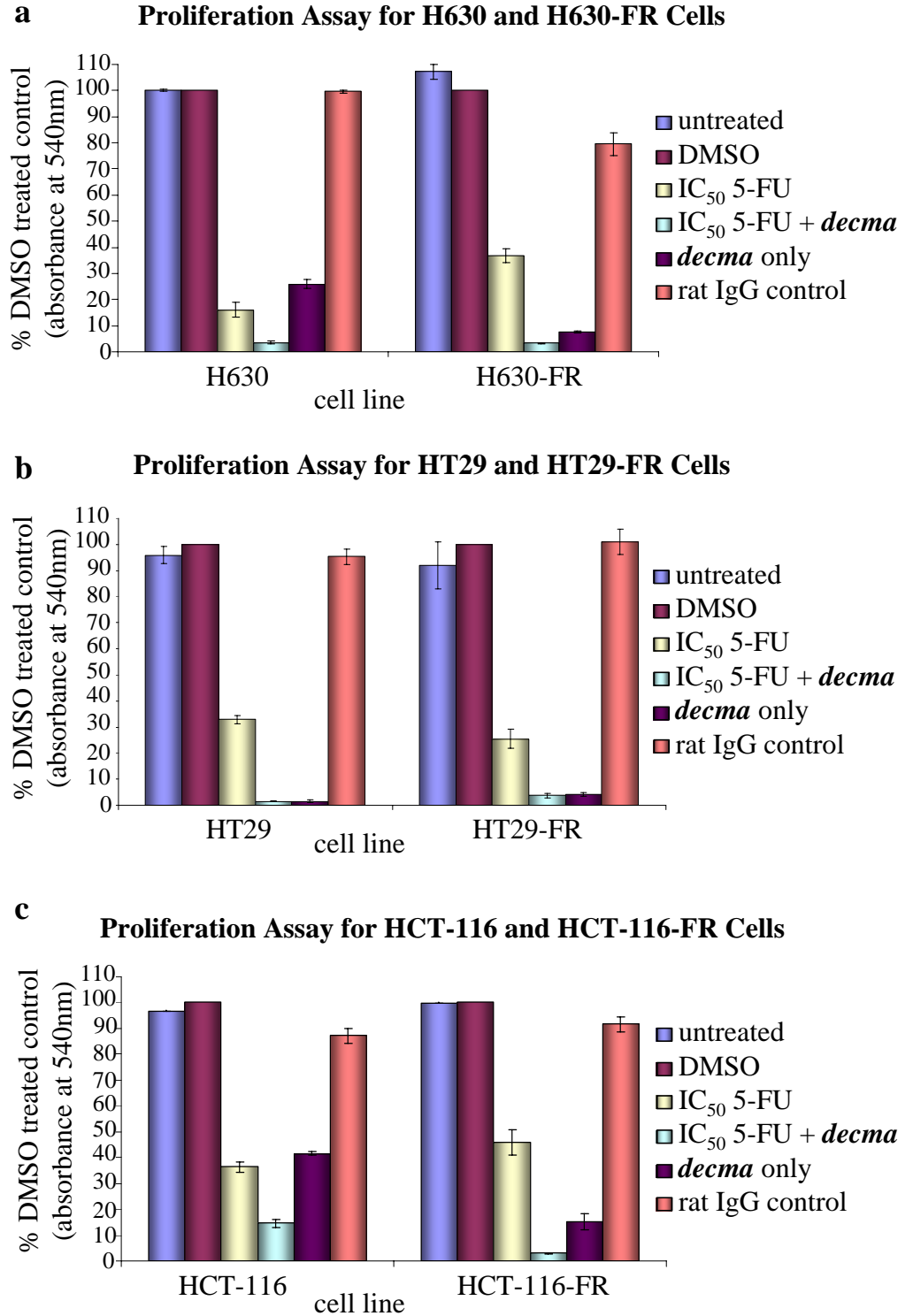


Figure 54 - Immunofluorescence of HCT-116 and HCT-116-FR Cells Treated with *Decma* before Removal for 7 days

HCT-116 and HCT-116-FR cells were trypsinised and single cells generated. 9×10^3 cells were plated on 19mm coverslips and incubated with *decma* antibody at 1:100 dilution for 7 days before being washed with complete medium to remove *decma* antibody and grown for a further 7 days. Cells were then fixed and stained with an antibody against; **a**) E-cadherin (shown in green; Alexa Fluor 488) or **b**) β -catenin (shown in green; Alexa Fluor 488). Incubation with rat IgG was used as a control (4.5×10^3 cells were plated on 19mm coverslips to account for increased assay time). Vectashield containing DAPI was used to visualise the nuclei (blue). Scale bars 20 μ m.

Figure 54

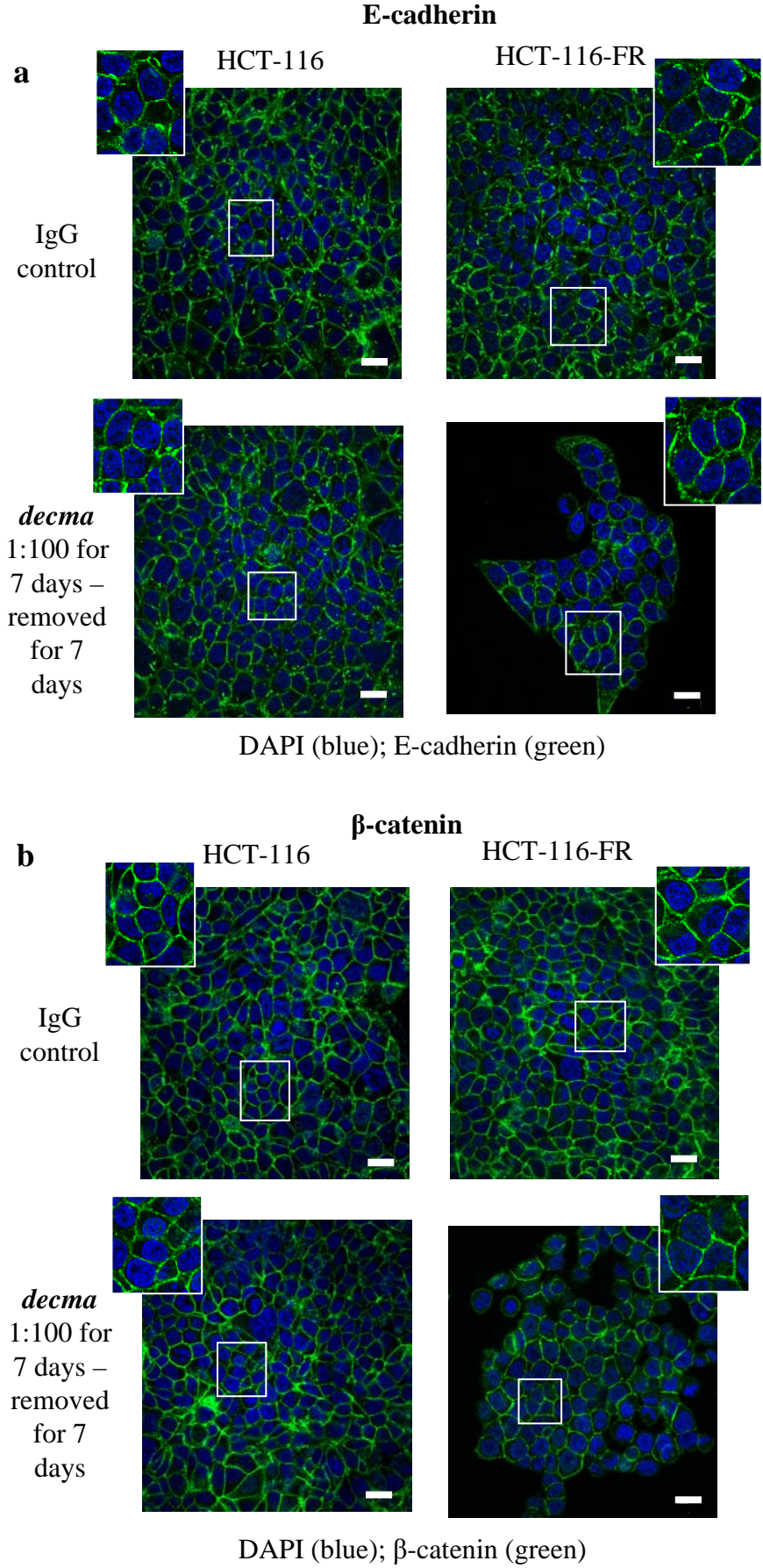
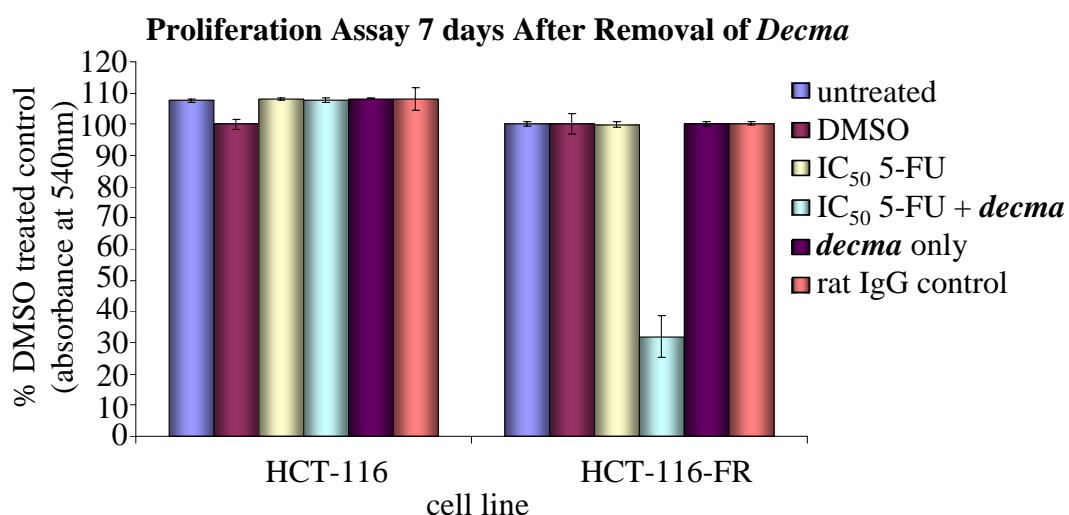


Figure 55

Proliferation in HCT-116 and HCT-116-FR Cells after Removal of *Decma*

An SRB cell proliferation assay was performed over 7 days on HCT-116 and HCT-116-FR cells (1×10^3 cells/well 96 well plate ($320\text{mm}^2/\text{well}$)), which were treated with the IC₅₀ concentration of 5-FU, *decma* only (1:100), or *decma* (1:100) plus the IC₅₀ concentration of 5-FU. Cells that were untreated, treated only with non-immune rat IgG or treated with DMSO vehicle were used as controls and plated with 0.5×10^3 cells/well 96 well plate to account for increased assay time (refer to figure key for treatment colour coding). After 7 days, treatments were removed and replaced with complete medium for another 7 days. Absorbance at 540nm of 6 replicates per treatment were averaged and displayed as a percentage of DMSO-treated control. Standard deviation was calculated from the percentage DMSO-treated control values of the 6 replicates. A representative experiment is shown.

5.6. Cell Survival after *Decma* Treatment

In order to determine whether *decma* was affecting cell survival (rather than proliferation per se) caused by the reduced cell number observed after *decma* treatment, a TUNEL assay was performed in HCT-116 (**Figure 56**) and HCT-116-FR cells (**Figure 57**). Breaks in DNA are highlighted by the incorporation of fluorescein (detected via excitation at 488 nm) at the free 3'-hydroxyl ends of the fragmented DNA (Gavrieli et al., 1992), thus allowing cell death to be monitored (**Figures 56a** and **57a**). Treatment with rat IgG was used as a control (**Figures 56b** and **57b**). Treatment with DNase, an enzyme that catalyzes the hydrolytic cleavage of phosphodiester linkages in the DNA backbone, was used as a positive control for TUNEL staining (**Figures 56c** and **57c**) and a negative control with no TUNEL staining was used to determine the degree of background staining (**Figures 56d** and **57d**). In HCT-116 cells treated with *decma*, no TUNEL staining was detected when compared to controls, whilst HCT-116-FR cells treated with *decma* displayed positive TUNEL staining.

Thus, *decma* treatment of HCT-116-FR cells resulted in cell death, whilst this does not occur in the HCT-116 cells. This is consistent with *decma* treatment resulting in cell death caused by loss of signals coming from E-cadherin-mediated junctions.

TUNEL staining indicated that during loss of cell-cell junctions by treatment with *decma*, HCT-116-FR cells undergo cell death unlike their non-resistant counterparts, HCT-116 cells, which only experience reduced cell proliferation. This may be an explanation for why the HCT-116-FR cells treated with *decma*, in addition to their IC₅₀ concentration of 5-FU, did not recover fully upon removal of treatment.

It is known that treatment with 5-FU utilises the p53 cell death pathway to kill cells (Longley et al., 2003). The localisation of p53 in either the nucleus or the cytoplasm

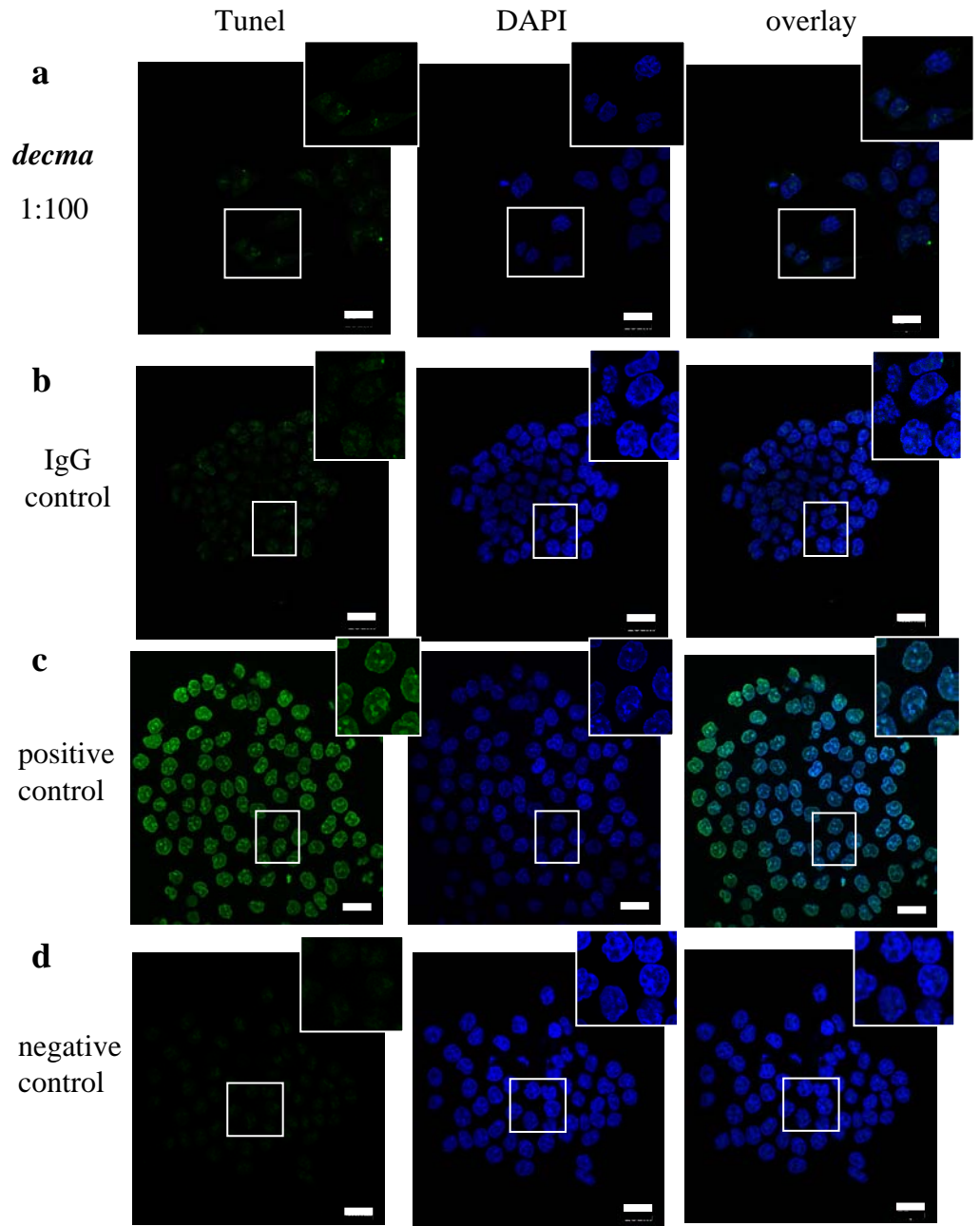
governs very defined, and sometimes opposing roles, played by p53 in the cells (Hollstein and Hainaut, 2010). Therefore, I initially investigated if there were any differences between the location of p53 in HCT-116 and HCT-116-FR cells, which both contain wild-type p53 and display differing basal levels between the cell lines (shown later). HCT-116 and HCT-116-FR cells were incubated with *decma* at 1:100 dilution and grown for 7 days. Cell treated with rat IgG were used as controls. Cells were fixed and stained with an antibody against p53 (**Figure 58**). The percentage of cells with positively stained p53 nuclei was calculated for each cell line and condition. IgG control treatment of HCT-116-FR cells showed a large proportion of cells contained nuclear p53 compared with a lower number in HCT-116 cells (**Figure 58a**). Treatment with *decma* resulted in a reduced number of cells containing p53 staining in the nucleus of the HCT-116-FR cells. Conversely, the HCT-116 cells experienced a rise in positive p53 staining in the nucleus (**Figure 58b**). This observation was quantified by counting positive nuclei and displayed as a percentage of total number of nuclei present (**Figure 58c**).

Thus, I concluded that basal nuclear staining of p53 was greater in the 5-FU-resistant cells when compared to their sensitive counterpart. However, upon *decma* treatment, and hence loss of junctions, the level of nuclear p53 staining in the 5-FU-resistant HCT-116-FR cells was reduced toward levels shown in the 5-FU sensitive HCT-116 cells. Conversely, HCT-116 cells, during loss of cell-cell junctions, experienced an increase in nuclear staining of p53. This suggested differing roles of p53 in 5-FU-sensitive and –resistant cells, based on localisation, when adherens junctions are removed.

Figure 56 - TUNEL Staining of HCT-116 Cells Treated with *Decma*

HCT-116 cells (9×10^3 cells/19mm coverslips) were incubated with **a)** *decma* at 1:100 dilution or **b)** rat IgG control and grown for 7 days before a TUNEL assay was performed (shown in green (fluorescein); described in Materials and Methods). **c)** Incubation for 5 minutes with DNase prior to TUNEL assay being performed was used as a positive control. **d)** A rat IgG control sample without TUNEL treatment was used as a negative control to determine the degree of background staining. Vectashield containing DAPI was used to visualise the nuclei (blue). An overlaid image is also shown. Scale bars 20 μ m.

Figure 56



DAPI (blue); Tunel (green)

Figure 57 - TUNEL Staining of HCT-116-FR Cells Treated with *Decma*

HCT-116-FR cells (9×10^3 cells/19mm coverslips) were incubated with **a)** *decma* at 1:100 dilution or **b)** rat IgG control and grown for 7 days before a TUNEL assay was performed (shown in green (fluorescein); described in Materials and Methods). **c)** Incubation for 5 minutes with DNase prior to TUNEL assay being performed was used as a positive control. **d)** A rat IgG control sample without TUNEL treatment was used as a negative control to determine the degree of background staining. Vectashield containing DAPI was used to visualise the nuclei (blue). An overlaid image is also shown. Scale bars 20 μ m.

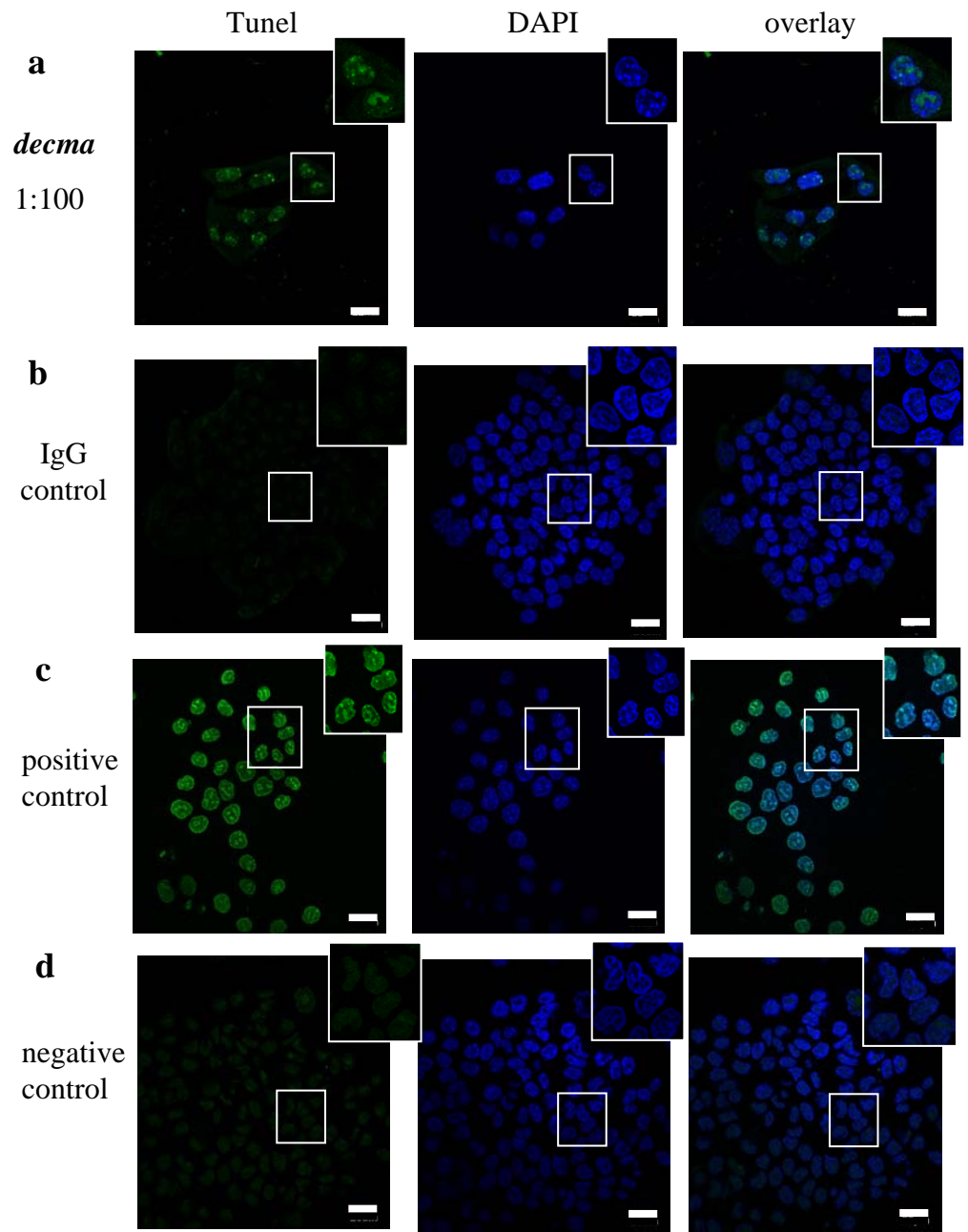
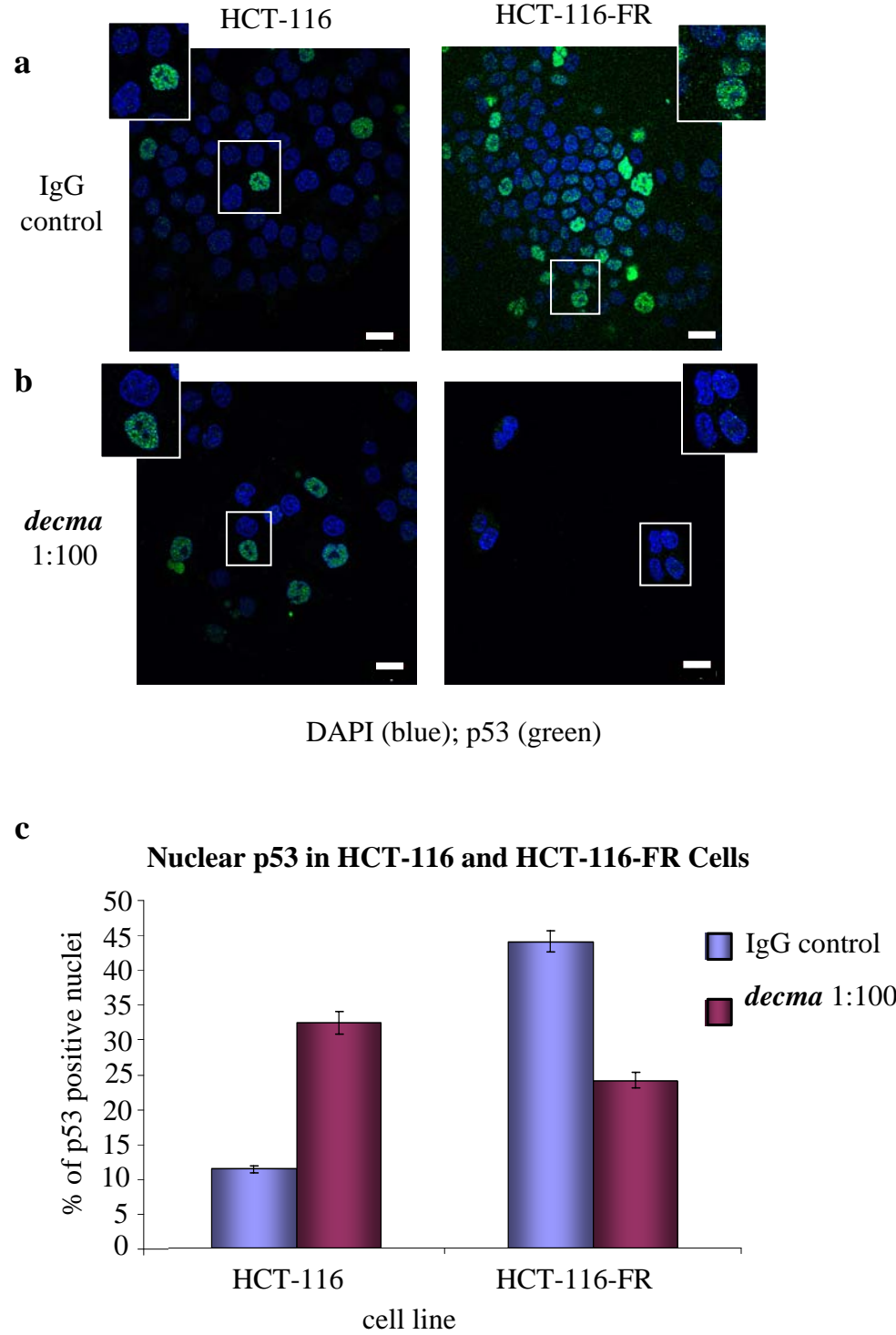
Figure 57

Figure 58 - p53 Localisation in HCT-116 and HCT-116-FR Cells

HCT-116 and HCT-116-FR cells were incubated with **a)** rat IgG control or **b)** *decma* at 1:100 dilution and grown for 7 days. Cells were then fixed using the formaldehyde method and stained with an antibody against p53 (shown in green; Alexa Fluor 488). Vectashield containing DAPI was used to visualise the nuclei (blue). A cell count of positively stained p53 nuclei in HCT-116 and HCT-116-FR cells was presented as a percentage calculated from total nuclei in 15 images (greater than 250 cells) analysed (**c**). Standard deviation was calculated from the 15 images analysed. A representative experiment is shown. Scale bars 20 μ m.

Figure 58



5.7. Signalling Effects of *Decma* Treatment

Since a reduction in proliferation was observed in both HCT-116 and HCT-116-FR cells upon *decma* treatment, which was greater in the HCT-116-FR cells (**Figure 53c**), I performed immunoblotting on lysates after 7 days of *decma* treatment (**Figure 59**). It is known that E-cadherin allows activation of the MAP kinase and PI-3-kinase (Akt) pathways (Pece et al., 1999; Pece and Gutkind, 2000). Hence, junction loss caused by *decma* treatment, may effect signalling through these pathways. As just described, nuclear staining of p53 was also altered upon *decma* treatment and I also studied p53 levels by immunoblotting.

Treatment of HCT-116 cells with *decma* caused an increase in phosphorylation of the pro-proliferation and/or survival signal proteins Akt and MAP kinase when compared to control cells, on sites that are specifically associated with kinase activity. This was not the case for the HCT-116-FR cells, which displayed a decrease in Akt and MAP kinase levels and phosphorylation when the cells were treated with *decma* (**Figure 59a and b**). This suggested that reduced Akt and/or MAP kinase activity correlated with the reduced proliferation and/or survival observed in the HCT-116-FR cells upon *decma*-induced loss of cell-cell junctions. As mentioned in the introduction, activity of PI3-kinase through the mTOR pathway will be determined by activation of p70 S6 kinase. The levels of phosphorylated p70 S6 kinase were unaltered in both cell lines with *decma* treatment. However, I was unable to specifically identify total p70 S6 kinase by immunoblotting as the antibody did not produce 'clean' blots, resulting in an inability to confirm total p70 S6 kinase expression level (**Figure 59c**). Thus the changes I observed in Akt and MAP kinase activities were not general activations of all downstream pathways.

An increase in the generally pro-apoptotic protein p53 was obtained in both HCT-116 and HCT-116-FR cells treated with *decma*. Both HCT-116 and HCT-116-FR cells contain wild type p53 (McDermott et al., 2005) and I noted that HCT-116 cells appear to have a

higher basal level of p53 than their 5-FU resistant counterparts, suggesting the protein is more stable or transcription levels differ between the cells. Since 5-FU operates via a p53 dependant mechanism to cause cell death (Longley et al., 2003), this decrease in basal p53 could be one mechanism that contributes to resistance in the HCT-116-FR cells. However, phosphorylation of p21^{CIP1}, which is a target of p53, at Threonine 145 (T145) did not appear to alter upon *decma* treatment in either cell line, although I was unable to determine total p21^{CIP1} expression levels, as antibodies proved to be unreliable (**Figure 59d**).

As *decma* treatment caused an effect on cell-cell contacts, I examined total levels of E-cadherin and p120-catenin. The total protein levels were unaltered in both cell lines after *decma* treatment. However, there was a faster migrating species present in the E-cadherin blot of the HCT-116 cells when treated with *decma*, which is absent in IgG control or untreated cells. The reason for this and its significance is currently unknown. In addition, there was a lower species of p120-catenin protein in the HCT-116-FR cells which is consistently lost upon *decma* treatment. Again, the significance of this is unknown (**Figure 59e**). Actin was used as a protein loading control, and was at similar levels in both sensitive and resistant HCT-116 cells and unaltered by *decma* treatment. From these results, I confirmed that E-cadherin and p120-catenin levels were not visibly altered upon *decma* treatment in HCT-116 and HCT-116-FR cells. Importantly, activation of the Akt and MAP kinase pathway were reduced in the HCT-116-FR cells upon *decma* treatment, suggesting there is a link between E-cadherin-mediated adherens junctions, signalling through the Akt and/or MAP kinase, and chemoresistance. In contrast to the resistant cells, *decma* treatment seemed to cause increased activity of Akt and MAP kinase.

These results suggest that the decrease in proliferation observed in the 5-FU resistant cells upon junction loss may correlate with reduced signalling from the Akt and MAP kinase pathways. HCT-116 cells also respond to *decma* by reduced proliferation and increases in

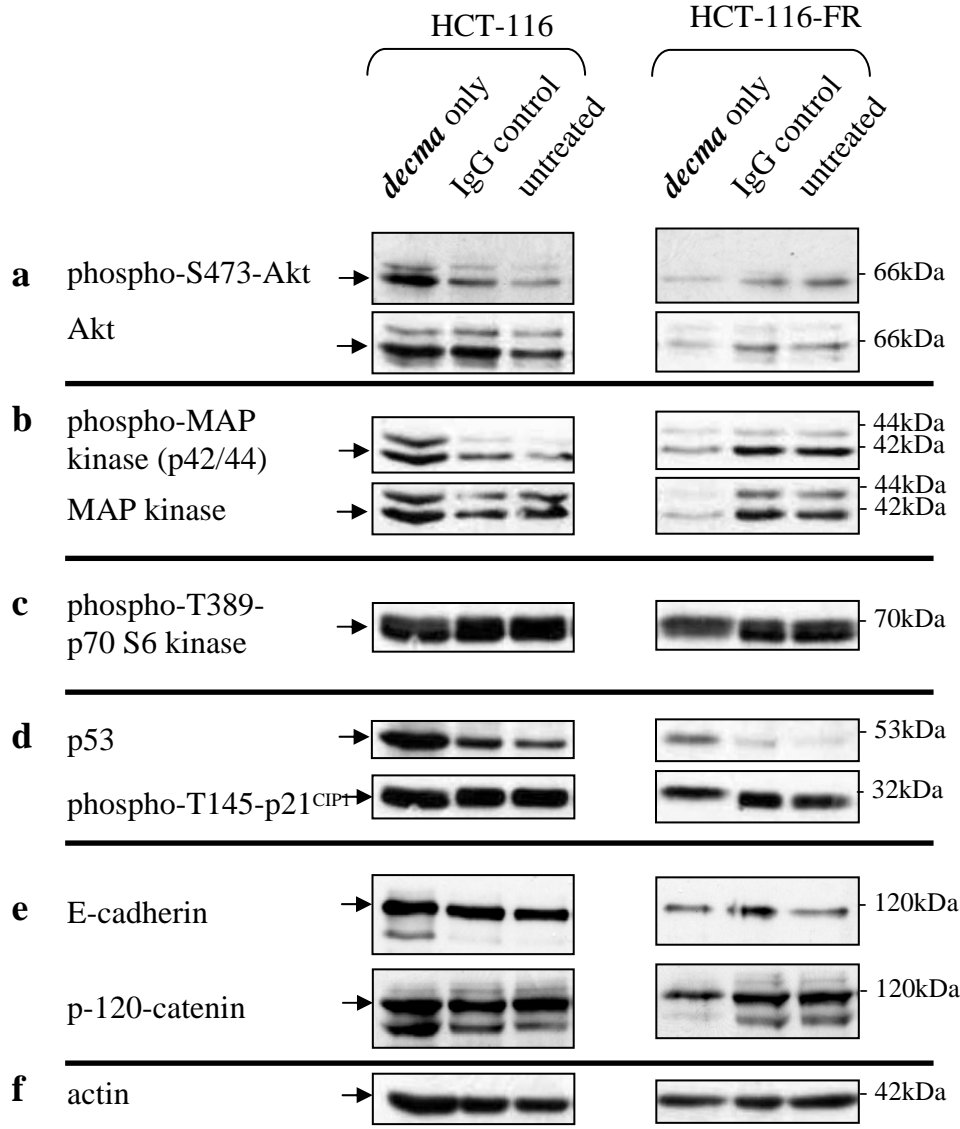
activation of both Akt and MAP kinase pathways may provide a mechanism for proliferation and/or survival that results in HCT-116 cells achieving greater proliferation than the HCT-116-FR cells during junction loss.

Thus, the HCT-116-FR cells were more sensitive to *decma* treatment and subsequent loss of adherens junctions than HCT-116 cells, which may be explained by loss of proliferation and/or survival signals from the Akt or MAP kinase pathways. Hence, the Akt and MAP kinase pathways were investigated in future experiments. Note:- Basal levels of activation differed in **Figure 61** and **Figure 63** from IgG control samples shown in this section in **Figure 59**. This was attributed to a greater density of cells being used to generate data in **Figure 59** which altered protein levels.

Figure 59 - Immunoblotting Signalling Effects in HCT-116 and HCT-116-FR Cells

Immunoblotting was carried out after 7 days on HCT-116 and HCT-116-FR cells that were untreated, or treated with *decma* (1:100) or rat IgG. Lysates were probed with antibodies against proteins involved in the PI3-kinase and MAP kinase pathways, i.e. phospho-S473-Akt and Akt (**a**), phospho-MAP kinase (p44/p42, Thr202/Tyr204) and MAP kinase (**b**) and phospho-p70 S6 kinase (**c**), apoptosis i.e. p53 and its target - phospho-T145-p21^{CIP1} (**d**) and cell-cell adhesion, i.e. E-cadherin and p120-catenin (**e**). Actin was used as a loading control (**f**). A representative experiment is shown. Molecular weight markers are shown.

Figure 59



5.7.1. Signalling Effect via the PI3-kinase/Akt and MAP Kinase Pathways

Immunoblotting of *decma*-treated HCT-116-FR cells suggested a link between the reduced proliferation of the HCT-116-FR and decreased signalling through the PI3-kinase/Akt and MAP kinase pathways. In *decma*-treated HCT-116 cells, the signalling via these pathways was enhanced when compared to rat IgG controls, implying that these pathways may be enhanced to mediate proliferation and/or survival when the junctions are lost in the HCT-116 cells. In order to test dependency on these pathways, an SRB cell proliferation assay was carried out over 7 days on HCT-116 and HCT-116-FR cells treated with increasing concentrations of either GDC-0941, a specific inhibitor of PI3-kinase p110- α subunit (**Figure 60**) or a commonly used MAP kinase kinase (MEK) inhibitor, U0126 (**Figure 62**).

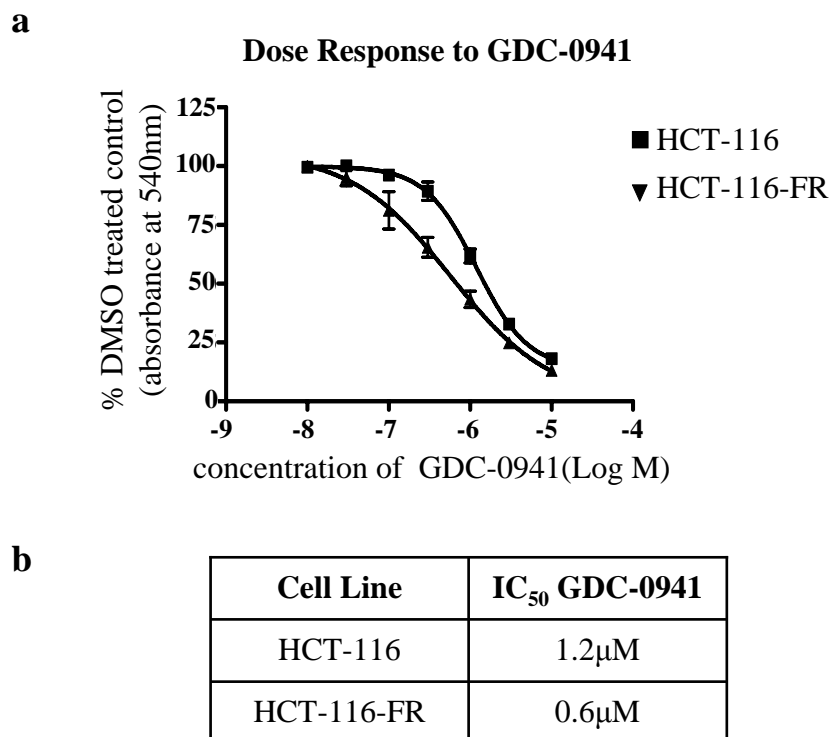
Treatment with GDC-0941 resulted in a dose dependent inhibition of proliferation of both the HCT-116 and HCT-116-FR cells (**Figure 60a**). However, this was more marked in the HCT-116-FR cells, with a lower IC₅₀ concentration of 0.6 μ M compared to the IC₅₀ concentration of 1.2 μ M for the HCT-116 cells (**Figure 60b**). Immunoblotting of HCT-116 and HCT-116-FR cells treated with increasing concentrations of GDC-0941 confirmed that the proliferation effects corresponded with a dose dependent decrease in phospho-S473-Akt (**Figure 61a**). DMSO treated samples were used as controls and they confirmed that the basal level of phospho-S473-Akt in the HCT-116-FR cells was greater than that in the HCT-116 cells. Protein expression levels of Akt remained unaltered in both cell lines and levels were the same in both HCT-116 and HCT-116-FR cells (**Figure 61b**). Increased activation of Akt in the HCT-116-FR cells compared to the HCT-116 cells may be a result of greater signalling from E-cadherin in these cells.

The levels of phospho-T389-p70 S6 kinase, total p53 and phospho-T145-p21^{CIP1} decreased in a dose dependent manner as the concentration of GDC-0941 increased (**Figure 61c, d** and **e**, respectively). Unfortunately, total p21^{CIP1} and p70 S6 kinase levels could not be

established. The levels of phospho-T145-p21^{CIP1} and phospho-T389-p70 S6 kinase did not differ between DMSO treated HCT-116 and HCT-116-FR cells. However, p53 levels were higher in DMSO treated HCT-116-FR cells when compared to HCT-116 cells. Total protein loading was unaltered in all samples as judged by immunoblotting with an antibody against actin (**Figure 61f**). From these results, I concluded that HCT-116-FR cells may rely on the PI3-kinase pathway for pro-proliferation and/or survival to a greater extent than the HCT-116 cells. Results thus far suggest that removal of E-cadherin-mediated junctions causes reduced Akt signalling, resulting in cell death, possibly by a p53 dependant mechanism in resistant cells but not in sensitive cells.

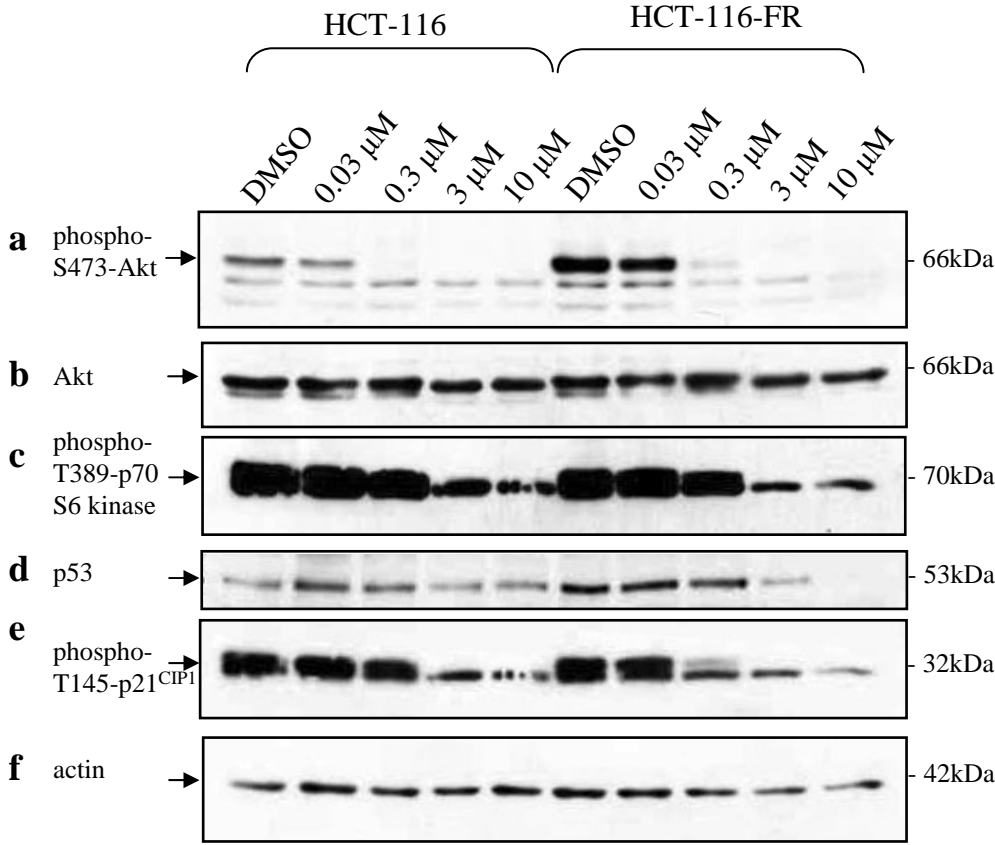
Treatment with U0126 resulted in a dose dependent inhibition of proliferation of both the HCT-116 and HCT-116-FR cells (**Figure 62a**). There was no apparent difference in sensitivity to U0126 between the HCT-116 and HCT-116-FR cells with IC₅₀ values of 6.7µM and 6.2µM, respectively (**Figure 62b**). Immunoblotting of HCT-116 and HCT-116-FR cells treated with increasing concentrations of U0126 produced a dose dependent decrease in phospho-MAP kinase (p42/44) (**Figure 63a**). Total protein expression levels of MAP kinase and p53 with U0126 treatment were not substantially altered in either cell lines (**Figures 63b** and **c**). The levels of phospho-T145-p21^{CIP1} decreased in a dose dependent manner as the concentration of U0126 increased (**Figure 63d**) suggesting signalling through MAP kinase contributes to activation of p21^{CIP1}.

Overall, these data suggest there was a difference on reliance of signals from the PI3-kinase pathway between the HCT-116 and HCT-116-FR cells, but not the MAP kinase pathway. The 5-FU resistant HCT-116-FR cells had an increased basal level of phospho-S473-Akt which was reduced on disruption of cell-cell adhesions after *decma* treatment. Thus, there is a strong correlation between cell-cell adhesion, phospho-S473-Akt and E-cadherin-mediated pro-proliferation and/or survival in HCT-116-FR cells.

Figure 60

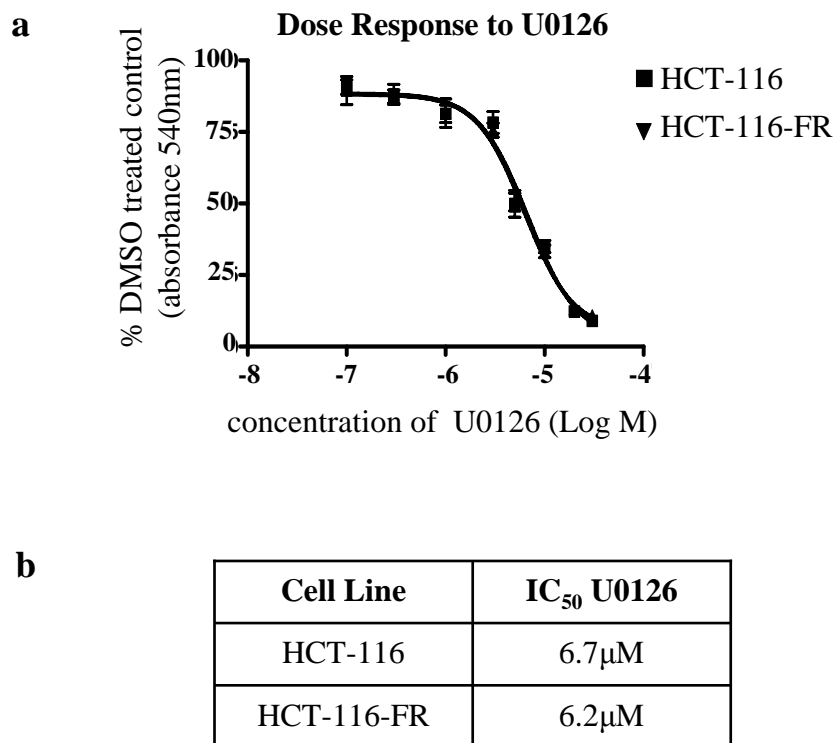
Proliferation of HCT-116 and HCT-116-FR Cells Treated with GDC-0941

a) An SRB proliferation assay was performed over 7 days on HCT-116 and HCT-116-FR cells (1×10^3 cells/well of 96 well plate ($320\text{mm}^2/\text{well}$)) which were treated with a range of concentrations of GDC-0941, a selective inhibitor of PI-3-kinase p110- α subunit. Cells that were DMSO treated were used as controls (refer to figure key for cell line coding). Absorbance at 540nm of 6 replicates were averaged and displayed as a percentage of DMSO-treated control. Standard deviation was calculated from the percentage DMSO-treated control values of the 6 replicates. A representative experiment is shown. **b)** IC₅₀ values for GDC-0941 in HCT-116 and HCT-116-FR cells were calculated using Graph Pad Prism software.

Figure 61

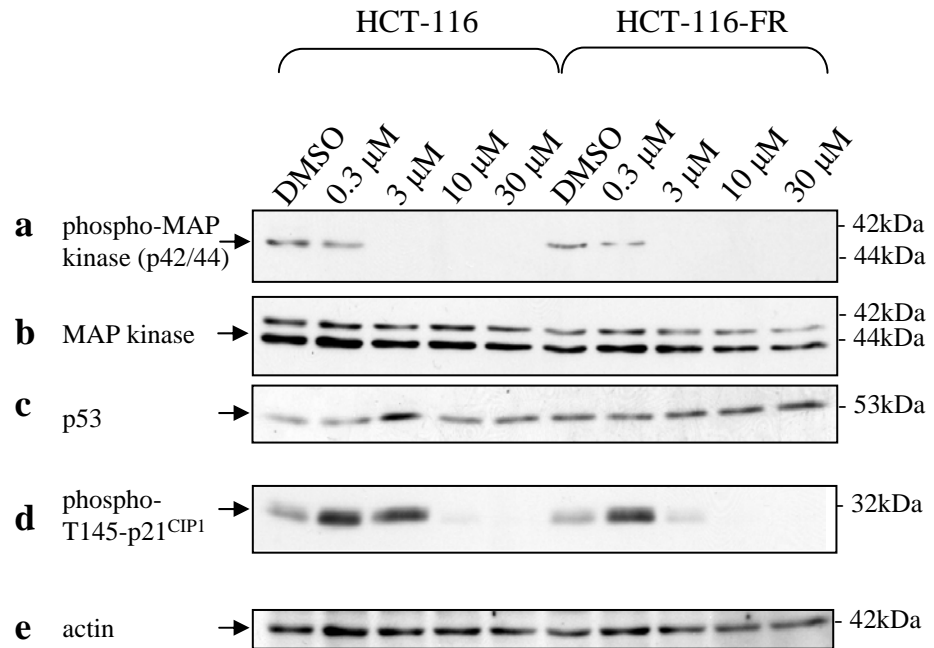
Signalling in HCT-116 and HCT-116-FR Cells Treated with GDC-0941

Immunoblotting was carried out on HCT-116 and HCT-116-FR cells (1×10^6 cells) plated for 24 hours and then treated for a further 24 hours with a range of concentrations of GDC-0941. Lysates were probed with antibodies against; **a**) phospho-S473-Akt, **b**) Akt, **c**) phospho-T389-p70 S6 kinase, **d**) p53, and **e**) phospho-T145-p21^{CIP1}. Actin was used as a loading control (**f**). Molecular weight markers are shown.

Figure 62

Proliferation of HCT-116 and HCT-116-FR Cells Treated with U0126

a) An SRB proliferation assay was performed over 7 days on HCT-116 and HCT-116-FR cells (1×10^3 cells/well of 96 well plate ($320\text{mm}^2/\text{well}$)) which were treated with a range of concentrations of U0126, a selective inhibitor of MEK. Cells that were DMSO treated were used as controls (refer to figure key for cell line coding). Absorbance at 540nm of 6 replicates were averaged and displayed as a percentage of DMSO-treated control. Standard deviation was calculated from the percentage DMSO-treated control values of the 6 replicates. A representative experiment is shown. **b)** IC₅₀ values for U0126 in HCT-116 and HCT-116-FR cells were calculated using Graph Pad Prism software.

Figure 63**Signalling in HCT-116 and HCT-116-FR Cells Treated with U0126**

Immunoblotting was carried out on HCT-116 and HCT-116-FR cells (1×10^6 cells) plated for 24 hours and then treated for a further 24 hours with a range of concentrations of U0126, a specific inhibitor of the MAP kinase pathway. Lysates were probed with antibodies against; **a**) phospho-MAP kinase (p42/44), **b**) MAP kinase, **c**) p53, and **d**) phospho-T145-p21^{CIP1}. Actin was used as a loading control (**e**). Molecular weight markers are shown.

5.8. Clonogenic Assays

Results from previous experiments implied that the 5-FU resistant cell line HCT-116-FR cells, were more reliant on their cell-cell junctions than their more sensitive counterparts, namely HCT-116 cells. Using the clonogenic assay, I investigated whether the effect of 5-FU on the proliferation of HCT-116 and HCT-116-FR cells was dependent on the presence of cell-cell junctions. In addition, I looked at whether the absence of these junctions affected the sensitivity of the cells to 5-FU in order to corroborate the earlier findings with *decma* treatment. HCT-116 and HCT-116-FR cells were trypsinised, single cells generated and cells were plated at 1000 cells/well of a 6 well dish (35mm diameter/well). After 24 hours, the medium was changed for medium containing the IC₅₀ concentration of 5-FU for each cell line. DMSO treatment was used as a vehicle control. The cells were then left for 14 days before being treated with the SRB cell proliferation assay method. Prior to solubilising the SRB, the number of colonies formed was counted and their areas measured (**Figures 64-66**).

The number of colonies formed were reduced in both HCT-116 and HCT-116-FR cells when treated with their corresponding IC₅₀ concentration of 5-FU when compared to their respective DMSO treated controls (**Figure 64**). The inhibition of colony formation was measurably greater in the HCT-116-FR cells. Since the appropriate IC₅₀ was used per cell line, this demonstrates greater sensitivity of the HCT-116-FR to 5-FU in the absence of cell-cell junctions suggesting that HCT-116-FR cells resistance is dependent on cells having cell-cell junctions.

The HCT-116-FR also displayed colonies of a smaller area when treated with DMSO when compared to the HCT-116 cells (**Figure 65**). Treatment with 5-FU, reduced colony area in both cell lines, but this effect appeared greater in the HCT-116 cells since the area of DMSO treated cells was initially larger. Therefore, I concluded that the IC₅₀ concentration

of 5-FU resulted in a measurable reduction in colony area in the HCT-116 cells, but 5-FU treatment had no substantial effect on the colony area of the HCT-116-FR cells. This data suggests that colonies formed from HCT-116-FR single cells are already at a reduced area upon DMSO treatment, due to lack of cell-cell contact, which cannot be substantially reduced during 5-FU treatment.

SRB cell proliferation assay results, from the clonogenic assays, allow a more accurate analysis of proliferation from the colonies formed. Both HCT-116 and HCT-116-FR cells indicated a reduction in proliferation by 5-FU treatment (**Figure 66a**). When these results were displayed as a percentage of DMSO control only 10% of HCT-116-FR cells survived 5-FU treatment (90% proliferation inhibition) compared to 23% of HCT-116 cells (77% proliferation inhibition). Therefore, upon 5-FU treatment, reduced proliferation was more apparent in the HCT-116-FR cells than in the HCT-116 cells.

The SRB cell proliferation assay results did not corroborate with the colony area observed. 5-FU treatment reduced colony area was more obvious in HCT-116 cells, but reduced proliferation was more apparent in HCT-116-FR cells. I noted that the HCT-116-FR cells appeared to have additional cells growing above the monolayer, suggesting preferential attachment by cell-cell junctions rather than colony spreading, mediated by cell-matrix attachment and that this observation may possibly correlate with 5-FU resistance acquisition. To examine this in 3-dimensions (3-D), HCT-116 and HCT-116-FR cells were plated sparsely on glass-bottomed dishes and grown for 4 days. The colonies formed during this time were fixed and stained with calcein, AM (cytoplasmic dye) and DAPI (nuclei dye) and 3-D images compiled using the Olympus FV1000 confocal microscope (**Figure 67**). I found that the HCT-116 cells grew in a flat monolayer with a colony height of 12 μ m. In contrast, the colonies formed in the HCT-116-FR cells were deeper with cells 'piled up' on top of one another and measured 100 μ m at the highest peak of cells with the main bulk of cells measuring 90 μ m high. This can be seen more clearly by a cross

sectional image through the deepest section of each colony, which showed that the HCT-116-FR cells grew in a bell-shaped form versus the relatively flat growth observed in the HCT-116 cells (**Figure 67b**).

Therefore, I concluded that HCT-116 cells are more able to proliferate from single cells than HCT-116-FR cells. In HCT-116 cells, 5-FU treatment reduced colony number by approximately 25% and had a major impact on colony area, which together resulted in an 80% proliferation inhibition. HCT-116-FR cells were less able to give rise to colonies from single cells than HCT-116 cells during DMSO treatment and this was markedly reduced by 5-FU addition. However, colony area was not greatly affected by the addition of 5-FU. The proliferation inhibition of 90% seen in the HCT-116-FR cells is therefore principally from the failure of HCT-116-FR cells to give rise to colonies when incubated in the presence of an IC_{50} dose of 5-FU.

Figure 64 - Clonogenic Assay of the HCT-116 and HCT-116-FR Cells

HCT-116 and HCT-116-FR cells were trypsinised and single cells generated. A clonogenic assay was performed by plating 100 cells/well of a 6 well dish (35mm diameter/well). After 24 hours the medium was changed for medium containing the corresponding DMSO concentration or IC_{50} concentration of 5-FU. The samples were then left for 14 days before being treated with the SRB cell proliferation assay method **(a)**. The number of colonies formed was counted for each cell line, and treatment, and shown as an average of 3 experiments **(b)**. Standard deviation was calculated from the 3 experiments analysed.

Figure 64

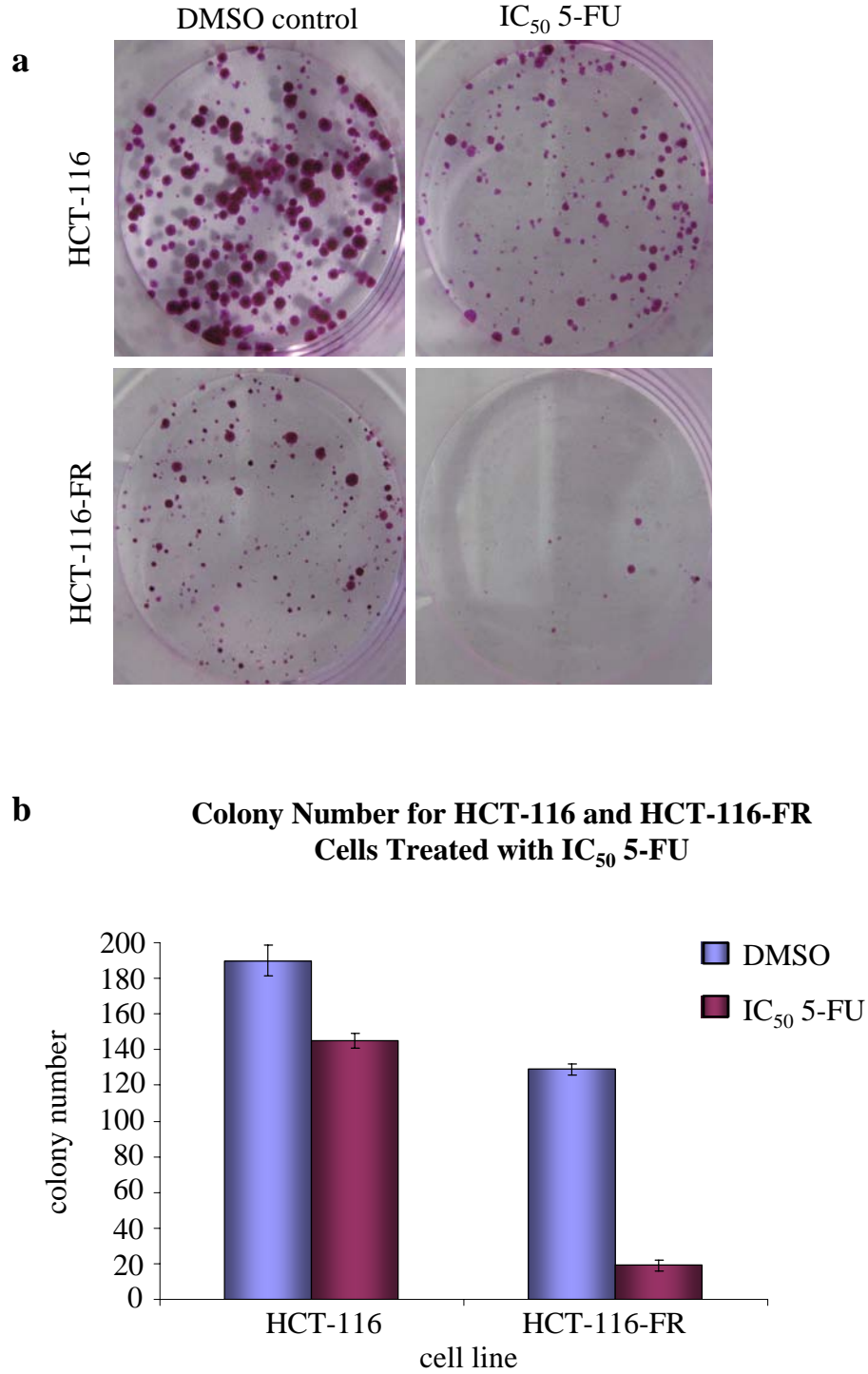


Figure 65 - Average Area of Colonies in HCT-116 and HCT-116-FR Cells

A clonogenic assay was performed with HCT-116 and HCT-116-FR cells (**Figure 64**). Image shown depicts colonies from which measurements were obtained (**a**). Colony area was measured for HCT-116 and HCT-116-FR cells with and without 5-FU treatment (**b**) and displayed as an average. Standard error for colony size was calculated and shown on graph. A representative experiment is shown.

Figure 65

a



b

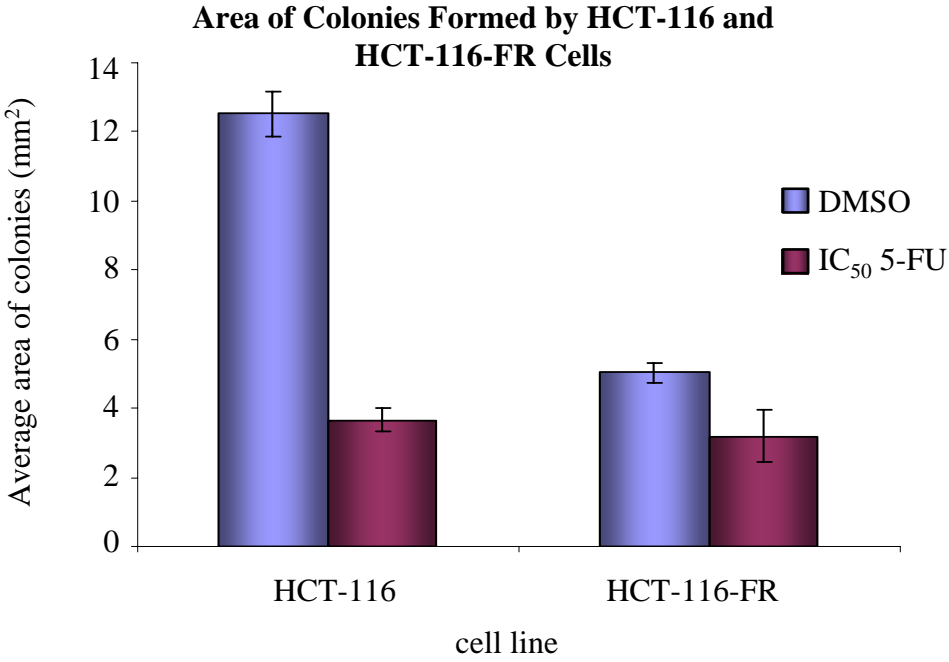


Figure 66 - Clonogenic Assays of HCT-116 and HCT-116-FR Cells

A clonogenic assay was performed with HCT-116 and HCT-116-FR cells with and without 5-FU treatment (**Figure 64**). After colony size measurements were obtained (**Figure 65**), the SRB dye was solubilised using SRB solubilising solution (described in Materials and Methods). **a)** An average absorbance at 540nm of 3 replicates per treatment was calculated. Standard deviation was derived from the values obtained from the 3 replicates. A representative experiment is shown. **b)** Values of percentage DMSO-treated control were calculated from the average results obtained with 5-FU treatment of HCT-116 and HCT-116-FR cells.

Figure 66

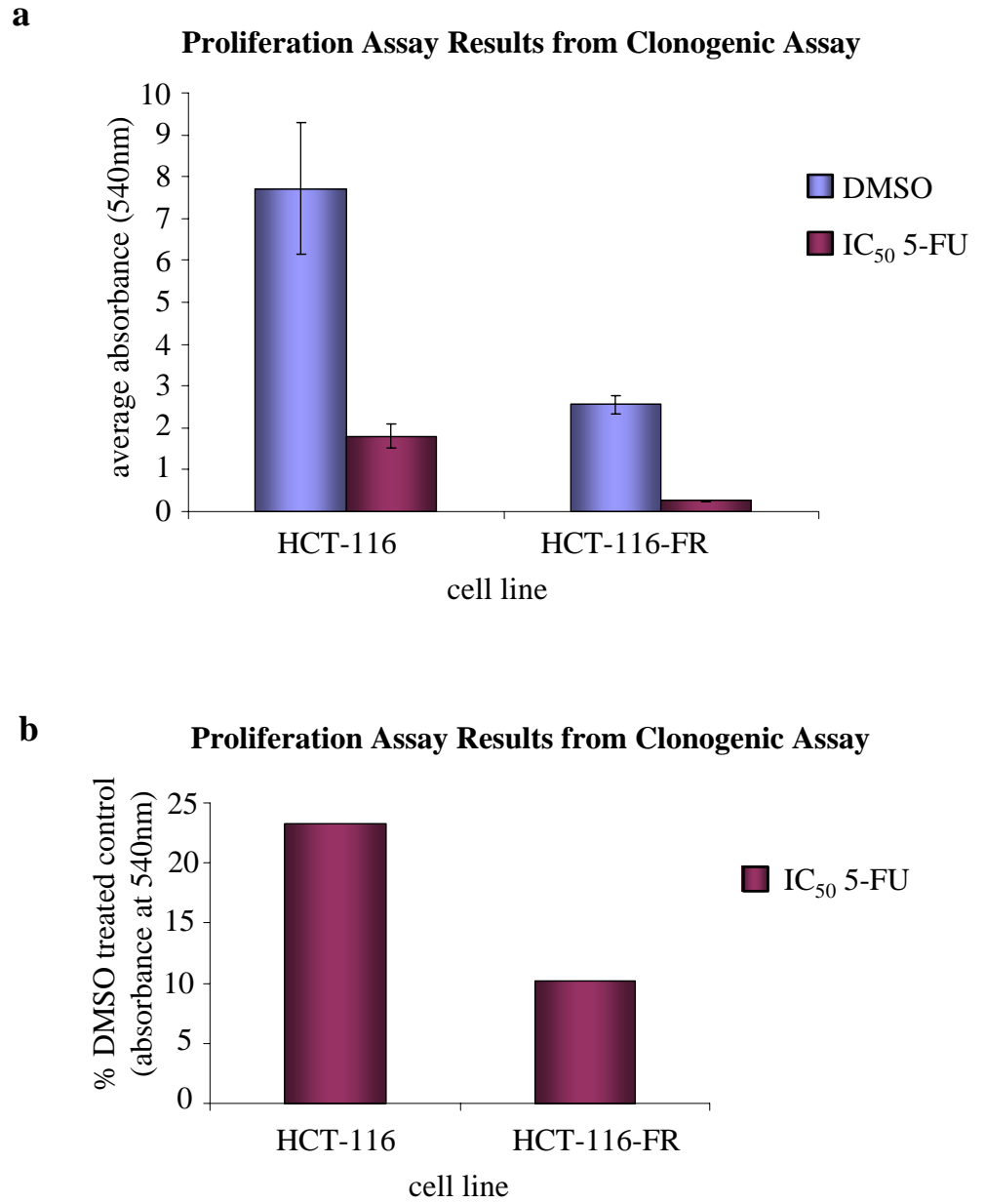
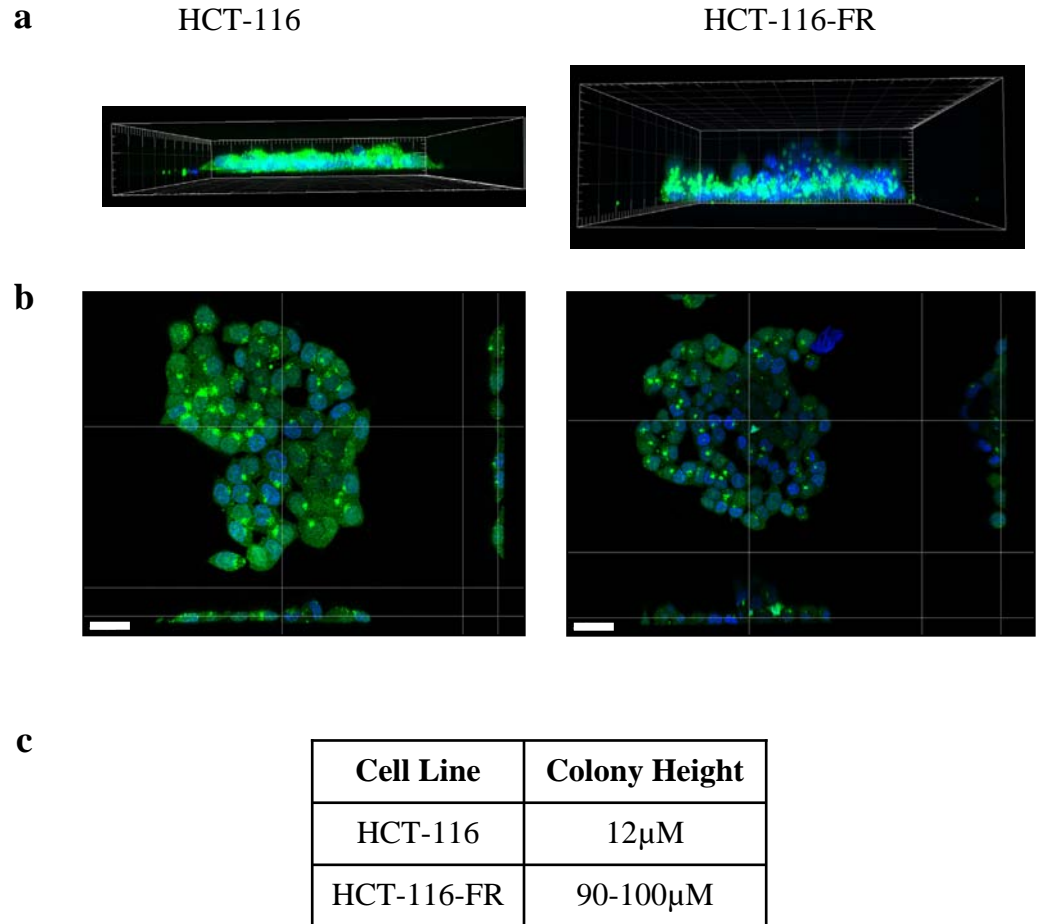


Figure 67

3-Dimensional (3-D) Analysis of HCT-116 and HCT-116-FR Cell Colonies

3-dimensional (3-D) analysis was performed on colonies grown by HCT-116 and HCT-116-FR cells. Cells were plated onto glass-bottomed 30mm dishes at low density (1×10^5 cells) and grown for 4 days. The cells were incubated with calcein, AM, for 1 hour at 37°C and then fixed with formaldehyde. DAPI was added to cells to visualise nuclei. Confocal images were taken in 0.5 μ M sections throughout a colony of cells. These sections were then compiled to give, **a**) a 3-D image that enabled **c**) the height of the colony of cells to be established. **b**) An image through a cross-section of the sample is also shown. Scale bars 40 μ m.

5.9. Use of siRNA as Another Approach

In order to find an alternative way to test the effect of interfering with E-cadherin functions on 5-FU sensitivity, I performed a preliminary experiment using siRNA to induce knockdown of E-cadherin and p120-catenin expression. E-cadherin RNAi would provide information on loss of the protein in the cells whereas p120-catenin RNAi would result in the inability to form adherens junctions thus testing the importance of adherens junction formation over E-cadherin protein expression. Cells were transiently transfected using Lipofectamine™ 2000 with siRNA against E-cadherin (**Figure 68b**) or p-120-catenin (**Figure 69b**) for 24 hours before being plated onto coverslips for a further 24 hours. Cells were then fixed using the paraformaldehyde method (E-cadherin siRNA) or the formaldehyde method (p120-catenin siRNA) and stained with antibodies against E-cadherin or p120-catenin. Control siRNA, composed of a scrambled sequence that is not directed to any human gene, was used to monitor any non-specific effects of the siRNA or transfection treatment (**Figures 68a** and **69a**).

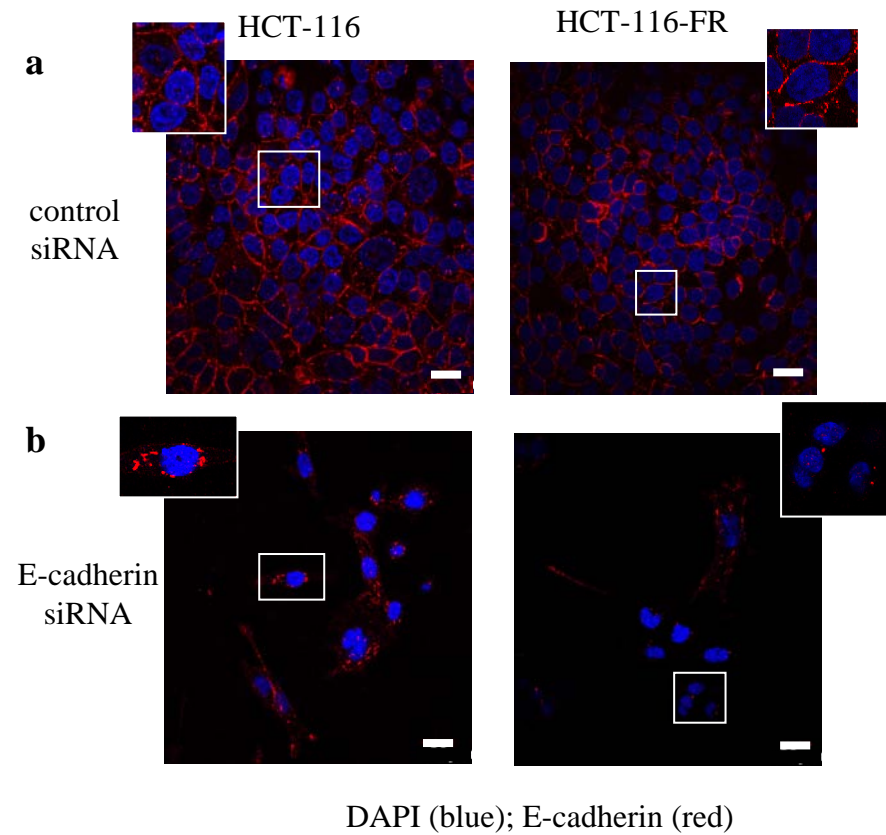
E-cadherin siRNA resulted in a visible reduction in E-cadherin protein and loss of cell-cell adhesions in both HCT-116 and HCT-116-FR cells when compared to control siRNA treated cells (**Figure 68**). Residual E-cadherin appeared to be internalised. Loss of cell-cell adhesions was also evident in HCT-116 and HCT-116-FR cells upon p120-catenin siRNA, where visible protein reduction was apparent (**Figure 69**). However, residual p120-catenin remained at the cell membrane although staining was weaker (**Figure 69b**). These observations were quantified by calculating the percentage of cells that had junctions remaining under each siRNA condition (**Figure 69c**). In control siRNA treated samples, HCT-116 and HCT-116-FR cells had 77% and 64% of cells with cell-cell junctions, respectively. E-cadherin siRNA reduced the percentage of junctions remaining in the HCT-116 and HCT-116-FR cells to 33% and 11%, respectively, whilst p120-catenin

siRNA treated HCT-116 and HCT-116-FR cells displayed 57% and 34% of junctions remaining, respectively. Thus, I concluded that siRNA against E-cadherin and p120-catenin resulted in a reduction of proteins in both HCT-116 and HCT-116-FR cells. Loss of cell to cell junctions was more obvious with E-cadherin siRNA, than with p120-catenin siRNA in this one experiment performed.

It was very obvious from immunofluorescence after E-cadherin siRNA and p120-catenin siRNA there was a greatly reduced cell number consistent with E-cadherin providing essential proliferation and/or survival signals in these colon cancer cells. This seemed to be consistent with the effect of *decma* treatment. However, this was not reflected in reduced cell proliferation as measured by an SRB cell proliferation assay where cells treated with siRNA were treated with a range of 5-FU concentrations (**Figure 70**). No alteration to IC₅₀ concentrations of 5-FU was experienced during knockdown of these proteins in the HCT-116-FR cells or in the p120-catenin siRNA in the HCT-116 cells. However, siRNA knock-down of E-cadherin protein in the HCT-116 cells significantly enhanced their resistance to 5-FU, as illustrated by performing a paired T-Test, generating a P-Value (**Figure 70d**). The lack of alteration to 5-FU IC₅₀ concentrations for HCT-116-FR cells or in the p120-catenin siRNA in the HCT-116 cells may have several explanations. Stable E-cadherin knockdown cells could not be generated as there was loss of cell viability during protein knockdown (data not shown) further indicating that HCT-116 and HCT-116-FR cells required cell-cell junctions for survival. After 2 days, transient knockdown in this preliminary experiment was successful by immunofluorescence and confirmed by immunoblotting (**Figures 71a and 72a**). However, over the period of time required for a cell proliferation assay to be performed, cell cultures recovered E-cadherin and p120-catenin expression (**Figure 71b and c, Figure 72b and c**). Levels of E-cadherin and p120-catenin protein in siRNA treated HCT-116 and HCT-116-FR cells had reached levels similar with control samples suggesting that recovery of protein had occurred during

the SRB cell proliferation assay resulting in no effect on the IC_{50} to 5-FU being displayed (**Figure 71b and c, Figure 72b and c**). This may be due to selection of cells which retained E-cadherin or p120-catenin providing a survival and/or proliferative advantage. Time did not permit me to distinguish possibilities.

From these results, I concluded that in at least one preliminary experiment, it was possible use siRNA to knockdown E-cadherin and p120-catenin, but the SRB cell proliferation assay was uninformative of their effects on cell survival and/or proliferation.

Figure 68

DAPI (blue); E-cadherin (red)

Immunofluorescence of HCT-116 and HCT-116-FR Cells after siRNA

HCT-116 and HCT-116-FR cells (5×10^4 cells/19mm glass coverslip) were plated for 24 hours and then transfected with **a)** control siRNA or **b)** E-cadherin siRNA using Lipofectamine™ 2000 and fixed 2 days after transfection using the paraformaldehyde method. Cells were stained with an antibody against E-cadherin (shown in red; Alexa Fluor 594). Vectashield containing DAPI was used to visualise the nuclei (blue). Scale bars 20 μ m.

Figure 69 - Immunofluorescence of HCT-116 and HCT-116-FR Cells after siRNA

HCT-116 and HCT-116-FR cells (5×10^4 cells/19mm glass coverslip) were plated for 24 hours and then transfected with **a)** control siRNA or **b)** p120-catenin siRNA using Lipofectamine™ 2000 and fixed 2 days after transfection using the formaldehyde method. Cells were stained with an antibody against p120-catenin (shown in red; Alexa Fluor 594). Vectashield containing DAPI was used to visualise the nuclei (blue). Scale bars 20µm. **c)** Cells containing cell-cell junctions were counted in control siRNA, E-cadherin siRNA (**Figure 68**) and p120-catenin siRNA and displayed as an average percentage of cells with junctions remaining. Standard deviation was calculated from an average of 15 images. A representative experiment is shown.

Figure 69

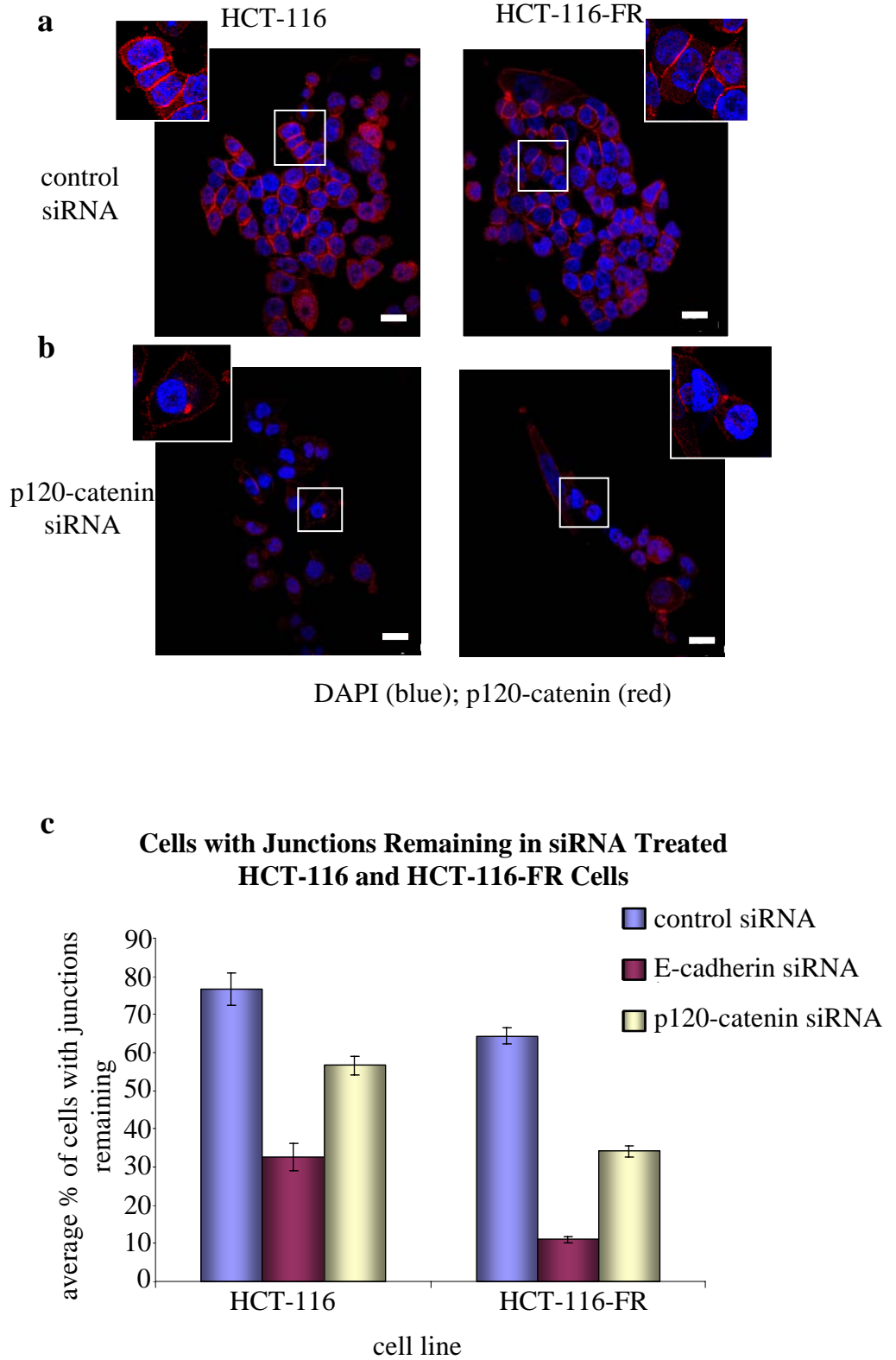
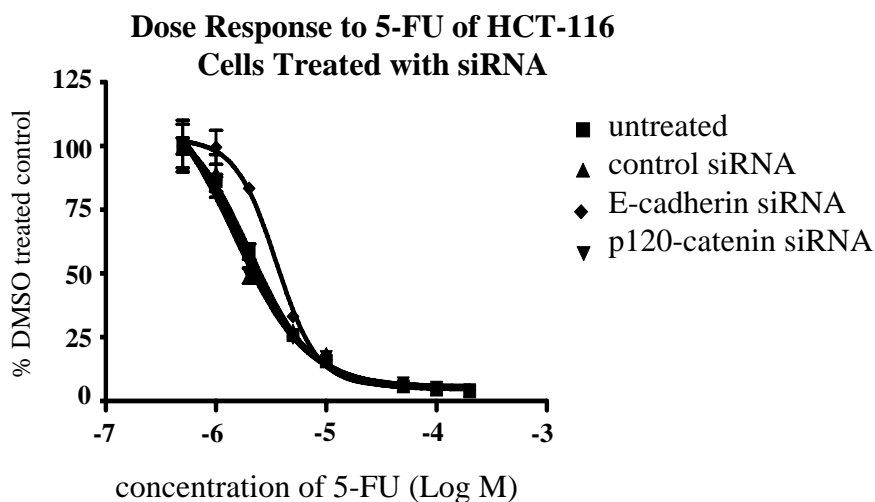


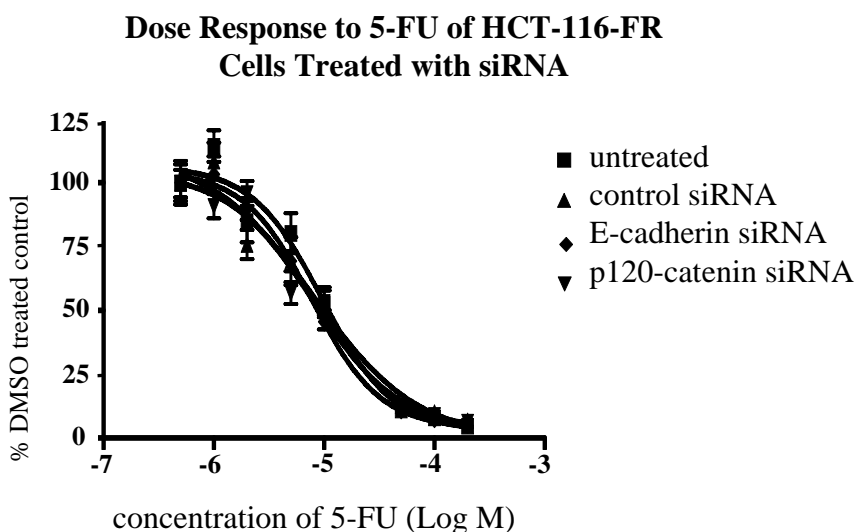
Figure 70 - Effects of siRNA Treatment on Proliferation of HCT-116 and HCT-116-FR Cells

Response to 5-FU of **a)** HCT-116 and **b)** HCT-116-FR cells transfected with control siRNA, E-cadherin siRNA or p120-catenin siRNA was analysed by performing SRB cell proliferation assays over 7 days (1×10^3 cells/well 96 well plate ($320\text{mm}^2/\text{well}$) were treated) with a range of 5-FU concentrations (shown on graph as Log Molar concentration). Refer to figure key for cell line coding. A representative experiment (of three replicates) is shown. Cells that were DMSO-treated were used as a control. Absorbance at 540nm of 6 replicates were averaged and displayed as a percentage of DMSO-treated control. Standard deviation was calculated from the percentage DMSO-treated control values of the 6 replicates. **c)** IC_{50} values for 5-FU for all siRNA treatment were calculated for each cell line using Graph Pad Prism software. **d)** P-Values were calculated by performing a paired T-test and significances indicated with an asterisk (*).

a



b



c

Treatment	HCT-116 cells - IC ₅₀ 5-FU	HCT-116-FR cells - IC ₅₀ 5-FU
untreated	1.9µM	10.1µM
control siRNA	1.6µM	8µM
E-cadherin siRNA	3.5µM	8µM
p120-catenin siRNA	1.5µM	7.7µM

d

Treatment	HCT-116 cells – P-Value	HCT-116-FR cells – P-Value
control siRNA	0.972	0.716
E-cadherin siRNA	0.008*	0.733
p120-catenin siRNA	0.341	0.952

Figure 71 – Immunoblotting of siRNA Treated HCT-116 and HCT-116-FR Cells

Immunoblotting was carried out on HCT-116 and HCT-116-FR cells (1×10^6 cells) plated for 24 hours and transfected with E-cadherin siRNA using Lipofectamine™ 2000. Cells that were untreated or transfected with control siRNA were used as controls. Lysates were harvested after; **a)** 2 days, **b)** 5 days and **c)** 7 days and probed with an antibody against E-cadherin. Actin was used as a loading control. Molecular weight markers are shown.

Figure 71

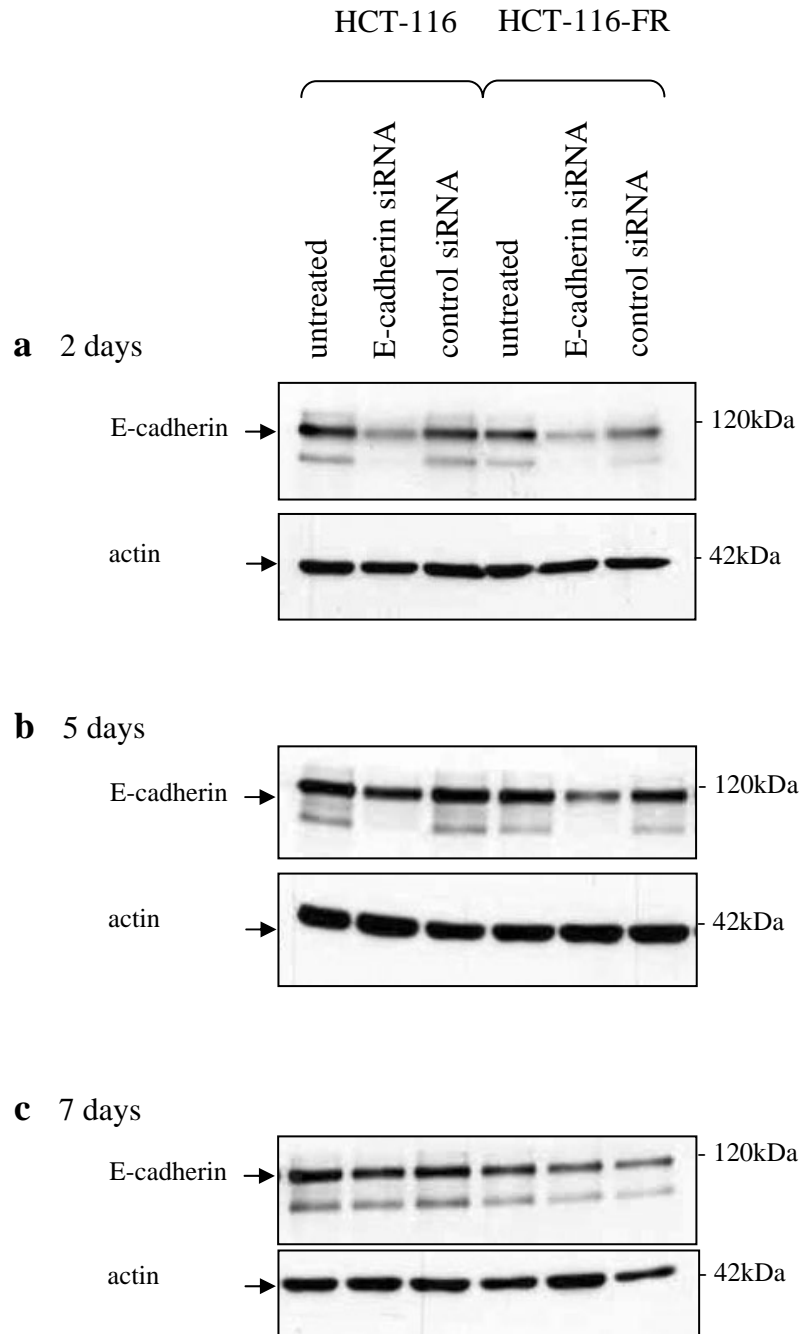
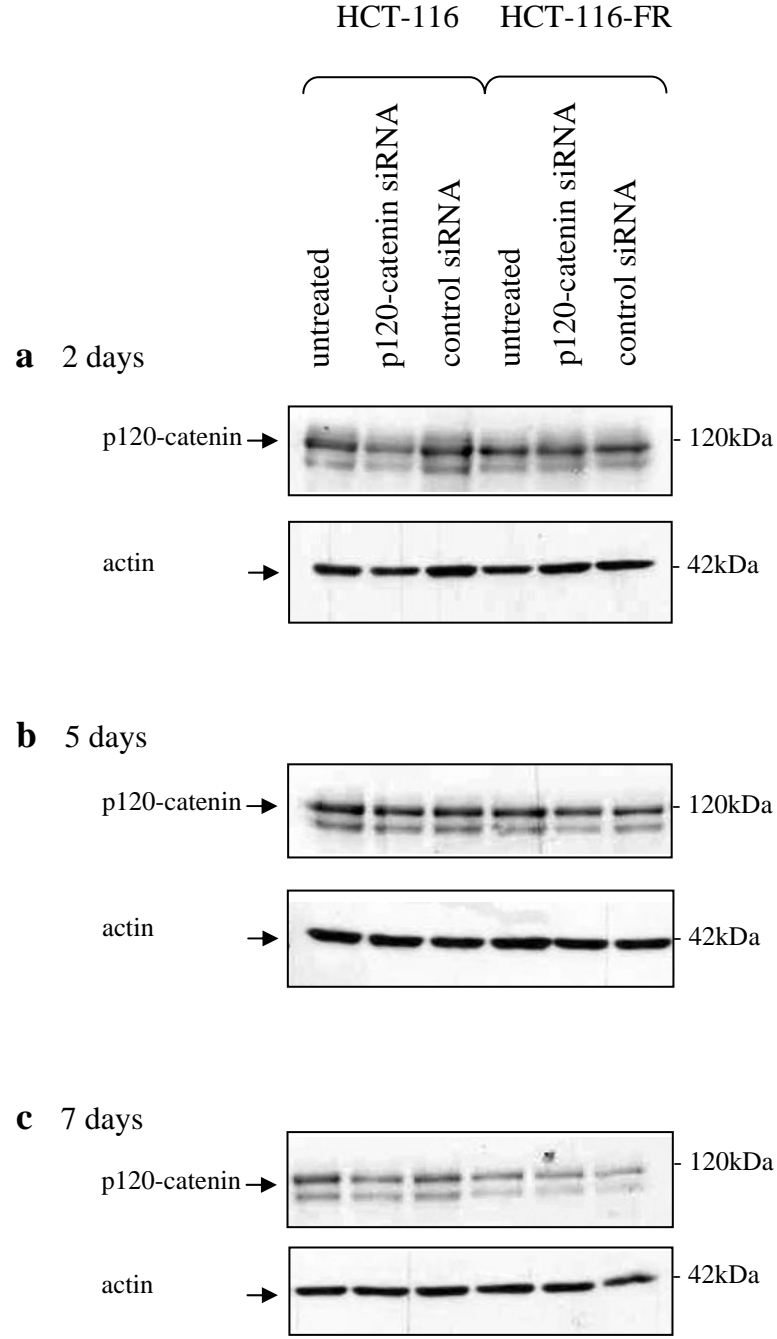


Figure 72 – Immunoblotting of siRNA Treated HCT-116 and HCT-116-FR Cells

Immunoblotting was carried out on HCT-116 and HCT-116-FR cells (1×10^6 cells) plated for 24 hours and transfected with p120-catenin siRNA using Lipofectamine™ 2000. Cells that were untreated or transfected with control siRNA were used as controls. Lysates were harvested after; **a)** 2 days, **b)** 5 days and **c)** 7 days and probed with an antibody against p120-catenin. Actin was used as a loading control. Molecular weight markers are shown.

Figure 72



5.10. Summary

The use of *decma* was a valuable tool in investigating the importance of E-cadherin-mediated cell-cell contacts. This interfering antibody had a pronounced effect, by inhibiting proliferation and/or survival of the epithelial-like colorectal cancer cell pair I tested here. It also resulted in some re-sensitisation of resistant cells to 5-FU. Preliminary results suggested that this was also the case when cell-cell junctions were perturbed by siRNA treatment to knock down expression of E-cadherin and p120-catenin, although this requires more investigation, probably with inducible protein knockdown. Proliferation assays highlighted the reverse result being observed in the RNAi experiments when compared to the *decma* treatment, however, due to the protein knockdown being unsuccessful for a prolonged period of time, this result cannot be substantiated. Initial observations indicated that the same trend, as was shown by *decma* treatment, would result if continued knockdown could be achieved by an inducible method.

Basal activation levels of the pro-proliferation and survival signalling pathways, namely the PI3-kinase/Akt and MAP kinase pathways, were consistently higher in the 5-FU-resistant HCT-116-FR cells. Activities of key components of both these pathways were suppressed upon *decma* treatment, implying that such signalling was dependent on adherens junctions. There was a different response in the 5-FU-sensitive HCT-116 cells, where *decma* induced activation of Akt and MAP kinase. These findings suggested that cell-cell contact-dependence of signalling to Akt and MAP kinase correlates with sensitivity to 5-FU. Specifically, these data implied that there was a greater reliance of 5-FU-resistant HCT-116-FR cells on their cell-cell contacts to induce at least some survival and/or proliferative signals. From experiments using selective chemical inhibitors of both the PI3-kinase/Akt and MAP kinase pathways, I concluded that it was most likely signalling via the PI3-kinase/Akt pathway that promoted survival in 5-FU-treated HCT-

116-FR cells. I also found differences in p53 localisation when *decma*-treated HCT-116-FR cells were compared with their more sensitive counterparts, suggesting that E-cadherin may indirectly control p53, perhaps contributing to 5-FU responses that are adhesion dependent. Specifically, HCT-116-FR cells had a larger proportion of nuclear p53 staining which was reduced upon *decma* treatment.

Overall, I conclude that 5-FU-resistant cells seem to be more susceptible to loss of E-cadherin-mediated adherens junctions than sensitive cells, at least for the clones examined from the resistant and sensitive HCT-116 cell pair. E-cadherin is required for survival and proliferation signalling, and early experiments suggest that the PI3-kinase pathway is important for survival which may be controlled by p53. However, I recognise that further experiments will be required to define precisely the molecular mechanisms by which E-cadherin-mediated signalling controls chemosensitivity, and how general these findings are. It would be very interesting to pursue this by examining multiple chemo-sensitive and -resistant colorectal cell lines (and other cancer cell types), and determine whether 5-FU resistance mechanisms are common to other chemotherapeutic agents.

6. Discussion

6.1. Models of 5-FU Resistance

Resistance is a major issue in the clinic for patient survival and *in vitro* studies using cell lines provide an important resource which enable scientists to better understand the mechanisms of resistance. Cell lines can be engineered to become resistant to cytotoxic agents by culturing cells in increasing concentrations of the drug and thereby selecting out resistant clones. In ovarian cancer it has also been possible to generate cell lines from the same patient following the acquisition of clinical resistance to cisplatin which provides a very powerful tool with which to study resistance. This is made possible in ovarian cancer through repeat collection of ascites fluid in these patients (Langdon et al., 1988).

In this study I have used three colorectal cancer cell lines which were inherently different in their sensitivity to 5-FU. This may reflect the different treatment regimes that the patients received before surgery and also the different origin of the cell lines. The HT29 and HCT-116 cells were both obtained from primary tumours which had received no treatment prior to resection (Boyer et al., 2004; Traverso et al., 2003). However, the H630 cells which were derived from a liver metastasis that had evaded previous treatment with 5-FU in combination with adriamycin, mitomycin C (FAM) and radiation (Copur et al., 1995; Park et al., 1987; Wang et al., 1999) were the most resistant of the three cell lines to 5-FU. In addition, as each cell line was obtained from a different patient the basal levels of proteins such as thymidylate synthase that are involved in 5-FU resistance may differ between cell lines and contribute to the different resistance observed.

Following continued treatment with increasing concentrations of 5-FU, each of the three cell lines became resistant to 5-FU. However, the degree of resistance achieved for each cell line varied. The parental H630 cells had a higher IC_{50} than either of the parental HT29

or HCT-116 cell lines and there was an almost 30-fold increase in the IC_{50} in the resistant H630 cells. In contrast there was only a 3-fold increase in the IC_{50} in the HT29 cells and a 5-fold increase in the HCT-116 resistant cells. The IC_{50} value for the resistant HT29 cells only reached the same value as the parental H630 cells. Thus there is a great deal of overlap in the IC_{50} s between the cell lines and also the degree of resistance that was achieved. This may reflect the inherent differences in the sensitivity of the different colorectal tumours to 5-FU. In addition, the *in vitro* selection of the individual resistant cell lines was carried out in different laboratories and different protocols are likely to have been used which may also contribute to these differences (Boyer et al., 2004; Copur et al., 1995). Furthermore the parental H630 cells may contain innate mechanisms of resistance that differ from the other two cell lines which allows them to adapt to much higher concentrations of 5-FU than the HT29 and HCT-116 cells. The location of the primary tumours may also have played a role in initial resistance and indeed any gained resistance after exposure to 5-FU. The H630 cells were derived from a liver metastasis from a patient with a primary rectal carcinoma, while the other two cell lines were from primary colon tumours. It has been reported that carcinomas derived from the colon and rectum differ in their behaviour at both early stage carcinogenesis and after cells have metastasised (Tsai et al., 2007). Furthermore, the location in the colon may also play a factor as it has been shown that cancers that arise in the distal colon differ than those that occur in the proximal colon (Bucfill, 1990; Delattre et al., 1989). The use of three paired 5-FU resistant cell lines with differing inherent and acquired resistant profiles provide a very useful model with which to study the mechanisms of 5-FU resistance.

6.2. 5-FU Resistance and E-cadherin

The sensitive H630 cells have a mesenchymal morphology and do not express E-cadherin. However, I observed that resistance to 5-FU resulted in an MET in these cells with the re-

expression of E-cadherin. In contrast the sensitive HT29 and HCT116 cells have retained E-cadherin expression and resistance to 5-FU did not alter E-cadherin protein expression. However, changes in the cell-cell adhesions, which are consistent with increased adhesiveness, were seen in the resistant variants of both these cells lines. Thus there was a trend in all three cell pairs towards a more adhesive phenotype upon acquisition of resistance to 5-FU. Interestingly, the most dramatic effect on cell-cell adhesions was seen in the H360 lines where the greatest gain in resistance to 5-FU was seen.

A number of assays were carried out to monitor the function of the cell-cell junctions within the cells. These included aggregation assays which directly measure cell-cell adhesion capacity and also FRAP, which gives a read-out of E-cadherin dynamics. E-cadherin is present in two pools within the membrane: diffusible E-cadherin molecules and transmembrane clusters engaged in cell-cell adhesion, and the movement of E-cadherin molecules between these two pools governs the formation of stable junctions (Klingelhofer et al., 2002; Sako et al., 1998; Yap et al., 1997). The concentration of E-cadherin molecules at the membrane is also controlled by endocytosis which in turn can control E-cadherin clustering and junction formation (Le et al., 1999; Troyanovsky et al., 2006). The mechanisms that regulate the movement of E-cadherin within, and away from, the membrane are not fully understood but recent studies using FRAP of GFP-E-cadherin have provided information on how the movement of E-cadherin molecules within the membrane are controlled (Serrels et al., 2009; Stehbens et al., 2006).

By performing FRAP, I showed that there was a slower recovery time for eGFP-E-cadherin in the resistant cell lines when compared to the sensitive counterparts. This does not necessarily indicate that the E-cadherin is more stable in these junctions but rather that the balance between the entry of un-bleached molecules and loss of eGFP-E- molecules out of the region of interest is altered in the resistant cells compared to the sensitive counterparts. Previously, FRAP has been used to assess changes in E-cadherin

accumulation at cell-cell contacts following treatment with nocodazole which disrupts the microtubule network (Stehbens et al., 2006). Treatment of cells with nocodazole reduced the amount of E-cadherin at cell-cell contacts as visualised by immunofluorescence and this was associated with a slower recovery rate. The authors therefore concluded that although trafficking of E-cadherin to the membrane was not affected by nocodazole treatment, the ability of the cell to concentrate fluorescent E-cadherin molecules at the bleached site was reduced resulting in a longer time to recover of the initial fluorescent intensity (Stehbens et al., 2006). Furthermore, previous work in our laboratory has shown that treatment with dasatinib, which stabilises cell-cell adhesions, results in a more rapid recovery following photobleaching (Serrels et al., 2009). In this study the ability of the resistant cells to form aggregates in the aggregation assay is increased when compared to sensitive cells suggesting that the concentration of E-cadherin on the membrane of the resistance cells may be greater despite no increase in protein level in the cell. However, this was associated with a decreased recovery rate in the resistant cells following photobleaching. As the recovery rate is controlled both by the movement of bleached molecules out of the area of interest and the movement of fluorescent molecules into the bleached area we cannot conclude from these assays whether this is associated with a change in concentration of E-cadherin molecules at the cell-cell contacts. For example, if the bleached molecules leave the area of interest at a slower rate then it is reasonable to assume that the time it would take to replace the bleached molecules would be increased. The FRAP analysis in this study was carried out on a confluent monolayer of cells which had established junctions and it is likely that the control of E-cadherin dynamics in these established junctions does not reflect the ability of cells to form aggregates in suspension (as monitored in the aggregation assay). These results highlight the problems of using this technology to address the function of E-cadherin junctions. FRAP gives a read-out of E-cadherin dynamics at the cell membrane but how this relates to adhesion strength is still

not clear. More direct analysis of adhesion strength in the 5-FU resistant cells is required. This can be measured by performing a disperse assay, which measures the decrease in the number of single cells that break away from a confluent monolayer as an indication of increased strength of the junctions (Calautti et al., 1998). Furthermore, a more direct approach would be to perform atomic force microscopy which enables the forces of atoms or molecules on the cell surface to be measured (Pittet et al., 2008).

6.3. Role of Yes in 5-FU Resistance

Cancer cells overcome direct inhibition of TS by 5-FU metabolites by up-regulating the TS gene following 5-FU treatment and as a consequence the SFK Yes, which is located on the same amplicon, is increased concurrently in 5-FU resistant cells. I therefore hypothesised that because of the known role of SFKs in the regulation of adherens junctions, that the increased expression of Yes in the resistant cells may play a role in cell-cell adhesions and that this may contribute to 5-FU resistance.

Previously Wang and co-workers had hypothesised that increased Yes expression did not confer resistance to 5-FU in colorectal cancer cells (Wang et al., 2004; Wang et al., 2001). This conclusion was based on microarray analysis of paired sensitive and 5-FU resistant colorectal cancer cell lines. Although the Yes gene was amplified in all the 5-FU resistant cell lines analysed, in one highly resistant cell line, there was no increased Yes protein expression despite the gene being amplified (Wang et al., 2001). This led to the hypothesis that 5-FU resistance did not correlate with Yes protein expression and that Yes therefore did not play a role in the mediating 5-FU resistance. Further analysis of the genes up-regulated or down-regulated in a wider panel of 5-FU resistant cells showed significant down regulation of genes involved in the activation of 5-FU in the resistant cells, for example, thymidine kinase, however, in some cell lines a corresponding decrease in protein expression this was not seen. Over-expression of TS protein was seen in all 5-FU

resistant cell lines although this was not always seen at the mRNA level indicating that TS expression is controlled post-transcriptionally. They consistently saw an up-regulation of Yes mRNA, but again in one breast cancer cell line no increase in Yes protein was observed (Wang et al., 2004). These types of correlative studies are useful but to address whether Yes was playing a role in 5-FU resistance a more direct approach was required.

I therefore used a vector based system to knockdown Yes expression in 5-FU resistant cells by RNAi. Down regulation of Yes expression did not restore sensitivity to 5-FU. In these experiments single cell clones were isolated with stable knock-down of Yes and it was noted that the IC_{50} for 5-FU in the Yes siRNA cells was higher than the vector control cells. However, when compared to the parental 5-FU resistant cells from which they were derived there was no change in IC_{50} . This highlights the problem of studying drug resistance in populations of cells which have been selected in culture. It is possible that the use of FACS and antibiotic treatment to isolate single cell clones may have changed the inherent resistance of the cells to 5-FU. Isolation of single cell clones rather than using a pooled population was carried out due to the wide range in levels of Yes knock-down in the pooled population which was felt may mask any effects of the 5-FU treatment. It may have been more useful to have used an inducible RNAi vector system which would rule out possible clonal variation in the cells. However, again inducible systems rely on treatment with drugs which are known to induce drug resistance such as doxycycline (Rooney et al., 2010).

6.4. Effects of Yes Knock-down on E-cadherin Junctions

Knock-down of Yes expression in 5-FU resistant cells reduced their ability to form aggregates to equivalent levels achieved in the sensitive cells. This result suggests that Yes affects the ability of cells to form cell-cell contacts. In contrast over expression of activated Src has been shown to result in an EMT with the breakdown of cell-cell contacts

(Avizienyte et al., 2002). Previously it has also been shown that inhibition of SFK activity by the use of a small molecule tyrosine kinase inhibitor or expression of a dominant negative Src protein induced stabilisation of cell-cell contacts in keratinocyte cultures (Owens et al., 2000). These approaches cannot distinguish between different Src family members and the use of RNAi to specifically knock-down Yes expression in the HCT-116-FR cells has provided the first evidence that the individual SFKs play differing roles at adherens junctions. Interestingly in another colorectal cancer cell line treatment with the pan SFK inhibitor, PP2 resulted in stronger cell-cell contacts (as shown by use of an aggregation assay as was used in this study). This was associated with decreased migration and metastasis *in vivo* following PP2 treatment (Nam et al., 2002). Again PP2 cannot distinguish between the SFKs due to the high degree of homology in the kinase domain of the family members and it may be that inhibition of Src (or other family members) in the PP2 treated cells may override the inhibition of Yes. Experiments using Src specific siRNA would have to be carried out to define the exact role Yes and Src in regulating adherens junctions.

6.5. Modulation of E-cadherin and EMT as Strategies to Overcome Drug Resistance

As there was a trend in all three cell pairs towards a more adhesive phenotype in the 5-FU resistant cells this raised the possibility that modulating E-cadherin within the cells may alter drug sensitivity. In support of this I have shown that treatment with the E-cadherin blocking antibody, *decma*, can re-sensitise the 5-FU resistant cells and furthermore that the resistant cells appear to be more dependent on cell-cell adhesions for their survival. Previous studies using three-dimensional spheroids, which are thought to more accurately mimic those conditions found in solid tumours (Sutherland and Durand, 1984), also showed that disruption of cell-cell adhesion using hyaluronidase resulted in increased sensitivity to the alkylating agent, cyclophosphamide (Croix et al., 1996). Other studies

using spheroid cultures also saw similar results; in HT29 cells treatment with an E-cadherin blocking antibody sensitised cells to a number of cytotoxics including 5-FU (no experiments were carried out in cells with acquired resistance to 5-FU) (Green et al., 2004) and in glioblastomas loss of cell-cell adhesions sensitised the cells to tumour necrosis factor-related apoptosis-inducing ligand (TRAIL) and CD95-induced apoptosis (Westhoff et al., 2008). In all of these experiments both cell matrix and cell-cell adhesions were disrupted, however, we observed a similar sensitisation in the presence of cell-matrix (integrin) adhesions suggesting that different survival signalling pathways may be involved. (These will be discussed in **6.6**).

To support the experiments carried out with *decma* I also used E-cadherin and p120-catenin siRNA to disrupt cell-cell adhesions. Initially I attempted to isolate cells with a stable knock-down of E-cadherin using the same vector based system utilised to generate the Yes knock-down cells. However, I was not able to generate stable cell lines which may reflect the requirement of the cells on E-cadherin for long term survival. I therefore carried out transient transfection experiments with E-cadherin and p120 siRNA oligonucleotides as they had been used successfully in the lab in other cell types. Preliminary results showed a reduced cell growth after 2 days and loss of E-cadherin and p120 was confirmed by both immunofluorescence analysis and immunoblotting. However, it was not possible to establish the effects of down regulating these proteins on the response to 5-FU treatment as over the period of time required for a cell proliferation assay to be performed, cell cultures recovered E-cadherin and p120-catenin expression. However, the preliminary data that I generated suggested that transient knock-down of E-cadherin protein levels was sufficient to significantly enhance the resistance to 5-FU in the parental HCT-116 cells. This raises the interesting question of whether inhibiting E-cadherin function (following treatment with *decma*) triggers pathways that induce cell death and chemo-sensitisation while a loss of E-cadherin protein protects against cytotoxic injury. This would be in keeping with

reports that loss of E-cadherin is associated with increased drug sensitivity as discussed below. Other approaches to down regulate E-cadherin expression include ectopic expression of the transcriptional repressors Twist and Snail and this would be an alternative approach that could be used to study the role of E-cadherin in drug resistance and further distinguish between these two possibilities (Hoshino et al., 2009; Yang et al., 2006).

Taken together the findings presented in this thesis along with previously published data indicate that cell-cell adhesion survival signals may contribute to the resistance of tumour cells to chemotherapy. However, as described in the Introduction (section **1.8.2**) there is a substantial body of evidence linking EMT with chemoresistance, where E-cadherin expression correlates with sensitivity to a number of therapeutic agents (Acloque et al., 2009; Voulgari and Pintzas, 2009). The role of E-cadherin in resistance has also been confirmed in the clinic where trials with the EGFR inhibitor erlotinib in non-small cell lung cancer confirmed a clinical benefit in patients with high expression of E-cadherin (Yauch et al., 2005). Acquired resistance in a number of tumour types is also associated with an induction of EMT (Hoshino et al., 2009). For example, in HT29 and KM12L4 colorectal cells acquired resistance to oxaliplatin is associated with increased expression of vimentin and decreased expression of E-cadherin. Although E-cadherin was not completely lost in these cells a translocation of E-cadherin from the membrane to the cytoplasm was seen which was accompanied by increased nuclear β -catenin (Yang et al., 2009). Interestingly, increased nuclear expression of Snail was seen in the KM12L4 cells but not the HT29 cells suggesting that cell-type specific mechanisms can regulate both E-cadherin expression and function.

An induction of EMT associated with drug resistance is also linked to a more invasive and migratory phenotype. For example oxaliplatin-induced resistance is associated with a loss

of polarity, increase in migration and invasion, while in breast cancer, cells that display an increased resistance to tamoxifen are also more migratory and invasive (Hiscox et al., 2004). This effect was partially mediated by signalling generated from the EGFR pathway. Use of the EGFR tyrosine kinase inhibitor, gefitinib (also known as Iressa) was able to reduce the aggressive phenotype associated with cells displaying a more mesenchymal morphology (Hiscox et al., 2004). These breast cancer cells also displayed a decreased binding of β -catenin to E-cadherin resulting in an increase proportion of β -catenin being present in the nucleus of the cell (Hiscox et al., 2006).

Targeting EMT has therefore become the focus of many groups and considerable effort is being put into the development of drugs that may revert the mesenchymal phenotype, thereby reducing the invasive and metastatic potential of the cells as well as restoring drug sensitivity when used in combination with conventional chemotherapy. Directly targeting transcriptional regulators of EMT would be a useful approach and for example, small molecule inhibitors do exist that disrupt β -catenin signalling although these are still at an early stage of pre-clinical development (Sabbah et al., 2008). Other approaches would be to target the upstream signalling pathways that regulate EMT and a number of inhibitors are already in preclinical or clinical development. For example, targeting Hedgehog signalling in pancreatic cancer induced EMT which was associated with reduced metastatic spread in mice. Furthermore, combination of gemcitabine (the standard of care in pancreatic cancer) with inhibitors of Hedgehog signalling significantly reduced primary tumour burden as compared to gemcitabine alone (Feldmann et al., 2007; Feldmann et al., 2008). Targeting SFK may also be effective as Src kinase is a key regulator of EMT. Dasatinib is an orally active SFK inhibitor which is currently in clinical development in a number of solid tumour types. In breast cancer cells it has been shown to preferentially kill mesenchymal or 'triple negative' cells (Finn et al., 2007) although a MET has not been reported following dasatinib inhibition. However, treatment of E-cadherin expressing

tumour cells with dasatinib results in a strengthening of cell-cell junctions (Serrels et al., 2009) but in my preliminary data (not presented here) I saw no change in the sensitivity of HCT-116 cells to 5-FU when pre-treated with dasatinib. This most probably reflects the fact that it is the loss or gain of E-cadherin protein expression that is the major determinant of drug sensitivity and that strengthening of junctions in cells which already express E-cadherin is not sufficient to change their sensitivity. However, simply re-expressing E-cadherin may not be sufficient to revert the EMT phenotype. In breast cancer cells that harbour activated Ras, inhibition of both the MAP kinase pathway, in addition to restoration of E-cadherin protein levels is required (Li and Mattingly, 2008). Therefore it is likely that the effectiveness of targeting EMT may be dependent on what other genetic alterations are present in the cell.

Although the focus of attention is on targeting pathways that induce EMT is there also a role for anti-E-cadherin antibody therapy in the treatment of resistant tumours? The use of antibodies as targeted therapies in the treatment of cancer is now well established (Chester et al., 2004; Segal and Saltz, 2009). A number of therapeutic antibodies are currently used within the clinic. For example, herceptin which is used for the treatment of HER2 positive breast cancer and bevacizumab, which targets VEGFR signalling, is licensed for the treatment of metastatic colon cancer in combination with 5-FU and is also being trialled in a number of other tumour types including breast and lung (Ferrara et al., 2004; O'Donovan et al.). It is not known whether significant toxicity would be seen upon treatment with E-cadherin antibodies as E-cadherin plays a critical role in the development and maintenance of a number of different tissues within the body (Yap et al., 2007). Loss of E-cadherin in the mouse is embryonic lethal (Larue et al., 1994) but conditional loss of E-cadherin in the skin of adult mice resulted in a loss of adherens junctions but overall tissue integrity was maintained via desmosomes (Young et al., 2003). When both P-cadherin and E-cadherin proteins levels were reduced in the skin of mice, adherens junctions were lost and this was

then accompanied by an increase in apoptosis (Tinkle et al., 2008). Additionally loss of E-cadherin in the breast does not result in abnormal duct development (Derksen et al., 2006) and in both the skin and breast loss of E-cadherin alone is not sufficient to induce tumour formation (Derksen et al., 2006; Young et al., 2003). This suggests that there may be enough redundancy within the cadherin family to prevent significant toxicity by using an antibody to specifically target E-cadherin. However, it may also be that by only targeting E-cadherin it is insufficient to breakdown adherens junctions in some cells. For example, in keratinocytes loss of cell-cell adhesions is only seen when a combination of both E- and P-cadherin antibodies are used (Owens et al., 2000). In this study despite the expression of P-cadherin in the cells, treatment with an E-cadherin specific antibody (*decma*) was sufficient to disrupt adherens junctions. However, β -catenin and p120-catenin did remain at the cell membrane suggesting that they may associate with P-cadherin, even though functional junctions were not apparent. In addition, p120-catenin has been shown to bind other cell membrane structures, for example, ZO and intercalated discs of cardiomyocytes (Golenhofen and Drenckhahn, 2000; Hartsock and Nelson, 2008).

So would it be possible to determine which patients may benefit from E-cadherin directed therapies? It is possible that in advanced metastatic tumours which have retained E-cadherin expression and become resistant to 5-FU that they may benefit from treatment with an anti-E-cadherin antibody. In contrast in resistant tumours which have undergone an EMT it may be beneficial to restore E-cadherin levels. It would therefore be necessary to screen tumours for both E-cadherin expression and localisation before treatment.

6.6. Signalling From Adherens Junctions

Cell-cell adhesions generate survival signals that may provide cancer cells with a mechanism to evade chemotherapy induced cell death. The resistant 5-FU cells appear to have an increased reliance on E-cadherin signalling and by manipulating their cell-cell

junctions, sensitivity to 5-FU treatment was restored. It is known that treatment with 5-FU utilises the p53 cell death pathway to kill cells (Longley et al., 2003). p53, which is wild-type in the HCT-116 cells, is found either in the nucleus or the cytoplasm and the localisation of p53 is known to govern the very defined, and sometimes opposing roles, played by p53 in the cells (Hollstein and Hainaut, 2010). Untreated sensitive and resistant HCT-116 displayed a differing proportion of positively stained p53 nuclei; resistance to 5-FU was associated with an increased number of cells with nuclear p53. It was not possible to determine the proportion of p53 in the cytoplasm; however, the total basal protein level of p53 between the cell lines was lower in the resistant cell line. Upon *decma* treatment, the localisation of the p53 changed with less staining observed in the nucleus of the resistant cells, while in the parental cell line there was an increase in nuclear p53 nuclear staining upon junction loss. These results show that upon loss of adherens junctions, the localisation of p53 changed in both cell lines but this change was different between sensitive and resistant cells.

Re-localisation of p53 was associated with changes in signalling through two key pro-survival/proliferation pathways, the PI3-kinase/Akt and MAP kinase (Hawkins et al., 2006; Pece and Gutkind, 2000). Basal levels of activation of both pathways were greater in the resistant cells in comparison to the sensitive cells when junctions were intact. This suggests that signalling from the adherens junctions, which are known to activate these survival pathways, was higher in the resistant cells than their sensitive counterparts. However, loss of cadherin mediated cell-cell junctions by *decma* treatment resulted in increased signalling via these pathways in the sensitive cells whereas in the resistance cells activation of these pathways was almost completely lost. Since these signals are linked with pro-survival and proliferation, it is reasonable to assume that loss of these signals would generate cell death in the resistant cells. Measurement of cell death was confirmed by means of a Tunel assay which showed that upon *decma* treatment in the resistant cells

displayed positive staining for Tunel, indicating apoptosis. This could be further confirmed by analysing a number of proteins linked to apoptosis, for example, the cleavage of the Caspase 3 protein or the detection of Annexin V on the cell membrane. The induction of apoptosis, however, was not seen in the sensitive cells. Although reduced proliferation was observed due to loss of junctions, cell death did not result. This may have been mediated by up-regulation of signalling from both the PI3-kinase and MAP kinase pathways during cell-cell junction loss in the sensitive cells. Unlike the resistant cells, the sensitive cells were able to up-regulate signalling by these two pathways even in the absence of cadherin mediated junctions. Focal adhesions have been shown to activate both these pathways (Guinebault et al., 1995; Schlaepfer et al., 1994) so it may be that loss of adherens junctions triggered an increased survival signalling through integrin-dependent cell matrix adhesions in the sensitive cells. Signalling from focal adhesions would replace the signalling lost from the adherens junctions which are known to also be able to activate PI3-kinase and MAP kinase pathways (Laprise et al., 2002; Pece and Gutkind, 2000). Induction of apoptosis has also been observed in an immortalised keratinocyte cell line following treatment with *decma* and this could be overcome by expressing a constitutively active form of either Ras or PI3-kinase indicating that these pathways are important for E-cadherin-dependent survival (Espada et al., 2009). Adherens junction dependent activation of PI3-kinase has also been linked with resistance to genotoxin-induced cell death in intestinal epithelial cells (Chae et al., 2009). Other survival pathways that have been linked to the adherens junction include p27^{KIP1}, which functions as a cyclin-dependent kinase inhibitor, and provides pro-survival signals following cell cycle growth arrest, and has been implicated in playing a role in adhesion-dependent resistance to cytotoxics (St Croix and Kerbel, 1997).

I then went on to test the hypothesis that the resistant cells may, not only be more reliant on their cell-cell junctions, but, that they may be more reliant on signalling through the

PI3-kinase/Akt and MAP kinase pathways for survival. Treating the sensitive and resistant cells with inhibitors of both pathways demonstrated a clear difference in the proliferation of the resistant cells following inhibition of the PI3-kinase pathway. Inhibition of proliferation in the resistance cells was 50% greater than in the sensitive cells, when PI3-kinase was inhibited, indicating that the resistant cells depend on this pathway for survival to a greater extent than their sensitive counterparts. In addition, upon *decma* treatment the resistant cells were not able to increase signalling via PI3-kinase in response to loss of adherens junctions. Reliance on the PI3-kinase pathway in addition to the MAP kinase pathway has been shown in cells resistant to gefitinib or imatinib (Ozaki et al., 2009). By inhibition of PI3-kinase and MAP kinase signalling, sensitivity to treatment with gefitinib or imatinib in resistant cells was improved (Ozaki et al., 2009). Inhibition of MAP-kinase signalling has also been shown to sensitise cells with increased MAP kinase signalling to treatment with the microtubule-destabilising agent, vincristine (Tanimura et al., 2009).

The signals generated from the PI3-kinase pathway may be controlled by p53 which could be altered by the location of the p53 in the cell, or vice versa. For example, basal levels of PI3-kinase are high in the resistant cells and are associated with increased nuclear p53 and increased cell-cell adhesiveness. Sensitive cells, on the other hand, have increased nuclear p53 and increased PI3-kinase activation following the loss of adherens junctions. In addition p53 is able to bind to TS mRNA and down regulate its expression in the cell (Peters and van Groeningen, 1991). The reduced basal p53 levels in the resistant cells may result from activated PI3-kinase signalling in these cells, as Akt is known to up-regulate Mdm2 which targets p53 for degradation (Datta et al., 1999; Vousden and Lane, 2007). The loss of p53 in turn could contribute to up-regulation of TS in the resistant cells. In addition, the sequestration of p53 to the nucleus in the resistant cells may also act to minimise p53 dependent down regulation of TS mRNA.

As previously mentioned, the location of p53 in the cell in either the nucleus, the cytoplasm or the mitochondria, can govern very defined, and sometimes opposing roles, played by p53 in the cells (Han et al., 2008; Hollstein and Hainaut, 2010). For example, the effect of p53 on autophagy in the cytoplasm results in a negative effect of cell survival resulting in apoptosis. However, p53 in the nucleus is able to up-regulate the protein, Damage-Regulated Autophagy Modulator (DRAM), which may possibly play a positive role in enabling the recovery of macromolecules from autophagy which can induce a positive effect on the survival of the cell (Tasdemir et al., 2008). With 10 different isoforms, p53 controls a wide diversity of cellular functions for example, as a cell cycle repressor, but also in metabolism and migration (O'Brate and Giannakakou, 2003). p53 has been named not only the 'guardian of the genome' but also the 'guardian of the tissue' due to its role in detecting damage in the genome in addition to mediating signals from E-cadherin in a tissue specific manner (Yamaguchi et al., 2004). This auspicious nomenclature results from experimental data generated in *Drosophila* where alterations in the adherens junctions or in the signals generated from them, results in p53 dependent apoptosis (Yamaguchi et al., 2004).

From the data generated in my thesis, I hypothesise that adherens junctions play a role in survival of resistant cells to 5-FU by the up-regulation of survival signals mediated via increased nuclear p53. However, upon loss of junctions, signalling generated from the adherens junctions is lost in the resistant cells, which, unlike the sensitive cells, cannot be rescued by survival signals potentially generated through focal adhesions. The reduction of survival signals from the down-regulation of adherens junctions also induces the loss of p53 in the nucleus, suggesting that its translocation to the cytoplasm is involved in the induction of cell death. I therefore propose that in the sensitive cells, the ability to rescue the signalling through PI3-kinase, and possibly MAP kinase, results in the ability to drive p53 into the nucleus when junctions are lost resulting in protection from cell death

analogous to that shown by the untreated resistant cells. This suggests a possible mechanism undertaken by the resistant cells during 5-FU treatment. I subsequently propose that resistance to 5-FU may be reversed by the translocation of p53 to the cytoplasm and loss of PI3-kinase signalling generated by increased cell-cell adhesions (Figure 73).

Figure 73 – Theory Regarding Cell Death in HCT-116-FR Cells upon Junction Loss

Diagram to represent the results obtained and theories hypothesised regarding junction loss in 5-FU-sensitive HCT-116 cells and -resistant HCT-116-FR cells. Untreated HCT-116-FR cells display an up-regulated activation of PI3-kinase and MAP kinase pathways which is lost upon *decma* treatment (**b**). HCT-116 cells are able to up-regulate these pathways upon junction loss resulting in cell survival (**a**). Reduced p53 staining in the nucleus of HCT-116-FR cells is observed whereas increased p53 staining in the nucleus is shown in the HCT-116. Therefore, translocation of p53 to the cytoplasm may occur in the HCT-116-FR cells while cell death is reduced by increased nuclear p53 in the HCT-116 cells. (c) Summary of theory.

Figure 73

a

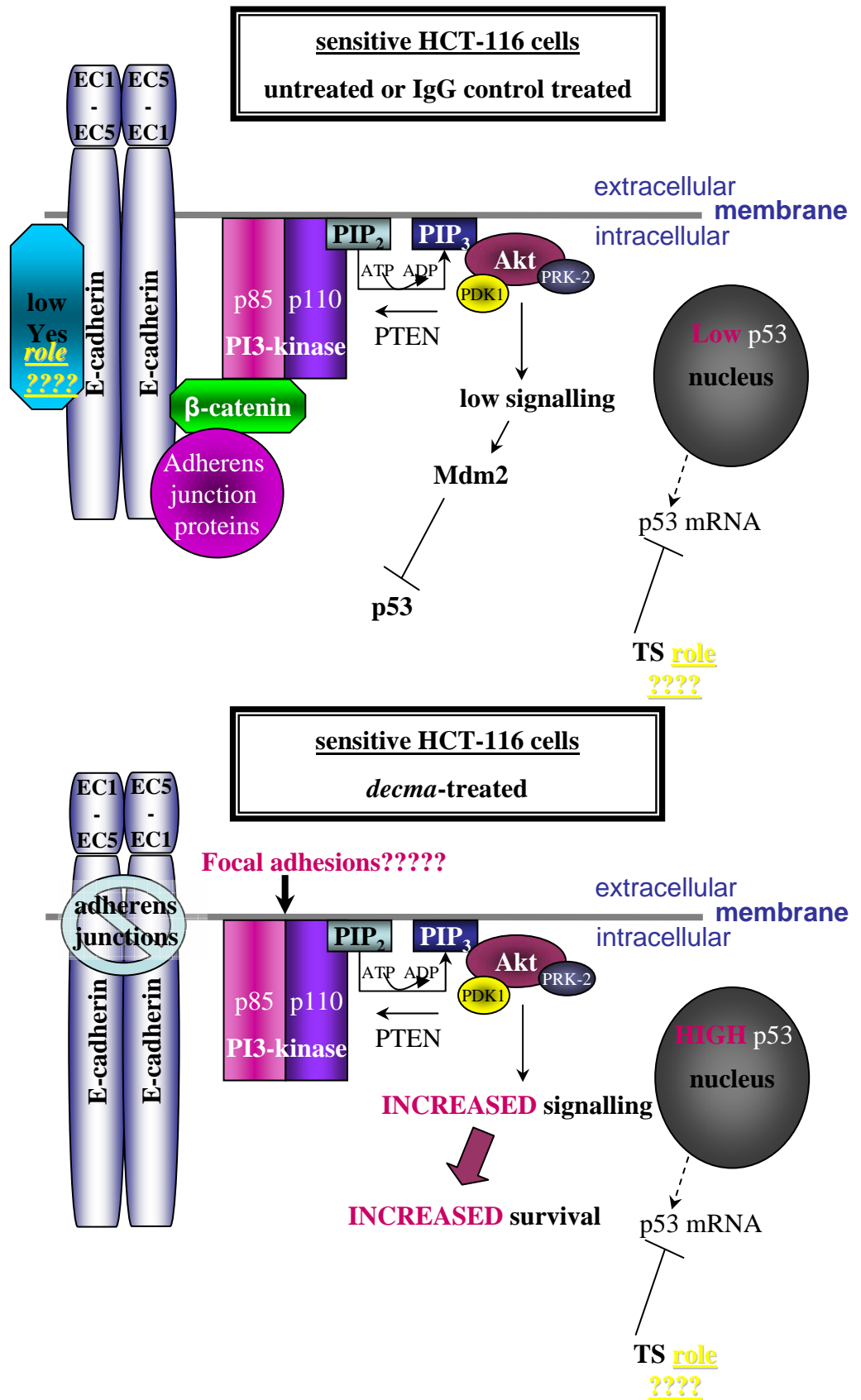
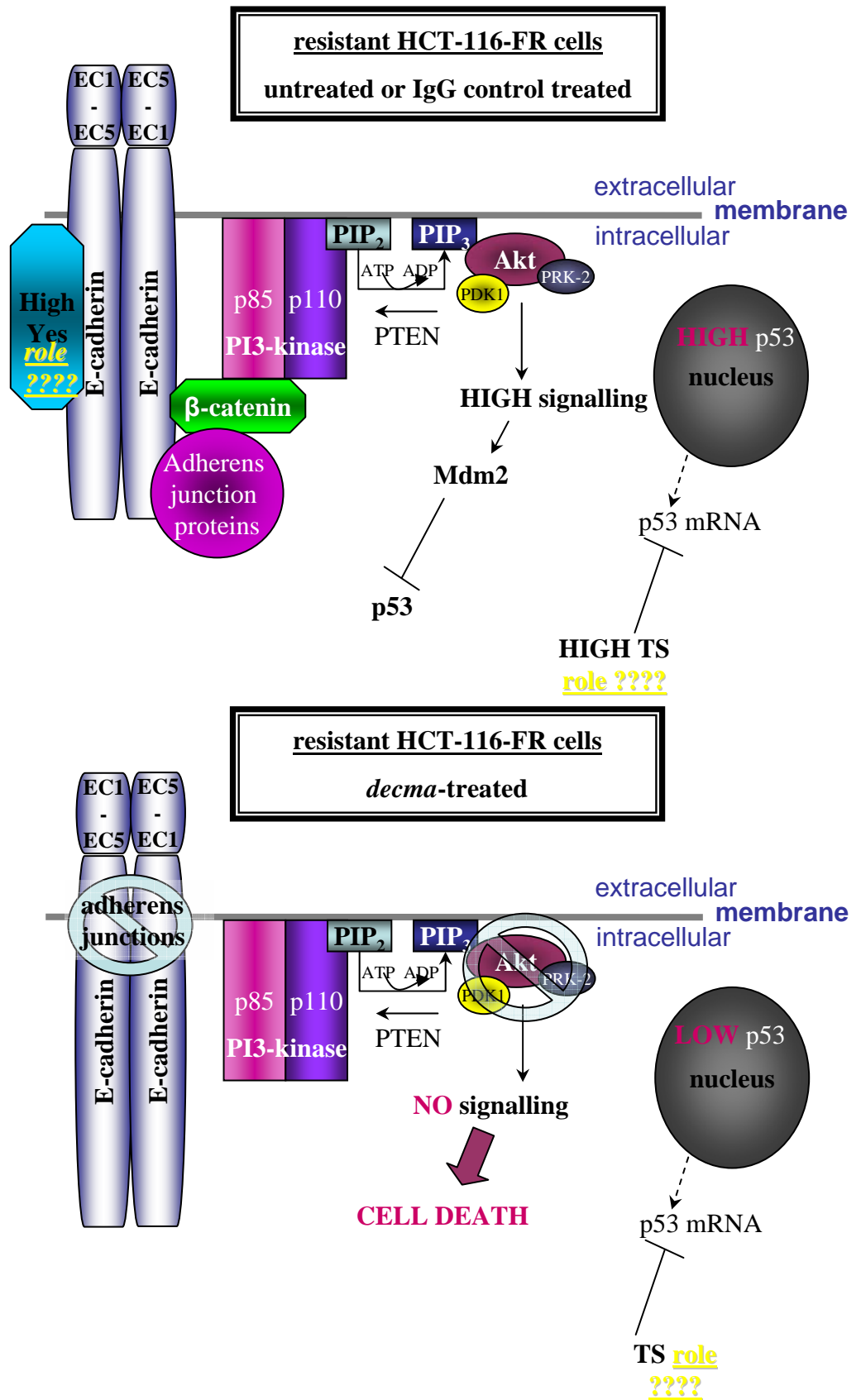


Figure 73

b



c

untreated or IgG control treated

	HCT-116	HCT-116-FR
Akt signalling	Low	High
p53 nucleus	Low	High
p53 cytoplasm??	High	Low
Yes	Low	High
Adherens junctions	Lower	Higher

***decma*-treated**

	HCT-116	HCT-116-FR
Akt signalling	High	Low
p53 nucleus	High	Low
p53 cytoplasm??	Low	High
Yes	High	Low
Adherens junctions	N/A – focal adhesions??	N/A

This theory requires much further analysis of both the pathways involved in cell survival and in addition the relationship to the apoptosis shown upon loss of adherens junctions. In this thesis we only showed p53 staining in the nucleus and did not measure the cytoplasmic pool of p53. Therefore translocation to cytoplasm is purely speculative. However, with this in mind, it poses the question of whether p53 has differing functions in the sensitive and resistant cells? Could this be due to increased cell-cell adhesion in the resistant cells that is co-ordinated with an increase in signalling generated from these adhesions and if this signalling is abated, does p53 cause apoptosis in the resistant cells as was shown in *Drosophila*? All these questions remain unanswered but it raises the intriguing possibility of whether modulation of p53 function could be used to re-sensitise resistant cells.

7. Future Work

If time had allowed, it would have been of great benefit to continue the work that I have started in this thesis. Experimental procedures that I would tackle would be to;

- establish the mode of cell death following *decma* treatment in the HCT-116-FR cells and the pathways involved. Initially I would analyse Annexin V staining, PARP cleavage, Caspase 3 cleavage, propidium iodide staining (followed by FACS analysis), Trypan blue exclusion assays and nuclear fragmentation with DAPI staining. I would further expand this to include the other cell pairs to address if cell death was also shown in resistant cells but not in sensitive cells
- investigate further the role of p53 in 5-FU resistance by looking at the phosphorylation status of p53 and downstream effectors e.g. p21
- induce p53 to the cytoplasm by treatment with Geldanamycin which blocks p53 binding to heat shock protein (hsp) 90 preventing nuclear import. This would induce the HCT-116 cells to more exactly mirror what is seen in the HCT-116-FR cells during *decma* treatment to interpret p53 role in cell death shown in the HCT-116-FR cells when junctions are lost
- explore other approaches to modulate E-cadherin expression to establish the role in 5-FU resistance. E.g. ectopic expression of Twist, Snail, Zeb-1 or Zeb-2
- establish whether Yes does play a role in 5-FU resistance. This could be done by the use of an inducible RNAi to Yes in order to rule out the possibility of clonal variation

- perform FRAP on Yes RNAi cells to further confirm the role of Yes in adherens junctions to further validate the results of previous FRAP data between sensitive and resistant cells and to confirm the aggregation assay
- establish whether Src and Yes have opposing roles in the regulation of adherens junctions. Generate cells with specific knockdown of Src and compare these with the Yes RNAi cells
- further assess the role of PI3-kinase in adherens junction-mediated survival and 5-FU resistance. For example, does inhibition of PI3-kinase sensitise cells to 5-FU. The PI3-kinase inhibitor used in this thesis was specific in the inhibition of the p110 α catalytic subunit of Class I PI3-kinases, however, it would be interesting to further investigate what role, if any, the other classes of these enzymes play in the resistance to 5-FU. Class III enzymes have been suggested to be able to signal downstream to mTOR implicating a possible role for them in cell survival
- examine multiple chemo-sensitive and -resistant colorectal cell lines (and other cancer cell types) and determine whether resistance mechanisms are common to other chemotherapeutic agents. This could include investigation of clinical samples to address if 5-FU resistance correlates with E-cadherin expression and/or localisation

Therefore, many questions are still unanswered but further investigation would provide a greater insight into the mechanisms employed by resistant cells. If this understanding could be transferred to the clinic, survival rates of patients presenting with recurrence of resistant disease could possibly be improved.

8. References

A.F.A. Smit, R.H.P.G. RepeatMasker.

- Acloque, H., Adams, M.S., Fishwick, K., Bronner-Fraser, M. and Nieto, M.A. (2009) Epithelial-mesenchymal transitions: the importance of changing cell state in development and disease. *J Clin Invest*, **119**, 1438-1449.
- Adlard, J.W., Richman, S.D., Seymour, M.T. and Quirke, P. (2002) Prediction of the response of colorectal cancer to systemic therapy. *Lancet Oncol*, **3**, 75-82.
- Alessi, D.R., James, S.R., Downes, C.P., Holmes, A.B., Gaffney, P.R., Reese, C.B. and Cohen, P. (1997) Characterization of a 3-phosphoinositide-dependent protein kinase which phosphorylates and activates protein kinase Balpha. *Curr Biol*, **7**, 261-269.
- Aligayer, H., Boyd, D.D., Heiss, M.M., Abdalla, E.K., Curley, S.A. and Gallick, G.E. (2002) Activation of Src kinase in primary colorectal carcinoma: an indicator of poor clinical prognosis. *Cancer*, **94**, 344-351.
- Arumugam, T., Ramachandran, V., Fournier, K.F., Wang, H., Marquis, L., Abbruzzese, J.L., Gallick, G.E., Logsdon, C.D., McConkey, D.J. and Choi, W. (2009) Epithelial to mesenchymal transition contributes to drug resistance in pancreatic cancer. *Cancer Res*, **69**, 5820-5828.
- Avizienyte, E., Wyke, A.W., Jones, R.J., McLean, G.W., Westhoff, M.A., Brunton, V.G. and Frame, M.C. (2002) Src-induced de-regulation of E-cadherin in colon cancer cells requires integrin signalling. *Nat Cell Biol*, **4**, 632-638.
- Avraham, S., Jiang, S., Ota, S., Fu, Y., Deng, B., Dowler, L.L., White, R.A. and Avraham, H. (1995) Structural and functional studies of the intracellular tyrosine kinase MATK gene and its translated product. *J Biol Chem*, **270**, 1833-1842.
- Balendran, A., Casamayor, A., Deak, M., Paterson, A., Gaffney, P., Currie, R., Downes, C.P. and Alessi, D.R. (1999a) PDK1 acquires PDK2 activity in the presence of a synthetic peptide derived from the carboxyl terminus of PRK2. *Curr Biol*, **9**, 393-404.
- Balendran, A., Currie, R., Armstrong, C.G., Avruch, J. and Alessi, D.R. (1999b) Evidence that 3-phosphoinositide-dependent protein kinase-1 mediates phosphorylation of p70 S6 kinase in vivo at Thr-412 as well as Thr-252. *J Biol Chem*, **274**, 37400-37406.
- Bataille, F., Rohrmeier, C., Bates, R., Weber, A., Rieder, F., Brenmoehl, J., Strauch, U., Farkas, S., Furst, A., Hofstadter, F., Scholmerich, J., Herfarth, H. and Rogler, G. (2008) Evidence for a role of epithelial mesenchymal transition during pathogenesis of fistulae in Crohn's disease. *Inflamm Bowel Dis*, **14**, 1514-1527.
- Beckenlehner, K., Bannke, S., Spruss, T., Bernhardt, G., Schonenberg, H. and Schiess, W. (1992) Hyaluronidase enhances the activity of adriamycin in breast cancer models in vitro and in vivo. *J Cancer Res Clin Oncol*, **118**, 591-596.

- Bjorge, J.D., Jakymiw, A. and Fujita, D.J. (2000) Selected glimpses into the activation and function of Src kinase. *Oncogene*, **19**, 5620-5635.
- Blaschuk, O.W. and Devemy, E. (2009) Cadherins as novel targets for anti-cancer therapy. *Eur J Pharmacol*, **625**, 195-198.
- Bolen, J.B., Veillette, A., Schwartz, A.M., DeSeau, V. and Rosen, N. (1987) Activation of pp60c-src protein kinase activity in human colon carcinoma. *Proc Natl Acad Sci U S A*, **84**, 2251-2255.
- Bonni, A., Brunet, A., West, A.E., Datta, S.R., Takasu, M.A. and Greenberg, M.E. (1999) Cell survival promoted by the Ras-MAPK signaling pathway by transcription-dependent and -independent mechanisms. *Science*, **286**, 1358-1362.
- Boonyaratanakornkit, V., Scott, M.P., Ribon, V., Sherman, L., Anderson, S.M., Maller, J.L., Miller, W.T. and Edwards, D.P. (2001) Progesterone receptor contains a proline-rich motif that directly interacts with SH3 domains and activates c-Src family tyrosine kinases. *Mol Cell*, **8**, 269-280.
- Boyer, J., McLean, E.G., Aroori, S., Wilson, P., McCulla, A., Carey, P.D., Longley, D.B. and Johnston, P.G. (2004) Characterization of p53 wild-type and null isogenic colorectal cancer cell lines resistant to 5-fluorouracil, oxaliplatin, and irinotecan. *Clin Cancer Res*, **10**, 2158-2167.
- Braga, V.M. (2002) Cell-cell adhesion and signalling. *Curr Opin Cell Biol*, **14**, 546-556.
- Braga, V.M., Machesky, L.M., Hall, A. and Hotchin, N.A. (1997) The small GTPases Rho and Rac are required for the establishment of cadherin-dependent cell-cell contacts. *J Cell Biol*, **137**, 1421-1431.
- Braga, V.M. and Yap, A.S. (2005) The challenges of abundance: epithelial junctions and small GTPase signalling. *Curr Opin Cell Biol*, **17**, 466-474.
- Brunton, V.G. and Frame, M.C. (2008) Src and focal adhesion kinase as therapeutic targets in cancer. *Curr Opin Pharmacol*, **8**, 427-432.
- Brunton, V.G., MacPherson, I.R. and Frame, M.C. (2004) Cell adhesion receptors, tyrosine kinases and actin modulators: a complex three-way circuitry. *Biochim Biophys Acta*, **1692**, 121-144.
- Bufill, J.A. (1990) Colorectal cancer: evidence for distinct genetic categories based on proximal or distal tumor location. *Ann Intern Med*, **113**, 779-788.
- Calautti, E., Cabodi, S., Stein, P.L., Hatzfeld, M., Kedersha, N. and Paolo Dotto, G. (1998) Tyrosine phosphorylation and src family kinases control keratinocyte cell-cell adhesion. *J Cell Biol*, **141**, 1449-1465.
- Calcagno, A.M. and Ambudkar, S.V. (2010) Molecular mechanisms of drug resistance in single-step and multi-step drug-selected cancer cells. *Methods Mol Biol*, **596**, 77-93.
- Calderwood, D.A. (2004) Talin controls integrin activation. *Biochem Soc Trans*, **32**, 434-437.

- Campbell, N.C., Elliott, A.M., Sharp, L., Ritchie, L.D., Cassidy, J. and Little, J. (2001) Rural and urban differences in stage at diagnosis of colorectal and lung cancers. *Br J Cancer*, **84**, 910-914.
- Carnrot, C., Wang, L., Topalis, D. and Eriksson, S. (2008) Mechanisms of substrate selectivity for Bacillus anthracis thymidylate kinase. *Protein Sci*, **17**, 1486-1493.
- Carreras, C.W. and Santi, D.V. (1995) The catalytic mechanism and structure of thymidylate synthase. *Annu Rev Biochem*, **64**, 721-762.
- Cartwright, C.A., Coad, C.A. and Egbert, B.M. (1994) Elevated c-Src tyrosine kinase activity in premalignant epithelia of ulcerative colitis. *J Clin Invest*, **93**, 509-515.
- Cartwright, C.A., Kamps, M.P., Meisler, A.I., Pipas, J.M. and Eckhart, W. (1989) pp60c-src activation in human colon carcinoma. *J Clin Invest*, **83**, 2025-2033.
- Cartwright, C.A., Meisler, A.I. and Eckhart, W. (1990) Activation of the pp60c-src protein kinase is an early event in colonic carcinogenesis. *Proc Natl Acad Sci U S A*, **87**, 558-562.
- Chae, B., Yang, K.M., Kim, T.I. and Kim, W.H. (2009) Adherens junction-dependent PI3K/Akt activation induces resistance to genotoxin-induced cell death in differentiated intestinal epithelial cells. *Biochem Biophys Res Commun*, **378**, 738-743.
- Chen, T.R., Drabkowski, D., Hay, R.J., Macy, M. and Peterson, W., Jr. (1987) WiDr is a derivative of another colon adenocarcinoma cell line, HT-29. *Cancer Genet Cytogenet*, **27**, 125-134.
- Chen, Y.H. and Lu, Q. (2003) Association of nonreceptor tyrosine kinase c-yes with tight junction protein occludin by coimmunoprecipitation assay. *Methods Mol Biol*, **218**, 127-132.
- Chen, Y.H., Lu, Q., Goodenough, D.A. and Jeansonne, B. (2002) Nonreceptor tyrosine kinase c-Yes interacts with occludin during tight junction formation in canine kidney epithelial cells. *Mol Biol Cell*, **13**, 1227-1237.
- Chester, K., Pedley, B., Tolner, B., Violet, J., Mayer, A., Sharma, S., Boxer, G., Green, A., Nagl, S. and Begent, R. (2004) Engineering antibodies for clinical applications in cancer. *Tumour Biol*, **25**, 91-98.
- Cho, K.B., Cho, M.K., Lee, W.Y. and Kang, K.W. (2010) Overexpression of c-myc induces epithelial mesenchymal transition in mammary epithelial cells. *Cancer Lett*.
- Chodniewicz, D. and Klemke, R.L. (2004) Regulation of integrin-mediated cellular responses through assembly of a CAS/Crk scaffold. *Biochim Biophys Acta*, **1692**, 63-76.
- Christiansen, J.J. and Rajasekaran, A.K. (2006) Reassessing epithelial to mesenchymal transition as a prerequisite for carcinoma invasion and metastasis. *Cancer Res*, **66**, 8319-8326.

- Cohen, P., Alessi, D.R. and Cross, D.A. (1997) PDK1, one of the missing links in insulin signal transduction? *FEBS Lett*, **410**, 3-10.
- Copple, B.L., Bustamante, J.J., Welch, T.P., Kim, N.D. and Moon, J.O. (2009) Hypoxia-inducible factor-dependent production of profibrotic mediators by hypoxic hepatocytes. *Liver Int*, **29**, 1010-1021.
- Copur, S., Aiba, K., Drake, J.C., Allegra, C.J. and Chu, E. (1995) Thymidylate synthase gene amplification in human colon cancer cell lines resistant to 5-fluorouracil. *Biochem Pharmacol*, **49**, 1419-1426.
- Croix, B.S., Rak, J.W., Kapitan, S., Sheehan, C., Graham, C.H. and Kerbel, R.S. (1996) Reversal by hyaluronidase of adhesion-dependent multicellular drug resistance in mammary carcinoma cells. *J Natl Cancer Inst*, **88**, 1285-1296.
- CRUK, C.R.U.K. (2009) Latest UK Cancer Incidence and Mortality Summary - numbers.
- Curran, S. and Murray, G.I. (1999) Matrix metalloproteinases in tumour invasion and metastasis. *J Pathol*, **189**, 300-308.
- Curreri, A.R., Ansfield, F.J., Mc, I.F., Waisman, H.A. and Heidelberger, C. (1958) Clinical studies with 5-fluorouracil. *Cancer Res*, **18**, 478-484.
- Daigo, Y., Furukawa, Y., Kawasoe, T., Ishiguro, H., Fujita, M., Sugai, S., Nakamori, S., Liefers, G.J., Tollenaar, R.A., van de Velde, C.J. and Nakamura, Y. (1999) Absence of genetic alteration at codon 531 of the human c-src gene in 479 advanced colorectal cancers from Japanese and Caucasian patients. *Cancer Res*, **59**, 4222-4224.
- Datta, S.R., Brunet, A. and Greenberg, M.E. (1999) Cellular survival: a play in three Akts. *Genes Dev*, **13**, 2905-2927.
- Datta, S.R., Dudek, H., Tao, X., Masters, S., Fu, H., Gotoh, Y. and Greenberg, M.E. (1997) Akt phosphorylation of BAD couples survival signals to the cell-intrinsic death machinery. *Cell*, **91**, 231-241.
- de Gramont, A., Bosset, J.F., Milan, C., Rougier, P., Bouche, O., Etienne, P.L., Morvan, F., Louvet, C., Guillot, T., Francois, E. and Bedenne, L. (1997) Randomized trial comparing monthly low-dose leucovorin and fluorouracil bolus with bimonthly high-dose leucovorin and fluorouracil bolus plus continuous infusion for advanced colorectal cancer: a French intergroup study. *J Clin Oncol*, **15**, 808-815.
- Delattre, O., Olschwang, S., Law, D.J., Melot, T., Remvikos, Y., Salmon, R.J., Sastre, X., Validire, P., Feinberg, A.P. and Thomas, G. (1989) Multiple genetic alterations in distal and proximal colorectal cancer. *Lancet*, **2**, 353-356.
- Derksen, P.W., Liu, X., Saridin, F., van der Gulden, H., Zevenhoven, J., Evers, B., van Beijnum, J.R., Griffioen, A.W., Vink, J., Krimpenfort, P., Peterse, J.L., Cardiff, R.D., Berns, A. and Jonkers, J. (2006) Somatic inactivation of E-cadherin and p53 in mice leads to metastatic lobular mammary carcinoma through induction of anoikis resistance and angiogenesis. *Cancer Cell*, **10**, 437-449.
- Di Paolo, A., Ibrahim, T., Danesi, R., Maltoni, M., Vannozzi, F., Flamini, E., Zoli, W., Amadori, D. and Del Tacca, M. (2002) Relationship between plasma

concentrations of 5-fluorouracil and 5-fluoro-5,6-dihydrouracil and toxicity of 5-fluorouracil infusions in cancer patients. *Ther Drug Monit*, **24**, 588-593.

- Domin, B.A., Mahony, W.B. and Zimmerman, T.P. (1993) Transport of 5-fluorouracil and uracil into human erythrocytes. *Biochem Pharmacol*, **46**, 503-510.
- Drubin, D.G. and Nelson, W.J. (1996) Origins of cell polarity. *Cell*, **84**, 335-344.
- Dunty, J.M., Gabarra-Niecko, V., King, M.L., Ceccarelli, D.F., Eck, M.J. and Schaller, M.D. (2004) FERM domain interaction promotes FAK signaling. *Mol Cell Biol*, **24**, 5353-5368.
- Edler, D., Glimelius, B., Hallstrom, M., Jakobsen, A., Johnston, P.G., Magnusson, I., Ragnhammar, P. and Blomgren, H. (2002) Thymidylate synthase expression in colorectal cancer: a prognostic and predictive marker of benefit from adjuvant fluorouracil-based chemotherapy. *J Clin Oncol*, **20**, 1721-1728.
- Engelman, J.A., Luo, J. and Cantley, L.C. (2006) The evolution of phosphatidylinositol 3-kinases as regulators of growth and metabolism. *Nat Rev Genet*, **7**, 606-619.
- Espada, J., Galaz, S., Sanz-Rodriguez, F., Blazquez-Castro, A., Stockert, J.C., Bagazgoitia, L., Jaen, P., Gonzalez, S., Cano, A. and Juarranz, A. (2009) Oncogenic H-Ras and PI3K signaling can inhibit E-cadherin-dependent apoptosis and promote cell survival after photodynamic therapy in mouse keratinocytes. *J Cell Physiol*, **219**, 84-93.
- Falcone, A., Ricci, S., Brunetti, I., Pfanner, E., Allegrini, G., Barbara, C., Crino, L., Benedetti, G., Evangelista, W., Fanchini, L., Cortesi, E., Picone, V., Vitello, S., Chiara, S., Granetto, C., Porcile, G., Fioretto, L., Orlandini, C., Andreuccetti, M. and Masi, G. (2007) Phase III trial of infusional fluorouracil, leucovorin, oxaliplatin, and irinotecan (FOLFOXIRI) compared with infusional fluorouracil, leucovorin, and irinotecan (FOLFIRI) as first-line treatment for metastatic colorectal cancer: the Gruppo Oncologico Nord Ovest. *J Clin Oncol*, **25**, 1670-1676.
- Feldmann, G., Dhara, S., Fendrich, V., Bedja, D., Beaty, R., Mullendore, M., Karikari, C., Alvarez, H., Iacobuzio-Donahue, C., Jimeno, A., Gabrielson, K.L., Matsui, W. and Maitra, A. (2007) Blockade of hedgehog signaling inhibits pancreatic cancer invasion and metastases: a new paradigm for combination therapy in solid cancers. *Cancer Res*, **67**, 2187-2196.
- Feldmann, G., Fendrich, V., McGovern, K., Bedja, D., Bisht, S., Alvarez, H., Koorstra, J.B., Habbe, N., Karikari, C., Mullendore, M., Gabrielson, K.L., Sharma, R., Matsui, W. and Maitra, A. (2008) An orally bioavailable small-molecule inhibitor of Hedgehog signaling inhibits tumor initiation and metastasis in pancreatic cancer. *Mol Cancer Ther*, **7**, 2725-2735.
- Ferrara, N., Hillan, K.J., Gerber, H.P. and Novotny, W. (2004) Discovery and development of bevacizumab, an anti-VEGF antibody for treating cancer. *Nat Rev Drug Discov*, **3**, 391-400.
- Fincham, V.J. and Frame, M.C. (1998) The catalytic activity of Src is dispensable for translocation to focal adhesions but controls the turnover of these structures during cell motility. *Embo J*, **17**, 81-92.

- Finn, R.S., Dering, J., Ginther, C., Wilson, C.A., Glaspy, P., Tchekmedyan, N. and Slamon, D.J. (2007) Dasatinib, an orally active small molecule inhibitor of both the src and abl kinases, selectively inhibits growth of basal-type/"triple-negative" breast cancer cell lines growing in vitro. *Breast Cancer Res Treat*, **105**, 319-326.
- Fischer, A.N., Fuchs, E., Mikula, M., Huber, H., Beug, H. and Mikulits, W. (2007) PDGF essentially links TGF-beta signaling to nuclear beta-catenin accumulation in hepatocellular carcinoma progression. *Oncogene*, **26**, 3395-3405.
- Folkes, A.J., Ahmadi, K., Alderton, W.K., Alix, S., Baker, S.J., Box, G., Chuckowree, I.S., Clarke, P.A., Depledge, P., Eccles, S.A., Friedman, L.S., Hayes, A., Hancox, T.C., Kugendradas, A., Lensun, L., Moore, P., Olivero, A.G., Pang, J., Patel, S., Pergl-Wilson, G.H., Raynaud, F.I., Robson, A., Saghir, N., Salphati, L., Sohal, S., Ultsch, M.H., Valenti, M., Wallweber, H.J., Wan, N.C., Wiesmann, C., Workman, P., Zhyvoloup, A., Zvelebil, M.J. and Shuttleworth, S.J. (2008) The identification of 2-(1H-indazol-4-yl)-6-(4-methanesulfonyl-piperazin-1-ylmethyl)-4-morpholin-4-yl-thieno[3,2-d]pyrimidine (GDC-0941) as a potent, selective, orally bioavailable inhibitor of class I PI3 kinase for the treatment of cancer. *J Med Chem*, **51**, 5522-5532.
- Frame, M.C. (2002) Src in cancer: deregulation and consequences for cell behaviour. *Biochim Biophys Acta*, **1602**, 114-130.
- Frame, M.C. (2004) Newest findings on the oldest oncogene; how activated src does it. *J Cell Sci*, **117**, 989-998.
- Franke, T.F., Kaplan, D.R., Cantley, L.C. and Toker, A. (1997) Direct regulation of the Akt proto-oncogene product by phosphatidylinositol-3,4-bisphosphate. *Science*, **275**, 665-668.
- Fujita, Y., Krause, G., Scheffner, M., Zechner, D., Leddy, H.E., Behrens, J., Sommer, T. and Birchmeier, W. (2002) Hakai, a c-Cbl-like protein, ubiquitinates and induces endocytosis of the E-cadherin complex. *Nat Cell Biol*, **4**, 222-231.
- Fukushima, M., Fujioka, A., Uchida, J., Nakagawa, F. and Takechi, T. (2001) Thymidylate synthase (TS) and ribonucleotide reductase (RNR) may be involved in acquired resistance to 5-fluorouracil (5-FU) in human cancer xenografts in vivo. *Eur J Cancer*, **37**, 1681-1687.
- Gaidarov, I., Smith, M.E., Domin, J. and Keen, J.H. (2001) The class II phosphoinositide 3-kinase C2alpha is activated by clathrin and regulates clathrin-mediated membrane trafficking. *Mol Cell*, **7**, 443-449.
- Gavrieli, Y., Sherman, Y. and Ben-Sasson, S.A. (1992) Identification of programmed cell death in situ via specific labeling of nuclear DNA fragmentation. *J Cell Biol*, **119**, 493-501.
- Geiger, T.R. and Peeper, D.S. (2009) Metastasis mechanisms. *Biochim Biophys Acta*, **1796**, 293-308.
- Ghysdael, J., Neil, J.C. and Vogt, P.K. (1981) A third class of avian sarcoma viruses, defined by related transformation-specific proteins of Yamaguchi 73 and Esh sarcoma viruses. *Proc Natl Acad Sci U S A*, **78**, 2611-2615.

- Goldberg, R.M. and Gill, S. (2004) Recent phase III trials of fluorouracil, irinotecan, and oxaliplatin as chemotherapy for metastatic colorectal cancer. *Cancer Chemother Pharmacol*, **54 Suppl 1**, S57-64.
- Golenhofen, N. and Drenckhahn, D. (2000) The catenin, p120^{ctn}, is a common membrane-associated protein in various epithelial and non-epithelial cells and tissues. *Histochem Cell Biol*, **114**, 147-155.
- Green, S.K., Francia, G., Isidoro, C. and Kerbel, R.S. (2004) Antiadhesive antibodies targeting E-cadherin sensitize multicellular tumor spheroids to chemotherapy in vitro. *Mol Cancer Ther*, **3**, 149-159.
- Gregory, P.A., Bert, A.G., Paterson, E.L., Barry, S.C., Tsykin, A., Farshid, G., Vadas, M.A., Khew-Goodall, Y. and Goodall, G.J. (2008) The miR-200 family and miR-205 regulate epithelial to mesenchymal transition by targeting ZEB1 and SIP1. *Nat Cell Biol*, **10**, 593-601.
- Grem, J.L. and Fischer, P.H. (1989) Enhancement of 5-fluorouracil's anticancer activity by dipyrindamole. *Pharmacol Ther*, **40**, 349-371.
- Guilford, P., Hopkins, J., Harraway, J., McLeod, M., McLeod, N., Harawira, P., Taite, H., Scoular, R., Miller, A. and Reeve, A.E. (1998) E-cadherin germline mutations in familial gastric cancer. *Nature*, **392**, 402-405.
- Guinebault, C., Payrastre, B., Racaud-Sultan, C., Mazarguil, H., Breton, M., Mauco, G., Plantavid, M. and Chap, H. (1995) Integrin-dependent translocation of phosphoinositide 3-kinase to the cytoskeleton of thrombin-activated platelets involves specific interactions of p85 alpha with actin filaments and focal adhesion kinase. *J Cell Biol*, **129**, 831-842.
- Gumbiner, B.M. (2000) Regulation of cadherin adhesive activity. *J Cell Biol*, **148**, 399-404.
- Gumbiner, B.M. (2005) Regulation of cadherin-mediated adhesion in morphogenesis. *Nat Rev Mol Cell Biol*, **6**, 622-634.
- Han, M.K., Song, E.K., Guo, Y., Ou, X., Mantel, C. and Broxmeyer, H.E. (2008) SIRT1 regulates apoptosis and Nanog expression in mouse embryonic stem cells by controlling p53 subcellular localization. *Cell Stem Cell*, **2**, 241-251.
- Hanks, S.K., Ryzhova, L., Shin, N.Y. and Brabek, J. (2003) Focal adhesion kinase signaling activities and their implications in the control of cell survival and motility. *Front Biosci*, **8**, d982-996.
- Hara, K., Maruki, Y., Long, X., Yoshino, K., Oshiro, N., Hidayat, S., Tokunaga, C., Avruch, J. and Yonezawa, K. (2002) Raptor, a binding partner of target of rapamycin (TOR), mediates TOR action. *Cell*, **110**, 177-189.
- Hartsock, A. and Nelson, W.J. (2008) Adherens and tight junctions: structure, function and connections to the actin cytoskeleton. *Biochim Biophys Acta*, **1778**, 660-669.
- Hawkins, P.T., Anderson, K.E., Davidson, K. and Stephens, L.R. (2006) Signalling through Class I PI3Ks in mammalian cells. *Biochem Soc Trans*, **34**, 647-662.

- Hay, N. and Sonenberg, N. (2004) Upstream and downstream of mTOR. *Genes Dev*, **18**, 1926-1945.
- Hill, R. and Wu, H. (2009) PTEN, stem cells, and cancer stem cells. *J Biol Chem*, **284**, 11755-11759.
- Hiscox, S., Jiang, W.G., Obermeier, K., Taylor, K., Morgan, L., Burmi, R., Barrow, D. and Nicholson, R.I. (2006) Tamoxifen resistance in MCF7 cells promotes EMT-like behaviour and involves modulation of beta-catenin phosphorylation. *Int J Cancer*, **118**, 290-301.
- Hiscox, S., Morgan, L., Barrow, D., Dutkowskil, C., Wakeling, A. and Nicholson, R.I. (2004) Tamoxifen resistance in breast cancer cells is accompanied by an enhanced motile and invasive phenotype: inhibition by gefitinib ('Iressa', ZD1839). *Clin Exp Metastasis*, **21**, 201-212.
- Hollstein, M. and Hainaut, P. (2010) Massively regulated genes: the example of TP53. *J Pathol*, **220**, 164-173.
- Hooijberg, J.H., de Vries, N.A., Kaspers, G.J., Pieters, R., Jansen, G. and Peters, G.J. (2006) Multidrug resistance proteins and folate supplementation: therapeutic implications for antifolates and other classes of drugs in cancer treatment. *Cancer Chemother Pharmacol*, **58**, 1-12.
- Hori, T., Takahashi, E., Ayusawa, D., Takeishi, K., Kaneda, S. and Seno, T. (1990) Regional assignment of the human thymidylate synthase (TS) gene to chromosome band 18p11.32 by nonisotopic in situ hybridization. *Hum Genet*, **85**, 576-580.
- Hoshino, H., Miyoshi, N., Nagai, K., Tomimaru, Y., Nagano, H., Sekimoto, M., Doki, Y., Mori, M. and Ishii, H. (2009) Epithelial-mesenchymal transition with expression of SNAI1-induced chemoresistance in colorectal cancer. *Biochem Biophys Res Commun*, **390**, 1061-1065.
- Hubbard, S.R. and Till, J.H. (2000) Protein tyrosine kinase structure and function. *Annu Rev Biochem*, **69**, 373-398.
- Huber, M.A., Kraut, N. and Beug, H. (2005) Molecular requirements for epithelial-mesenchymal transition during tumor progression. *Curr Opin Cell Biol*, **17**, 548-558.
- Hughey, C.T., Barbour, K.W., Berger, F.G. and Berger, S.H. (1993) Functional effects of a naturally occurring amino acid substitution in human thymidylate synthase. *Mol Pharmacol*, **44**, 316-323.
- Hulpiau, P. and van Roy, F. (2009) Molecular evolution of the cadherin superfamily. *Int J Biochem Cell Biol*, **41**, 349-369.
- Humar, B. and Guilford, P. (2009) Hereditary diffuse gastric cancer: a manifestation of lost cell polarity. *Cancer Sci*, **100**, 1151-1157.
- Hynes, R.O. (2009) The extracellular matrix: not just pretty fibrils. *Science*, **326**, 1216-1219.

- Ingley, E., Schneider, J.R., Payne, C.J., McCarthy, D.J., Harder, K.W., Hibbs, M.L. and Klinken, S.P. (2006) Csk-binding protein mediates sequential enzymatic down-regulation and degradation of Lyn in erythropoietin-stimulated cells. *J Biol Chem*, **281**, 31920-31929.
- Irby, R.B., Mao, W., Coppola, D., Kang, J., Loubeau, J.M., Trudeau, W., Karl, R., Fujita, D.J., Jove, R. and Yeatman, T.J. (1999) Activating SRC mutation in a subset of advanced human colon cancers. *Nat Genet*, **21**, 187-190.
- Irby, R.B. and Yeatman, T.J. (2000) Role of Src expression and activation in human cancer. *Oncogene*, **19**, 5636-5642.
- Izaguirre, G., Aguirre, L., Hu, Y.P., Lee, H.Y., Schlaepfer, D.D., Aneskievich, B.J. and Haimovich, B. (2001) The cytoskeletal/non-muscle isoform of alpha-actinin is phosphorylated on its actin-binding domain by the focal adhesion kinase. *J Biol Chem*, **276**, 28676-28685.
- Jager, T., Becker, M., Eisenhardt, A., Tilki, D., Totsch, M., Schmid, K.W., Romics, I., Rubben, H., Ergun, S. and Szarvas, T. (2010) The prognostic value of cadherin switch in bladder cancer. *Oncol Rep*, **23**, 1125-1132.
- Jamora, C. and Fuchs, E. (2002) Intercellular adhesion, signalling and the cytoskeleton. *Nat Cell Biol*, **4**, E101-108.
- Jin, H. and Varner, J. (2004) Integrins: roles in cancer development and as treatment targets. *Br J Cancer*, **90**, 561-565.
- Johnston, P.G., Drake, J.C., Trepel, J. and Allegra, C.J. (1992) Immunological quantitation of thymidylate synthase using the monoclonal antibody TS 106 in 5-fluorouracil-sensitive and -resistant human cancer cell lines. *Cancer Res*, **52**, 4306-4312.
- Johnston, P.G., Fisher, E.R., Rockette, H.E., Fisher, B., Wolmark, N., Drake, J.C., Chabner, B.A. and Allegra, C.J. (1994) The role of thymidylate synthase expression in prognosis and outcome of adjuvant chemotherapy in patients with rectal cancer. *J Clin Oncol*, **12**, 2640-2647.
- Johnston, P.G., Lenz, H.J., Leichman, C.G., Danenberg, K.D., Allegra, C.J., Danenberg, P.V. and Leichman, L. (1995) Thymidylate synthase gene and protein expression correlate and are associated with response to 5-fluorouracil in human colorectal and gastric tumors. *Cancer Res*, **55**, 1407-1412.
- Kalluri, R. (2009) EMT: when epithelial cells decide to become mesenchymal-like cells. *J Clin Invest*, **119**, 1417-1419.
- Kamei, T., Machida, K., Nimura, Y., Senga, T., Yamada, I., Yoshii, S., Matsuda, S. and Hamaguchi, M. (2000) C-Cbl protein in human cancer tissues is frequently tyrosine phosphorylated in a tumor-specific manner. *Int J Oncol*, **17**, 335-339.
- Kanaan, N., Marti, S., Moliner, V. and Kohen, A. (2007) A quantum mechanics/molecular mechanics study of the catalytic mechanism of the thymidylate synthase. *Biochemistry*, **46**, 3704-3713.
- Kaplan, J.M., Varmus, H.E. and Bishop, J.M. (1990) The src protein contains multiple domains for specific attachment to membranes. *Mol Cell Biol*, **10**, 1000-1009.

- Kaplan, K.B., Bibbins, K.B., Swedlow, J.R., Arnaud, M., Morgan, D.O. and Varmus, H.E. (1994) Association of the amino-terminal half of c-Src with focal adhesions alters their properties and is regulated by phosphorylation of tyrosine 527. *Embo J*, **13**, 4745-4756.
- Karhadkar, S.S., Bova, G.S., Abdallah, N., Dhara, S., Gardner, D., Maitra, A., Isaacs, J.T., Berman, D.M. and Beachy, P.A. (2004) Hedgehog signalling in prostate regeneration, neoplasia and metastasis. *Nature*, **431**, 707-712.
- Kartenbeck, J., Schmelz, M., Franke, W.W. and Geiger, B. (1991) Endocytosis of junctional cadherins in bovine kidney epithelial (MDBK) cells cultured in low Ca²⁺ ion medium. *J Cell Biol*, **113**, 881-892.
- Katoh, Y. and Katoh, M. (2008) Hedgehog signaling, epithelial-to-mesenchymal transition and miRNA (review). *Int J Mol Med*, **22**, 271-275.
- Khanna, S., Roy, S., Park, H.A. and Sen, C.K. (2007) Regulation of c-Src activity in glutamate-induced neurodegeneration. *J Biol Chem*, **282**, 23482-23490.
- Kim, M., Tezuka, T., Tanaka, K. and Yamamoto, T. (2004) Cbl-c suppresses v-Src-induced transformation through ubiquitin-dependent protein degradation. *Oncogene*, **23**, 1645-1655.
- Kinsella, A.R., Smith, D. and Pickard, M. (1997) Resistance to chemotherapeutic antimetabolites: a function of salvage pathway involvement and cellular response to DNA damage. *Br J Cancer*, **75**, 935-945.
- Klingelhofer, J., Laur, O.Y., Troyanovsky, R.B. and Troyanovsky, S.M. (2002) Dynamic interplay between adhesive and lateral E-cadherin dimers. *Mol Cell Biol*, **22**, 7449-7458.
- Klinghoffer, R.A., Sachsenmaier, C., Cooper, J.A. and Soriano, P. (1999) Src family kinases are required for integrin but not PDGFR signal transduction. *Embo J*, **18**, 2459-2471.
- Klippel, A., Reinhard, C., Kavanaugh, W.M., Apell, G., Escobedo, M.A. and Williams, L.T. (1996) Membrane localization of phosphatidylinositol 3-kinase is sufficient to activate multiple signal-transducing kinase pathways. *Mol Cell Biol*, **16**, 4117-4127.
- Knudsen, K.A. and Wheelock, M.J. (1992) Plakoglobin, or an 83-kD homologue distinct from beta-catenin, interacts with E-cadherin and N-cadherin. *J Cell Biol*, **118**, 671-679.
- Kodaki, T., Woscholski, R., Hallberg, B., Rodriguez-Viciana, P., Downward, J. and Parker, P.J. (1994) The activation of phosphatidylinositol 3-kinase by Ras. *Curr Biol*, **4**, 798-806.
- Kolch, W. (2000) Meaningful relationships: the regulation of the Ras/Raf/MEK/ERK pathway by protein interactions. *Biochem J*, **351 Pt 2**, 289-305.
- Kong, D. and Yamori, T. (2009) Advances in development of phosphatidylinositol 3-kinase inhibitors. *Curr Med Chem*, **16**, 2839-2854.

- Kornmann, M., Schwabe, W., Sander, S., Kron, M., Strater, J., Polat, S., Kettner, E., Weiser, H.F., Baumann, W., Schramm, H., Hausler, P., Ott, K., Behnke, D., Staib, L., Beger, H.G. and Link, K.H. (2003) Thymidylate synthase and dihydropyrimidine dehydrogenase mRNA expression levels: predictors for survival in colorectal cancer patients receiving adjuvant 5-fluorouracil. *Clin Cancer Res*, **9**, 4116-4124.
- Korpala, M., Lee, E.S., Hu, G. and Kang, Y. (2008) The miR-200 family inhibits epithelial-mesenchymal transition and cancer cell migration by direct targeting of E-cadherin transcriptional repressors ZEB1 and ZEB2. *J Biol Chem*, **283**, 14910-14914.
- Kroczyńska, B., Kaur, S. and Plataniotis, L.C. (2009) Growth suppressive cytokines and the AKT/mTOR pathway. *Cytokine*, **48**, 138-143.
- Kruser, T.J. and Wheeler, D.L. (2010) Mechanisms of resistance to HER family targeting antibodies. *Exp Cell Res*.
- Kypta, R.M., Goldberg, Y., Ulug, E.T. and Courtneidge, S.A. (1990) Association between the PDGF receptor and members of the src family of tyrosine kinases. *Cell*, **62**, 481-492.
- Lane, D.P. (1992) Cancer. p53, guardian of the genome. *Nature*, **358**, 15-16.
- Langdon, S.P., Lawrie, S.S., Hay, F.G., Hawkes, M.M., McDonald, A., Hayward, I.P., Schol, D.J., Hilgers, J., Leonard, R.C. and Smyth, J.F. (1988) Characterization and properties of nine human ovarian adenocarcinoma cell lines. *Cancer Res*, **48**, 6166-6172.
- Laprise, P., Chailier, P., Houde, M., Beaulieu, J.F., Boucher, M.J. and Rivard, N. (2002) Phosphatidylinositol 3-kinase controls human intestinal epithelial cell differentiation by promoting adherens junction assembly and p38 MAPK activation. *J Biol Chem*, **277**, 8226-8234.
- Larue, L., Ohsugi, M., Hirchenhain, J. and Kemler, R. (1994) E-cadherin null mutant embryos fail to form a trophectoderm epithelium. *Proc Natl Acad Sci U S A*, **91**, 8263-8267.
- Le, T.L., Yap, A.S. and Stow, J.L. (1999) Recycling of E-cadherin: a potential mechanism for regulating cadherin dynamics. *J Cell Biol*, **146**, 219-232.
- Lehembre, F., Yilmaz, M., Wicki, A., Schomber, T., Strittmatter, K., Ziegler, D., Kren, A., Went, P., Derksen, P.W., Berns, A., Jonkers, J. and Christofori, G. (2008) NCAM-induced focal adhesion assembly: a functional switch upon loss of E-cadherin. *Embo J*, **27**, 2603-2615.
- Leichman, C.G., Lenz, H.J., Leichman, L., Danenberg, K., Baranda, J., Groshen, S., Boswell, W., Metzger, R., Tan, M. and Danenberg, P.V. (1997) Quantitation of intratumoral thymidylate synthase expression predicts for disseminated colorectal cancer response and resistance to protracted-infusion fluorouracil and weekly leucovorin. *J Clin Oncol*, **15**, 3223-3229.
- Li, L.S., Morales, J.C., Veigl, M., Sedwick, D., Greer, S., Meyers, M., Wagner, M., Fishel, R. and Boothman, D.A. (2009) DNA mismatch repair (MMR)-dependent 5-

- fluorouracil cytotoxicity and the potential for new therapeutic targets. *Br J Pharmacol*, **158**, 679-692.
- Li, Q. and Mattingly, R.R. (2008) Restoration of E-cadherin cell-cell junctions requires both expression of E-cadherin and suppression of ERK MAP kinase activation in Ras-transformed breast epithelial cells. *Neoplasia*, **10**, 1444-1458.
- Li, S.S. (2005) Specificity and versatility of SH3 and other proline-recognition domains: structural basis and implications for cellular signal transduction. *Biochem J*, **390**, 641-653.
- Liu, F.S. (2009) Mechanisms of chemotherapeutic drug resistance in cancer therapy--a quick review. *Taiwan J Obstet Gynecol*, **48**, 239-244.
- Liu, P., Cheng, H., Roberts, T.M. and Zhao, J.J. (2009) Targeting the phosphoinositide 3-kinase pathway in cancer. *Nat Rev Drug Discov*, **8**, 627-644.
- Liwosz, A., Lei, T. and Kukuruzinska, M.A. (2006) N-glycosylation affects the molecular organization and stability of E-cadherin junctions. *J Biol Chem*, **281**, 23138-23149.
- Longley, D.B., Harkin, D.P. and Johnston, P.G. (2003) 5-fluorouracil: mechanisms of action and clinical strategies. *Nat Rev Cancer*, **3**, 330-338.
- Longley, D.B. and Johnston, P.G. (2005) Molecular mechanisms of drug resistance. *J Pathol*, **205**, 275-292.
- Luton, F., Verges, M., Vaerman, J.P., Sudol, M. and Mostov, K.E. (1999) The SRC family protein tyrosine kinase p62yes controls polymeric IgA transcytosis in vivo. *Mol Cell*, **4**, 627-632.
- Maeda, M., Johnson, K.R. and Wheelock, M.J. (2005) Cadherin switching: essential for behavioral but not morphological changes during an epithelium-to-mesenchyme transition. *J Cell Sci*, **118**, 873-887.
- Maehama, T. and Dixon, J.E. (1998) The tumor suppressor, PTEN/MMAC1, dephosphorylates the lipid second messenger, phosphatidylinositol 3,4,5-trisphosphate. *J Biol Chem*, **273**, 13375-13378.
- Mani, S.A., Guo, W., Liao, M.J., Eaton, E.N., Ayyanan, A., Zhou, A.Y., Brooks, M., Reinhard, F., Zhang, C.C., Shipitsin, M., Campbell, L.L., Polyak, K., Brisken, C., Yang, J. and Weinberg, R.A. (2008) The epithelial-mesenchymal transition generates cells with properties of stem cells. *Cell*, **133**, 704-715.
- Martin, G.S. (2001) The hunting of the Src. *Nat Rev Mol Cell Biol*, **2**, 467-475.
- Martin, G.S. (2003) Cell signaling and cancer. *Cancer Cell*, **4**, 167-174.
- Martin, G.S. (2004) The road to Src. *Oncogene*, **23**, 7910-7917.
- Massague, J. (1998) TGF-beta signal transduction. *Annu Rev Biochem*, **67**, 753-791.
- McConkey, D.J., Choi, W., Marquis, L., Martin, F., Williams, M.B., Shah, J., Svatek, R., Das, A., Adam, L., Kamat, A., Siefker-Radtke, A. and Dinney, C. (2009) Role of

epithelial-to-mesenchymal transition (EMT) in drug sensitivity and metastasis in bladder cancer. *Cancer Metastasis Rev*, **28**, 335-344.

- McDermott, U., Longley, D.B., Galligan, L., Allen, W., Wilson, T. and Johnston, P.G. (2005) Effect of p53 status and STAT1 on chemotherapy-induced, Fas-mediated apoptosis in colorectal cancer. *Cancer Res*, **65**, 8951-8960.
- Metzger, R., Danenberg, K., Leichman, C.G., Salonga, D., Schwartz, E.L., Wadler, S., Lenz, H.J., Groshen, S., Leichman, L. and Danenberg, P.V. (1998) High basal level gene expression of thymidine phosphorylase (platelet-derived endothelial cell growth factor) in colorectal tumors is associated with nonresponse to 5-fluorouracil. *Clin Cancer Res*, **4**, 2371-2376.
- Mitra, S.K., Hanson, D.A. and Schlaepfer, D.D. (2005) Focal adhesion kinase: in command and control of cell motility. *Nat Rev Mol Cell Biol*, **6**, 56-68.
- Miyashita, Y. and Ozawa, M. (2007) Increased internalization of p120-uncoupled E-cadherin and a requirement for a dileucine motif in the cytoplasmic domain for endocytosis of the protein. *J Biol Chem*, **282**, 11540-11548.
- Moarefi, I., LaFevre-Bernt, M., Sicheri, F., Huse, M., Lee, C.H., Kuriyan, J. and Miller, W.T. (1997) Activation of the Src-family tyrosine kinase Hck by SH3 domain displacement. *Nature*, **385**, 650-653.
- Montagnani, F., Chiriatti, A., Turrisi, G., Francini, G. and Fiorentini, G. (2010) A systematic review of FOLFOXIRI chemotherapy for the first-line treatment of metastatic colorectal cancer: improved efficacy at the cost of increased toxicity. *Colorectal Dis*.
- Moustakas, A. and Heldin, C.H. (2007) Signaling networks guiding epithelial-mesenchymal transitions during embryogenesis and cancer progression. *Cancer Sci*, **98**, 1512-1520.
- Muneoka, K., Shirai, Y., Sasaki, M., Wakai, T., Sakata, J. and Hatakeyama, K. (2009) Interstitial pneumonia arising in a patient treated with oxaliplatin, 5-fluorouracil, and, leucovorin (FOLFOX). *Int J Clin Oncol*, **14**, 457-459.
- Nada, S., Okada, M., MacAuley, A., Cooper, J.A. and Nakagawa, H. (1991) Cloning of a complementary DNA for a protein-tyrosine kinase that specifically phosphorylates a negative regulatory site of p60c-src. *Nature*, **351**, 69-72.
- Nakagawa, T., Tanaka, S., Suzuki, H., Takayanagi, H., Miyazaki, T., Nakamura, K. and Tsuruo, T. (2000) Overexpression of the csk gene suppresses tumor metastasis in vivo. *Int J Cancer*, **88**, 384-391.
- Nam, J.S., Ino, Y., Sakamoto, M. and Hirohashi, S. (2002) Src family kinase inhibitor PP2 restores the E-cadherin/catenin cell adhesion system in human cancer cells and reduces cancer metastasis. *Clin Cancer Res*, **8**, 2430-2436.
- Nave, B.T., Ouwens, M., Withers, D.J., Alessi, D.R. and Shepherd, P.R. (1999) Mammalian target of rapamycin is a direct target for protein kinase B: identification of a convergence point for opposing effects of insulin and amino-acid deficiency on protein translation. *Biochem J*, **344 Pt 2**, 427-431.

- Nawshad, A., Medici, D., Liu, C.C. and Hay, E.D. (2007) TGFbeta3 inhibits E-cadherin gene expression in palate medial-edge epithelial cells through a Smad2-Smad4-LEF1 transcription complex. *J Cell Sci*, **120**, 1646-1653.
- NCBI.
- Nilbert, M. and Fernebro, E. (2000) Lack of activating c-SRC mutations at codon 531 in rectal cancer. *Cancer Genet Cytogenet*, **121**, 94-95.
- Nusrat, A., Chen, J.A., Foley, C.S., Liang, T.W., Tom, J., Cromwell, M., Quan, C. and Mrsny, R.J. (2000) The coiled-coil domain of occludin can act to organize structural and functional elements of the epithelial tight junction. *J Biol Chem*, **275**, 29816-29822.
- O'Brate, A. and Giannakakou, P. (2003) The importance of p53 location: nuclear or cytoplasmic zip code? *Drug Resist Updat*, **6**, 313-322.
- O'Donovan, N., Byrne, A.T., O'Connor, A.E., McGee, S., Gallagher, W.M. and Crown, J. Synergistic interaction between trastuzumab and EGFR/HER-2 tyrosine kinase inhibitors in HER-2 positive breast cancer cells. *Invest New Drugs*.
- Office-for-National-Statistics. (2008) Registrations of cancer diagnosed in 2006, England.
- Ogawa, A., Takayama, Y., Sakai, H., Chong, K.T., Takeuchi, S., Nakagawa, A., Nada, S., Okada, M. and Tsukihara, T. (2002) Structure of the carboxyl-terminal Src kinase, Csk. *J Biol Chem*, **277**, 14351-14354.
- Ooyama, A., Okayama, Y., Takechi, T., Sugimoto, Y., Oka, T. and Fukushima, M. (2007) Genome-wide screening of loci associated with drug resistance to 5-fluorouracil-based drugs. *Cancer Sci*, **98**, 577-583.
- Orton, R.J., Sturm, O.E., Vyshemirsky, V., Calder, M., Gilbert, D.R. and Kolch, W. (2005) Computational modelling of the receptor-tyrosine-kinase-activated MAPK pathway. *Biochem J*, **392**, 249-261.
- Otey, C.A. and Carpen, O. (2004) Alpha-actinin revisited: a fresh look at an old player. *Cell Motil Cytoskeleton*, **58**, 104-111.
- Otey, C.A., Pavalko, F.M. and Burrige, K. (1990) An interaction between alpha-actinin and the beta 1 integrin subunit in vitro. *J Cell Biol*, **111**, 721-729.
- Otsu, M., Hiles, I., Gout, I., Fry, M.J., Ruiz-Larrea, F., Panayotou, G., Thompson, A., Dhand, R., Hsuan, J., Totty, N. and et al. (1991) Characterization of two 85 kd proteins that associate with receptor tyrosine kinases, middle-T/pp60c-src complexes, and PI3-kinase. *Cell*, **65**, 91-104.
- Owens, D.W., McLean, G.W., Wyke, A.W., Paraskeva, C., Parkinson, E.K., Frame, M.C. and Brunton, V.G. (2000) The catalytic activity of the Src family kinases is required to disrupt cadherin-dependent cell-cell contacts. *Mol Biol Cell*, **11**, 51-64.
- Ozaki, K., Kosugi, M., Baba, N., Fujio, K., Sakamoto, T., Kimura, S., Tanimura, S. and Kohno, M. (2009) Blockade of the ERK or PI3K-Akt signaling pathway enhances the cytotoxicity of histone deacetylase inhibitors in tumor cells resistant to gefitinib or imatinib. *Biochem Biophys Res Commun*, **391**, 1610-1615.

- Ozawa, M., Baribault, H. and Kemler, R. (1989) The cytoplasmic domain of the cell adhesion molecule uvomorulin associates with three independent proteins structurally related in different species. *Embo J*, **8**, 1711-1717.
- Ozawa, M., Hoschutzky, H., Herrenknecht, K. and Kemler, R. (1990) A possible new adhesive site in the cell-adhesion molecule uvomorulin. *Mech Dev*, **33**, 49-56.
- Park, J. and Cartwright, C.A. (1995) Src activity increases and Yes activity decreases during mitosis of human colon carcinoma cells. *Mol Cell Biol*, **15**, 2374-2382.
- Park, J., Meisler, A.I. and Cartwright, C.A. (1993) c-Yes tyrosine kinase activity in human colon carcinoma. *Oncogene*, **8**, 2627-2635.
- Park, J.G., Oie, H.K., Sugarbaker, P.H., Henslee, J.G., Chen, T.R., Johnson, B.E. and Gazdar, A. (1987) Characteristics of cell lines established from human colorectal carcinoma. *Cancer Res*, **47**, 6710-6718.
- Park, S.M., Gaur, A.B., Lengyel, E. and Peter, M.E. (2008) The miR-200 family determines the epithelial phenotype of cancer cells by targeting the E-cadherin repressors ZEB1 and ZEB2. *Genes Dev*, **22**, 894-907.
- Pawson, T. (1995) Protein-tyrosine kinases. Getting down to specifics. *Nature*, **373**, 477-478.
- Pawson, T. and Gish, G.D. (1992) SH2 and SH3 domains: from structure to function. *Cell*, **71**, 359-362.
- Pawson, T., Gish, G.D. and Nash, P. (2001) SH2 domains, interaction modules and cellular wiring. *Trends Cell Biol*, **11**, 504-511.
- Pece, S., Chiariello, M., Murga, C. and Gutkind, J.S. (1999) Activation of the protein kinase Akt/PKB by the formation of E-cadherin-mediated cell-cell junctions. Evidence for the association of phosphatidylinositol 3-kinase with the E-cadherin adhesion complex. *J Biol Chem*, **274**, 19347-19351.
- Pece, S. and Gutkind, J.S. (2000) Signaling from E-cadherins to the MAPK pathway by the recruitment and activation of epidermal growth factor receptors upon cell-cell contact formation. *J Biol Chem*, **275**, 41227-41233.
- Pena, S.V., Melhem, M.F., Meisler, A.I. and Cartwright, C.A. (1995) Elevated c-yes tyrosine kinase activity in premalignant lesions of the colon. *Gastroenterology*, **108**, 117-124.
- Peters, G.J. and van Groeningen, C.J. (1991) Clinical relevance of biochemical modulation of 5-fluorouracil. *Ann Oncol*, **2**, 469-480.
- Pickard, M. and Kinsella, A. (1996) Influence of both salvage and DNA damage response pathways on resistance to chemotherapeutic antimetabolites. *Biochem Pharmacol*, **52**, 425-431.
- Pittet, P., Lee, K., Kulik, A.J., Meister, J.J. and Hinz, B. (2008) Fibrogenic fibroblasts increase intercellular adhesion strength by reinforcing individual OB-cadherin bonds. *J Cell Sci*, **121**, 877-886.

- Pollard, T.D. and Cooper, J.A. (2009) Actin, a central player in cell shape and movement. *Science*, **326**, 1208-1212.
- Primer3.
- Ramanathan, R.K., Clark, J.W., Kemeny, N.E., Lenz, H.J., Gococo, K.O., Haller, D.G., Mitchell, E.P. and Kardinal, C.G. (2003) Safety and toxicity analysis of oxaliplatin combined with fluorouracil or as a single agent in patients with previously treated advanced colorectal cancer. *J Clin Oncol*, **21**, 2904-2911.
- Rastaldi, M.P., Ferrario, F., Giardino, L., Dell'Antonio, G., Grillo, C., Grillo, P., Strutz, F., Muller, G.A., Colasanti, G. and D'Amico, G. (2002) Epithelial-mesenchymal transition of tubular epithelial cells in human renal biopsies. *Kidney Int*, **62**, 137-146.
- Reits, E.A. and Neefjes, J.J. (2001) From fixed to FRAP: measuring protein mobility and activity in living cells. *Nat Cell Biol*, **3**, E145-147.
- Reynolds, A.B., Daniel, J., McCrea, P.D., Wheelock, M.J., Wu, J. and Zhang, Z. (1994) Identification of a new catenin: the tyrosine kinase substrate p120cas associates with E-cadherin complexes. *Mol Cell Biol*, **14**, 8333-8342.
- Reynolds, A.B. and Roczniak-Ferguson, A. (2004) Emerging roles for p120-catenin in cell adhesion and cancer. *Oncogene*, **23**, 7947-7956.
- Ribeiro, A.S., Albergaria, A., Sousa, B., Correia, A.L., Bracke, M., Seruca, R., Schmitt, F.C. and Paredes, J. (2009) Extracellular cleavage and shedding of P-cadherin: a mechanism underlying the invasive behaviour of breast cancer cells. *Oncogene*.
- Rivard, N. (2009) Phosphatidylinositol 3-kinase: a key regulator in adherens junction formation and function. *Front Biosci*, **14**, 510-522.
- Roche, S., Fumagalli, S. and Courtneidge, S.A. (1995) Requirement for Src family protein tyrosine kinases in G2 for fibroblast cell division. *Science*, **269**, 1567-1569.
- Rodriguez-Viciano, P., Marte, B.M., Warne, P.H. and Downward, J. (1996) Phosphatidylinositol 3' kinase: one of the effectors of Ras. *Philos Trans R Soc Lond B Biol Sci*, **351**, 225-231; discussion 231-222.
- Rooney, C., White, G., Nazgiewicz, A., Woodcock, S.A., Anderson, K.I., Ballestrem, C. and Malliri, A. (2010) The Rac activator STEF (Tiam2) regulates cell migration by microtubule-mediated focal adhesion disassembly. *EMBO Rep*.
- Rosen, S.A., Buell, J.F., Yoshida, A., Kazsuba, S., Hurst, R., Michelassi, F., Millis, J.M. and Posner, M.C. (2000) Initial presentation with stage IV colorectal cancer: how aggressive should we be? *Arch Surg*, **135**, 530-534; discussion 534-535.
- Roura, S., Miravet, S., Piedra, J., Garcia de Herreros, A. and Dunach, M. (1999) Regulation of E-cadherin/Catenin association by tyrosine phosphorylation. *J Biol Chem*, **274**, 36734-36740.
- Rous, P. (1983) Landmark article (JAMA 1911;56:198). Transmission of a malignant new growth by means of a cell-free filtrate. By Peyton Rous. *Jama*, **250**, 1445-1449.

- Rudini, N. and Dejana, E. (2008) Adherens junctions. *Curr Biol*, **18**, R1080-1082.
- Sabbah, M., Emami, S., Redeuilh, G., Julien, S., Prevost, G., Zimber, A., Ouelaa, R., Bracke, M., De Wever, O. and Gespach, C. (2008) Molecular signature and therapeutic perspective of the epithelial-to-mesenchymal transitions in epithelial cancers. *Drug Resist Updat*, **11**, 123-151.
- Sabe, H., Hata, A., Okada, M., Nakagawa, H. and Hanafusa, H. (1994) Analysis of the binding of the Src homology 2 domain of Csk to tyrosine-phosphorylated proteins in the suppression and mitotic activation of c-Src. *Proc Natl Acad Sci U S A*, **91**, 3984-3988.
- Sako, Y., Nagafuchi, A., Tsukita, S., Takeichi, M. and Kusumi, A. (1998) Cytoplasmic regulation of the movement of E-cadherin on the free cell surface as studied by optical tweezers and single particle tracking: corraling and tethering by the membrane skeleton. *J Cell Biol*, **140**, 1227-1240.
- Salonga, D., Danenberg, K.D., Johnson, M., Metzger, R., Groshen, S., Tsao-Wei, D.D., Lenz, H.J., Leichman, C.G., Leichman, L., Diasio, R.B. and Danenberg, P.V. (2000) Colorectal tumors responding to 5-fluorouracil have low gene expression levels of dihydropyrimidine dehydrogenase, thymidylate synthase, and thymidine phosphorylase. *Clin Cancer Res*, **6**, 1322-1327.
- Sansom, O.J., Meniel, V.S., Muncan, V., Pheese, T.J., Wilkins, J.A., Reed, K.R., Vass, J.K., Athineos, D., Clevers, H. and Clarke, A.R. (2007) Myc deletion rescues Apc deficiency in the small intestine. *Nature*, **446**, 676-679.
- Schlaepfer, D.D., Hanks, S.K., Hunter, T. and van der Geer, P. (1994) Integrin-mediated signal transduction linked to Ras pathway by GRB2 binding to focal adhesion kinase. *Nature*, **372**, 786-791.
- Schlaepfer, D.D. and Hunter, T. (1996) Signal transduction from the extracellular matrix--a role for the focal adhesion protein-tyrosine kinase FAK. *Cell Struct Funct*, **21**, 445-450.
- Schlaepfer, D.D. and Mitra, S.K. (2004) Multiple connections link FAK to cell motility and invasion. *Curr Opin Genet Dev*, **14**, 92-101.
- Schlaepfer, D.D., Mitra, S.K. and Ilic, D. (2004) Control of motile and invasive cell phenotypes by focal adhesion kinase. *Biochim Biophys Acta*, **1692**, 77-102.
- Segal, N.H. and Saltz, L.B. (2009) Evolving treatment of advanced colon cancer. *Annu Rev Med*, **60**, 207-219.
- Serrels, A., Timpson, P., Canel, M., Schwarz, J.P., Carragher, N.O., Frame, M.C., Brunton, V.G. and Anderson, K.I. (2009) Real-time study of E-cadherin and membrane dynamics in living animals: implications for disease modeling and drug development. *Cancer Res*, **69**, 2714-2719.
- Shimizu, D., Ishikawa, T., Ichikawa, Y., Togo, S., Hayasizaki, Y., Okazaki, Y., Danenberg, P.V. and Shimada, H. (2005) Prediction of chemosensitivity of colorectal cancer to 5-fluorouracil by gene expression profiling with cDNA microarrays. *Int J Oncol*, **27**, 371-376.

- Silverman, G.A., Kuo, W.L., Taillon-Miller, P. and Gray, J.W. (1993) Chromosomal reassignment: YACs containing both YES1 and thymidylate synthase map to the short arm of chromosome 18. *Genomics*, **15**, 442-445.
- Smellie, R.M. (1965) Biochemistry of deoxyribonucleic acid and ribonucleic acid replication. *Br Med Bull*, **21**, 195-202.
- Somani, A.K., Bignon, J.S., Mills, G.B., Siminovitch, K.A. and Branch, D.R. (1997) Src kinase activity is regulated by the SHP-1 protein-tyrosine phosphatase. *J Biol Chem*, **272**, 21113-21119.
- Soriano, P., Montgomery, C., Geske, R. and Bradley, A. (1991) Targeted disruption of the c-src proto-oncogene leads to osteopetrosis in mice. *Cell*, **64**, 693-702.
- Soussi, T. (2000) The p53 tumor suppressor gene: from molecular biology to clinical investigation. *Ann N Y Acad Sci*, **910**, 121-137; discussion 137-129.
- Spears, C.P., Gustavsson, B.G., Berne, M., Frosing, R., Bernstein, L. and Hayes, A.A. (1988) Mechanisms of innate resistance to thymidylate synthase inhibition after 5-fluorouracil. *Cancer Res*, **48**, 5894-5900.
- St Croix, B. and Kerbel, R.S. (1997) Cell adhesion and drug resistance in cancer. *Curr Opin Oncol*, **9**, 549-556.
- Stehbens, S.J., Paterson, A.D., Crampton, M.S., Shewan, A.M., Ferguson, C., Akhmanova, A., Parton, R.G. and Yap, A.S. (2006) Dynamic microtubules regulate the local concentration of E-cadherin at cell-cell contacts. *J Cell Sci*, **119**, 1801-1811.
- Sukegawa, J., Semba, K., Yamanashi, Y., Nishizawa, M., Miyajima, N., Yamamoto, T. and Toyoshima, K. (1987) Characterization of cDNA clones for the human c-yes gene. *Mol Cell Biol*, **7**, 41-47.
- Summy, J.M., Qian, Y., Jiang, B.H., Guappone-Koay, A., Gatesman, A., Shi, X. and Flynn, D.C. (2003a) The SH4-Unique-SH3-SH2 domains dictate specificity in signaling that differentiate c-Yes from c-Src. *J Cell Sci*, **116**, 2585-2598.
- Summy, J.M., Sudol, M., Eck, M.J., Monteiro, A.N., Gatesman, A. and Flynn, D.C. (2003b) Specificity in signaling by c-Yes. *Front Biosci*, **8**, s185-205.
- Sutherland, R.M. and Durand, R.E. (1984) Growth and cellular characteristics of multicell spheroids. *Recent Results Cancer Res*, **95**, 24-49.
- Takeishi, K., Kaneda, S., Ayusawa, D., Shimizu, K., Gotoh, O. and Seno, T. (1985) Nucleotide sequence of a functional cDNA for human thymidylate synthase. *Nucleic Acids Res*, **13**, 2035-2043.
- Tanimura, S., Uchiyama, A., Watanabe, K., Yasunaga, M., Inada, Y., Kawabata, T., Iwashita, K., Noda, S., Ozaki, K. and Kohno, M. (2009) Blockade of constitutively activated ERK signaling enhances cytotoxicity of microtubule-destabilizing agents in tumor cells. *Biochem Biophys Res Commun*, **378**, 650-655.
- Tasdemir, E., Chiara Maiuri, M., Morselli, E., Criollo, A., D'Amelio, M., Djavaheri-Mergny, M., Cecconi, F., Tavernarakis, N. and Kroemer, G. (2008) A dual role of p53 in the control of autophagy. *Autophagy*, **4**, 810-814.

- Thiery, J.P. (2002) Epithelial-mesenchymal transitions in tumour progression. *Nat Rev Cancer*, **2**, 442-454.
- Thiery, J.P. and Sleeman, J.P. (2006) Complex networks orchestrate epithelial-mesenchymal transitions. *Nat Rev Mol Cell Biol*, **7**, 131-142.
- Thomas, S.M. and Brugge, J.S. (1997) Cellular functions regulated by Src family kinases. *Annu Rev Cell Dev Biol*, **13**, 513-609.
- Thoreson, M.A., Anastasiadis, P.Z., Daniel, J.M., Ireton, R.C., Wheelock, M.J., Johnson, K.R., Hummingbird, D.K. and Reynolds, A.B. (2000) Selective uncoupling of p120(ctn) from E-cadherin disrupts strong adhesion. *J Cell Biol*, **148**, 189-202.
- Thorstensen, L., Lind, G.E., Lovig, T., Diep, C.B., Meling, G.I., Rognum, T.O. and Lothe, R.A. (2005) Genetic and epigenetic changes of components affecting the WNT pathway in colorectal carcinomas stratified by microsatellite instability. *Neoplasia*, **7**, 99-108.
- Thuault, S., Valcourt, U., Petersen, M., Manfioletti, G., Heldin, C.H. and Moustakas, A. (2006) Transforming growth factor-beta employs HMGA2 to elicit epithelial-mesenchymal transition. *J Cell Biol*, **174**, 175-183.
- Tinkle, C.L., Pasolli, H.A., Stokes, N. and Fuchs, E. (2008) New insights into cadherin function in epidermal sheet formation and maintenance of tissue integrity. *Proc Natl Acad Sci U S A*, **105**, 15405-15410.
- Traverso, G., Bettegowda, C., Kraus, J., Speicher, M.R., Kinzler, K.W., Vogelstein, B. and Lengauer, C. (2003) Hyper-recombination and genetic instability in BLM-deficient epithelial cells. *Cancer Res*, **63**, 8578-8581.
- Troyanovsky, R.B., Sokolov, E.P. and Troyanovsky, S.M. (2006) Endocytosis of cadherin from intracellular junctions is the driving force for cadherin adhesive dimer disassembly. *Mol Biol Cell*, **17**, 3484-3493.
- Tsai, M.S., Su, Y.H., Ho, M.C., Liang, J.T., Chen, T.P., Lai, H.S. and Lee, P.H. (2007) Clinicopathological features and prognosis in resectable synchronous and metachronous colorectal liver metastasis. *Ann Surg Oncol*, **14**, 786-794.
- Tsukita, S., Oishi, K., Akiyama, T., Yamanashi, Y., Yamamoto, T. and Tsukita, S. (1991) Specific proto-oncogenic tyrosine kinases of src family are enriched in cell-to-cell adherens junctions where the level of tyrosine phosphorylation is elevated. *J Cell Biol*, **113**, 867-879.
- Turner, C.E. (2000) Paxillin and focal adhesion signalling. *Nat Cell Biol*, **2**, E231-236.
- Vivanco, I. and Sawyers, C.L. (2002) The phosphatidylinositol 3-Kinase AKT pathway in human cancer. *Nat Rev Cancer*, **2**, 489-501.
- Vogelmann, R., Nguyen-Tat, M.D., Giehl, K., Adler, G., Wedlich, D. and Menke, A. (2005) TGFbeta-induced downregulation of E-cadherin-based cell-cell adhesion depends on PI3-kinase and PTEN. *J Cell Sci*, **118**, 4901-4912.

- Voulgari, A. and Pintzas, A. (2009) Epithelial-mesenchymal transition in cancer metastasis: mechanisms, markers and strategies to overcome drug resistance in the clinic. *Biochim Biophys Acta*, **1796**, 75-90.
- Vousden, K.H. and Lane, D.P. (2007) p53 in health and disease. *Nat Rev Mol Cell Biol*, **8**, 275-283.
- Waldner, M.J. and Neurath, M.F. (2010) The molecular therapy of colorectal cancer. *Mol Aspects Med*.
- Walther, A., Johnstone, E., Swanton, C., Midgley, R., Tomlinson, I. and Kerr, D. (2009) Genetic prognostic and predictive markers in colorectal cancer. *Nat Rev Cancer*, **9**, 489-499.
- Wang, H., Cai, Q., Zeng, X., Yu, D., Agrawal, S. and Zhang, R. (1999) Antitumor activity and pharmacokinetics of a mixed-backbone antisense oligonucleotide targeted to the R1alpha subunit of protein kinase A after oral administration. *Proc Natl Acad Sci U S A*, **96**, 13989-13994.
- Wang, L.H., Duesberg, P.H., Kawai, S. and Hanafusa, H. (1976) Location of envelope-specific and sarcoma-specific oligonucleotides on RNA of Schmidt-Ruppin Rous sarcoma virus. *Proc Natl Acad Sci U S A*, **73**, 447-451.
- Wang, N.M., Yeh, K.T., Tsai, C.H., Chen, S.J. and Chang, J.G. (2000) No evidence of correlation between mutation at codon 531 of src and the risk of colon cancer in Chinese. *Cancer Lett*, **150**, 201-204.
- Wang, W., Cassidy, J., O'Brien, V., Ryan, K.M. and Collie-Duguid, E. (2004) Mechanistic and predictive profiling of 5-Fluorouracil resistance in human cancer cells. *Cancer Res*, **64**, 8167-8176.
- Wang, W., Marsh, S., Cassidy, J. and McLeod, H.L. (2001) Pharmacogenomic dissection of resistance to thymidylate synthase inhibitors. *Cancer Res*, **61**, 5505-5510.
- Webb, J.D., Coleman, M.L. and Pugh, C.W. (2009) Hypoxia, hypoxia-inducible factors (HIF), HIF hydroxylases and oxygen sensing. *Cell Mol Life Sci*, **66**, 3539-3554.
- Westhoff, M.A., Zhou, S., Bachem, M.G., Debatin, K.M. and Fulda, S. (2008) Identification of a novel switch in the dominant forms of cell adhesion-mediated drug resistance in glioblastoma cells. *Oncogene*, **27**, 5169-5181.
- Wheeler, D.L., Huang, S., Kruser, T.J., Nechrebecki, M.M., Armstrong, E.A., Benavente, S., Gondi, V., Hsu, K.T. and Harari, P.M. (2008) Mechanisms of acquired resistance to cetuximab: role of HER (ErbB) family members. *Oncogene*, **27**, 3944-3956.
- Wildenberg, G.A., Dohn, M.R., Carnahan, R.H., Davis, M.A., Lobdell, N.A., Settleman, J. and Reynolds, A.B. (2006) p120-catenin and p190RhoGAP regulate cell-cell adhesion by coordinating antagonism between Rac and Rho. *Cell*, **127**, 1027-1039.
- Xu, J., Lamouille, S. and Derynck, R. (2009) TGF-beta-induced epithelial to mesenchymal transition. *Cell Res*, **19**, 156-172.

- Yagi, T. and Takeichi, M. (2000) Cadherin superfamily genes: functions, genomic organization, and neurologic diversity. *Genes Dev*, **14**, 1169-1180.
- Yamaguchi, M., Hirose, F., Inoue, Y.H., Ohno, K., Yoshida, H., Hayashi, Y., Deak, P. and Matsukage, A. (2004) Genetic link between p53 and genes required for formation of the zonula adherens junction. *Cancer Sci*, **95**, 436-441.
- Yang, A.D., Fan, F., Camp, E.R., van Buren, G., Liu, W., Somcio, R., Gray, M.J., Cheng, H., Hoff, P.M. and Ellis, L.M. (2006) Chronic oxaliplatin resistance induces epithelial-to-mesenchymal transition in colorectal cancer cell lines. *Clin Cancer Res*, **12**, 4147-4153.
- Yang, S., Guo, X., Debnath, G., Mohandas, N. and An, X. (2009) Protein 4.1R links E-cadherin/beta-catenin complex to the cytoskeleton through its direct interaction with beta-catenin and modulates adherens junction integrity. *Biochim Biophys Acta*, **1788**, 1458-1465.
- Yap, A.S., Briehner, W.M. and Gumbiner, B.M. (1997) Molecular and functional analysis of cadherin-based adherens junctions. *Annu Rev Cell Dev Biol*, **13**, 119-146.
- Yap, A.S., Crampton, M.S. and Hardin, J. (2007) Making and breaking contacts: the cellular biology of cadherin regulation. *Curr Opin Cell Biol*, **19**, 508-514.
- Yauch, R.L., Januario, T., Eberhard, D.A., Cavet, G., Zhu, W., Fu, L., Pham, T.Q., Soriano, R., Stinson, J., Seshagiri, S., Modrusan, Z., Lin, C.Y., O'Neill, V. and Amler, L.C. (2005) Epithelial versus mesenchymal phenotype determines in vitro sensitivity and predicts clinical activity of erlotinib in lung cancer patients. *Clin Cancer Res*, **11**, 8686-8698.
- Yeatman, T.J. (2004) A renaissance for SRC. *Nat Rev Cancer*, **4**, 470-480.
- Yokouchi, M., Kondo, T., Sanjay, A., Houghton, A., Yoshimura, A., Komiyama, S., Zhang, H. and Baron, R. (2001) Src-catalyzed phosphorylation of c-Cbl leads to the interdependent ubiquitination of both proteins. *J Biol Chem*, **276**, 35185-35193.
- Young, P., Boussadia, O., Halfter, H., Grose, R., Berger, P., Leone, D.P., Robenek, H., Charnay, P., Kemler, R. and Suter, U. (2003) E-cadherin controls adherens junctions in the epidermis and the renewal of hair follicles. *Embo J*, **22**, 5723-5733.
- Zeisberg, M., Yang, C., Martino, M., Duncan, M.B., Rieder, F., Tanjore, H. and Kalluri, R. (2007) Fibroblasts derive from hepatocytes in liver fibrosis via epithelial to mesenchymal transition. *J Biol Chem*, **282**, 23337-23347.
- Zheng, X.M., Resnick, R.J. and Shalloway, D. (2000) A phosphotyrosine displacement mechanism for activation of Src by PTPalpha. *Embo J*, **19**, 964-978.
- Zheng, X.M., Wang, Y. and Pallen, C.J. (1992) Cell transformation and activation of pp60c-src by overexpression of a protein tyrosine phosphatase. *Nature*, **359**, 336-339.
- Zhu, S., Bjorge, J.D., Cheng, H.C. and Fujita, D.J. (2008) Decreased CHK protein levels are associated with Src activation in colon cancer cells. *Oncogene*, **27**, 2027-2034.

- Ziegler, W.H., Gingras, A.R., Critchley, D.R. and Emsley, J. (2008) Integrin connections to the cytoskeleton through talin and vinculin. *Biochem Soc Trans*, **36**, 235-239.
- Zwick, E., Bange, J. and Ullrich, A. (2001) Receptor tyrosine kinase signalling as a target for cancer intervention strategies. *Endocr Relat Cancer*, **8**, 161-173.